Stony Brook University

Using Plant Traits to Predict Denitrification in Wetland Ecosystems

A Dissertation Presented

by

Mary Alldred

to

The Graduate School

in Partial Fulfillment of the

Requirements

for the Degree of

Doctor of Philosophy

in

Ecology and Evolution

Stony Brook University

August 2015

Stony Brook University
The Graduate School

Mary Alldred

We, the dissertation committee for the above candidate for the
Doctor of Philosophy degree, hereby recommend
acceptance of this dissertation.

Stephen B. Baines – Dissertation Advisor
Associate Professor, Department of Ecology and Evolution

Dianna Padilla – Chairperson of Defense
Professor, Department of Ecology and Evolution

Jessica Gurevitch
Professor, Department of Ecology and Evolution

Alistair Rogers
Scientist, Biological, Environmental, and Climate Sciences
Brookhaven National Laboratory

Stuart Findlay
Senior Scientist, Aquatic Ecology
Cary Institute of Ecosystem Studies

This dissertation is accepted by the Graduate School

_____
Charles Taber
Dean of the Graduate School

Abstract of the Dissertation

Using Plant Traits to Predict Denitrification in Wetland Ecosystems

by

Mary Alldred

Doctor of Philosophy

in

Ecology and Evolution

Stony Brook University

2013

Understanding how changes in ecological communities affect ecosystem function, including the provisioning of ecosystem services, is a critical challenge in the field of ecology. I apply a trait-based approach to link the characteristics of plant communities to their effects on denitrification and nitrogen-removal ecosystem services. My work has addressed this challenge at multiple scales using literature syntheses, field surveys, field manipulations, and greenhouse experiments. In a meta-analysis of 419 published measurements of denitrification, I estimated that vegetation on average increases the ability of marshes to remove nitrogen by 55% and that this effect differs among species. My study was the first to quantify the general effect of wetland vegetation on this globally important term of the nitrogen cycle. I pursued two field projects to explain variation among species by investigating interactions among plant traits and sediment properties and processes. In the first, I determined that removing an invasive marsh grass, *Phragmites australis*, increased sediment nitrogen concentrations and decreased denitrification relative to marshes containing invasive *Phragmites* or native cattail species. These results suggest a trade-off between removing invasive species to conserve biodiversity and managing wetlands to promote nitrogen removal. The second field project addressed interactions between traits of dominant salt marsh grass *Spartina alterniflora* and ecosystem properties and processes along a land-use gradient on Long Island, NY. Root growth of *S. alterniflora* responded positively to salinity and negatively to nitrogen availability, suggesting that eutrophication and sea-level rise may have opposing effects on root mass, and therefore marsh stability, in the future. Results from greenhouse experiments, which employed a novel combination of oxygen-sensitive planar optodes and microbial process measurements, suggested that *S. alterniflora* roots influence nitrification and denitrification rates by introducing oxygen to sediments. Field measurements from Long Island marshes confirmed that plant traits are useful predictors of denitrification potential among wetland sites, offering superior estimates relative to those obtained from abiotic predictors. Results also suggest that the influence of plant communities on denitrification scales positively with aboveground biomass. Together my results support the utility of trait-based approaches in understanding the role of plant communities in promoting nitrogen-removal services in wetland ecosystems.

Dedication Page

For my father. By cultivating interests in football and scuba, he coaxed this shy scholar outside into nature.

For my mother. My earliest childhood memories are of watching Star Trek with her and seeing science and discovery as something important and, on occasion, heroic.

And for both of them, who supported me unconditionally.

Table of Contents

List of Tables

List of Figures

Chapter 6

Acknowledgments

I would first like to thank my advisor Stephen Baines for his constant support, even as my early project discussions veered away from his academic comfort zone into the messy world of mud and nitrogen. I cannot emphasize enough how fortunate I feel to have had an advisor that mitigated the many traumas of graduate school, rather than adding to them. Stephen helped me considerably in making my research project a reality, and by his own example helped me to become a more thoughtful scientist and a more patient and compassionate mentor. I would also like to thank my doctoral committee: Dianna Padilla for convincing me that I would find a home in the scholarly community at Stony Brook and for adopting me into her extended lab family early in my graduate career, Jessica Gurevitch for imparting wisdom on plant ecology and statistical design but perhaps more importantly for inspiring me to be more observant of the natural world, Stuart Findlay for making the complexities of marsh chemistry and ecology appear as simple and straightforward as I think anyone ever could, and Alistair Rogers for his considerable logistical support and guidance on the topic of plant physiology.

My dissertation research would not have been possible without the assistance of my labmates Dr. Katie Schneider, Lucas Merlo, Emily Herstoff, Stoycho Velkovsky, and Kevin Doyle. Stoycho collaborated with me to complete the mesocosm experiments presented in Chapter 3 and performed all nutrient extractions and nitrification assays reported in Chapters 3 and 4. Many incredible undergraduate assistants from Stony Brook and other nearby universities contributed substantially to field and laboratory analyses: Nawal Ahmed, Jordan Bader (Drew University), Diana Lenis, Douglas Lerner, Anne Liberti, Steven Lundi, Vashtidevi Mahadeo, Priscilla Moley, Ashley Moreno, Sangmin Pak, Louis Piscopo (SUNY Oswego), Matthew Sarubbi, Jordan Schwartzberg, and Michael Tong. Several graduate students in Ecology and Evolution also assisted with field work: Jonathan Borrelli, Emily Herstoff, Theresa Miranda, Hae Yeong Ryu, Laurel Yohe, Charles DiRienzo, and Zachary Chejanovski.

A number of students, professors, and staff in the Department of Ecology and Evolution contributed to my development as a scientist and scholar and my mental and emotional well-being. I would like to especially thank Dana Opulente for being my friend, confidant, and office mate throughout my time in New York and her family for making me feel welcome and that I have a home and family here. Emily Rollinson, Abigail Cahill, Jennifer Rollins, Mica McCarty-Glenn, Emily Herstoff and countless others in E&E have provided a truly exceptional network of support, friendship, and collegial discourse that have added to my academic and personal well-being, and I cannot thank them enough. And to Jonathan Borrelli, I offer my deepest gratitude and appreciation for keeping me sane, understanding and sharing my passion for science, and reminding me to take care of myself and enjoy life.

This work was supported by New York Sea Grant (R/CMC-10), a Tibor T. Polgar Fellowship and Graduate Research Fellowship from the Hudson River Foundation, the ENY Chapter of the Nature Conservancy, a Robert R. Sokal Award for Research in Statistical Biology, and a Lawrence Slobodkin Award for Research in Ecology from the Department of Ecology and Evolution, Stony Brook University. Site access was generously provided by the Nature Conservancy, Suffolk County Parks, U.S. Fish and Wildlife, the Town of Hempstead, the Village of Sands Point, and the Ward Melville Heritage Organization. Nicole Maher and Jim Browne were exceptionally helpful in identifying field locations and providing information on the natural history of Long Island marshes. Zoe Cardon at Woods Hole Marine Laboratory provided extensive methodological advice on the use of oxygen measurement methods, and

Anne Giblin, also at Woods Hole, performed the membrane-inlet mass spectroscopy measurements reported in Chapter 3. I would also like to thank Alistair Rogers and Stefanie Lasota at Brookhaven National Laboratory and Stuart Findlay, David Fischer, and Lisa Martel at the Cary Institute of Ecosystem Studies for analytical assistance. Cathleen Wigand, Kelly Addy, Timothy Hollein, Lisa Martel, and Mary Scranton provided advice on conducting gas chromatography measurements.

Chapter 1

Introduction

Human activities have profoundly transformed the structure and function of ecosystems on a global scale. Many of these transformations, including agricultural and industrial land-use development, have increased the well-being and economic prosperity of human societies. However, these transformations have also caused substantial negative impacts on ecosystem services, including regulation of air and water quality, with potentially severe consequences for human health and well-being (Millennium Ecosystem Assessment 2005). Simultaneously, humans have altered biodiversity and the composition of ecological communities worldwide (Chapin III et al. 2000). Ecological communities are generally understood to affect ecosystem processes and services (Tilman 1999, Loreau et al. 2001, Hooper et al. 2005). However, predicting how changes in biodiversity will alter ecosystem services remains a central problem in the field of ecology, and one that requires a synthesis of knowledge from the subdisciplines of physiological, community, and ecosystem ecology (Naeem 2002, Kremen 2005).

A trait-based framework offers one promising approach to bridge the gaps among various subdisciplines of ecology and to address interactions between community and ecosystem processes. Trait-based approaches have been around for some time (Keddy 1992, Eviner and Chapin III 2003) and continue to generate enthusiasm for their potential to produce general, predictive models in ecology by focusing on the mechanistic links among organism characteristics, organism performance, and the environment (Lavorel and Garnier 2002, McGill et al. 2006, Lavorel and Grigulis 2012). Unfortunately, adoption of the word "trait" by multiple subdisciplines in ecology has led to considerable confusion over what measurements a trait, or a "functional trait," can encompass (Violle et al. 2007). Most of this confusion arises from the

several reasons traits may be studied. In physiology or functional ecology, traits are typically studied to infer how a particular organism will respond to fluctuations or directional changes in its environment. The idea of a trait as a species characteristic is also employed by community ecologists when defining the fundamental niches of species, and to explain patterns of species interactions that ultimately govern the realized niches of species (McGill et al. 2006). This usage is similar to the concept of "response trait" proposed by Lavorel and colleagues to explain responses of plant communities to abiotic change or disturbance (Lavorel and Garnier 2002). In ecosystem ecology, traits most commonly refer to those characteristics of organisms that affect ecosystem properties or processes (Suding et al. 2008, Ehrenfeld 2010). Since the focus is the effect of the trait on the environment, it is not necessary that the trait be a stable characteristic of a species; the same effect would result if the trait value were the result of changing species composition or plastic phenotypic responses to the environment within resident species. Moreover, when traits are studied for their influence on the ecosystem, they are measured or integrated at a scale that is relevant to the ecosystem process of interest. Often this means averaging a trait value over many co-existing species within an ecosystem. This usage is similar to the concept of "effect trait" proposed by Lavorel and colleagues (Lavorel and Garnier 2002).

An organismal trait can simultaneously be both an effect and a response trait. In fact, where the goal of a study is to predict how a change in community structure may alter ecosystem function, an overlap in response and effect traits is the ideal scenario (Lavorel and Garnier 2002). For example, in grasslands of Central Europe, nutrient enrichment favored the dominance of plant species with higher specific leaf area, leaf nitrogen content, and maximum photosynthetic rate, without having an overall impact on standing biomass of the plant community. The net effect of this change in the trait composition of the plant community was to increase the annual

net primary productivity (ANPP) of the nutrient-enriched grasslands (Lavorel and Garnier 2002). In this example, using a trait-based approach offered a mechanistic explanation of how plant communities responded to nutrient enrichment and how this community-level response in trait composition affected ANPP, an important ecosystem process. Rather than favoring species that achieve higher peak biomass, nutrient enrichment in this case resulted in selection for species with traits that conferred higher maximum photosynthetic rates per unit biomass. To the extent that these traits respond to other environmental changes (e.g., drought, temperature, rising atmospheric CO_2), the same framework could be applied to predict the consequences of trait responses for community composition, as well as the effect of the new community on ANPP.

A fundamental strength of a trait-based approach is that it is flexible enough to be applied at multiple scales, depending on the question of interest. For example, in systems dominated by a single species (e.g., agricultural or monospecific wetland systems), trait dynamics may operate on an intraspecific level, often resulting from phenotypic plasticity or selection on standing genetic variation. In contrast, in extremely diverse communities, the trait variation of interest may result from replacement of some taxa with others possessing different traits. In either case similar trait-based frameworks can be applied, in which the response and effect traits of interest are identified, assessed at a scale relevant to the ecosystem process of interest, and mechanistically linked to predict outcomes for ecosystem function.

Human modification of the global nitrogen cycle presents a considerable management challenge for which a trait-based approach may prove useful. By adding an industrial fixation term to the global nitrogen cycle and increasing rates of biological fixation (Figure 1.1), human activities have more than doubled the amount of biologically available nitrogen added to landscapes (Vitousek et al. 1997). In aquatic ecosystems, excess nitrogen can result in

eutrophication, hypoxia, and harmful algal blooms, all of which have severe consequences for human health and economics (Millennium Ecosystem Assessment 2005). Denitrification, a microbial respiratory process in which nitrate is permanently removed from ecosystems to the atmosphere as inert dinitrogen gas (Figure 1.1), helps to counteract these effects and thus represents a critical ecosystem service (Zedler 2003, Hinga et al. 2005).

Wetland ecosystems are important sites of denitrification, and wetland plant communities are known to influence sediment chemistry and denitrification rates by altering organic carbon availability and the redox conditions of sediments through root aeration (Figure 1.2) (Sherr and Payne 1978, Weisner et al. 1994, Bachand and Horne 2000). Denitrifying microbes require organic carbon as an energy source and nitrate as an electron acceptor. Because oxygen yields greater energy, microbes will use oxygen preferentially when it is available; therefore, oxygen concentrations must be low before denitrifiers will use nitrate as a terminal electron acceptor for respiration. However, because the dominant form of nitrogen in anoxic systems tends to be ammonium (Figure 1.2A), denitrifiers commonly rely on the production of nitrate via microbial nitrification, which requires oxygen to proceed (Figure 1.2B). Therefore, highest denitrification rates are often observed in systems that experience variation in oxygen availability, such that sufficient oxygen is available for the production of nitrate via nitrification, but low oxygen conditions also exist and induce denitrifiers to switch from reducing oxygen to reducing nitrate (Seitzinger et al. 2006). Plant-mediated sediment aeration is one mechanism that may promote coupled nitrification-denitrification by increasing spatial (Figure 1.2C) or temporal (Figure 1.2D) variation in sediment oxygen availability.

Figure 1.3 presents a conceptual framework that incorporates the various possible influences of plant communities on denitrification potential as interactions between components

of the nitrogen cycle and traits of the plant community. In general, traits that increase sediment aeration may have a direct negative influence on denitrification by providing a superior oxidant or an indirect positive influence on denitrification by enhancing the production of nitrate via nitrification (Figure 1.2B). Belowground traits associated with sediment ventilation, like root mass or rhizome width, could impact delivery of oxygen or spatial variation in oxygen delivery (Armstrong and Armstrong 1990, Armstrong et al. 1996). Aboveground traits like maximum photosynthetic rate, or proxies of photosynthetic potential including specific leaf area or leaf nitrogen content, could also be related to diurnal variation in oxygen production (Armstrong and Armstrong 1990, Wright et al. 2004, Reich et al. 2007). Litter quality and root production may influence carbon availability and quality and enhance denitrification potential, albeit on very different timescales, with root exudation influencing short-term carbon dynamics and litter quality influencing long-term carbon dynamics via decomposition and nutrient recycling (Hume et al. 2002a, b). Conversely, traits associated with high nitrogen demand or accumulation of nitrogen in recalcitrant biomass would result in competition with microbes for nitrogen and may inhibit denitrification rates.

The goal of my dissertation was to apply a trait-based framework to understand how plant communities modify nitrogen cycling processes and nitrogen-removal services in wetland sediments. In Chapter 2, I conducted a systematic review and meta-analysis of 419 published measurements of denitrification to determine whether denitrification rates vary systematically among different wetland communities, defined by the dominant species in the community. I also determined the general effect of vegetation on denitrification rates and whether this effect varies among wetland communities. Chapters 3 and 4 applied an effect-trait approach to predict the influence of dominant salt marsh grass *Spartina alterniflora* on denitrification potential. In

Chapter 3, to establish sediment aeration as a mechanism by which *S. alterniflora* influences denitrification rates, I applied a novel combination of oxygen-sensitive planar optode methods, microbial process assays, measurements of sediment chemistry, and quantification of plant traits in mesocosm-scale greenhouse experiments. In Chapter 4, I used plant traits to predict denitrification potential among 11 salt marsh locations on Long Island, NY that span a gradient of land-use and nitrogen-loading intensity.

Wetlands have been heavily impacted by humans, with over 50% of global wetland area lost to human development and much of the remaining area degraded or threatened due to such pressures as sea-level rise, salinization, eutrophication, and invasion by exotic plant species (Zedler and Kercher 2005). In Chapters 5 and 6, I focused on trait responses in wetland plant communities resulting from sea-level rise, eutrophication, and invasive-species management. Belowground growth in coastal plants is a critical determinant of marsh stability and the ability of wetlands to keep pace with sea-level rise; however, the responses of belowground traits to nutrient enrichment and salinity remains an open question in coastal marsh ecology despite a long history of study (Valiela et al. 1976, Mendelssohn and Morris 2000). In Chapter 5, I established the responses of belowground traits of *Spartina alterniflora* to salinity and nutrient conditions among 11 field sites varying in nitrogen-loading intensity and salinity. In Chapter 6, I monitored removals of *Phragmites australis*, an invasive marsh grass, from freshwater tidal wetlands of the Hudson River and compared treated removal sites to intact *Phragmites* communities and native *Typha angustifolia* communities. The trait composition of plant communities that recolonized treated sites was compared to both *Phragmites*- and *Typha*-dominated communities, and changes in nitrogen-removal services were assessed following invasive-plant management.

Together, these chapters represent the application of a trait-based conceptual framework to address the critical and difficult challenge of predicting how changes in wetland plant communities may alter present and future patterns of denitrification and nitrogen-removal ecosystem services.

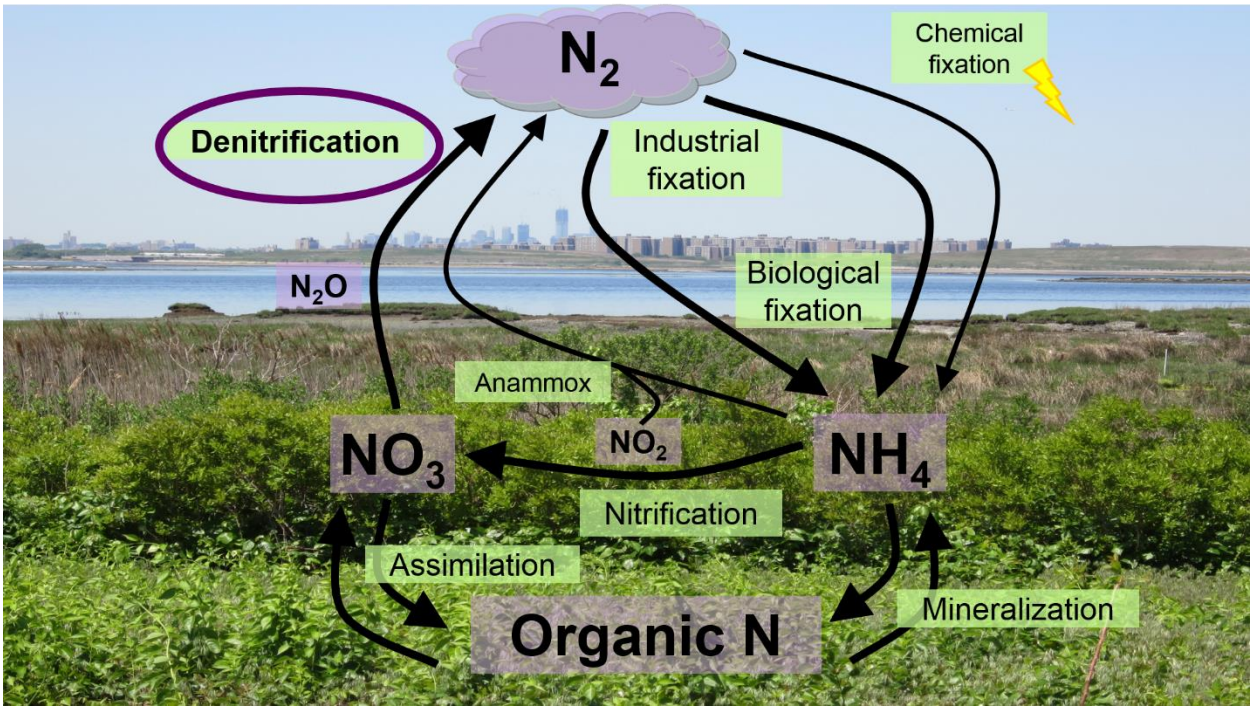

Figure 1.1: Diagram showing major transformations of the nitrogen cycle. Human activities have increased inputs of biologically available nitrogen to ecosystems by increasing rates of biological fixation and adding an industrial fixation term to the global nitrogen cycle. Microbial denitrification permanently removes biologically available nitrogen in the form of nitrate (NO_3^-) from ecosystems to the atmosphere as inert nitrogen gas (N_2).

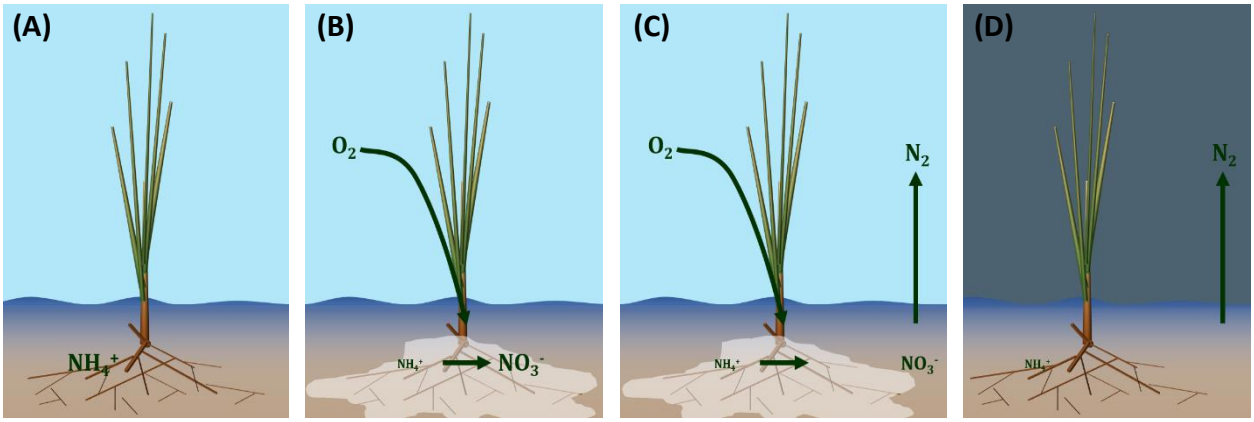

Figure 1.2: Example of root-mediated sediment aeration, one potential mechanism by which plants may influence sediment chemistry and denitrification. (A) Because wetland sediments are saturated, the dominant form of inorganic nitrogen is reduced ammonium (NH_4^+). (B) Plants may introduce oxygen to sediments via stems and roots, either diffusively from the atmosphere or as a product of photosynthesis. (C) Once oxygen is present, nitrifying bacteria may oxidize ammonium to nitrate (NO_3^-). Nitrate from nitrification may diffuse to anoxic sediment sites, or (D) remain in the sediment until oxygen is depleted (e.g. via net respiration at night), and be reduced to N_2 gas by denitrifying bacteria. Therefore, plant characteristics that enhance spatial or temporal variation in oxygen availability should also be expected to promote coupled nitrification-denitrification.

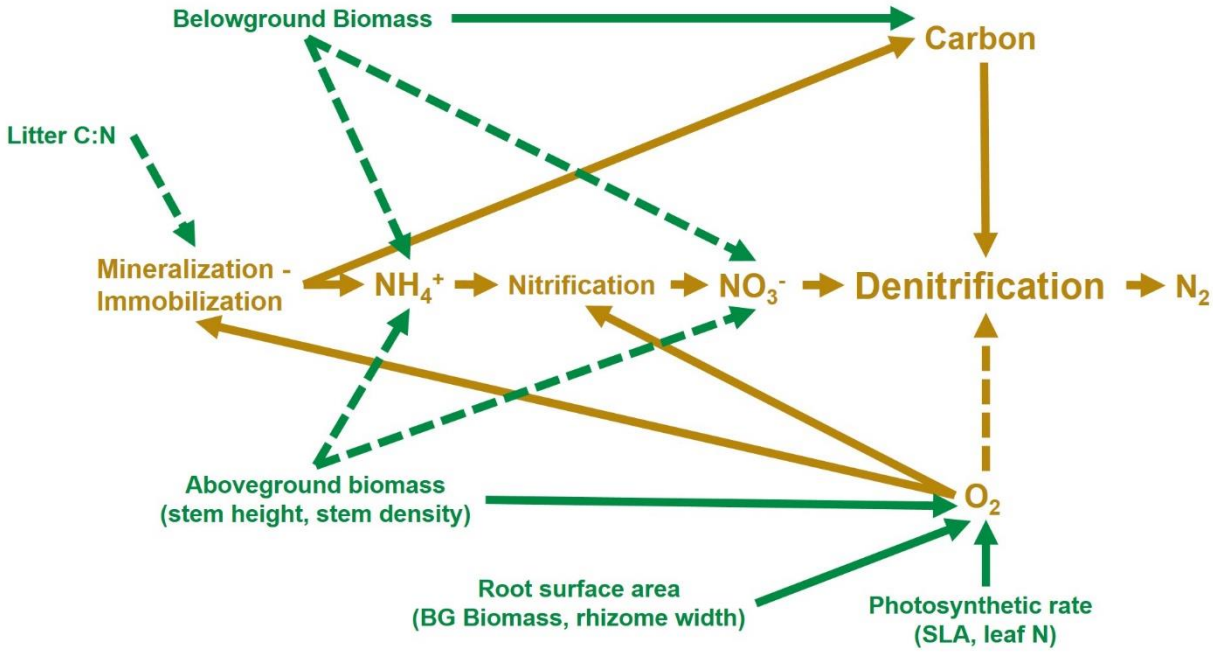

Figure 1.3: Conceptual framework linking key processes of nitrogen cycling and nitrogen-removal services (brown) to changes in the trait composition of plant communities (green). Solid lines indicate positive interactions, and dashed lines indicate negative interactions.

Chapter 2

Effects of wetland plants on denitrification rates: a meta-analysis

Abstract

Human activity is accelerating changes in biotic communities worldwide. Predicting impacts of these changes on ecosystem services such as denitrification, a process that mitigates the consequences of nitrogen pollution, remains one of the most important challenges facing ecologists. Wetlands especially are valued as important sites of denitrification, and wetland plants are expected to have differing effects on denitrification. Here I present the results of a meta-analysis, conducted on 419 published estimates of denitrification in wetlands dominated by different plant species. Plants increased denitrification rates by 55% on average. This effect varied significantly among communities as defined by the dominant plant species, but surprisingly did not differ substantially among methods for measuring denitrification or among types of wetlands. I conclude that mechanistically linking functional plant traits to denitrification will be key to predicting the role of wetlands in nitrogen mitigation in a changing world.

Introduction

Identifying general relationships between biotic community structure and ecosystem function is a key challenge facing ecologists. Changes to biotic communities that result from global climate change, sea-level rise, species introductions, or selected harvesting are likely to have a substantial effect on biogeochemical processes (Chapin III et al. 2000, Lavorel and Garnier 2002, Kremen and Ostfeld 2005). Nonetheless, attempts to link simple measures of community structure to ecosystem process have often met with limited success (Lawton 1999, Simberloff 2004). For example, a large number of studies has found that relationships between

biodiversity and a number of biogeochemical processes are often complex and statistically weak (Hooper et al. 2005). Such a result is not necessarily surprising. Ecosystem processes are often most strongly influenced by those organisms in a community that contribute most to biomass and productivity, or which play unique biogeochemical roles (Lavorel and Garnier 2002, Suding et al. 2008). Due to differences in key traits, dominant organisms can vary widely in their effects on the local chemical and physical environment, as well as on other species in the community (Eviner and Chapin III 2003, Laughlin 2011). Therefore, one may expect ecosystem processes to be closely linked to the identity of the dominant species in an ecosystem.

Here I apply meta-analytic techniques to relate published values of wetland denitrification to plant community composition as defined by the dominant species present. This study represents an important first step in a broader effort to develop a more mechanistic incorporation of community structure into models of the nitrogen cycle. Humans have more than doubled the amount of nitrogen fixation on a global basis, with highly industrialized areas experiencing mineralized nitrogen concentrations up to 25 times that of pre-development concentrations (Vitousek et al. 1997, Hinga et al. 2005). Movement of excess fixed nitrogen into downstream ecosystems, particularly nitrogen-limited coastal ecosystems, results in eutrophication, hypoxia, and harmful algal blooms, all of which may have severe consequences for the economy and human health (Hooper and Vitousek 1997, Vitousek et al. 1997, Hinga et al. 2005, Howarth et al. 2011). Denitrification, a microbial process in which nitrate is permanently removed from ecosystems to the atmosphere as inert dinitrogen gas (N_2), can help to mitigate the effects of mineralized-nitrogen pollution (Zedler 2003, Jordan et al. 2011). Consequently, estimating denitrification at landscape scales is a critical goal for managers of aquatic and coastal ecosystems (Hinga et al. 2005, Groffman et al. 2009). Wetland sediments are particularly

important sites of denitrification because their anaerobic nature favors complete reduction of mineralized nitrogen to N_2 gas, while minimizing the release of the intermediate product, N_2O, a powerful greenhouse gas (Kralova et al. 1992, Schlesinger 2009).

Wetland plants are generally understood to play an important role in nitrogen removal by altering the sediment environment in which denitrification occurs (Caffrey et al. 2007). Denitrification is an anaerobic bacterial respiratory process that requires nitrate (NO_3^-, an oxidizing agent), organic carbon (as a reducing agent) and low O_2 concentrations to proceed. In several cases, plants have been shown to control sediment denitrification dynamics by competing for nitrate (Schimel et al. 1989, Kirk and Kronzucker 2005), supplying labile organic carbon (Hume et al. 2002b), and introducing oxygen via diffusion from roots (Caffrey and Kemp 1990, Caffrey and Kemp 1992). Research on plant invasions has further revealed that changes in the composition of plant communities can have a major effect on sediment microbial processes (Ehrenfeld 2003), including denitrification (Windham and Meyerson 2003). The extent and composition of wetland plant communities are changing rapidly due to species introductions, land-use changes, sea level rise, and climate change (Bertness et al. 2002, Ehrenfeld 2003). Because plants differ in functional characteristics that may influence denitrification, broad scale changes in the composition of plant communities may substantially alter denitrification rates of future landscapes.

Despite the growing realization that vegetation may exert considerable control over denitrification rates, to date no attempts have been made to assess the generality of plant-mediated effects and incorporate these effects into predictive denitrification models (Boyer et al. 2006). Instead, efforts have more typically focused on abiotic factors, such as hydrography, water chemistry, and sediment characteristics, which are relatively easy to characterize and

whose potential influence on denitrification is often more clearly understood. The influence of plant communities on denitrification may be hard to disentangle from the influence of abiotic variables because plant community structure may be correlated to a number of physical and chemical variables. Methodological concerns also pose problems for attempts to build predictive models from existing observations. Researchers have developed diverse techniques for measuring small rates of N_2 production against the enormous background concentrations in the atmosphere (Groffman et al. 2006). Whether these various methods provide comparable estimates of denitrification rates remains one of the greatest concerns in denitrification research. As an example, acetylene-inhibition methods have been found to underestimate denitrification rates relative to direct measurements of nitrogen-gas production (Watts and Seitzinger 2000). If any type of method tends to be used more in a given plant community, spurious correlations between plant communities and measured denitrification could result. Alternatively, variation among methods may obscure any relationships between plant community structure and denitrification that actually exist.

Here I synthesize the results of a large number of denitrification studies conducted in well characterized plant communities from across the ecological and engineering literature. Using this extensive database, I determine whether denitrification rates differ among communities dominated by specific plant species. I also evaluate the relative importance of the type of wetland system in which the studies were conducted and the methods used to measure denitrification in explaining the variation in denitrification rates among studies. The presence of nearby non-vegetated control plots or treatments in a number of studies allow me to control for geophysical context and methodology by calculating an effect size for vegetation on denitrification rates. Using the effect-size metric, I test for generality in the effect of vegetation

on denitrification rates among plant communities. I conclude by exploring possible approaches for predicting what effects specific plant communities will have on sediment denitrification rates.

Methods

To develop an exhaustive data set, I performed a systematic review using Web of Science and Google Scholar databases using the key terms "wetland AND plant AND denitrification." I expanded this search by including all studies cited in key review papers examining variation in denitrification rates or the effects of plants on geochemical processes (Cornwell et al. 1999, Ehrenfeld 2003, Caffrey et al. 2007), and I searched for all papers citing any of these reviews. Publication dates ranged from earliest available publications to studies published in 2010. Once a list of potentially useful studies was compiled, I examined each study systematically to include only those that measured denitrification rates within well characterized plant communities. Among these studies, plant communities were most often characterized by the dominant species inhabiting the community; therefore, I only included studies that reported a denitrification rate measurement associated with a dominant species in the community. Where percent composition was specified, the "dominant species" classification was only used if the species comprised greater than 50% of the biomass or cover within a plant community. On several occasions in which the inputs to a wetland system were known or easily determined, investigators quantified other fates of nitrogen, such as plant uptake, and calculated denitrification by mass balance. If studies used either nitrogen removal (ammonium or nitrate removal) or mass balance to calculate denitrification, I required that they quantify other fates of nitrogen inputs or justify that denitrification was the dominant form of nitrogen removal within their system. Mass-balance studies that failed to meet these criteria were assumed to overestimate denitrification rates and were discarded.

For each plant community studied in an article, the average denitrification rate, as well as the error and sample size for that average, was recorded. Where multiple averages were recorded, I included only those averages that were collected during the growing season at independent wetland locations (or in separate laboratory or field containers). For each average denitrification measurement, I recorded the type of wetland system within which the measurement was made as well as the method used to measure denitrification. Denitrification rates were converted to common units (g N m^{-2} h^{-1}) prior to analyses. For studies that measured denitrification per volume of sediment, volume measurements were converted to area equivalents, given the dimensions of sediment cores analyzed. Studies that failed to report error or sample size, or failed to provide enough methodological information to convert denitrification rates to common units, were excluded from further examination. My search yielded average measurements of denitrification in vegetated sediments from 419 independent sites or mesocosms collected from 55 publications. Ninety-two of these measurements could be paired with estimates of denitrification from nearby non-vegetated control plots or treatments. A final list of measurements included in this analysis is provided in Table S1 in Supporting Information.

Effect sizes were calculated as the average denitrification rate for each measurement, weighted by the inverse of the sampling variance. This calculation gives greater weight to measurements of denitrification rates with greater precision or greater replication (Osenberg et al. 1999). Data were then grouped by plant community, wetland system, and method of denitrification measurement. Any differences observed in average denitrification rates among plant communities may be the result of physiological differences in the plants themselves; however, they could also be an artifact of geophysical conditions (e.g., hydrology, nitrogen loading, salinity), which influence denitrification and coincidentally affect the composition of

wetland plant communities. Unfortunately, geophysical conditions such as nitrogen loading were rarely reported in a way that would facilitate inclusion in this analysis. To estimate the effect of vegetation independent of geophysical context, I made use of the subset of 92 measurements that included denitrification measurements in non-vegetated control sites or treatments. For each of these measurements, I calculated the logarithm of the ratio of denitrification rate in vegetated sediments to that in nearby non-vegetated sediments. This ratio provided me with a measure of the local effect of vegetation on denitrification (Hedges et al. 1999). To test whether functional or taxonomic groupings of plant communities may explain variation in vegetation effects, I repeated this analysis, grouping plant communities at the family and genus level and into functional groups based on growth form. Growth-form categories included trees and shrubs, emergents (including grasses, sedges, and rushes), emergent forbs, submersed macrophytes, and floating plants. Q-tests of heterogeneity were performed to test the ability of each grouping variable to explain both the variation in the effect of plants on denitrification and the variation in average denitrification rates among all measurements. A random-effects model was used for these tests (Gurevitch and Hedges 2001). In the context of meta-analysis, a random-effects model is a more conservative test of differences among groups in that it does not assume that a common true effect size exists for each group among measurements; rather, it includes an additional variance term which accounts for random variation in the effect of interest among measurements (Gurevitch and Hedges 2001). For both sets of analyses, confidence intervals and probability values were estimated by bootstrapping, using 999 iterations of the data. All calculations were performed in MetaWin 2.0 (Rosenberg et al. 2000).

Results

Overview of the Data

Average net denitrification rates reported among all the measurements included in this analysis varied over six orders of magnitude, from -6.4 to 880 mg-N m^{-2} h^{-1}. Studies varied widely in purpose from documenting the effects of species invasions on denitrification rates to comparing treatment-wetland designs employing different plant species. Often, the dominant plant species at a site was reported under site characterization and was not the main focus of the study. Results were obtained from a variety of wetland systems, including 168 constructed wetland sites, 53 experimental microcosms or mesocosms, and 198 naturally occurring wetlands (including salt marshes, tidal freshwater marshes, riparian wetlands, and depressional wetlands). More than 82% of the measurements involved emergent plant communities dominated by monocots, with 49% of the monocot species belonging to the family Poaceae.

Of the many methods available to measure denitrification (for a complete review, see Groffman et al. 2006), the most commonly used method was denitrification enzyme activity (DEA) and other similar acetylene-reduction techniques (Appendix A); DEAs and other acetylene reduction techniques accounted for over 59% of the measurements included in my analysis. The methods used to measure denitrification and the systems in which measurements were made did not appear to be strongly associated with any particular type of plant community (for complete list, see Appendix A). However, instances in which investigators have used multiple denitrification measurements to investigate the same plant community, or instances in which the same community was investigated in multiple wetland systems, were rarely available. Consequently I was unable to calculate interaction terms or perform multiple regression analyses with my predictor variables.

Do Denitrification Rates Differ among Plant Communities?

Measurements of denitrification differed significantly among plant communities, with differences among dominant plant species ranging over four orders of magnitude (Figure 2.1A). The highest observed denitrification rates occurred in sites dominated by *Spartina alterniflora* and *Oryza sativa* (Figure 2.1A). Grouping by the dominant species in a plant community explained 28% of the variation in denitrification rates among measurements (Table 2.1). These results were not sensitive to the removal of high-denitrification and low-denitrification plant communities from the analysis. Because I was unable to determine if there was an interaction between plant communities and denitrification measurements using the whole data set, I repeated this analysis for only those studies using DEA and similar acetylene-reduction methods in order to rule out a confounding effect of variation in methods among studies. This subset analysis provided statistically similar results to an analysis of the full dataset ($p = 0.002$; $df = 23, 221$; variance explained = 31%).

A notably large amount of variation remained within many of the plant community groupings, including cases for which a large number of measurements were available. For example, denitrification rates observed at sites dominated by *Phragmites australis* ($n = 55$) varied by over an order of magnitude (Figure 2.1A). Grouping denitrification measurements by the wetland type explained only 14% of the total variation in denitrification rates, less than half of the variation explained when grouping by plant community (Table 2.1). Most of this variation was explained by very low denitrification rates in experimental estuarine ponds and very high denitrification rates in mesocosm experiments (Figure 2.1B). When studies conducted in experimental ponds and mesocosm experiments were removed from the analysis, differences

among the remaining wetland types ranged within only one order of magnitude and explained only 2.1% of the variation in denitrification measurements.

Denitrification measurements were found to differ significantly among the various methods used to measure denitrification, but grouping by method explained only 8% of the variation in denitrification rates among measurements. The greatest estimates of denitrification were based on ammonium removal, although denitrification measurements obtained by direct N_2 flux methods—including membrane inlet mass spectrometry (MIMS) and N_2:Ar measurements—also appeared higher than those obtained by acetylene reduction methods (including DEA) and ^{15}N tracer methods. When studies employing ammonium removal were removed from my analysis, grouping by denitrification-measurement method explained only 2.3% of the variation in denitrification measurements (Figure 2.1C). Though average denitrification rates varied significantly among functional groups (Table 2.1), grouping dominant species into functional groups based on their growth forms explained only 2% of the variation in denitrification measurements (Figure 2.1D).

Does "the Effect of Vegetation" on Denitrification Rates Differ among Plant Communities?

When normalized to rates in nearby non-vegetated sediments, denitrification rates in vegetated sediments varied over three orders of magnitude and differed significantly among plant communities. Average denitrification among communities with different dominant species ranged over two orders of magnitude (Figure 2.2A), a reduction from the four orders of magnitude variation observed in non-normalized average denitrification rates. Grouping plant communities by the dominant species accounted for 38% of the variation in the effect of vegetation (Table 2.2). This result was not sensitive to the removal of high-denitrification and low-denitrification plant communities from the analysis. Significant variation remained within

individual community groupings, most notably in *Salix*-dominated communities, for which the greatest average effect of vegetation was observed but for which this effect varied over two orders of magnitude (Figure 2.2A). Vegetation effects on denitrification rates were positive for 12 out of the 16 plant communities included in this analysis, with 9 of these having a positive effect on denitrification that differed significantly from zero. In four plant communities denitrification rates were lower than those in non-vegetated sediments, but none of these differences were statistically significant. The same analysis failed to detect differences among plant communities when dominant species were grouped at either the family ($p = 0.551$, $df = 9, 59$) or genus level ($p = 0.271$, $df = 12, 57$) or by growth form (Table 2.2, Figure 2.2D).

When normalized to denitrification rates in non-vegetated sediments, denitrification rates in vegetated sediments did not differ significantly either among different types of wetland systems or among the various methods used to measure denitrification (Table 2.2). Average vegetation effects ranged within one order of magnitude (Figure 2.2B-C). These variables also explained far less variation in the vegetation effect than did the dominant species in the plant community (Table 2.2). Because this dataset contained little to no overlap in predictor variables among studies, I was unable to compute interaction terms between predictors or to perform the subset analysis described for denitrification rates.

On average, I found that denitrification rates were 55% higher in vegetated sediments, relative to denitrification rates in non-vegetated sediments ($\ln R = 0.4380$, confidence interval = 0.1460-0.7357). Thus the overall "effect of vegetation" was a 1.55 factor increase in denitrification rates.

Discussion

The data set used in this study is the largest currently available on wetland denitrification, bridging extensive literatures in both ecology and environmental engineering. My analysis of this huge dataset established several key points regarding controls on denitrification. First, I found that the type of wetland studied and the method used to measure denitrification was poorly related to variability in denitrification rates. Instead, what mattered most was the presence of vegetation, which caused denitrification to be on average ~50% greater than in nearby non-vegetated sediments. Furthermore, I found that the size of this vegetative effect varied widely with plant community composition as defined by the dominant species, suggesting that the characteristics of dominant species need to be considered in future models of wetland denitrification. In the following discussion, I will explore the implications of my main findings and their ramifications for estimation of denitrification at a landscape level.

The general lack of a systematic effect of methodology on denitrification rates was perhaps the most surprising finding. While I found some influence of methodology on raw denitrification estimates, differences in denitrification between vegetated and adjacent non-vegetated sediments were unrelated to the methods employed. Attempts to predict denitrification across ecosystems have been limited because of uncertainty concerning the comparability and accuracy of different methods, and because many methods can only be used under certain circumstances (Groffman et al. 2006). For example, the technique widely believed to be most accurate, changes in N_2:Ar as measured by membrane inlet mass spectrometry, is technically challenging and can only be used routinely in saturated environments where interference from atmospheric N_2 is minimal (Kana et al. 1994). My analysis suggests that the measurement of denitrification potential using acetylene reduction, which is cheap, technically straightforward

and feasible in most environments, can be used to assess wide scale variation in relative denitrification rates, making broad comparative studies feasible. It also raises the possibility that absolute rates may be estimated from relative measures by calibrating them against more robust and intensive methods, such as change in N_2:Ar, in reference habitats that allow the use of both methods. Future analyses would strongly benefit from a greater availability of studies that estimate denitrification rates for the same plant community using multiple measurement techniques (e.g., Watts and Seitzinger 2000, Hopfensperger et al. 2009). With these data, one could more conclusively assess relative differences in the estimates that various denitrification methods provide, without the confounding influence of differences among plant communities.

A major goal of this study was to determine if vegetation exerted a positive influence on denitrification. While enhancement of denitrification by vegetation had been observed in previous experimental studies, it was not clear that it would be broadly observed across wetland ecosystems. In addition to promoting denitrification by adding organic substrates and introducing oxygen that enhances generation of nitrate from nitrification, plants may inhibit denitrification by flooding the sediments with oxygen or competing with nitrifying and denitrifying bacteria for nitrogenous compounds (Schimel et al. 1989, Kirk and Kronzucker 2005). This competition for nitrogen should be particularly important in wetlands since primary production in these systems is often limited by nitrogen (Howarth 1988, LeBauer and Treseder 2008). That such competition was not sufficient to offset the positive effect of plants on denitrification would seem at first to suggest that nitrifying and denitrifying microbes significantly out-compete the plants for nitrogen. However, other studies have suggested that nitrifiers are in fact poor competitors for ammonium (Verhagen et al. 1994, Verhagen et al. 1995). Alternatively, at the scale of microbes, both nitrogen sufficient and nitrogen deficient

conditions could coexist side by side in soils over relatively small spatial scales. Over the larger scales experienced by plants, however, the actions of denitrifying microbes may result in an overall deficit of nitrogen relative to plant needs, resulting paradoxically in the limitation of primary production by nitrogen in an ecosystem with enough free nitrate to allow substantial denitrification.

My analyses indicate that over a third of the variability in the effect of vegetation can be explained by the dominant species in the plant community. Along with previous studies of pair-wise species comparisons (Caffrey and Kemp 1990) and studies of species invasions (Ehrenfeld 2003, Windham and Ehrenfeld 2003), my findings make a clear case that community composition plays an important role in determining denitrification. That effect may actually be larger than observed here. The identity of the dominant species is an incomplete description of plant community structure, and the composition and biomass of the subdominant community, as well as interactions among dominant and subdominant species, could vary substantially within one of the community categories in ways that could significantly influence denitrification. In any case, community structure should be considered when making landscape scale assessments of denitrification from remote sensing data, or when predicting the effects of sea-level rise or species invasions on denitrification.

One obvious approach for including species composition in future assessments of denitrification would be to estimate the average rates associated with each dominant species using analyses like those conducted here. It might be possible to do so using factorial laboratory experiments under controlled conditions and technically straightforward denitrification methods, such as denitrification potential. While conceptually simple, such an approach may be complicated in practice. Relevant traits like oxygen production, nitrogen demand, and root:shoot

allocation can be very plastic and may vary substantially with ambient conditions in ways that are particular to each species. Moreover, the effects of these important traits on denitrification could vary substantially with abiotic variables, such as hydrologic regime, or sediment and water chemistry. Establishing separate, context-specific relationships to predict denitrification for each community type, even for the limited number of dominant species included in this analysis, could soon prove to be a quixotic effort. Even if successfully obtained, such relationships would not necessarily account for the influence of subdominant species and may therefore fail to replicate real patterns in nature.

An alternative approach would be to identify a few distinct functional groupings of species based on their effects on denitrification. For example, emergent plants, whose leaves are in contact with the atmosphere and whose roots penetrate sediments, would be expected to have very different effects on sediment oxygen relative to submerged or floating plants that have little or no rooting structure. Consequently, functional groupings based on morphology are often expected to explain variation in the influence of plant communities on sediment processes like denitrification (Keddy 1992, Boutin and Keddy 1993). Contrary to this expectation, I found that morphological groupings of dominant species did not explain significant variation in raw denitrification rates or in the influence of plant communities on denitrification. This result is perhaps not surprising given that the highest and lowest denitrification rates observed in this study occur in emergent plant communities dominated by species in Poales (Figure 2.1A), while plant communities dominated by different species in the genus *Typha* are associated with low, intermediate, and high effects on denitrification rates (Figure 2.2A). Furthermore, vegetation effects were not found to differ significantly when measurements were grouped by either the family or the genus of the dominant plant in the community. These results are consistent with

previous assessments that conventional functional or taxonomic groupings are relatively less useful in predicting rates of ecosystem processes than is information about plant community composition or functional trait composition (Eviner and Chapin III 2003, Wright et al. 2006).

A third approach is to describe the plant community along several continuous functional trait axes that may be relevant to denitrification, rather than by the dominant species (Eviner and Chapin III 2003, Suding et al. 2008). These "aggregate functional traits" would be those likely to influence denitrification through specific effects on oxygen concentrations, nitrogen availability or labile carbon in associated sediments. A list of such traits could include above- or belowground biomass, rooting area or depth, elemental composition of tissues, litter quality, etc. When applied at the community level, a trait based approach promises to address the effect of the dominant species on denitrification while accommodating for plasticity within species and for some of the influence of subdominant species. By addressing only a few relevant functional traits at a time, it also simplifies the task of characterizing the community in ways that are relevant to denitrification. Moreover, determining how specific traits relate to denitrification can reveal which critical factors seem to be the most important determinants of this process.

Although I wanted to explore the possibility of using functional traits to predict denitrification on a preliminary basis, most denitrification-relevant traits were not reported consistently enough among taxa to be of use in my meta-analysis. Wetland plants also tend to be underrepresented in online plant trait databases (Wright et al. 2004, Kleyer et al. 2008, Kattge et al. 2011). Nonetheless, I was able to find information on "average shoot height" for 16 of the taxa in my analysis belonging to the order Poales in the United States Department of Agriculture Plants Database (USDA 2014). Over some time scale, I expect that average shoot height should be correlated to nutrient demand and photosynthetic rate, which may be relevant for oxygen and

nitrogen levels in associated sediments. Below a certain value, shoot height should be positively related to denitrification due to the effects of diel oxygenation of sediments on denitrification (Figure 2.3A). Above a certain shoot height one may expect sediment oxygenation will be enough to inhibit denitrification, or that plants will sequester enough nitrogen that they effectively compete with nitrifiers and denitrifiers. Consequently, I expected a unimodal relationship between denitrification and shoot height. When I plotted weighted average denitrification rates calculated in my analysis to average shoot heights from the USDA database, I did observe a general trend of maximum denitrification rates occurring in communities dominated by species of intermediate height (Figure 2.3B); this pattern became even clearer when I removed the extremely high denitrification measurements obtained in *Oryza sativa* and *Spartina alterniflora* communities (Figure 2.3C).

Clearly, much more information is required in order to understand how various other plant traits, as well as sediment properties and site history, interact to influence the effects of plant communities on denitrification. However, the patterns observed here suggest that a functional-trait approach may offer a promising way forward, particularly as the characterizations of wetland plant species that are already underway continue to become available. Functional-trait variables offer many of the same advantages as abiotic factors in that they are relatively easy to quantify using established methods and can be generalizable, in this case according to physiological trade-offs for plants that have been shown to operate independently of plant functional type, growth form, or environment (Wright et al. 2004). A focus on key plant traits offers a general and, therefore, flexible way to link plant community composition and structure to important ecosystem process such as denitrification. Such

approaches will become increasingly important as plant community distributions and compositions are expected to change in the future.

Table 2.1: Summary of Q-tests of heterogeneity for each of the three grouping variables, performed on weighted average denitrification rates. P-values were estimated from bootstrapping, using 999 iterations. Results significant at $\alpha = 0.05$ are shown in bold.

Source of Heterogeneity	Plant Community		Wetland System		Method		Functional Group	
	Q	df	Q	Df	Q	df	Q	df
Among	4865	37	2533	7	1479	10	174	4
Within	12773	355	15330	402	16471	405	7899	382
Total	17637	392	17863	409	17950	415	8073	386
p		**0.004**		**0.004**		**0.041**		**0.043**
% Variation Explained		28		14*		8†		2

* Percent variation explained is equal to 2.1% when studies conducted in experimental estuarine ponds and constructed wetlands are excluded from analysis.

† Percent variation explained is equal to 2.3% when measurements obtained by ammonium removal are excluded from analysis.

Table 2.2: Summary of Q-tests of heterogeneity for each of the three grouping variables, performed on log response ratios of denitrification in vegetated and non-vegetated sediments. P-values were estimated from bootstrapping, using 999 iterations. Results significant at $\alpha = 0.05$ are shown in bold.

Source of Heterogeneity	Plant Community		Wetland System		Method		Functional Group	
	Q	df	Q	Df	Q	df	Q	df
Among	81	15	16	4	23	7	9	3
Within	134	39	149	59	144	56	84	55
Total	214	54	165	63	166	63	93	58
p		**0.04**		0.187		0.284		0.207
% Variation Explained		38		10		14		10

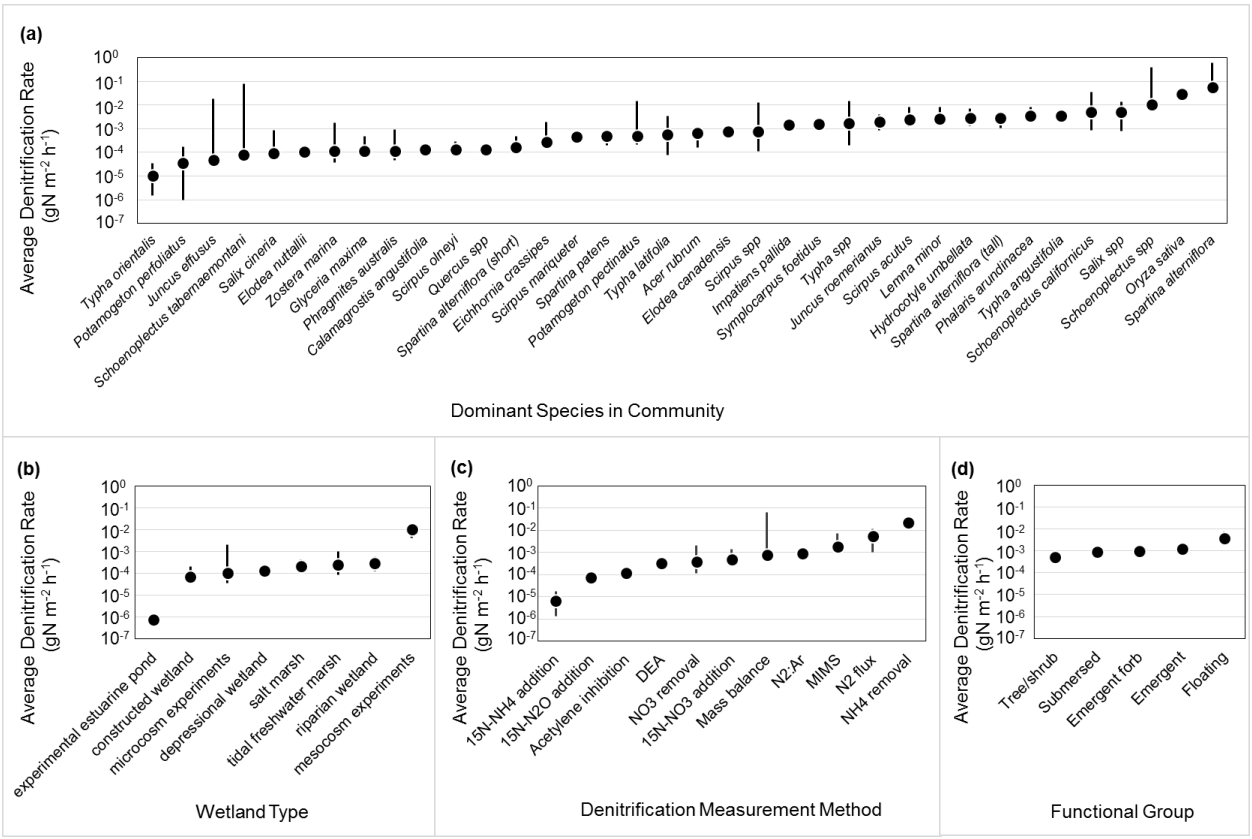

Figure 2.1: Weighted average denitrification rates among (a) dominant species in the wetland plant community, (b) types of wetland in which the studies were conducted, (c) methods used to measure denitrification rates (DEA = denitrification enzyme activity, MIMS = membrane inlet mass spectroscopy), and (d) functional groups based on growth forms. Average rates are plotted on a $\log_{10}$ scale. Error bars show bootstrapped confidence intervals, generated from 999 sampling iterations.

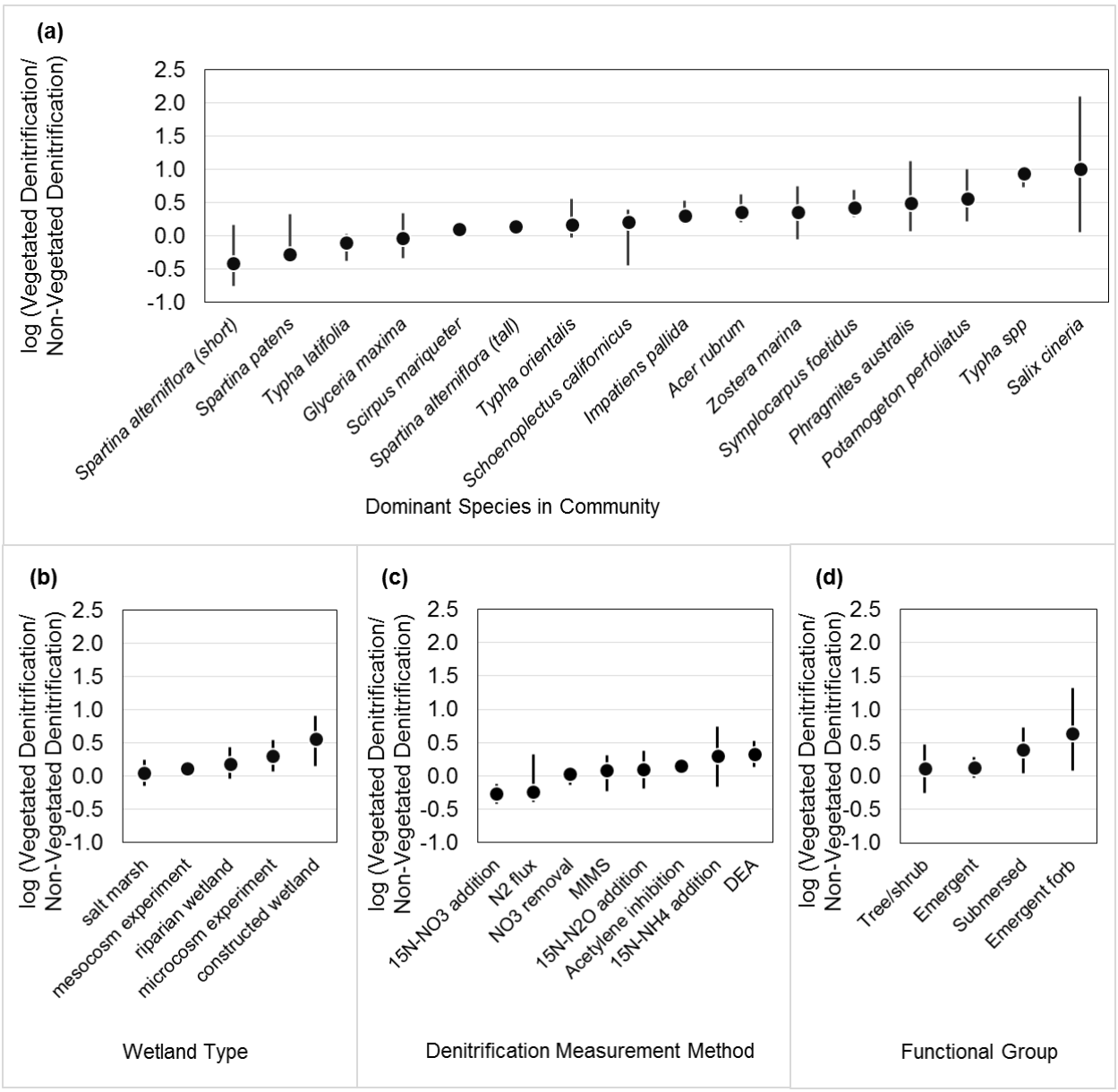

Figure 2.2: Denitrification rates in vegetated sediments, normalized as a log response relative to denitrification rates in paired non-vegetated plots or treatments. Weighted means are grouped by (a) the dominant species in the wetland plant community, (b) the type of wetland system in which the studies were conducted, (c) measurements used to measure denitrification rates (DEA = denitrification enzyme activity, MIMS = membrane inlet mass spectroscopy), and (d) functional groups based on growth forms. Error bars show bootstrapped confidence intervals, generated from 999 sampling iterations.

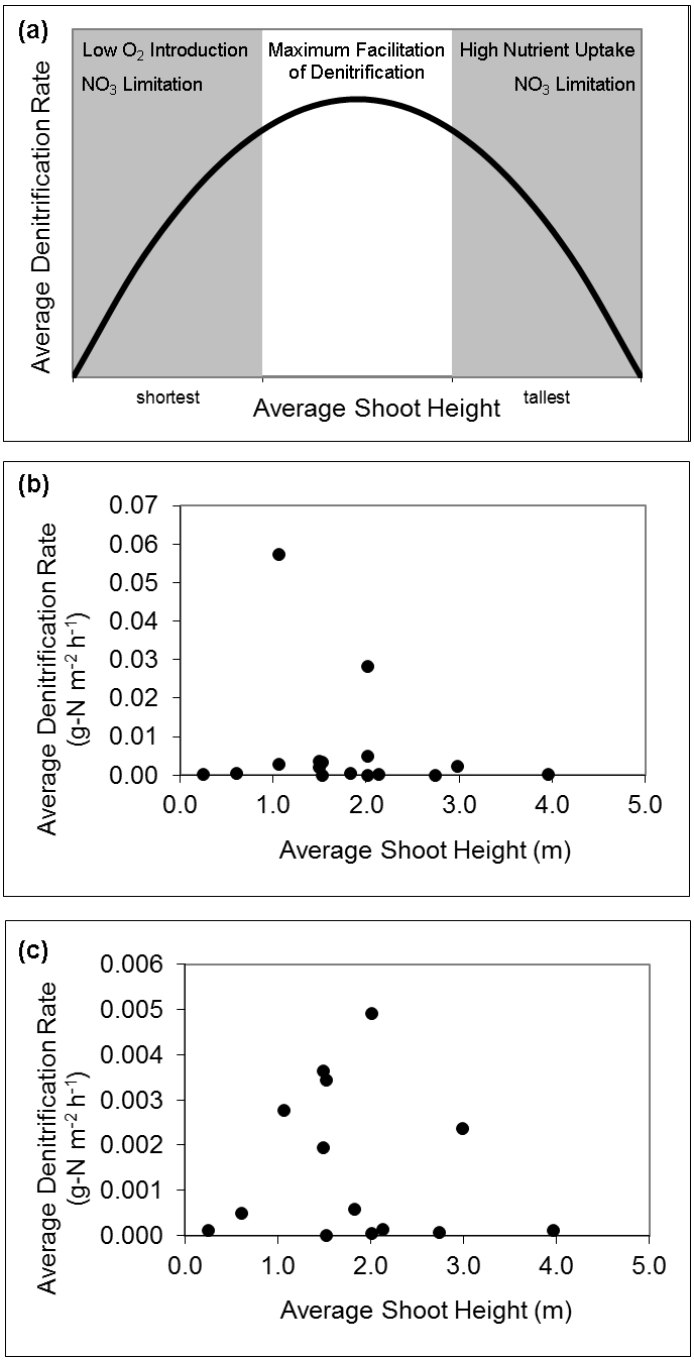

Figure 2.3: (a) Denitrification may be expected to vary with plant size such that small plants introduce insufficient oxygen to sediments to facilitate production of nitrate, and larger plants compete with denitrifiers for nitrate, both limiting denitrification rates. Maximum rates of denitrification would occur at intermediate plant size. (b) Among emergent plant communities, maximum rates of denitrification are observed in communities dominated by 1.0-2.0 m plants. (c) When the highest rates in *Spartina alterniflora* (1.0 m) and *Oryza sativa* communities (2.0 m) are excluded, the pattern persists. Data for average shoot height for grasses, sedges, and rushes were obtained from the USDA database.

Chapter 3

Plant traits predict the influence of wetland plants on sediment oxygen and denitrification potential

Abstract

Human activities have altered major biogeochemical cycles and the diversity and distribution of species on a global scale, yet our ability to quantify the effects that changes in ecological communities have on ecosystem processes lags far behind management needs. Specifically, microbial denitrification represents an ecosystem service on which human societies depend for nitrogen removal and maintenance of water quality. Denitrification is known to respond to differences in the characteristics of wetland plant communities but remains a notoriously difficult process to measure and predict. Here I examine the influence of the dominant salt-marsh grass *Spartina alterniflora* on sediment oxygenation and microbial nitrogen-cycling processes in replicated experimental mesocosms. I apply a novel combination of oxygen-sensitive planar optode methods, microbial process assays, measurements of sediment chemistry, and quantification of plant traits to determine associations between characteristics of wetland vegetation and the potential for wetland sediments to remove nitrogen. Denitrification potentials were found to correlate strongly to plant traits that enhance sediment aeration, and thus facilitate coupled nitrification-denitrification. My results suggest that knowledge of the trait composition of wetland plant communities may simplify the task of predicting denitrification potential of wetland ecosystems. Trait-process associations offer one promising approach to the challenge of predicting rates of ecosystem processes such as denitrification in the face of rapid changes in wetland plant communities due to land development, sea-level rise, and species invasions.

Introduction

Human activities have profoundly altered the diversity and distribution of species and ecological communities on a global scale (Chapin III et al. 2000). Changes in the diversity and structure of ecological communities are known to alter provisioning of ecosystem services on which we depend (e.g., storm and flood protection, clean water, food resources, recreation and aesthetics) (Chapin III et al. 2000, Loreau et al. 2001, Hooper et al. 2005). However, our ability to quantify and predict how specific changes in communities, especially those that result in novel or "no analog" communities, will alter ecosystem services lags far behind management needs. One promising approach to this problem involves using traits of organisms within communities to mechanistically link community structure with the effects those communities have on specific ecosystem properties or processes (Chapter 1, Lavorel and Garnier 2002, McGill et al. 2006). Here I use "trait" to refer to any measurable characteristic of a plant or plant community that may affect specific ecosystem processes; this usage is synonymous with the definition of "effect trait" used by Lavorel and colleagues to link plant communities to the effects they have on ecosystem processes and services (Lavorel and Garnier 2002, Lavorel et al. 2011).

In many areas worldwide, humans have doubled the amount of biologically available nitrogen entering watersheds, resulting in severe water-quality degradation in aquatic and coastal systems (Vitousek et al. 1997, Millennium Ecosystem Assessment 2005). Wetland ecosystems are hotspots of microbial denitrification, a valuable ecosystem service that permanently removes nitrogen from aquatic systems to the atmosphere as inert nitrogen gas (Zedler 2003, Hinga et al. 2005). Understanding the characteristics of wetland ecosystems that promote high rates of denitrification is essential both in valuing current wetland resources and in managing future water quality in rapidly changing coastal and aquatic systems. Whereas the ability to rapidly

assess the nitrogen-removal capacity of wetlands is critical to this endeavor, denitrification itself is a notoriously difficult process to measure due to the challenges associated with measuring tiny fluxes of N_2 gas against an 80% atmospheric background (Groffman et al. 2006). Constructing models to predict denitrification is also difficult because the physical, chemical, and biological characteristics of ecosystems that determine rates of nitrogen removal are extremely diverse (Boyer et al. 2006, Seitzinger 2008, Groffman et al. 2009). For all of these reasons, denitrification remains one of the least well quantified terms in the global nitrogen cycle despite its ecological and economic importance (Schlesinger 2009).

Wetland vegetation is known to alter sediment chemistry in ways that influence denitrification rates (Chapter 1, Sherr and Payne 1978, Weisner et al. 1994, Bachand and Horne 2000). Denitrifying microbes are heterotrophs that require organic carbon as an energy source and nitrate as an oxidizing agent. When oxygen is available in their environment, denitrifiers will favor it as an electron acceptor as it yields greater energy; only when oxygen becomes depleted will they switch to nitrate as a terminal electron acceptor. However, in saturated systems like wetlands, oxygen is rarely abundant and much of the available nitrogen is in the reduced form of ammonium. In these systems, denitrifiers rely on microbial nitrification to oxidize ammonium into nitrate (see Figure 1.2). As a result, denitrification rates are maximized by processes that create spatial and temporal variation in sediment oxygen, producing a scenario in which enough oxygen is available to favor nitrification of ammonium to nitrate and in which hypoxic or anoxic conditions cause denitrifiers to use nitrate as an electron acceptor. Therefore, highest denitrification rates are often observed in systems that experience either spatial or temporal variation in oxygen availability, such that sufficient oxygen (Seitzinger et al. 2006).

Because denitrification potential is maximized by variation in oxygen conditions, I would expect plant traits that increase spatial or temporal variation in oxygen availability to enhance rates of coupled nitrification-denitrification (Figure 1.3). These traits could include belowground characteristics that would facilitate delivery of oxygen from the atmosphere to the rhizosphere or that would lead to spatial variation in oxygen delivery such as total root mass or maximum rhizome or root width. Oxidized areas surrounding the roots would promote the production of nitrate via microbial nitrification, which could then diffuse into adjacent anoxic areas of the sediment and be denitrified (Figure 1.2). Traits could also include those related to photosynthesis, or traits that are commonly related to photosynthetic potential including leaf nitrogen and specific leaf area, which would increase diurnal variation in oxygen production (Wright et al. 2004, Reich et al. 2007). When plants are photosynthetically active during the day, oxygen delivery to the sediments would promote nitrification, and nitrate produced during the day could undergo denitrification at night when root and microbial respiration results in depletion of oxygen. Such diel cycles in sediment oxygen have been observed for a variety of both submerged and emergent wetland plants (Sand-Jensen et al. 1982, Armstrong and Armstrong 1990, Caffrey and Kemp 1991, Brix et al. 1992). Though this chapter focuses on the influence of wetland plants on sediment oxygen availability and denitrification potential, similar trait-based approaches could address other pathways through which plants may influence sediment chemistry and denitrification (Figure 1.3).

I examined the influence of common salt marsh dominant *Spartina alterniflora* on sediment oxygen dynamics and nitrogen cycling processes in experimental mesocosms. Using oxygen-sensitive photographic films and direct measurements of sediment oxygen concentrations, I investigated potential relationships among key plant traits, spatial and temporal

variation in sediment oxygen availability, and microbial process rates. For the multiple reasons listed earlier, denitrification offers a powerful test of a trait-based predictive approach. If successful, predictions of denitrification potential using relatively easily quantifiable plant traits would greatly simplify the considerable challenges of understanding current mechanisms that determine sediment denitrification rates and predicting the potential for future wetland ecosystems to remove nitrogen.

Methods

Experimental Design

Plugs of sediment were collected from two salt marshes on the northern coast of Long Island, NY, Flax Pond and West Meadow Creek (40.965249, -73.133750 and 40.936468, -73.143173, respectively) in July 2013. The sampling time was chosen to correspond to peak biomass of the vegetation when the effect of plants was expected to be readily detectable, but prior to the onset of seed production, when plants begin reallocating resources to reproduction and dormancy and become less physiologically active. At each site, I randomly collected two plugs from mudflats containing no vegetation, two plugs from the marsh edge containing tall-form *Spartina alterniflora*, and two plugs from the marsh platform containing short-form *Spartina alterniflora*. I transferred the sediment plugs to PVC mesocosms (20 cm wide x 30 cm tall x 10 cm deep) in the field under deoxygenated site water and installed a deoxygenated PVC porewater equilibrator along one side (Hesslein 1976). The fronts of the mesocosms were each sealed with a transparent plexiglass panel containing the oxygen-sensitive optode film. Mesocosms were returned to the Life Sciences Greenhouse at Stony Brook University within two hours of initial collection and placed in rigid photographic darkroom structures in a growth

chamber at 25°C, with the vegetation and surface sediments exposed to saturating light conditions on a 16:8 hour light-dark cycle.

Darkroom structures consisted of a rigid steel frame to hold mesocosms, cameras, and LED light fixtures in place under light-proof black cloth, while allowing emergent plant structures and the sediment surface to be exposed to light. Within the darkroom structures, I affixed LED lights that transmitted at 390 nm (the excitation wavelength of our O_2-sensitive dye) at an angle of 45° relative to the optode film and fitted with a diffuser and 475 nm short-pass filter. Photos were acquired using Canon Powershot A480 point-and-shoot cameras that I modified by removing the infrared filter and fitting with an OG-530 long-pass filter. Raw images were captured every 5 minutes for 36 hours using an automatic image-capture program CHDK (Canon Hack Development Kit).

Mesocosms containing the various sediment treatments were allowed to acclimate under growth chamber conditions for three days, and sediment O_2 data were collected via photography of the optode films for three days following the initial acclimation period. At the end of the experimental period, plant traits, equilibrated and extractable sediment porewater nutrients, and microbial process rates were measured.

Preparation of Oxygen-Sensitive Optode Films

Methods for preparing and calibrating optode films were adopted from Larsen et al. (2011) following the modifications employed by Forbes et al. (2014). Optode films consisted of a 20 cm x 15 cm polyethylene film coated with a layer of oxygen-sensitive and reference dyes and a second layer of black-carbon coating to control for contrast in sediment color. The oxygen-sensitive dye I used was Pt (II) meso-tetra (pentafluorophenyl) porphrine, or PtTFPP, which fluoresces at 650 nm. It is an oxygen-quenched fluorophore, meaning that it fluoresces

more brightly when oxygen is absent and less brightly as oxygen increases. Macrolex Yellow 10GN, which fluoresces at 480 nm and does not respond to oxygen, was used as a reference dye to control for uneven distribution of dye mixture on the optode surface. Films were first affixed to a water-coated PVC block, taped securely, and placed on a perfectly level surface in a fume hood. A mixture of 1% (wt/wt) oxygen-sensitive PtTFPP, 2% (wt/wt) reference fluorophore Macrolex Yellow 10GN, and 4% (wt/wt) polystyrene beads were dissolved in chloroform and applied to the films. When the fluorophore layer was completely dry, I added a second layer of black silicone sealant dissolved in hexane. When the second layer was completely dry, optodes were removed from the PVC block and affixed over immersion oil to the transparent plexiglass front panels of the mesocosms with several layers of black electrical tape.

For initial calibrations of the optode films, fully assembled mesocosms were filled with distilled water and randomly placed in the darkroom structures. I bubbled the mesocosms with air to achieve maximum oxygen saturation, measured oxygen using a dissolved oxygen meter, and captured five images for later calibration. Subsequent oxygen-saturation points were obtained by bubbling with prepure nitrogen gas, and a near-zero point was achieved with the addition of several grams of sodium sulfite. No fewer than eight oxygen-saturation points were collected for calibration of each optode film. Oxygen signals were extracted from raw images in ImageJ as the fluorescence of the red channel (O_2-sensitive signal) normalized to the fluorescence of the green channel (the reference-dye signal) as (Red-Green)/Green (Schneider et al. 2012). I fit a calibration plot for each optode to a modified Stern-Volmer standard curve

[3.1] $$\frac{R}{R_0} = \alpha + \left[(1-\alpha) \times \left(\frac{1}{1 + K_{SV} \times O_2}\right)\right]$$

where R/R_0 is the pixel intensity at a given O_2 concentration divided by the pixel intensity at zero, α represents the non-quenchable fraction of the optode, K_{SV} is the Stern-Volmer coefficient, and O_2 is the known oxygen saturation obtained by the dissolved oxygen meter.

Temporal variability in oxygenation for each mesocosm was estimated as the difference in mean oxygen saturation over the optode surface between light and dark conditions in the growth chamber. Spatial variability was estimated under light and dark conditions as the standard deviation of oxygen saturation over the optode surface at a given time point.

Sediment Chemistry

During the experiment, porewater samples were collected every 12 hours using syringe-vacuum porewater sippers to monitor any changes in dissolved nutrients and salinity (Kolker 2005). Prior to experiments, I prepared PVC porewater equilibrators with duplicate 20 ml sampling wells spaced vertically at 3 cm intervals. Equilibrators were filled with deionized water, covered with a Spectr-Por cellulose membrane, and deoxygenated overnight by bubbling with nitrogen gas prior to installation in mesocosms (Hesslein 1976). The equilibrators were undisturbed for six days, three days of acclimation prior to the experiment and during the three days the experiment was running. Upon completion of the experiments, porewater was extracted by syringe from PVC porewater equilibrators and acidified until analysis of ammonium, nitrate, phosphate, and salinity using standard methods (Jones 1984, Parsons et al. 1984b, Wetzel and Likens 2000). I also collected a subfraction of equilibrated water in each mesocosm from 6 and 12 cm below the sediment surface, corresponding to the top and bottom of the optode film, and shipped these samples in gas-tight glass vials to Woods Hole Marine Laboratory for analysis of N_2:Ar and O_2:Ar using membrane inlet mass spectroscopy (MIMS) (Kana et al. 1994).

Sediment subsamples were collected at the end of the experiment from 6 and 12 cm below the sediment surface, extracted with 2N potassium chloride solution, and analyzed for ammonium, nitrate, and phosphate following the same methods used for porewater samples. I also used sediment subsamples at these depths for determination of moisture content (change in mass after drying at 70°C for a minimum of 24 hours) and total carbon and nitrogen content using a Perkin Elmer Series II CHNS Analyzer. Sediment composition was measured at 3 cm intervals as sand content after wet-sieving through a 63 µm mesh, drying at 70ºC for at least 24 hours, and calculating mass of sand relative to the total mass of the sample.

Microbial Processes

At the end of the experiment, sediment samples were collected from each mesocosm at 6 and 12 cm below the sediment surface for determination of denitrification rates using denitrification enzyme activity (DEA) measurements, nitrification measurements, and net mineralization-immobilization measurements. All microbial-process measurements began within 24 hours of initial sediment sampling. For DEAs, I amended a 5 g subsample of sediment with potassium nitrate, glucose, chloramphenicol, and acetylene gas under anaerobic conditions for 90 minutes (Smith and Tiedje 1979b). Headspace samples were collected at 30 and 90 minutes, stored in pre-evacuated gas-tight vials, and analyzed for N_2O concentration on a Hewlett Packard 5890 gas chromatograph, equipped with a ^{63}Ni electron-capture detector and a 2.5 m x 0.318 cm stainless steel column packed with Poropak Q (80/100 mesh); the column was operated at 40ºC with a detector temperature of 350ºC and an ultrahigh purity N_2 carrier gas at a flow rate of 30 ml/min. The denitrification potential of the microbial community was calculated from the change in concentration of N_2O during the incubation time using the equation:

[3.2] $$denitrification\ potential\ (\mu gN\ g^{-1}h^{-1}) = \frac{v\ (N_2O_{T1} - N_2O_{T0})}{MT}$$

where *v* is the volume of the headspace and porespace, *M* is the mass of the sediment in the incubation, and *T* is the incubation time (Smith and Tiedje 1979a, Watts and Seitzinger 2000). This method provides an estimate of the maximum potential of the microbial community to perform denitrification and is therefore a useful variable for determining differences between experimental treatments or locations, but it should not be interpreted as an exact measurement of N_2 flux from sediments (Groffman et al. 2006).

Nitrification and mineralization assays were performed using three replicate 2 g sediment subsamples, also collected from 6 and 12 cm depths from each mesocosm. For each measurement, one "initial" 2 g subsample was immediately used to determine initial ammonium content using extraction methods described above, one "blocked" 2 g subsample was amended with nitrification inhibitor nitrapyrin in a 10 mg/L dimethyl sulfoxide (DMSO) solution, and one "control" subsample was amended with DMSO only (Hall 1984, Bédard and Knowles 1989, Strauss and Lamberti 2000). "Blocked" and "control" sediments were incubated in 20 mL site-collected water for 48 hours in the dark on a shaker table at 20-25º C. At the end of the incubation period, I added 20 mL of 2N potassium chloride solution and measured extractable ammonium concentrations as described above. I determined gross nitrification from the difference in final ammonium concentrations between "blocked" and "control" incubations, controlling for dilution and incubation time, in the following equation:

[3.3] $$gross\ nitrification\ (\mu gN\ cm^{-3}h^{-1}) = \frac{0.2([NH_4{-}N_{blocked}] - [NH_4{-}N_{control}])}{VT}$$

where *V* is the volume of sediment, *T* is the incubation time, and 0.2 is a constant to account for dilution of the nutrient extraction (Starry et al. 2005). Net mineralization/immobilization was determined from the difference between "control" incubations and "initial" measurements of extractable ammonium:

[3.4] $$net\ mineralization\ (\mu gN\ cm^{-3}h^{-1}) = \frac{0.2([NH_4{-}N_{control}] - [NH_4{-}N_{initial}])}{VT}$$

Positive values for mineralization indicate net mineralization, whereas negative values indicate net immobilization (Starry et al. 2005).

Vegetation characteristics

Duplicate sediment cores were collected from each mesocosm using a bulb planter (5 cm diameter, ~20 cm length or to bottom of root zone) and PVC coring device and kept frozen at -20°C until determination of total root and rhizome mass at 3 cm intervals by wet sieving onto a 2000 µm mesh filter, removing non-organic fragments by hand, and determining mass after drying at 70ºC for at least 24 hours. For each 3 cm subsection that contained root material, the maximum width of the root or rhizome (hereafter referred to as "rhizome width" for simplicity) was also recorded. I measured total stem density and aboveground biomass for each mesocosm, as well as the stem height of each plant within each mesocosm. For each stem, I randomly selected two leaves for determination of leaf width and thickness, specific leaf area (area of leaf per gram of dry mass), and carbon and nitrogen content using a Perkin Elmer Series II CHNS Analyzer. For non-vegetated treatments, the majority of plant trait data are not available; out of necessity, models using these variables had 4 fewer observations than those for which non-vegetated treatments were included (e.g., root mass and stem density for which values of 0 or near-0 were logical).

Statistical analysis

All data analysis was performed in R *version 3.0.2* (R Core Team 2012). I first computed Pearson correlations among plant traits and the two sediment-chemistry variables I expected plants would influence (i.e., oxygen enrichment and extractable ammonium content) at the scale of the whole mesocosm. I avoided including redundant plant traits ($r \geq 0.50$) in subsequent

models used to predict responses in sediment chemistry and rates of microbial processes. Initial general linear models (GLMs) were constructed to predict oxygen and ammonium, initially containing the microsite treatment (i.e., marsh edge, marsh platform) as a categorical predictor and the plant trait most correlated to oxygen or ammonium as continuous predictors. Plant traits that were redundant but found to be useful predictors were evaluated in separate initial models. Predictors that were not found to be significantly related to oxygen or ammonium ($\alpha = 0.10$) were eliminated from models in a stepwise fashion. At each step of elimination, the fit of the previous and resulting model were compared. Residuals of the best model were inspected for normality using a Kolmogorov-Smirnov Lilliefors test.

I next constructed GLMs to predict microbial process rates (i.e., mineralization, nitrification, and denitrification and N_2 enrichment) using extractable ammonium and oxygen enrichment as continuous predictors using the methods described above. Denitrification rates obtained from DEA measurements were normalized to carbon content of sediments and $\log_{10}$ transformed prior to analysis to achieve normal distributions of model residuals. N_2 and O_2 measurements in equilibrated sediment porewater, obtained from MIMS measurements, were expressed as an enrichment relative to atmosphere-equilibrated site water. Plant traits that were found to be best predictors of sediment oxygen and ammonium were then used in general linear models to predict denitrification rates, and fits of best models were compared to those including ammonium and oxygen as predictors.

R code used to perform all statistical tests, the output of all statistical comparisons performed, and code used to generate figures is reported in Appendix B.

Results

Many plant traits included in this analysis were highly correlated (Table 1). Total aboveground biomass was positively correlated with both stem density and root width at $\alpha = 0.05$, root width was negatively correlated with specific leaf area (SLA) at $\alpha = 0.10$, and maximum stem height was negatively correlated with the ratio of carbon to nitrogen in leaf tissue at $\alpha = 0.05$. Several additional trait combinations were correlated at marginally non-significant α levels of 0.10-0.30 (see Table 3.1). Traits that best predicted O_2 enrichment in equilibrated sediment porewater were root width and maximum stem height (Figure 3.1), which were found to be redundant and thus considered in separate predictive models (Table 3.1). SLA was the best predictor of extractable ammonium content of sediments (Figure 3.1).

Net mineralization/immobilization rates indicated that microbial immobilization was occurring across all treatments, and that immobilization rates responded strongly to extractable ammonium concentrations in sediments (Figure 3.2A). Nitrification rates and denitrification potentials (DEAs normalized to sediment carbon) depended on the interaction between sediment oxygen and sediment ammonium concentrations (Figure 3.2B and 3.2C). No combination of sediment variables was able to predict net N_2 enrichment in sediment porewater. In all cases, I observed no significant effect of the microsite treatment on the relationship between plant traits and sediment chemistry, nor any interaction between microsite treatments and plant traits; thus, microsite and its interaction terms were eliminated from final models.

While models including ammonium and oxygen concentrations provided the best fit to observed denitrification potentials, comparable fits could also be achieved with univariate models including only maximum rhizome width or maximum stem height of plants in mesocosms (Table 3.2), traits which were also strong predictors of sediment oxygen

concentrations (Figure 3.1). Denitrification potentials were positively associated with both rhizome width and stem height (Figure 3.3A and 3.3B). Net N_2 enrichment measured with MIMS did not correlate with denitrification potentials ($r = 0.02$, $p = 0.98$) and responded differently to vegetation treatments, with higher N_2 enrichment measurements observed in vegetated mesocosms relative to non-vegetated mesocosms. The best predictor of net N_2 enrichment was the density of plant stems in mesocosms, with the lowest values of N_2 enrichment occurring in mesocosms with highest stem densities (Figure 3.3C).

Discussion

I found that the same plant traits that best predicted sediment oxygen enrichment, root width and maximum stem height (Figure 3.1), were also successful in predicting variation in denitrification rates among experimental mesocosms (Table 3.2). Moreover, models including only univariate relationships with rhizome width or maximum stem height were nearly as successful in explaining variation in denitrification potentials, 58% and 49% respectively, as models parameterized with both sediment oxygen and ammonium availability, 77% (Table 3.2).

Sediment ammonium availability was predictably a key variable in determining the rates of all of nitrogen cycling processes measured in this study (Figure 3.2). That I observed high rates of microbial immobilization in all mesocosms is not surprising, given that the mean ratio of carbon to nitrogen in *S. alterniflora* leaves was 36 (± 7) in this study, which indicated that leaf litter alone was highly unlikely to meet the nitrogen requirements of typical decomposing microbes (Goldman et al. 1987). However, both nitrification and denitrification were also dependent on sediment oxygen availability (Figure 3.2B and 3.2C), suggesting that rates of denitrification are as dependent on the production of nitrate via nitrification as on total availability of mineralized nitrogen in this system. This observation lends considerable support

to my hypothesis that plant traits influencing oxygen delivery to sediments could play a key role in determining rates of microbial denitrification (Figure 1.3).

Contrary to my expectations (Figure 1.3), measurements of N_2 enrichment in sediment porewater did not correlate well with denitrification potentials. While measurements of N_2 enrichment relative to argon using membrane inlet mass spectroscopy (MIMS) methods indicated that net denitrification occurred in all treatment groups, N_2 enrichment followed the opposite patterns observed in measurements of denitrification potential using denitrification enzyme activity (DEA) assays. Denitrification potentials responded positively to plant traits that enhanced oxygenation of sediments (Figure 3.3A and 3.3B), whereas N_2 concentrations in sediment porewater decreased with increasing stem density (Figure 3.3C). Two possible mechanisms could explain this discrepancy. Higher rates of nitrogen fixation in vegetated plots could have removed N_2 from porewater, resulting in lower apparent net denitrification. This mechanism seems unlikely in this specific study because oxygen, which inhibits nitrogen fixation by free living heterotrophs, was higher in vegetated mesocosms; furthermore, fixation should decrease with increasing ammonium availability, but N_2 concentrations were unrelated to sediment ammonium concentrations. The more likely explanation is that plant stems provided a conduit that facilitated equilibration of N_2 produced from denitrification with the atmosphere. Plant ventilation of sediments would explain why N_2 in sediment porewater decreased with increasing stem density, causing N_2:Ar ratios to more closely resemble atmosphere-equilibrated water (Figure 3.3C). If true, this mechanism would represent a potential pathway for expediting the flux of N_2 from sediments. Further experiments involving direct measurements of nitrogen fixation or ^{15}N tracers would be needed to fully resolve the fate of N_2 produced by denitrification in vegetated marsh sediments.

Wetland plant communities worldwide are undergoing rapid transitions due to land development, sea-level rise, and species invasions (Zedler and Kercher 2005). Acclimation of current communities and changes in the species composition of communities are known to alter sediment chemistry and denitrification rates (Ehrenfeld 2003, Craft et al. 2008). To the extent that potential responses of plant traits to various management scenarios are predictable, our analysis offers hope that the impacts of community-level changes on denitrification potentials could also be predicted using trait-based models. Further investigation of associations between plant traits and sediment microbial processes is clearly needed to develop more general trait-based models that would apply to multiple plant species and abiotic contexts.

Encouragingly, relationships between plant traits influencing sediment oxygen and resulting denitrification potentials were observed despite considerable background variation in sediment ammonium among mesocosms in this study (Figure 3.3). This consistency may simply be a result of an extreme dependence of denitrification on coupled nitrification in the particularly anoxic sediments of our confined mesocosms. Alternatively, it may be that covariance of plant traits arising from economic trade-offs described elsewhere result in plant-trait relationships that remain robust to differences in sediment nutrient context (Wright et al. 2004, Freschet et al. 2010). For example, if opportunistic traits associated with nutrient uptake also enhance sediment oxygenation (e.g., root width, stem height), then one may expect these traits to consistently covary with higher rates of microbial nitrogen removal. Further investigation of trait associations with microbial rates across a range of nutrient-loading conditions would allow one to test this hypothesis. If true, this result leads to the intriguing possibility of building general models to predict nitrogen removal with simple measures of plant-community characteristics,

while eliminating the need to painstakingly establish trait-process relationships for every plant species of interest.

My results indicate that trait-based models could greatly simplify our ability to predict processes as complicated as denitrification. Both plant-trait data (Kattge et al. 2011) and tools to incorporate trait data into predictive ecosystem models (LeBauer et al. 2013) are increasingly available in public-access formats. The field of ecology is now well placed to address critical management decisions concerning both the conservation of functional diversity in ecological communities and the maintenance of ecosystem services on which human societies depend. Coupling characteristics of ecological communities to the various effects that these communities have on key ecosystem processes is a necessary first step in this endeavor.

Table 3.1: Correlations among plant traits included in analyses. Values above the diagonal correspond to Pearson's correlation coefficient; values below the diagonal correspond to p-values (n = 8). (• Significant at α = 0.10, * Significant at α = 0.05, ** Significant at α = 0.01, AG = aboveground, SLA = specific leaf area)

	AG biomass ($g\ m^{-2}$)	Stem density (m^{-2})	Root mass ($g\ m^{-2}$)	Root width (mm)	Stem height (cm)	SLA ($cm^2 g^{-1}$)	Leaf C:N
AG biomass ($g\ m^{-2}$)	1	** 0.75	0.12	* 0.77	0.61	-0.50	-0.44
Stem density (m^{-2})	** 0.0054	1	0.19	-0.42	0.11	0.58	-0.17
Root mass ($g\ m^{-2}$)	0.7095	0.5448	1	-0.05	0.36	0.45	-0.02
Root width (mm)	* 0.0253	0.3013	0.9006	1	0.56	• -0.63	-0.27
Stem height (cm)	0.1059	0.8029	0.3803	0.1466	1	0.04	* -0.73
SLA ($cm^2 g^{-1}$)	0.2076	0.1297	0.2600	• 0.0919	0.9300	1	-0.08
Leaf C:N	0.2746	0.6810	0.9648	0.5191	* 0.0389	0.8432	1

Table 3.2: Alternate general linear models to predict denitrification using (1) sediment ammonium and oxygen concentrations, (2) rhizome width, and (3) maximum stem height. Denitrification potentials were normalized to sediment carbon and $\log_{10}$ transformed prior to analysis.

	Model 1 NH_4^+ and O_2		**Model 2 Root width**		**Model 3 Max. stem height**	
Parameter	Estimate	p	Estimate	p	Estimate	p
Intercept	5.8	2.2×10^{-5}	0.50	0.656	-0.087	0.956
$[NH_4^+]$ (µM)	-4.4×10^{-3}	0.054				
$[O_2]/[O_2$ atm] (ppt)	1.9×10^{-2}	0.003				
$[NH_4^+] \times [O_2]$	-3.4×10^{-5}	0.052				
Rhizome width (mm)			0.46	0.028		
Stem height (cm)					0.032	0.052
R^2	**0.77**		**0.58**		**0.49**	
p	**0.006**		**0.028**		**0.052**	
df (model, error)	**3, 8**		**1, 6**		**1, 6**	

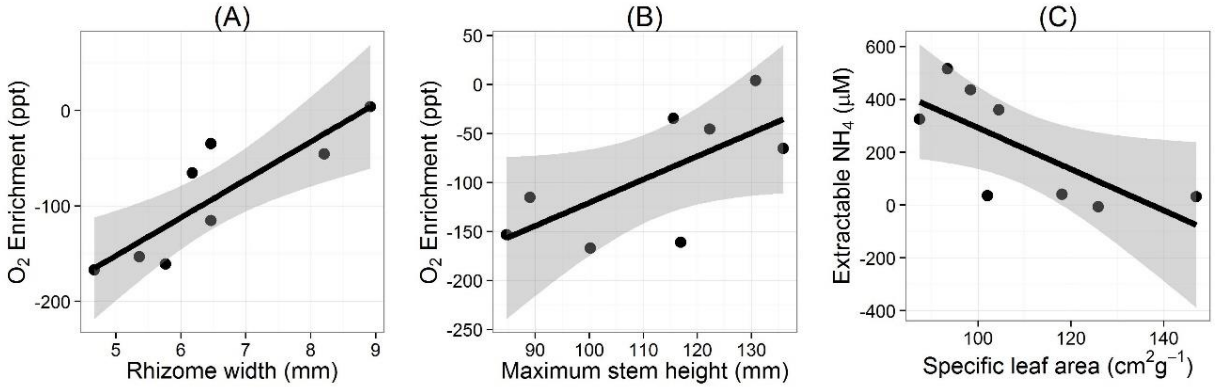

Figure 3.1: Sediment oxygen concentration increased linearly with (A) rhizome width (y = -351.0+ 39.80 x, R^2 = 0.74, p = 0.006) and (B) maximum stem height (y = -357.4 +2.37 x, R^2 = 0.46, p = 0.063) of plants in mesocosms. Oxygen is reported as the concentration in sediment equilibrators relative to atmosphere-equilibrated standards (O_2 enrichment = 0). (C) Extractable ammonium content in sediments was negatively associated with specific leaf area (y = 1076 – 7.829 x, R^2 = 0.52, p = 0.044).

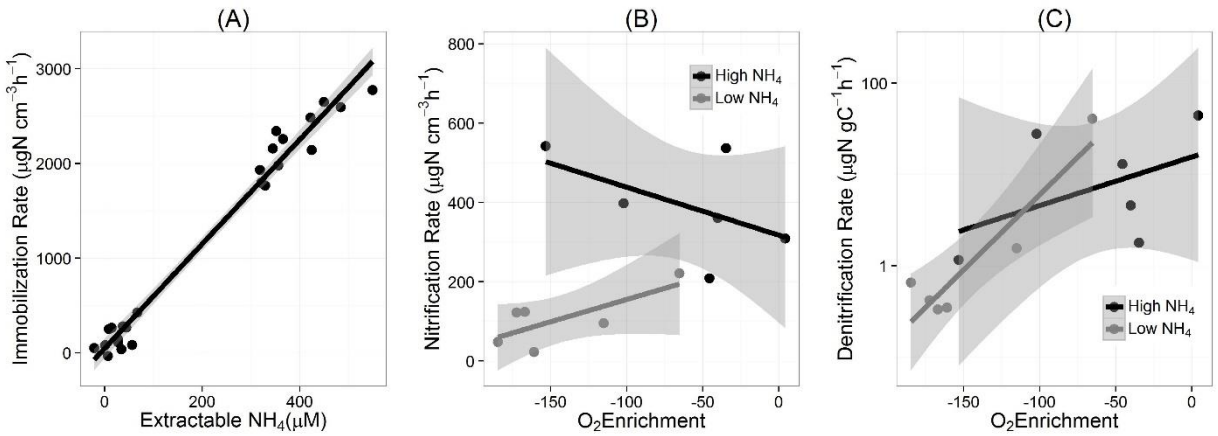

Figure 3.2: Relationships between sediment chemistry (ammonium and oxygen) and microbial processes. (A) Immobilization rates are linearly related to ammonium ($y = -44.81 – 5.53\ x$, $R^2 = 0.98$, $p < 10^{-10}$). (B) Nitrification rates and (C) denitrification rates depend on the interaction between sediment oxygen and ammonium availability.

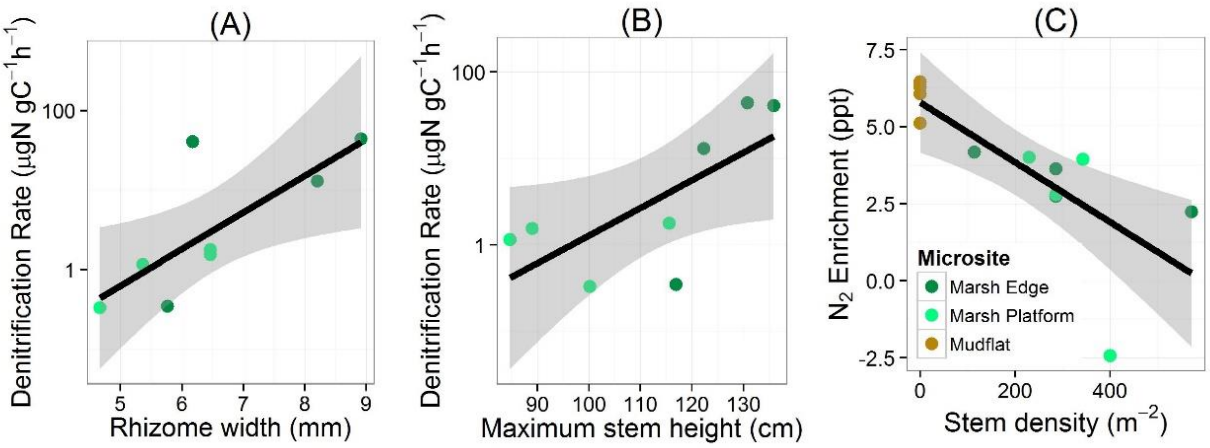

Figure 3.3: Denitrification potentials correlated positively with (A) rhizome width and (B) maximum stem height. N_2 enrichment in equilibrated sediment porewater decreased with increasing stem density ($y = 5.78 – 0.009\ x$, $R^2 = 0.57$, $p = 0.004$).

Chapter 4

Using plant traits to predict denitrification potential in salt marsh ecosystems

Abstract

Microbial denitrification, a critical ecosystem service on which humans depend for nitrogen removal and the maintenance of water quality, remains a notoriously difficult process to measure and predict. Models that incorporate traits of wetland plant communities may provide a complementary approach to traditional hydrologically and chemically based models in predicting rates of denitrification among wetland ecosystems. I examined the influence of the dominant salt-marsh grass *Spartina alterniflora* on microbial nitrogen-cycling processes in eleven field sites spanning a range of land-use conditions on Long Island, NY. My analysis revealed that simple linear models of plant traits provided predictions of denitrification potentials among sites that were comparable to models using measurements of sediment carbon and nitrogen content as predictors. Among all sites, denitrification potentials in *Spartina*-dominated sediments were double those measured in adjacent non-vegetated control plots on average, with the influence of vegetation increasing with total aboveground and belowground biomass of the plant community. Together these results support the utility of trait-based approaches in understanding the role of plant communities in promoting nitrogen-removal services in wetland ecosystems. Trait-based models offer a powerful way to estimate denitrification rates at the whole-ecosystem scale and could be used to predict how changes in the composition of ecological communities alter the provisioning of ecosystem services in future landscapes.

Introduction

Denitrification remains one of the most important but least well-quantified terms in the global nitrogen cycle (Galloway et al. 2004, Schlesinger 2009). Humans have augmented inputs

of nitrogen to ecosystems on a global scale, resulting in an accumulation of biologically available nitrogen within many ecosystems (Vitousek et al. 1997, Galloway et al. 2004). In aquatic ecosystems, excess nitrogen can have severe negative consequences for human health and local water quality, including eutrophication, hypoxia, and harmful algal blooms (Millennium Ecosystem Assessment 2005). Denitrification, a microbial respiratory process in which nitrate is permanently removed from ecosystems to the atmosphere as inert dinitrogen gas, helps to counteract these effects and thus represents a critical ecosystem service (Zedler 2003, Hinga et al. 2005). For this reason, denitrification is perhaps the most essential term in the nitrogen cycle for those aiming to mitigate the impacts of excess nitrogen availability.

Much of the uncertainty in estimating denitrification at the scale of whole ecosystems is due to the difficulty of measuring and modeling this process. Directly measuring denitrification requires the detection of tiny fluxes of N_2 gas against an atmosphere that is 80% N_2. Different techniques developed to address this challenge often provide conflicting estimates (Groffman et al. 2006). Because many of these methods are expensive and technically challenging, whatever measurements of denitrification exist are often very limited in spatial and temporal scale (Boyer et al. 2006). For these reasons, managers and biogeochemists often rely on predictive models of denitrification, which usually incorporate the various hydrological and chemical factors controlling denitrification rates (Boyer et al. 2006, Groffman et al. 2009). Denitrifying microbes are facultative anaerobic heterotrophs that use organic carbon as an energy source and can switch to using nitrate as an electron acceptor when molecular oxygen becomes depleted. Models that have been developed to predict denitrification typically use nitrogen loading and organic carbon as predictor variables. Sediment temperature, measurements or predictions of sediment redox conditions, and factors associated with hydrology and residence time are also commonly

incorporated to identify environments in which denitrification is likely to occur (Boyer et al. 2006).

Though these models serve a useful purpose, they do not try account for the influence of organisms and ecological communities on ecosystem process rates (Boyer et al. 2006, Groffman et al. 2009). A trait-based framework offers one potential approach to improving these models by linking community structure and dynamics with ecosystem processes (Lavorel and Garnier 2002, McGill et al. 2006). Wetland plant communities are known to influence sediment chemistry and denitrification rates by altering organic carbon availability and the redox conditions of sediments through root aeration (Sherr and Payne 1978, Weisner et al. 1994, Bachand and Horne 2000). Traits represent useful parameters for describing mechanistic relationships between organisms and their environments, in this case between wetland plants and the sediment environment (Keddy 1992).

The conceptual framework introduced in Chapter 1 illustrates that plant traits may affect denitrification via multiple pathways, possibly leading to complex relationships that depend on environmental context (Figure 1.3). Traits that increase sediment aeration may suppress denitrification by introducing molecular oxygen, the favored electron acceptor in respiration. Alternatively, they may enhance denitrification by encouraging the production of nitrate from ammonium via nitrification. Both belowground traits such as root mass or rhizome width, and aboveground traits such as like photosynthetic rate, specific leaf area or leaf nitrogen content, could be related to diurnal variation in oxygen within sediments (Wright et al. 2004, Reich et al. 2007). Litter quality and root production may influence carbon availability and quality and enhance denitrification potential, albeit on very different timescales, with root exudation influencing short-term carbon dynamics and litter quality influencing long-term carbon dynamics

via decomposition and nutrient recycling (Hume et al. 2002a, b). Conversely, traits associated with higher nitrogen demands or accumulation of nitrogen in recalcitrant biomass would result in competition with microbes for nitrogen and may inhibit denitrification rates (Figure 1.3).

In this chapter, I examined the association of traits of coastal salt marsh communities dominated by *Spartina alterniflora* with sediment characteristics and microbial nitrogen cycling rates in a comparative field study on Long Island, NY. Long Island represents a well-established gradient of high-intensity land use in urban areas of western Long Island near New York City to comparatively low-intensity land use in agricultural and forested areas of eastern Long Island (O'Shea and Brosnan 2000, Scorca and Monti 2001, Monti and Scorca 2003, Benotti et al. 2007) (Figure 4.1), with corresponding variation in inorganic nitrogen availability in sediments as a result of the various land uses (see Chapter 5). I examined potential associations between the traits of *Spartina*-dominated communities and nitrogen-cycling rates across Long Island. I then used trait associations to predict denitrification rates among sites and compared my predictions to predictions obtained from sediment variables commonly used in predictive denitrification models (organic carbon and nitrate availability).

Because my approach is correlative, I expected that both the *Spartina*-dominated plant community and the microbial community may be responding to differences in nitrogen availability sites. Therefore, correlations between plant traits and denitrification rates could indicate a direct effect of the plant community on denitrification, or they could simply represent a biologically meaningful proxy for nitrogen availability to which both the plant and microbial communities are responding. To directly evaluate the influence of marsh vegetation, I calculated an effect of the plant community on denitrification potential, relative to adjacent non-vegetated plots at the same marsh sites, and attempted to explain this effect using aggregate traits of the

plant community. This study represents a regional-scale attempt to establish predictive associations between characteristics of an ecological community and a microbial process that constitutes a critical service in many ecosystems.

Methods

Field Sampling

Eleven coastal salt marshes on Long Island, each dominated by *Spartina alterniflora*, were selected for sampling to examine relationships among plant traits, sediment characteristics, and microbial nitrogen transformations (Figure 4.1). I sampled all sites in June and August of 2013, times that correspond to the onset of plant growth and peak biomass. To control for tidal height and time of day, all sampling occurred within two hours of low tide and within two hours of solar noon, when physiological rates of both the vegetation and microbes were expected to be maximized. For each marsh location, 12 quadrats (25 x 25 cm) were randomly placed at a minimum of one meter apart, five within the marsh platform where short-form *S. alterniflora* is typically found, five near a creek edge where tall-form *S. alterniflora* is typically more common, and two in adjacent non-vegetated mudflats.

Vegetation measurements

Within each quadrat location, two canopy leaves from different *S. alterniflora* stems were randomly selected for measurements of photosynthetic rate, stomatal conductance, and photosystem II efficiency (Fv/Fm) using an LI-6400XT portable photosynthesis system, equipped with a 6400-40 leaf chamber fluorometer. When leaf width was insufficient to fill the leaf chamber, area corrections were applied prior to final calculations of photosynthetic rate and stomatal conductance (Box 4.1). I collected a 10 cm long leaf fragment from the leaves used in physiological measurements for measurements of leaf width and specific leaf area. Leaf

fragments were dried at 50°C for a minimum of 24 hours, weighed, and analyzed for carbon and nitrogen content with a Perkin Elmer Series II CHNS Analyzer. All aboveground material in the quadrats was harvested, dried at 50°C for at least 24 hours, and weighed to determine aboveground biomass. A sediment core (diameter ≈ 5 cm, depth ≈ 10 cm) was collected from near a stem closest to the center of each quadrat for determination of belowground biomass and maximum rhizome width. Total belowground biomass, including living and dead roots and rhizomes, was determined by wet sieving sediment through a 1000 µm sieve and removing non-vegetative material by hand. Both physiological and morphological traits are expressed as a weighted mean of the traits of individual constituents of the community within the plot area.

Sediment Chemistry

Porewater samples were collected from each quadrat using syringe-vacuum porewater sippers (Kolker 2005) and were kept frozen at -20° C until analysis for salinity using a refractometer and ammonium, nitrate, and phosphate content using standard colorimetric techniques (Jones 1984, Parsons et al. 1984b, Wetzel and Likens 2000). Sediment subsamples from each quadrat were extracted with 2N potassium chloride solution and analyzed for nutrient contents using the same methods used for porewater samples. Sediment subsamples were also used to measure moisture content (change in mass after drying at 70°C for at least 24 hours) and total carbon and nitrogen content with a Perkin Elmer Series II CHNS Analyzer. Sediment composition was determined as sand content by wet-sieving through a 63 µm mesh, drying at 70°C for 24 hours, and calculating mass of sand relative to the total mass of sediment subsample.

At the end of each sampling season, porewater nutrient profiles were obtained for each site with PVC porewater equilibrators using the same methods described in Chapter 3 (Hesslein 1976). Porewater equilibrators were installed in the transition zone between the marsh edge and

marsh platform at each marsh site and left in the field for 7 to 10 days; porewater was collected from sampling wells using a syringe and stored in acidified scintillation vials until analysis.

Microbial Processes

Sediment samples were collected from each quadrat for determination of denitrification rates using denitrification enzyme activity (DEA) measurements, gross nitrification measurements, and net mineralization-immobilization measurements. All microbial process measurements began within 24 hours of initial sediment sampling. DEA measurements followed the same protocols detailed in Chapter 3 (Smith and Tiedje 1979a, Watts and Seitzinger 2000). DEAs provide an estimate of the maximum potential of the microbial community to perform denitrification and are therefore useful for determining differences in denitrification potential between locations, but should not be interpreted as an absolute measurement of N_2 flux from sediments (Groffman et al. 2006). Nitrification and mineralization assays were performed on sediment subsamples from the same sediment cores used to measure DEA, using methods described in Chapter 3 (Hall 1984, Bédard and Knowles 1989, Strauss and Lamberti 2000, Starry et al. 2005).

Statistical Analysis

All data analyses were performed in R *version 3.0.2* (R Core Team 2012). I first computed Pearson correlations among plant traits using the function rcorr{Hmisc} (Harrell 2014, Schloerke et al. 2014) in order to avoid including redundant plant traits in subsequent models used to predict response rates of microbial processes. General linear models (GLMs) were constructed to predict denitrification rates, gross nitrification rates, and net mineralization-immobilization rates for site-level means using both plant-trait predictors and sediment-variable predictors. Rates measured in tall- and short-form *S. alterniflora* were not found to differ

systematically and were pooled at the site level in all models. Denitrification and nitrification rates were found to be log-normally distributed and were logarithmically transformed prior to analysis to achieve normal distribution of model residuals. Because logarithmic transformations cannot be performed on negative values, net immobilization and net mineralization measurements were analyzed as untransformed rates. Both nitrification and mineralization rates showed unequal variance among sampling groups when untransformed; therefore, weighted linear regressions were attempted in predictive models for both of these variables. Weights were calculated as the inverse of the site-level sampling variance.

I examined pairwise correlations between process rates and plant traits, and between process rates and sediment parameters. Initial GLMs contained "sampling time" as a categorical predictor, the two most informative trait or sediment predictor variables (most correlated to the process of interest) as continuous predictors, and all potential interactions. Non-significant factors and interactions ($p \geq 0.10$) were eliminated from models in a forward step-wise procedure. Residuals of final models were tested for normality using a Kolmogorov-Smirnov Lilliefors test (Lilliefors 1967).

For each marsh site, I computed the effect of plants on denitrification rates as a $\log_{10}$-response ratio of denitrification potentials in vegetated sediments divided by denitrification potentials in non-vegetated sediments:

[Equation 4.1] $logR = log_{10}\left(\frac{DEA_{VEG}}{DEA_{SED}}\right)$

The error in effect was calculated as the propagated error of sampling denitrification in both vegetated and non-vegetated locations at the site level:

[Equation 4.2] $logR(s) = \frac{\sqrt{(s_{VEG})^2+(s_{SED})^2}}{2}$

where *s* refers to the standard deviation in denitrification rates in vegetated and sediment plots at each site. I evaluated the ability of plant traits to explain the effect of plants on denitrification in weighted GLMs, where weights were equal to the inverse of the variance in *logR*. All model formulations, and code used to generate models and figures, are available in Appendix C.

Results

At the site level, plant traits explained 52% of the variation in denitrification rates, with a model fit comparable to the 56% explained by sediment variables (Table 4.1). In the bivariate plant-trait model (Figure 4.2A), denitrification rates were negatively associated with root mass (Figure 4.2B) and positively associated with leaf nitrogen content (Figure 4.2C). In the bivariate sediment model (Figure 4.2D), denitrification rates were positively associated with both carbon content (Figure 4.2E) and extractable nitrate content of sediments (Figure 4.2F). Denitrification rates were also positively associated with gross nitrification rates (Figure 4.3). Variation in gross nitrification rates (Figure 4.4A) and net mineralization rates (Figure 4.4B) at the site level was best explained by a weighted univariate relationship with extractable ammonium availability (Table 4.2). Nitrification was positively associated with ammonium availability (Figure 4.4A), whereas net mineralization declined with increasing ammonium (Figure 4.4B). No significant relationships were found between plant traits and nitrification rates (Appendix C); however, mineralization was found to be positively associated with both root mass and stomatal conductance, with these traits explaining 34% of the site-level variation in net mineralization in a weighted linear model (Table 4.2). Negative net mineralization (net immobilization) was observed in the vast majority of the sediments I surveyed, with positive net mineralization detected in only 40 of the 220 measurements conducted in vegetated sediments. In all cases,

there were no significant differences in microbial process rates between sampling times, and sampling time was eliminated from final models.

The effect of plants on denitrification rates was positive for seven out of eleven sites, but the average effect among all sites was not significantly different from zero. On average vegetation resulted in a doubling of denitrification potential relative to adjacent non-vegetated sediments. The effects of plants on denitrification are best explained by a linear additive model using aboveground and belowground biomass as predictors (Table 4.3, Figure 4.5A). Vegetation effects were significantly and positively associated with total aboveground biomass of the plant community (Figure 4.5B) and positively associated with total belowground biomass (Figure 4.5C) at $\alpha = 0.10$ (Table 4.3). However, the effect of vegetation was also highly variable, with a negative effect occurring in four of eleven sites, and much of the variation in effect remains unexplained (Table 4.3). Maximum plant effects appeared to occur at intermediate values of aboveground and belowground biomass, but our sampling was insufficient at extreme values of these variables to fit a monotonic relationship to the data (Figure 4.5A).

Discussion

Field observations from *Spartina alterniflora* salt marshes provided strong support for associations between plant traits and potential rates of microbial denitrification. Together, the negative association with root mass and positive association with leaf nitrogen content explained over 52% of the variation in denitrification rates at the site level (Figure 4.2), performing comparably to models parameterized with sediment carbon and nitrate availability (Table 4.1). Notably, these plant traits were associated with both nitrogen assimilation and sediment aeration, two separate but related plant-mediated pathways that I hypothesized would influence sediment conditions and denitrification potential (Figure 1.3). The negative association with root mass is

consistent with my hypothesis that sediment oxygenation may have a direct inhibitory effect on denitrification by providing a superior oxidant for denitrifiers such that they do not switch to using nitrate as a terminal electron acceptor. Likewise, the positive association between denitrification potential and leaf nitrogen content was consistent with the hypothesized influence of photosynthetic rate on enhancing coupled nitrification-denitrification. Specifically, I expected that higher photosynthetic rates would increase the diurnal variation in oxygen delivery to sediments, wherein oxygen loss from plant roots is high during the day when plants are photosynthetically active but low at night when continued root and microbial respiration results in a net loss of oxygen. This diurnal cycling in oxygen could result in a dynamic in which nitrification is favored during conditions of high oxygen, producing nitrate that can be consumed by denitrifiers when oxygen becomes depleted. A positive association with leaf nitrogen content, a well-supported proxy of photosynthetic potential, provides some support for this hypothesis (Reich et al. 2007, Kattge et al. 2009). That denitrification potential is positively associated with gross nitrification rates among sites (Figure 4.3) lends further support to the indirect enhancement of denitrification via coupled nitrification-denitrification (Figure 1.3).

An alternate explanation for these results could be that both plant and microbial communities are responding to the same gradient in nitrogen enrichment among the marsh sites on Long Island. One would expect that leaf nitrogen would be greater in sites where more inorganic nitrogen is available. Likewise, root mass in *Spartina alterniflora* has been shown to decrease in response to nutrient enrichment because plants require less belowground growth to obtain sufficient nutrients and allocate more growth to aboveground, photosynthetically active tissues (see Chapter 5) (Deegan et al. 2012, Watson et al. 2014). Therefore, both plant responses that are associated with higher denitrification potentials are also potentially correlated to

increasing nitrogen availability. That the plant-trait model performs comparably to sediment models in explaining variation in denitrification potential among sites (Table 4.1) is itself an interesting result because it suggests that plant traits may provide an informative proxy of biologically available nitrogen.

Both nitrification and mineralization rates were strongly associated with sediment nitrogen availability (Figure 4.4), while plant traits were relatively less successful in predicting rates of these processes (Table 4.2, Appendix C). Net immobilization was observed for over 80% of the vegetated plots that I surveyed, with a strong positive association between immobilization and nitrogen enrichment in sediments (Figure 4.4). This result indicates first that the nutrient content of *Spartina alterniflora* litter is insufficient to meet microbial needs, which is unsurprising given that the mean leaf C:N among sites is 32.6, well below the needs of typical decomposing microbes (Goldman et al. 1987). It also suggests that as nutrient enrichment increases, net storage of nitrogen in organic forms would increase simultaneously in these systems (Bowden 1986, Groffman et al. 1992). Notably, I did detect a significant positive association between net mineralization rates and root mass (Table 4.2), which may lend further support for the possibility that plant traits provide a useful indicator of biologically available nitrogen.

Associations between plant traits and denitrification potential do not themselves allow me to distinguish between alternate mechanisms that could be responsible for observed patterns in denitrification among sites. To begin to address this challenge, I made use of observations obtained from nearby non-vegetated sediments, and computed an "effect of vegetation" metric for each site. This metric should control for factors such as nitrogen enrichment that would contribute to responses in both the plant and microbial community. I found that denitrification

potentials in vegetated plots were on average double those observed in nearby non-vegetated plots, though significant variation was detected in the effect of vegetation among sites. Moreover, the influence of plants on denitrification potential generally increased with increasing aboveground biomass (Figure 4.5B) and belowground biomass (Figure 4.5C). This observation is consistent with the idea that trait relationships may be scaled to ecosystem-level processes using measurements of plant abundance as an indicator of plant influence (Lavorel and Grigulis 2012). If true, extending these relationships to multi-species communities may simply be a matter of computing community-trait means, weighted by the biomass of individual constituents of the community.

Overall my results support the usefulness of plant traits in predicting patterns of microbial processes, likely due to a combination of the direct influence of plants on sediment chemistry and the usefulness of plant traits as indicators of biologically available nitrogen. Though further experimental and observational work is clearly needed to assess the relative importance of the various mechanisms by which plant communities influence sediment processes, as well as the generality of these mechanisms for multi-species communities, my findings indicate great potential for plant traits to inform predictions of denitrification in wetland ecosystems. All of the components of the nitrogen cycle that I measured—denitrification, nitrification, and net mineralization—were closely associated with nitrogen availability in sediment porewater (Figure 4.2F, Figure 4.4). To the extent that plant traits provide useful proxies of biologically available nitrogen, surveys of plant traits within an ecosystem may provide valuable insight into this key determinant of the nitrogen cycle. Plant-trait predictors provide additional advantages in that they may be assessed relatively quickly and inexpensively, and many traits including foliar nitrogen can be measured at the landscape scale using

hyperspectral remote-sensing methods (Serbin et al. 2014, Asner et al. 2015). When combined with moisture and geophysical measurements obtained by remote sensing, such variables offer the potential for landscape-scale predictions of the nitrogen removal capacity of ecosystems (Boyer et al. 2006, Kulkarni et al. 2008).

Table 4.1: Results of general linear models to predict denitrification potential in salt marshes dominated by *Spartina alterniflora*. Denitrification potentials were log_{10} transformed prior to analysis. (Root mass = total belowground biomass g m^{-2}, Leaf N = leaf nitrogen content mgN g^{-1}dry weight, Carbon = sediment carbon content mgC g^{-1}dry weight, Nitrate = extractable nitrate content of sediments µM)

Plant-trait Model $R^2 = 0.52$ $F_{2,19} = 10.21$ $p = 9.7 \times 10^{-4}$				**Sediment Model** $R^2 = 0.56$ $F_{2,19} = 12.04$ $p = 4.2 \times 10^{-4}$			
Factor	Estimate	t	p	Factor	Estimate	t	p
Intercept	2.0	4.2	4.6×10^{-4}	Intercept	1.9	9.0	2.9×10^{-8}
Root mass	-3.4×10^{-4}	-3.5	2.6×10^{-3}	Carbon	1.8×10^{-3}	1.4	1.9×10^{-1}
Leaf N	8.4×10^{-2}	3.1	5.9×10^{-3}	Nitrate	7.1×10^{-3}	3.6	1.2×10^{-3}

Table 4.2: Results of general linear models to predict net mineralization rates; models were weighted by the inverse of the sampling variance in mineralization at the site level. (Root mass = total belowground biomass g m^{-2}, Conductance = stomatal conductance mol H_2O m^{-2} s^{-1}, Leaf N = leaf nitrogen content mgN g^{-1}dry weight, Ammonium = extractable ammonium content of sediments µM)

Plant-trait Model $R^2 = 0.34$ $F_{2,19} = 4.81$ $p = 5.1 \times 10^{-3}$				**Sediment Model** $R^2 = 0.55$ $F_{1,17} = 24.64$ $p = 7.5 \times 10^{-5}$			
Factor	Estimate	t	p	Factor	Estimate	t	p
Intercept	-8.6×10^{2}	-5.4	3.4×10^{-5}	Intercept	-22.5	-0.3	0.79
Root mass	1.6×10^{-1}	2.6	0.02	Ammonium	-4.6	-5.0	7.5×10^{-5}
Conductance	1.5×10^{3}	1.7	0.10				

Table 4.3: Results of weighted general linear model to predict the effect of plants on denitrification rates. The effect of plants was calculated as the $\log_{10}$ response ratio of denitrification rates in vegetated sediments, relative to denitrification rates in non-vegetated sediments. The regression was weighted by the inverse of the combined sampling variance of vegetated and non-vegetated means at each site. ($R^2 = 0.23$, $F_{2, 19} = 1.73$, $p = 0.08$)

Factor	Estimate	t	p
Intercept	-1.3	-1.7	0.10
Aboveground Biomass	1.6×10^{-3}	2.1	0.05
Root Mass	3.6×10^{-4}	1.8	0.09

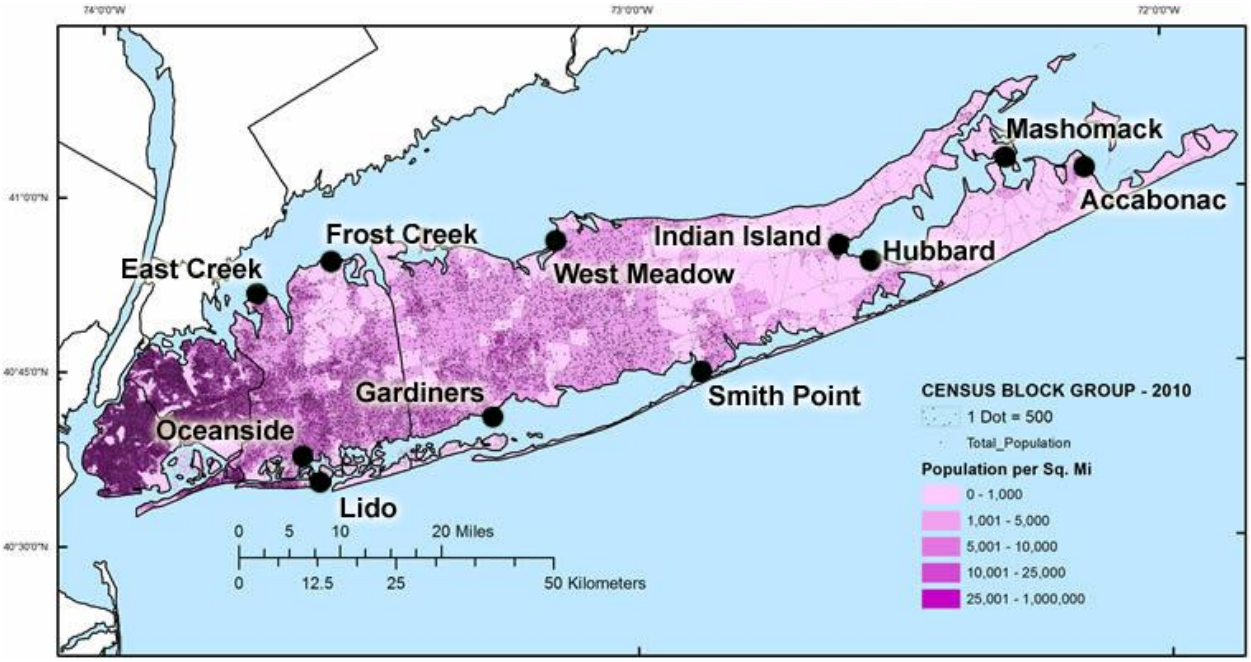

Figure 4.1: Research locations on Long Island, NY, ranging from high human population density in western Long Island to rural areas in eastern Long Island (United States Geological Survey 2010). Each salt-marsh location was dominated by *Spartina alterniflora* and sampled in June and August, 2013. At each site, five plots were sampled along the marsh edge, five along the marsh platform, and five on non-vegetated mudflats.

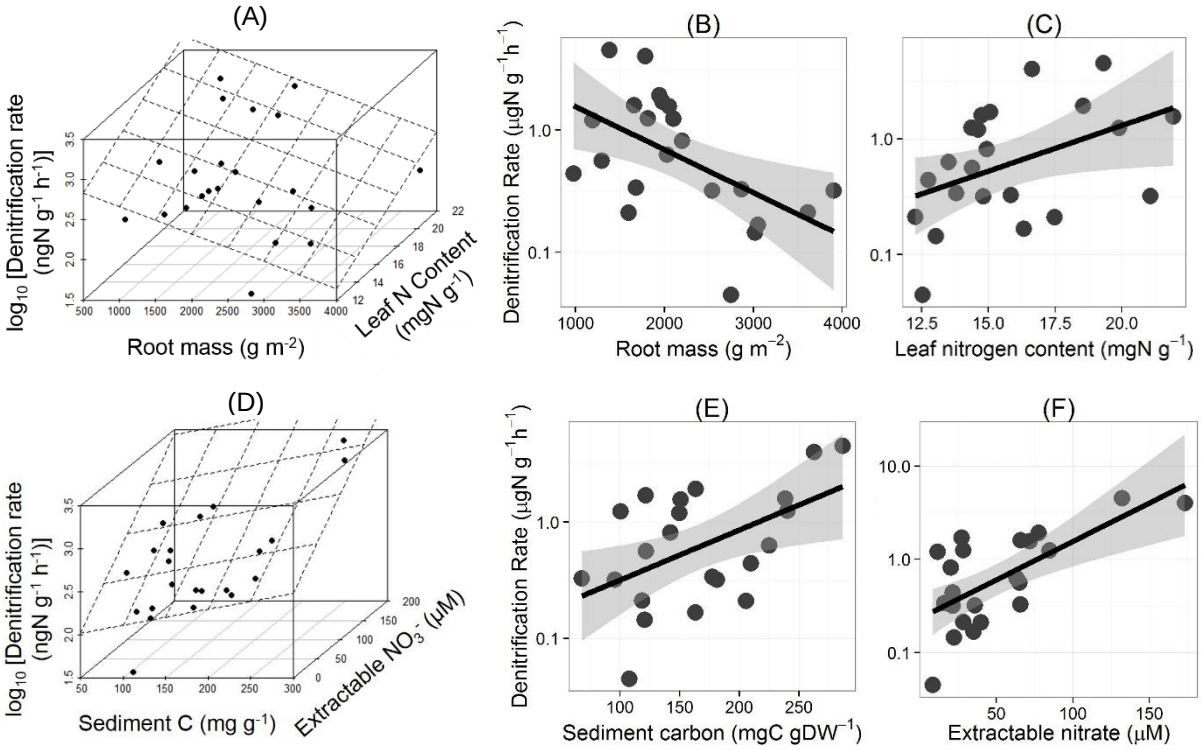

Figure 4.2: Result of best models to predict denitrification rates at the site level. (A) A linear, additive model including root mass and leaf nitrogen content as predictors explained 52% of variation in denitrification rates. Denitrification was (B) negatively associated with root mass and (C) positively associated with leaf nitrogen content. (D) A linear, additive model including sediment carbon and extractable nitrate as predictors explained 56% of variation in denitrification rates. Denitrification was positively associated with (E) sediment carbon and (F) extractable nitrate content.

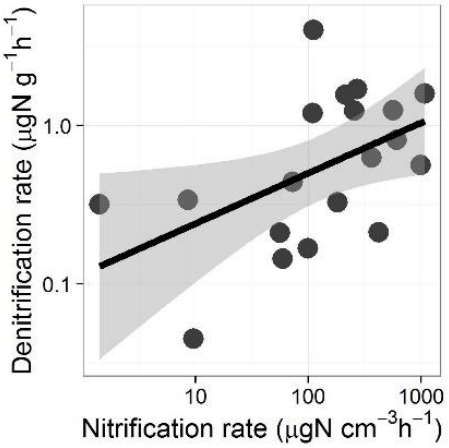

Figure 4.3: Denitrification rates were positively associated with nitrification rates at the site level ($y = 1.6 + 0.45\ x$, $R^2 = 0.18$, $F_{1, 20} = 4.4$, $p = 0.05$).

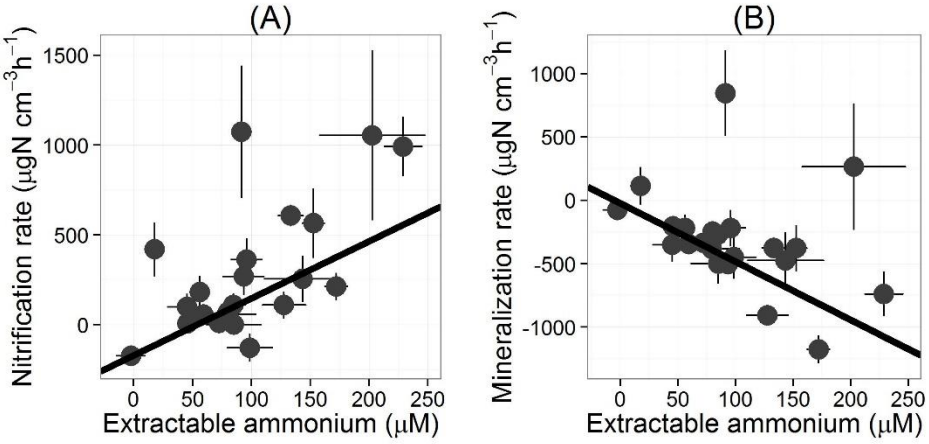

Figure 4.4: (A) Variation in nitrification rates among sites was best explained by extractable ammonium content of sediments, using a univariate linear model, weighted by the inverse of the site-level sampling variance in nitrification ($y = -170 + 3.2\ x$, $p = 5.2 \times 10^{-4}$, $R^2 = 0.46$). (B) Variation in mineralization rates was best also best explained by extractable ammonium in a weighted, linear model.

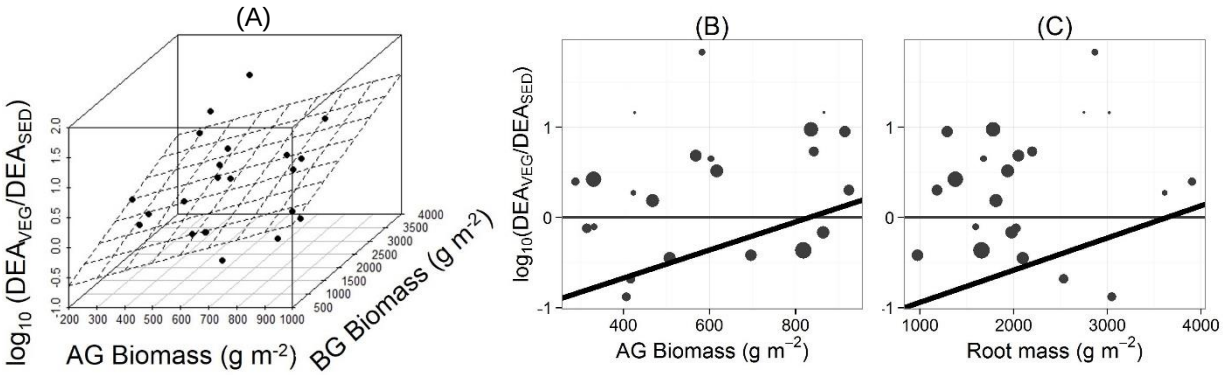

Figure 4.5: (A) The effect of plants on denitrification rates, shown here as a log-response ratio of denitrification potential in vegetated plots to denitrification potential in sediment plots, increased with both (B) aboveground biomass and (C) root mass at the site level. Sizes of the points in B and C correspond to their relative weights in the weighted linear model (Table 4.5). A log-response ratio of 0 indicates no effect of vegetation; a positive value indicates a positive effect, and a negative value indicates a negative effect.

Box 4.1 Derivation of leaf-area correction for the LI-COR 6400-40 leaf chamber fluorometer

The area of the leaf inside the chamber was determined by calculating the area of the two circular segments not covered with leaf area [Equation 4.3-4.4] and subtracting these segments from the total area of the leaf chamber [Equation 4.5]. The only inputs necessary to make the final calculation is chamber area (2 cm^2), chamber radius (R, or the square-root of the area, divided by π), and the mid-leaf width (d).

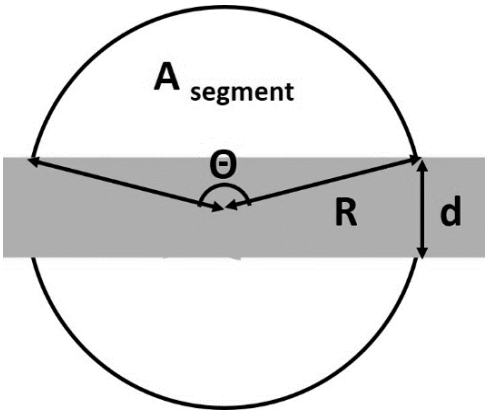

[Equation 4.3] $A_{segment} = \frac{1}{2}\theta^2[\theta - \sin(\theta)]$

[Equation 4.4] where $\theta = 2\,arccos\left(\frac{\frac{1}{2}d}{R}\right)$

[Equation 4.5] $A_{leaf} = A_{chamber} - 2\left(A_{segment}\right)$

Chapter 5

Impacts of salinity and nutrients on salt marsh stability

Abstract

Belowground growth in coastal plants is a critical determinant of marsh stability and the ability of wetlands to keep pace with sea-level rise. Quantifying the multiple effects of nutrient loading on root biomass and marsh stability is an ongoing controversy in wetland research. Though some physiological models for marsh vegetation predict that root mass should increase with increasing nutrient availability, fertilization experiments and field measurements have indicated that plants shift growth allocation from belowground to aboveground as nitrogen availability increases. Likewise, salinity may decrease belowground growth through sulfide toxicity, or it may increase belowground allocation as plants respond to sulfide stress by increasing root growth to oxidize sediments. Here, I made use of an urban to rural range of land-use conditions among coastal marshes dominated by *Spartina alterniflora* on Long Island, NY to test for correlates of root growth. Based on two years of data from both low- and high-marsh *S. alterniflora* in 11 field sites, I found that belowground biomass was related positively to salinity and negatively to extractable nitrogen content in sediments. These results indicate that further eutrophication may reduce marsh stability and that increasing salinity, perhaps as a result of future sea level rise, may increase marsh stability.

Introduction

Coastal salt marsh ecosystems provide valuable services such as shoreline stabilization, flood and storm surge protection, and maintenance of coastal water quality (Zedler 2003, Costanza et al. 2008, Gedan et al. 2011). The resilience of these ecosystems to multiple anthropogenic pressures, including coastal eutrophication and accelerated sea-level rise, is

therefore critical for the health and economic well-being of coastal communities worldwide (Millennium Ecosystem Assessment 2005). For salt marshes to keep pace with projected sea level-rise, they must accumulate sufficient sediment and organic matter for vertical growth, while maintaining sediment stability despite periodic hydrologic disturbances (e.g. storm surges and overland flow). Both of these features of resilient marshes depend on well-developed root systems (Nyman et al. 2006, Perillo et al. 2009). However, despite a long history of study (Valiela et al. 1976, Mendelssohn and Morris 2000), the relative importance of abiotic factors in influencing root-mass production and accumulation remains controversial in coastal marsh ecology. To predict future patterns of marsh stability and the ability of marshes to provide critical ecosystem services, one must first resolve which abiotic factors are positively or negatively associated with belowground growth.

One of the abiotic factors influencing root growth in coastal marsh vegetation is the availability of inorganic nitrogen, which is thought to be a limiting nutrient in coastal marshes (Mendelssohn and Morris 2000, Bertness et al. 2002). Human activities have more than doubled nitrogen inputs worldwide relative to preindustrial levels, with inputs from synthetic fertilizers and animal wastes accompanying industrialized agricultural development, and human wastes from septic systems, sewage treatment, and combined sewer overflows accompanying urban development (Vitousek et al. 1997, Millennium Ecosystem Assessment 2005). However, the consequences of increased nitrogen loading for root growth and stability in coastal ecosystems remains an open question. Growth allocation in plants is typically assumed to shift from belowground to aboveground with increasing nutrient availability; that is, when nutrient limitation is relieved by fertilization, plants require fewer roots to acquire sufficient nutrients and can allocate more growth to photosynthetic tissues (Ericsson 1995). Therefore, one may expect

to observe a reduction in belowground growth in coastal marshes that receive higher nutrient loads. Reductions in living root mass have been observed in long-term nutrient enrichment studies and were often accompanied by a decrease in sediment stability (Turner et al. 2009, Kearney et al. 2011, Deegan et al. 2012, Watson et al. 2014). However, physiological models of salt marsh vegetation and other enrichment studies have shown that nitrogen additions result in increased belowground growth, as well as increased sediment capture and accretion due to enhanced aboveground growth (Morris et al. 2002, Anisfeld and Hill 2012, Fox et al. 2012, Graham and Mendelssohn 2014). An increase in root growth with increasing nitrogen amendments may be predicted if alleviating nitrogen limitation increases total plant production, including allocation to photosynthetic tissues, rhizomes, *and* roots (Morris et al. 2013), or if nitrogen fertilization results in a shift to phosphorus limitation and stimulates the growth of plant roots to scavenge for phosphorus (Turner 2011). In any case, the net impact that increasing nitrogen loads have on belowground plant growth deserves further scrutiny at whole-marsh scales over multidecadal time periods and multiple nutrient-loading regimes.

As a consequence of sea-level rise, salinity is also expected to increase across many brackish, coastal marshes; however, in coastal areas where climate change results in increased precipitation events or river discharge, salinity may also be expected to decrease (Craft et al. 2008). Additionally, greater tidal ranges may also reduce salinity in what were previously poorly flushed, high evaporation portions of the marsh. However salinity changes in the future, understanding the effects of salinity on root mass in coastal vegetation is critical to our ability to forecast future marsh stability. Increasing salinity translates to a higher concentration of sulfate ions, which when reduced to hydrogen sulfide in low redox marsh sediments, is toxic to plants (Mendelssohn and Morris 2000). Therefore, one may expect to observe decreasing plant

production, including root production, with increasing salinity in anoxic marsh sediments (Linthurst and Seneca 1981). However, marsh plants may also respond to sulfide stress under low redox conditions by introducing oxygen to sediments via their roots and specialized aerynchymatous tissues (Armstrong et al. 1994). Considering plant responses to sulfide, increased salinity stress may lead to an increase in root growth. The impacts of salinity on belowground growth in coastal vegetation are complicated by interactions and between nitrogen and salinity (Mendelssohn and Morris 2000). Salinity is known to increase ammonium fluxes from sediments, leading to net nitrogen loss (Giblin et al. 2010), as well as to directly inhibit ammonium assimilation by plants (Bradley and Morris 1990). Therefore, given the mixed responses described above, counteracting effects of nitrogen and salinity on root mass may be expected. Field evidence for effects of salinity on belowground growth is sparse and does not clearly support either alternative hypothesis, nor test potential interactions with nutrient assimilation (Drake and Gallagher 1984, Howes et al. 2010). Further field assessments are needed to fully resolve the influence of salinity on marsh stability.

Here I examined the simultaneous influences of salinity and sediment nutrient availability on belowground growth of *Spartina alterniflora* across 11 coastal salt marshes that span an urban to rural land-use gradient from western to eastern Long Island, NY (Figure 4.1). Using 430 observations of total belowground biomass collected in June and August over two years, I assessed the ability of salinity and inorganic nutrients to explain site-level variation in root mass. The sites examined in this study form a 50-100 year chronosequence of development from forested to agricultural to urban land-use types, a series of land-use transitions that reflects development patterns occurring worldwide (Millennium Ecosystem Assessment 2005). This comparative study complements long-term fertilization experiments (13-17 year) by identifying

correlates of root mass, and thus marsh stability, which have established on a multidecadal scale under a common pattern of land-use development.

Methods

Long Island, NY represents a well-established gradient of high-intensity land use in urban areas of western Long Island near New York City to comparatively low-intensity land use in agricultural and forested areas of eastern Long Island (O'Shea and Brosnan 2000, Scorca and Monti 2001, Monti and Scorca 2003, Benotti et al. 2007). As an example, nitrogen loads to the entirety of Jamaica Bay in western Long Island have risen from 35 kg/day in 1900 prior to extensive development to an estimated 15,800 kg/day as of 2005 (Benotti et al. 2007). Whereas pre-development nitrogen fluxes to Long Island marshes originated almost entirely from groundwater flow, post-development fluxes are dominated by sewage-treatment outflows, combined-sewer overflows, septic systems and cesspools, and agricultural drainage (including legacy effects from historically extensive duck farms in eastern portions of the island) (Ayers et al. 2000, Benotti et al. 2007). Total nitrogen inputs are generally found to be greatest in areas of highest human population density (United States Geological Survey 2010). Additionally, variation in tidal range between Long Island Sound on the northern coast of Long Island and the various coastal embayments of southern and eastern Long Island, as well as variation in stream-flow discharge, offered a high probability that average salinity would vary among marsh sites independently of variation in nitrogen loading (Scorca and Monti 2001, Monti and Scorca 2003).

Eleven coastal salt marshes on Long Island, each dominated by *Spartina alterniflora*, were selected for sampling (Figure 4.1) to examine the effects of nutrient availability and salinity on aboveground and belowground plant growth. Sampling was conducted in June and August of 2012 and 2013, chosen to correspond to the onset of plant growth and peak biomass. For each

marsh location, ten 25 x 25 cm quadrats were randomly placed at a minimum of one meter apart, five within the marsh platform where short-form *S. alterniflora* are typically found, and five near a creek edge where tall-form *S. alterniflora* are typically more common. For each quadrat location I measured aboveground and belowground biomass, sand content, sediment carbon content, sediment porewater salinity, and sediment porewater nutrient availability (ammonium, nitrate, and phosphate).

Within each sampling quadrat, I clipped all aboveground vegetation; clippings were dried at 50° C for at least 48 hours and weighed to determine aboveground biomass. A sediment core (diameter ≈ 5 cm, length ≈ 10 cm) was taken from near a stem closest to the center of each quadrat for determination of belowground biomass, maximum rhizome width, and sand content. Total belowground biomass, including living and dead roots and rhizomes, was determined by wet sieving core samples through a 1000 µm sieve and removing non-vegetative material by hand. Sand particles larger than 63 µm were likewise collected by sieving and weighed to determine sand content of marsh sediments. Vegetated sediment from duplicate cores within the same quadrat, was subsampled, dried, and analyzed for total nitrogen and carbon content using a Perkin Elmer Series II CHNS Analyzer. I collected sediment porewater from each quadrat using syringe-vacuum porewater sippers. Porewater samples kept on ice, returned to the lab, and frozen at -20° C until analysis of salinity with a refractometer, and ammonium and nitrate content using standard colorimetric methods (Jones 1984, Parsons et al. 1984b); unless otherwise specified, measurements of nitrate and ammonium were summed prior to analysis and reported as "dissolved inorganic nitrogen (DIN)." In 2013, an additional 5 g sediment subsample from the duplicate sediment cores was extracted with 10 ml 2N KCl solution and analyzed for ammonium, nitrate, and phosphate content using standard colorimetric methods (Jones 1984,

Parsons et al. 1984b, Wetzel and Likens 2000). I also obtained nutrient and salinity profiles for each wetland location in April, June, and August of each year using PVC porewater equilibrators with 12 ml sampling wells spaced vertically at 3 cm intervals. Equilibrators were filled with dionized water, covered with a Spectr-Por cellulose membrane, and deoxygenated overnight by bubbling with nitrogen gas prior to installation (Hesslein 1976). Equilibrators were installed in vegetated sediments at the transition zone between tall- and short-form *S. alterniflora* at each site and left in the field for 7-10 days. Porewater was collected from sampling wells using a syringe and stored in acidified scintillation vials until analysis.

I performed all data analyses on site-level means in R *version 3.0.2* (R Core Team 2012). Measurements obtained in tall- and short-form *S. alterniflora* (marsh edge and platform, respectively) were not found to differ systematically in total aboveground or belowground biomass and were pooled at the site level. Because all predictor variables were not measured in all years, two separate sets of linear models were constructed, one initially containing all predictor variables collected in 2012-2013 [salinity, porewater DIN] and one initially containing all predictor variables collected in 2013 [salinity, extractable DIN, extractable phosphate]. Models were constructed to predict aboveground biomass, root mass, and maximum rhizome width. For all variables included in initial models, distributions and pairwise correlations were examined using the R function ggpairs (Schloerke et al. 2014) and tested for significance using the R function rcorr (Harrell 2014). Extractable phosphate and all porewater nutrient measurements were $\log_{10}$ transformed to satisfy assumptions of normality prior to testing.

Significance testing for each model was performed as an ANCOVA, with "Sampling Time" included as a categorical predictor, and nutrients and salinity included as continuous predictors in a sequential linear model. Factors and interactions that did not add predictive value

were eliminated from models; after each elimination, changes in model fits were evaluated for significance. Relationships between predictor variables and root mass were calculated (Legendre 2013) and plotted (Wickham and Chang 2015) as standard-major-axis (SMA) regressions to account for appreciable measurement error in both dependent and independent variables. Code for analyses and figures is provided in Appendix D.

Results

Extractable inorganic nitrogen and salinity varied independently among Long Island field sites (Figure 5.1, Appendix D). High concentrations of nitrogen were detected in areas of western Long Island, as predicted, but concentrations were also high in central Long Island near Peconic Bay, where duck farms were historically abundant. Salinity was greatest at sites near the westernmost and easternmost ends of Long Island (Figure 5.1), and was uncorrelated to variation in nitrogen availability (Appendix D).

For measurements conducted in June and August 2013, initial models to predict root mass included sampling time, salinity, extractable inorganic nitrogen, and extractable phosphate. Total root mass was negatively related to extractable inorganic nitrogen (Figure 5.2A), but positively related to porewater salinity at $\alpha = 0.05$ (Figure 5.2B). Though mean root mass differed between sampling times, the effect of salinity and nitrogen on root mass did not, and no interaction was detected between salinity and nitrogen. Overall, I detected a 60-70% reduction in standing root mass and a 70% increase in standing aboveground biomass with increasing nitrogen availability at the site level (Figure 5.2A, 5.2C). Additionally, root mass was found to increase with increasing porewater salinity by as much as 70% at the site level; the effect of salinity on root mass was remarkably consistent among all sampling times included in this analysis (Figure 5.2B).

Aboveground biomass was positively related only to extractable inorganic nitrogen at $\alpha = 0.10$ (Figure 5.2C) but had no obvious response to variation in salinity (Figure 5.2D). In all cases, extractable phosphate was a poor predictor of vegetation responses and was removed from final models. Overall, I was able to explain over 51% of the total variation in root mass with extractable nitrogen, salinity, and seasonal information; with only nitrogen and seasonal information, I was able to explain 42% of the total variation in aboveground biomass among marsh sites (Table 5.1). For the full set of root mass measurements (2012-2013), only porewater inorganic nitrogen and salinity were available as independent variables. Porewater nitrogen did not explain a significant amount of variation in root mass and was discarded from the model. Salinity was positively related to root mass at $\alpha = 0.05$, and although mean root mass again differed significantly among sampling times, the effect of salinity on root mass did not. No variables sampled in both 2012 and 2013 were significantly associated with aboveground biomass. Sampling time and salinity explained 34% of the variation in root mass for the 2012-2013 dataset. In all cases, porewater nutrient measurements obtained from vacuum porewater sippers were found to be poor predictors of root mass and aboveground biomass and were ultimately discarded from final models. No linear combination of sediment variables was capable of explaining a significant amount of variation in maximum rhizome width in either set of analyses. Vegetation response variables—aboveground biomass, root mass, and maximum rhizome width—were uncorrelated at the site level; likewise, no significant correlations were detected among predictor variables—extractable nitrogen, extractable phosphorus, porewater nitrogen, porewater phosphorus, porewater salinity (see Appendix D for full analysis).

Discussion

This work supports the hypothesis that eutrophication due to nitrogen loading exerts a negative influence on belowground biomass, and thus marsh stability, in coastal marshes. This result is consistent with a growing body of evidence suggesting that increasing nutrient availability increases the amount of growth marsh plants allocate to aboveground production and decreases the amount of growth allocated to roots and rhizomes (Valiela et al. 1976, Deegan et al. 2012, Watson et al. 2014). Notably, most studies have been based on enrichment experiments and have witnessed a response in only the living fraction of belowground biomass. My study is one of the few that has detected a response in total belowground biomass, including both living and dead root material, in a coastal marsh (Morris and Bradley 1999). Because the long-term stability of marshes experiencing sea-level rise ultimately depends on the *total* accumulation of organic material and mineral sediments, my results suggest one biological mechanism under which chronic nutrient enrichment may inhibit the ability of marshes to grow vertically. A reduction in total belowground biomass, resulting from both the accumulation and decomposition of dead root matter, is a slow response variable that is perhaps unlikely to be detected in short- to moderate-term (i.e., 5-15 year) enrichment experiments. In contrast, the variation in standing total root mass in Long Island salt marshes could be viewed as a 50 to 100 year enrichment experiment in which the effects of chronic eutrophication on total biomass are more likely to be detected. This finding has important implications for the long-term stability of marshes that are believed to be currently stabilized by nutrient enrichment.

An alternate explanation for my observed pattern of reduced belowground biomass with increased nitrogen is that increasing aboveground production through nutrient enrichment enhances mineral sedimentation rate, thus decreasing the proportion of organic material in

sediments relative to non-organic components (Morris et al. 2002). If true, I would expect to observe an inverse relationship between aboveground biomass and total belowground biomass or organic content of sediments at the site level. Although I did detect an increase in aboveground production in sites with higher nutrient availability (Figure 5.2C), I found no correlation between aboveground biomass and belowground biomass among sites, nor with total organic sediment content (Appendix D). However, aboveground biomass was weakly correlated with the sand content of sediments for samples collected in 2013 (Appendix D). Together, these results suggest that aboveground biomass does influence sediment capture, but that the amount of sediment captured is insufficient to affect the total fraction of sediments composed of organic material. Such a result is not surprising given that stream discharge and thus overall particle delivery to Long Island marshes is small relative to tidal influence (Kim and Bokuniewicz 1991). The lack of a negative correlation between aboveground and belowground production (Appendix D) further suggests that controls on these vegetation responses may be decoupled, which seems counterintuitive since both responses depend on nitrogen availability (Figure 5.2A, 5.2C). In addition to nitrogen, these biomass components may be responding to alternate abiotic variables, such as salinity in the case of root mass (Figure 5.2B) or tidal range in the case of aboveground biomass (Steever et al. 1976). The relative importance of enhanced sediment capture due to increasing aboveground biomass, versus reduced sediment accumulation resulting from decreasing belowground biomass, may depend strongly on rates of sediment delivery via stream discharge and the strength of tidal influences on coastal marshes. My findings indicate that, in marshes with relatively low rates of sediment deposition, factors controlling belowground growth and organic-matter accumulation are likely to be more important determinants of vertical marsh growth than sediment capture by aboveground biomass.

The nutrient-loading context of a marsh may also influence large-scale patterns. I found no evidence of phosphate effects in our analysis (Appendix D); however, because the mean N:P ratio in sediment porewater never exceeded 15 for any of the sites included in this study, marsh vegetation in these sites is extremely unlikely to be phosphorus limited (Verhoeven et al. 1996). In marshes with lower phosphorus availability, nitrogen enrichment may cause plants to become increasingly phosphorus limited, in which case they may allocate more growth to roots to scavenge for phosphate (Turner 2011). If the phosphorus-scavenging hypothesis is true, nitrogen enrichment of sites experiencing nitrogen and phosphorus co-limitation could result in an increase in root mass.

The most surprising pattern I observed was the positive and remarkably consistent effect of salinity on belowground biomass in *Spartina alterniflora* marshes (Figure 5.2B). This result supports the hypothesis that plants allocate more growth to roots as a stress response, aerating sediments to increase sulfide oxidation and alleviate sulfide stress (McKee et al. 1988). My results are consistent with at least one other field study (Howes et al. 2010), which found that high-salinity marshes produce more roots and have a higher sediment shear strength than nearby low-salinity marshes. However, these field studies appear to conflict with greenhouse studies that have found reductions in root production under sulfide stress (Mendelssohn and Morris 2000). This discrepancy may arise because greenhouse plants kept in static conditions may not have sufficient opportunity to influence redox conditions in the sediments via responses in root growth, whereas observations of field conditions include longer term acclimation responses of plants (Mendelssohn and Morris 2000). Overall, results from field studies suggest that increasing salinity from sea-level rise may enhance stability of existing coastal marshes, assuming that sediment delivery and total production is sufficient for vertical marsh growth.

Though consistent with previous work showing that nutrient loading negatively impacts root mass, my findings suggest a much larger role for salinity in determining total root mass than is commonly expected. Together, these results indicate that further eutrophication may reduce marsh stability and that increasing salinity experienced by inland marshes as sea level rises may increase stability of those marshes. Because high sulfide concentrations inhibit the ability of roots to assimilate nitrogen (Mendelssohn and Morris 2000), I expected an interaction between the effects of salinity and nitrogen availability on root mass. However, I found that salinity and nitrogen acted independently to influence total root mass. Therefore, though the effects of these two anthropogenic stressors on root mass are likely to exhibit complex spatial signatures over time, the fact that they act independently and consistently means that it should be possible to predict a significant proportion of the variation using relatively simple biological relationships. Given sufficient knowledge of hydrology and particle load for a site, a holistic management approach that accounts for both hydrological and chemical determinants of vegetative growth may well be within reach. Such an approach would greatly enhance our ability to properly assess the stability of marshes under future scenarios of sea-level rise and eutrophication.

Table 5.1: Results of ANCOVAs explaining variation in root mass (g/m^2) and aboveground biomass of *Spartina alterniflora* at the site level in June-August 2013. In both cases, interaction terms were non-significant and were removed from final models. DIN = Extractable Dissolved Inorganic Nitrogen, SS = Sum of Squares.

Root mass (g/m^2) Model $R^2 = 0.5133$					**Aboveground Biomass (g/m^2)** Model $R^2 = 0.4185$				
Parameter	df	SS	F	p	Parameter	df	SS	F	p
Sampling Time	1	2.051×10^6	5.796	0.0285	Sampling Time	1	2.722×10^5	9.136	0.007
Salinity (ppt)	1	1.695×10^6	4.790	0.0438					
DIN (µM)	1	2.225×10^6	6.288	0.0233	DIN (µM)	1	1.138×10^5	3.819	0.066
Residuals	16	5.661×10^6			Residuals	18	5.364×10^5		

Table 5.2: Results of ANCOVA explaining variation in root mass (g/m^2) of *Spartina alterniflora* at the site level in June and August 2012-2013. Interaction terms were non-significant and were removed from the final model. Model $R^2 = 0.3426$.

Parameter	df	Sum of Squares	F value	p value
Sampling Time	3	3.904×10^6	2.993	0.0435
Salinity (ppt)	1	4.251×10^6	9.778	0.0035
Residuals	36	1.565×10^7		

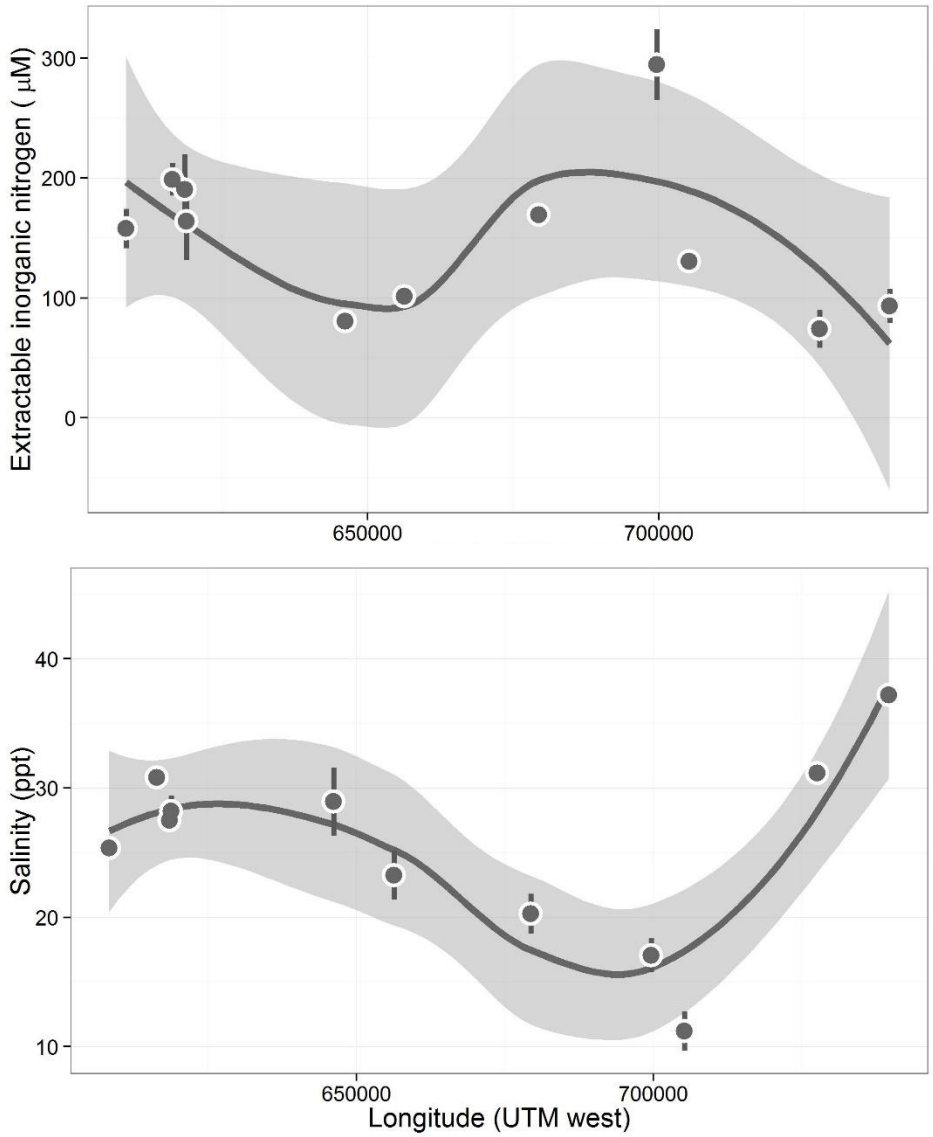

Figure 5.1: Variation in extractable inorganic nitrogen and salinity in sediments across the 11 Long Island field sites included in this study. Error bars show standard error for site-level means (n = 10); the moving averages (solid lines) and confidence regions (shaded areas) were computed using a loess smoothing function.

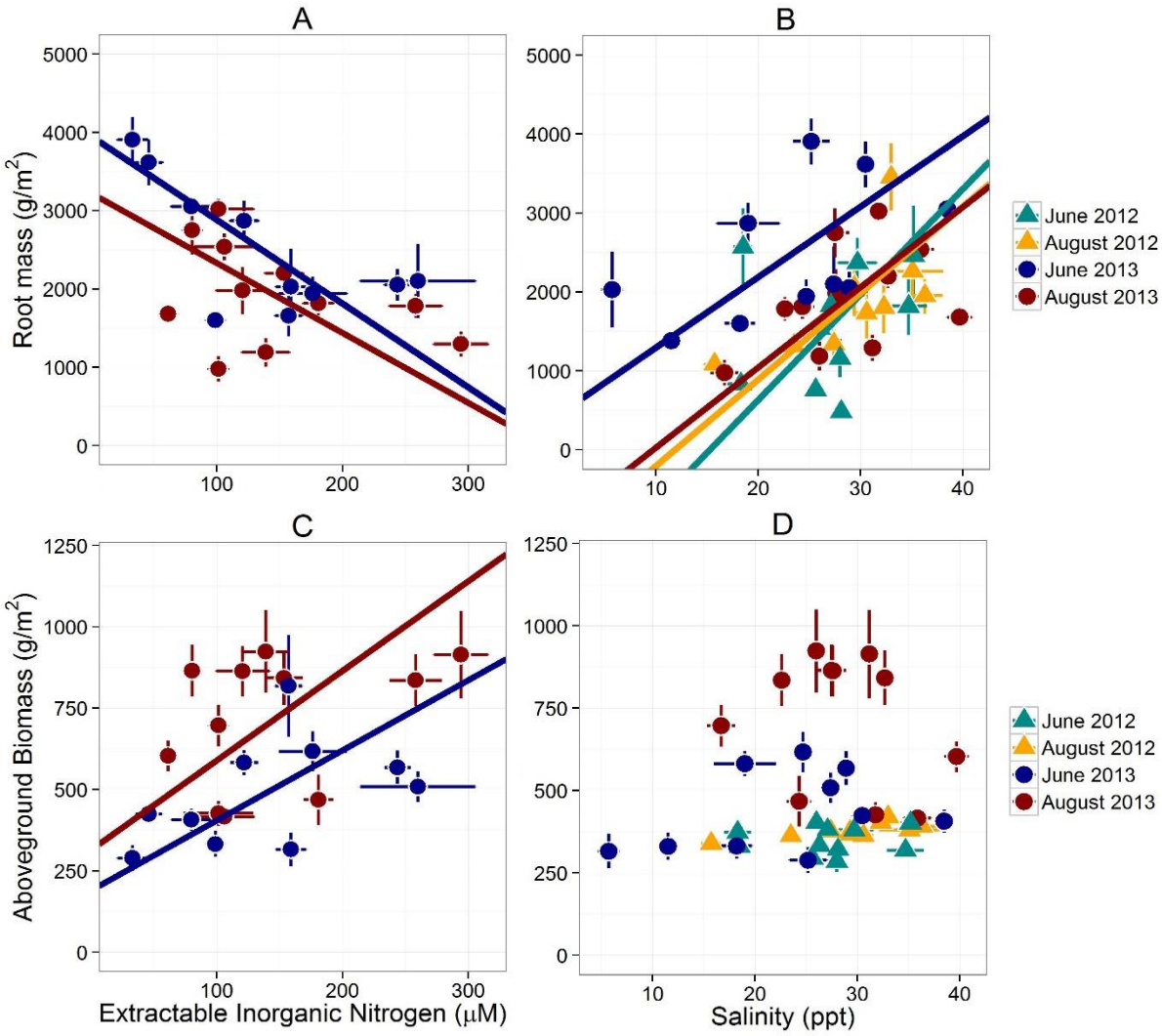

Figure 5.2: (A) At the site level, root mass of *Spartina alterniflora* was negatively associated with extractable inorganic nitrogen content of sediments in June 2013 [$slope_{SMA}$ = -10.72, n = 10, R^2 = 0.49] and August 2013 [$slope_{SMA}$ = -8.94, n = 11, R^2 = 0.13]. (B) Root mass was positively associated with the salinity of sediment porewater in June 2012 [$slope_{SMA}$ = 133.4, n = 10, R^2 = 0.05], August 2012 [$slope_{SMA}$ = 109.4, n = 10, p = 0.044, R^2 = 0.42], June 2013 [$slope_{SMA}$ = 89.19, n = 10, R^2 = 0.27], and August 2013 [$slope_{SMA}$ = 101.4, n = 11, R^2 = 0.19]. (C) Total aboveground biomass was positively associated with extractable inorganic nitrogen in June 2013 [$slope_{SMA}$ = 2.18, n = 10, R^2 = 0.23] and August 2013 [$slope_{SMA}$ = 2.75, n = 11, R^2 = 0.14], but (D) aboveground biomass was not related to salinity.

Chapter 6

Impacts of invasive-plant management on nitrogen-removal services in freshwater tidal marshes

Abstract

Establishing relationships between biodiversity and ecosystem function is an ongoing endeavor in contemporary ecosystem and community ecology, with important practical implications for conservation and the maintenance of ecosystem services. Removal of invasive plant species to conserve native diversity is a common management objective in many ecosystems, including wetlands. However, substantial changes in plant community composition have the potential to alter sediment characteristics and ecosystem services, including permanent removal of nitrogen from these systems via microbial denitrification. A balanced assessment of costs associated with keeping and removing invasive plants is needed to manage simultaneously for biodiversity and pollution targets. I monitored small-scale removals of *Phragmites australis* over four years to determine their effects on potential denitrification rates relative to three untreated *Phragmites* sites and adjacent sites dominated by native *Typha angustifolia*. Sediment ammonium increased following the removal of vegetation from treated sites, likely as a result of decreases in both plant uptake and nitrification. Denitrification potentials were lower in removal sites relative to untreated *Phragmites* sites, a pattern that persisted at least two years following removal as native plant species began to re-colonize treated sites. These results suggest the potential for a trade-off between invasive-plant management and nitrogen-removal services. A balanced assessment of costs associated with keeping versus removing invasive plants is needed to adequately manage simultaneously for biodiversity and pollution targets.

Introduction

Characterizing relationships between biodiversity and ecosystem function is a central goal in contemporary ecological research (Loreau et al. 2001). Because many ecosystem functions provide essential services for human survival and well-being, this discussion is of vital importance to environmental management (Kremen 2005). For ecosystems that provide multiple ecosystem services, conserving biodiversity or functional diversity of the community is considered essential to preserving ecosystem function (Tilman 1999, Loreau et al. 2001). The increasing prevalence of invasive or exotic species, which are often responsible for reducing biodiversity and causing local extinctions of native species, is commonly thought to be antithetical to this goal (Simberloff 2015). Eradicating invasive species has become a common management practice, with the implicit assumption that removing invasives will increase biodiversity and restore one or more functions of the local ecosystem. However, relationships between biodiversity and ecosystem function depend on complex interactions between organisms and their environments, which themselves may be context dependent, making broad generalizations difficult (Hooper et al. 2005). In many cases, the traits of the dominant species in a community can be more important than diversity in controlling ecosystem services (Grime 1998, Smith and Knapp 2003, Díaz et al. 2007). Invasive species, which often become dominant species in a community and are known to impact sediment nutrient cycling processes, therefore have the potential to create conflicting management goals (Ehrenfeld 2003, Stein et al. 2014).

This tradeoff may be especially important in wetlands. Wetland ecosystems provide a wealth of services, including flood abatement, support for biodiversity, and improvement of water quality, that together has been valued at approximately $3000 per hectare annually (Zedler 2003). At least 50% of the global wetland area has been lost to agricultural, urban, and rural

development, and many of the remaining wetlands are considered to be “degraded” due to eutrophication and the increasing dominance of invasive species (Bertness et al. 2002, Zedler and Kercher 2005). Wetlands have been found to be particularly susceptible to invasions by opportunistic plant invaders that form monotypic stands and displace native plant species; in fact, over 24% of the "worst plant invaders" are wetland plants (Zedler and Kercher 2004). Removal of invasive species to restore native plant biodiversity is thus a frequent target of restoration in wetland ecosystems (Martin and Blossey 2013). Some invasive plants are associated with differing rates of existing ecological processes or even novel processes (Vitousek and Walker 1989, Ehrenfeld 2003). One attribute of a successful invader is sequestration of limiting resources, and certain invasive plants are known to increase rates of nutrient removal in the wetlands they invade (Ehrenfeld 2003, Hansson et al. 2005). Removing invasive plants in these wetlands to restore native biodiversity could thus have negative consequences for nutrient-removal ecosystem services. Understanding the interactions between the various impacts of invasive species, as well as the consequences of removing invasives, is critical to determine a proper balance among potentially conflicting management goals for wetland systems.

In this chapter I investigated the impacts of small-scale *Phragmites australis* herbicide removals on sediment nutrient concentrations and denitrification potential. Using two years of pre-removal monitoring data and two years of post-removal monitoring data, I compared the nitrogen removal rates of treated sites to intact *Phragmites* stands and sites dominated by native *Typha angustifolia*. I also assessed the species composition of treated sites two years following removal, and compared traits relevant to nitrogen removal of the recolonizing plant community to plant communities at sites dominated by *Phragmites* and *Typha*. *Phragmites australis*, a clonal marsh grass, has been a frequent target of invasive-species management efforts (Kiviat

2006). Though *Phragmites australis* has been at least a minor component of brackish marshes in the United States for at least 40,000 years (Orson 1999), cryptic invasions of European haplotypes of *Phragmites* beginning in the 1800s caused a dramatic increase in abundance and size of existing *Phragmites* stands, as well as aggressive colonization into freshwater and brackish marshes beyond the limits of the native's historic range (Saltonstall 2002). The invasive haplotypes of *Phragmites* are particularly adept at colonizing disturbed or nutrient-rich aquatic systems (Kettenring et al. 2012), and once established reach heights of up to 4 meters and biomass densities of 727-3663 g/m^2 (Meyerson et al. 2000a). Due to the dense, tall growth associated with *Phragmites*, local reductions in the native diversity of plant species are often observed following invasions (Chambers et al. 1999, Keller 2000, Silliman and Bertness 2004). *Phragmites* is also often considered to provide poor habitat conditions for native birds, fish, and invertebrates relative to native wetland plants (Benoit and Askins 1999, Fell et al. 2003), although it clearly provides habitat for some organisms (Kiviat 2013). For these reasons and for general aesthetic reasons, management organizations in the United States invest considerable sums, an estimated $4.6 million annually (Martin and Blossey 2013), on the control and eradication of *Phragmites*.

However, the same traits that allow *Phragmites* to form dense monocultures can also promote desired ecosystem services such as nutrient and pollutant remediation (Meyerson et al. 2000b, Windham et al. 2001), shoreline stabilization (Rooth and Stevenson 2000), and maintenance of wetland habitat in disturbed and urban areas (Kiviat 2013). In the Hudson Valley and throughout many highly developed regions of the United States, excessive nitrogen loading poses a considerable challenge to managing local water quality. *Phragmites* dominance in these areas may serve to improve water quality. *Phragmites* sequesters larger pools of

nitrogen aboveground because it exhibits much higher aboveground growth than native wetland plants, and its stems tend to remain standing following senescence (Meyerson et al. 2000b). *Phragmites* also aerates wetland sediments that would otherwise remain anoxic (Armstrong and Armstrong 1990), allowing greater production of nitrate (nitrification) and thus greater removal of nitrogen to the atmosphere as inert dinitrogen gas (via denitrification) (Otto et al. 1999, Windham and Ehrenfeld 2003).

Though a great deal of research has focused on the removal of *Phragmites* through mechanical, chemical, or biological means (Hazelton et al. 2014), most of these studies have focused on evaluating the success of these methods in eradicating *Phragmites*. Relatively less attention has been given to monitoring the impacts of *Phragmites* removal on nitrogen-removal ecosystem services (but see Meyerson et al. 1999, Findlay et al. 2003), and the plant communities that recolonize treated areas are only infrequently characterized (Hazelton et al. 2014). Following removal of vegetation with herbicide, lower rates of sediment aeration should decrease rates of nitrate production from ammonium via nitrification and limit the supply of nitrate to denitrifying microbes. The absence of plant uptake should further limit removal of ammonium from sediments to plant biomass. Therefore, I predicted that ammonium concentrations should increase in sediments following *Phragmites* removal and that denitrification potentials should decrease relative to vegetated sites. To my knowledge, this is only the second study to investigate the impacts of *Phragmites* removal on sediment denitrification potential (Findlay et al. 2003) and the first to have the opportunity to do so within replicated removal stands.

Methods

Site Description

In September 2010, the Eastern New York (ENY) Chapter of the Nature Conservancy initiated small-scale (0.30-0.76 ha) eradications of three stands of *Phragmites australis* from Ramshorn Marsh (N 42.216059, W -73.854959), a 308 ha freshwater tidal marsh located on the west shore of the Hudson river near Catskill, NY (Figure 6.1). Initial removals were performed with an application of Aquapro^{TM} glyphosate herbicide (7.0 L/ha) and LI-700 aquatic surfactant (1.25 ppm) from a Marsh Master^{TM} using a mounted spray system. Subsequent spot treatments of Aquapro^{TM} (1%) and LI-700 were applied in September 2011 and 2012 using low-volume backpack sprayers (Zimmerman and Shirer 2013).

I conducted an initial survey of denitrification potential, sediment organic content, and sediment ammonium and nitrate concentrations in the three *Phragmites* stands in Ramshorn Marsh in August 2009 prior to removal; four replicate locations were sampled in each of the stands. In August 2010, I expanded my pre-treatment survey to include three reference stands of *Phragmites*, one at Brandow Point (N 42.249440, W -73.824390) and two at West Flats (N 42.295549, W -73.786796), which were not selected for removal (Figure 6.1). These sites were similar to Ramshorn in terms of sediment chemistry and hydrology prior to treatment (Alldred and Baines 2011), and are located on the west shore of the Hudson River 5.4 km and 11.3 km northeast of Ramshorn Marsh, respectively. In August 2010, I sampled two locations within each *Phragmites* reference stand, one location within each *Phragmites* stand in Ramshorn designated for removal, and one paired *Typha*-dominated area near each Ramshorn *Phragmites* stand (total of 12 sampling locations). Following removal in September 2010, I repeated my sampling in September 2011, June 2012, and September 2012. At each of these times, I sampled

three locations in the reference *Phragmites* stands (hereafter "Reference-*Phragmites*"), three locations in the treated *Phragmites* stands ("Ramshorn-Removal"), and six locations in *Typha*-dominated areas near each of the *Phragmites* stands ("Reference-*Typha*" and "Ramshorn-*Typha*").

Vegetation

In September 2011 and June 2012, I measured aboveground biomass and leaf carbon and nitrogen content for all locations sampled at the reference sites, but I refrained from collecting biomass samples at Ramshorn due to concerns that *Phragmites* regrowth could escape follow-up herbicide treatments if clipped. In September 2012 I received permission from the Nature Conservancy to add biomass and leaf carbon and nitrogen content measurements to sampling at Ramshorn locations as well. I harvested all aboveground biomass within two haphazardly placed quadrats (25 x 25 cm) within a 2 m radius of each sediment-sampling location. Harvested biomass was dried, weighed, and subsampled for analysis of leaf carbon and nitrogen content using a Perkin Elmer Series II CHNS Analyzer. For September 2012 data, I identified harvested biomass to species and determined dry mass and leaf carbon and nitrogen content for each component plant species within each quadrat. Plot-level data for vegetation measurements were calculated as an average weighted by the biomass of the component species.

Porewater Nutrients

I measured sediment nutrient profiles using PVC porewater equilibrators with 12 ml sampling wells spaced vertically at 3 cm intervals. Equilibrators were filled with dionized water, covered with a Spectr-Por cellulose membrane, and deoxygenated overnight by bubbling with nitrogen gas prior to installation in sediments (Hesslein 1976). Equilibrators were left in vegetated sediments at each sampling location for 7-10 days. Porewater was collected from

sampling wells using a syringe and stored in acidified vials until analysis. In 2009, samples were analyzed for ammonium and nitrate by ion chromatography and in all subsequent years using standard colorimetric methods (Jones 1984, Parsons et al. 1984a). After 2010, porewater was also sampled from ~5-10 cm below the sediment surface using a syringe-vacuum porewater sipper; sipper samples were frozen at -20° C until analysis using standard colorimetric methods.

Denitrification potential

Duplicate sediment cores from each sampling location were collected with a 7 cm diameter metal corer to a depth of ~10-15 cm for assays of denitrification potential. Samples were stored at 4 C and analyzed within 24 hours of sampling. A five gram subsample was amended with potassium nitrate (KNO_3), glucose, chloramphenicol, and acetylene and incubated under anaerobic conditions for 90 minutes (Smith and Tiedje 1979b). Headspace samples were collected at 30 and 90 minutes and stored in pre-evacuated glass vials. Gas samples were analyzed for N_2O using electron capture gas chromatography. This method provides a relative measurement of the maximum potential of the microbial community to perform denitrification and has been demonstrated to be a useful measurement for comparing experimental treatments (Groffman et al. 2006), but it should not be interpreted as a measure of absolute denitrification rates.

A subsample of each core was also used to determine sediment moisture content (change in mass after drying at 70°C for a minimum of 24 hours), total organic content (loss after combustion at 450°C for 4 hr), and total nitrogen and carbon content (CHNS analysis as described for vegetation samples).

Statistical Analysis

Differences in plant community composition among the three dominant vegetation types [*Phragmites*, *Typha*, Removal] were assessed using discriminant analysis of duplicate aboveground-biomass plots in September 2012. This method attempts to characterize an a priori grouping (in this case, three dominant vegetation types), based on a linear combination of predictor variables (in this case, biomass of the component species occupying the plots). If the plant community at the removal sites reverted to a *Typha*- or *Phragmites*-dominated community within the time frame of my study, the discriminant analysis would fail to distinguish the removal sites from one of these dominant vegetation types. If the plant community at removal sites switched to a novel community following herbicide treatment, the discriminant analysis would succeed in assigning removal plots to this novel vegetation type. Differences in plant traits [aboveground biomass, leaf nitrogen content, total plant nitrogen content] measured in September 2012 among the three dominant vegetation types [*Phragmites*, *Typha*, Removal] were analyzed with a one-way ANOVA. A separate two-way ANOVA was used to compare *Phragmites* and *Typha* communities sampled at the reference sites at two additional sampling times [September 2011, June 2012, September 2012]. Measurements of sediment nitrogen and carbon collected August 2010-September 2012 were also analyzed with a two-way ANOVA to compare the three dominant vegetation groups.

Measurements of denitrification potential, sediment porewater nutrients, and total sediment organic content were analyzed at the stand scale using 2-way ANOVA. Because the "Reference-*Typha*" treatment group was not added until September 2011, it was necessary to analyze the data using two different statistical designs. The first compared the three "treatments" [Ramshorn-Removal, Ramshorn-*Typha*, Reference-*Phragmites*] that were sampled across all

"sampling times" [August 2010, September 2011, June 2012, September 2012], both before *and* after herbicide treatment. For these ANOVAs, significant impacts of herbicide treatment on dependent variables [denitrification potential, sediment ammonium content, and sediment organic content] were tested as planned comparisons within the interaction term (treatment x sampling time). In the second statistical design, I compared four treatments [Ramshorn-Removal, Ramshorn-*Typha*, Reference-*Typha*, Reference-*Phragmites*] for sampling times that occurred after herbicide treatment [September 2011, June 2012, September 2012]. For these ANOVAs, significance of herbicide treatment was assessed for the dependent variables listed above and additional measurements added in 2011 [total organic carbon and nitrogen content of sediments] using planned comparisons of treatments. Planned comparisons of Ramshorn-Removal and Reference-*Phragmites* sampling times were used to test for significant differences between sites where *Phragmites* was removed relative to sites where *Phragmites* was left intact. Planned comparisons of Reference-*Typha* and Reference-*Phragmites* were used to test whether sites dominated by plant species differed when left undisturbed. Though I attempted to control for phenology by sampling at peak biomass in each of our sampling years (late August/early September), I acknowledge that other factors such as temperature may influence sediment chemistry and microbial activity. The planned comparisons of treatment and reference sites statistically control for interannual and seasonal variability when detecting treatment effects. Statistical analyses were performed in JMP (JMP(R) 1989-2007). Graphs were produced in R using the package ggplot2 (Wickham and Chang 2015).

Results

Vegetation

In September 2011, one year following initial herbicide application, the removal sites in Ramshorn Marsh remained largely unvegetated, except for sparse regrowth of *Peltandra virginica* (Figure 6.2B). By September 2012 the removal sites had been colonized by a community dominated by *Leersia oryzoides*, *Polygonum arifolium*, *Peltandra virginica*, *Impatiens capensis*, *Scirpus fluviatilis*, and *Scirpus tabernaemontani* (Figure 6.2C). This community was distinct in species composition from other marsh communities dominated by *Typha angustifolia* or *Phragmites australis* (Figure 6.3, Table 6.1). Removal communities were also characterized by lower aboveground biomass (Figure 6.4A, Table 6.2) and leaf nitrogen content (Figure 6.4B, Table 6.2), relative to *Phragmites*-dominated reference sites. In all cases, *Phragmites*-dominated sites greatly exceeded other plant communities in aboveground biomass production and leaf nitrogen content (Table 6.2). For both *Typha*-dominated communities and removal communities, leaf nitrogen content was negatively correlated with aboveground biomass at the plot level; for *Phragmites*-dominated communities, this correlation was weak and of small effect (Figure 6.4C). Sediments in *Phragmites*-dominated sites on average contained slightly more organic carbon than *Typha*-dominated sites (Figure 6.5A), but the variation in this measurement was sufficiently high that results were non-significant at $\alpha = 0.05$ (Table 6.2). Sediment organic nitrogen, however, was significantly greater for *Phragmites*-dominated sites than *Typha*-dominated sites, and slightly higher on average than in removal communities (Figure 6.5B, Table 6.2).

Porewater Nutrients

Average porewater nitrate concentrations remained at or below 0.02 mg/L (i.e., the detection limit for our analytical methods) across all treatments throughout our study; therefore, only results of porewater ammonium are reported. Following initial herbicide treatment, porewater ammonium concentrations in removal sites increased by over an order of magnitude relative to all vegetated sites (Figure 6.6, Table 6.2); they returned to pretreatment levels within two years (Figure 6.6).

Denitrification Potential

The most striking source of variation in denitrification potential was time, with average measurements varying nearly 8-fold among seasons and years (Figure 6.7, Table 6.2). Nevertheless, denitrification potential in removal sites decreased significantly by approximately 50% relative to intact *Phragmites*-dominated reference locations (Figure 6.7, Table 6.2); this effect remained remarkably constant two years following initial herbicide application (Figure 6.7). With the exception of anomalously high denitrification potential measurements at the reference *Typha* sites in September 2011, denitrification potentials were consistently highest in *Phragmites*-dominated sites, and were significantly higher than *Typha*-dominated sites in Ramshorn Marsh at $\alpha = 0.10$ (Table 6.2).

Discussion

The removal of invasive *Phragmites australis* had a significant negative impact on nitrogen-removal processes in Ramshorn Marsh. Following removal, available inorganic ammonium concentrations in the sediments rose by over an order of magnitude (Figure 6.6), and denitrification potential decreased by 50% relative to sites with intact *Phragmites* (Figure 6.7). This difference in denitrification potential between treated and untreated sites persisted for at

least two years following initial herbicide application (Figure 6.7). The impacts I observed in this study are consistent with the results of the only other study to examine changes in denitrification potential following eradication of *Phragmites* (Findlay et al. 2003). Moreover, the effectiveness of *Phragmites* in promoting nitrogen-removal services, relative to native plant communities in our sites, is consistent with what one would expect based on extensive characterization of this plant invader (Meyerson et al. 1999, Meyerson et al. 2000b, Windham and Meyerson 2003). *Phragmites* is known to sequester larger pools of nitrogen in both above and belowground growth (Meyerson et al. 2000b), as well as to aerate otherwise anoxic sediments (Armstrong and Armstrong 1990), promoting removal of nitrogen via coupled nitrification-denitrification. Following herbicide treatment, assimilation of inorganic nitrogen into plant tissues would cease, and roots would no longer introduce oxygen to sediments, hindering oxidation of ammonium to nitrate. This sequence of events should result in a build-up of sediment ammonium, which I clearly observed (Figure 6.6). Though total inorganic nitrogen levels increased, I expected denitrification potential to decrease due to limitation of denitrifying microbes by nitrate (oxidant). Not only did I observe an initial decrease in denitrification potential in treated sites relative to intact *Phragmites*-dominated sites, this effect persisted two years following the initial treatment, even as native plant communities began to recolonize the treated sites.

This study is one of the few that have characterized the plant community that recolonized sites following *Phragmites* eradication (Hazelton et al. 2014). Consistent with those studies, I found that, rather than recovering to a similar native plant community found elsewhere in the marsh, the sites shifted to a completely different suite of species. The results of my vegetation surveys were consistent with surveys of 1.0 m^2 plots conducted by the Nature Conservancy at the

same marsh locations (Zimmerman and Shirer 2013). In this case, the new community was characterized primarily by the presence of *Leersia oryzoides* and *Polygonum arifolium*, rather than *Typha*-dominated marshes that are typical of emergent wetlands in the Hudson River (Figure 6.3). Notably, many of these species are commonly found in the understory of *Typha*-dominated marshes in the Hudson River, and may represent an early stage in the succession of a tidal marsh community in this system (Zimmerman and Shirer 2009). This new community attained only 1/4 of the peak biomass of a *Phragmites*-dominated community and contained less than half the nitrogen content of a mature *Phragmites* leaf (Figure 6.4A and 6.4B). Overall, the capacity of this community to store nitrogen in aboveground tissue is severely reduced relative to both *Phragmites*- and *Typha*-dominated communities (Figure 6.4). The net effect of species succession in this case could serve to increase the amount of time needed for a site to recover nitrogen-removal capacity following invasive species removal. Though I did not measure belowground traits of the plant communities, the lag in recovery of denitrification potential (Figure 6.7) suggests that plant communities may also differ in their belowground impacts on microbial processes. In order to fully understand impacts of plant-community alterations on ecosystem processes, belowground measurements should be given greater attention in future studies.

The success of *Phragmites* as an invader is often attributed to its ability to alter sediment nutrient cycles such that it has a competitive advantage relative to native plant species (Meyerson et al. 2000b). Specifically, *Phragmites* has been shown to increase pools of organic nitrogen relative to inorganic nitrogen in sediments, which other native plants are less efficient at assimilating (Meyerson et al. 2000b, Mozdzer et al. 2010). My results suggest that such a mechanism may be at work in the Hudson River. I found significantly higher concentrations of

total organic nitrogen in sediments of *Phragmites*-dominated sites, relative to sites inhabited by native *Typha*-dominated plant communities (Figure 4B, Table 2). Moreover, total aboveground biomass was negatively correlated with leaf nitrogen in native plant communities, which is a common sign of nutrient competition within a plant community (Figure 3C). This correlation was much weaker for *Phragmites*, which is consistent with relaxed nutrient competition in *Phragmites*-dominated sites due to access to an additional pool of organic nitrogen. Relaxed nutrient competition, along with resprouting from rhizomes and quickly producing high aboveground biomass, may explain the difficulty in permanently eradicating stands of *Phragmites* (Hazelton et al. 2014).

Overall, *Phragmites*-dominated plant communities assimilate more nitrogen in aboveground biomass (Figure 3) and store more nitrogen in organic form in sediments (Figure 4) than native plant communities. Further, the removal of *Phragmites* resulted in significant increases in dissolved inorganic nitrogen pools (Figure 6) and significant decreases in the potential of the microbial community to permanently remove nitrogen to the atmosphere via denitrification (Figure 7). Together, these results suggest a management trade-off between eradicating *Phragmites* to restore a diverse native plant community and promoting nitrogen-removal ecosystem services in the wetland. Certainly, management actions such as immediate replanting of native plants could help ameliorate these impacts, but follow-up herbicide treatments are always required, and some degree of disturbance is likely to be inevitable (Kettenring and Adams 2011, Lombard et al. 2012). In light of this trade-off in management priorities, the question then becomes: When and where is *Phragmites* eradication likely to significantly impact local water quality? For small, isolated patches of *Phragmites* in a system like the Hudson, which is relatively hydrologically open and well flushed by periodic tidal

inundation, the impact on water quality is likely to be quite small relative to the benefit of restoring native diversity and improving habitat conditions for wildlife. However, for systems in which *Phragmites* has become the major plant community in the landscape, complete eradication is not only unlikely (Kettenring and Adams 2011) but may result in water quality problems that outweigh the benefits of biodiversity restoration, particularly for aquatic systems where water sources are smaller or hyrologically isolated. Invasive-species management highlights the need to develop specific management priorities for ecosystems. Frameworks are continually being developed that seek to optimize the provisioning of multiple ecosystem services, with the understanding that management priorities may in some cases conflict (Findlay et al. 2002, Wainger et al. 2010, Truitt et al. 2015).

Phragmites management in the Hudson River Estuary provides one example of a situation in which biodiversity does not maximize delivery of an ecosystem service; in this case a dominant species with traits that maximize opportunistic nutrient acquisition and high biomass production also maximizes nitrogen-removal ecosystem services. In addition to nitrogen removal, *Phragmites* is credited with additional ecosystem services including carbon and heavy metal sequestration, soil stabilization, and habitat provisioning for both common and rare native animals (Kiviat 2013). Other exotic grasses have been found to store carbon and provide forage for grazing animals (Stein et al. 2014). Ecosystems dominated by invasive species and low-diversity communities challenge simple assumptions that biodiversity should beget greater value for multiple ecosystem functions. Particularly in urbanized and highly modified systems, invasive species like *Phragmites* can have quantifiable functional value both to the environment and local human societies that may not be easily achieved with native communities. In such cases, a holistic approach that begins with explicit management priorities, and considers potential

trade-offs among management outcomes, is likely to provide the best solutions to management and restoration.

Table 6.1: Discriminant analysis of plant communities. Three a priori vegetation-cover types [*Phragmites*, *Typha*, Removal] were distinguished based on a weighted linear combination of component species' biomass. (Wilks' $\Lambda = 0.017$, Approx. $F_{18,26} = 9.603$, $p < 0.001$, percent misclassified = 4.167)

Canonical Axis	Eigenvalue	% Variance Explained	Cumulative % Explained	Canonical Correlation
1	12.705	79.54	79.54	0.96
2	3.268	20.46	100.00	0.87

Table 6.2: Summary of p values from ANOVAs comparing vegetated communities before and after herbicide application to "Removal" sites in Ramshorn Marsh. Results significant at $\alpha = 0.10$ are shown in bold. For full ANOVA tables, see Appendix E.

Dependent Variable	Years Included in Analysis	Time	Vegetation	Before-Treatment Comparisons			After-Treatment Comparisons			Time x Vegetation
				Phragmites v Removal	*Typha* v Removal	*Phragmites* v Typha	*Phragmites* v Removal	*Typha* v Removal	*Phragmites* v *Typha*	
Denitrification Potential	2010-2012	**0.0018**	0.1122	0.8896	0.9675	0.9269	**0.0471**	0.9134	**0.0591**	0.9066
	2011-2012	**0.0046**	0.1938				**0.0874**	0.9259	0.7594	0.2590
Sediment Ammonium	2010-2012	**0.0335**	**0.0162**	0.9858	0.9772	0.9472	**0.0007**	**0.0054**	0.4215	**0.0330**
	2011-2012	**0.0861**	**0.0016**				**0.0007**	**0.0055**	0.9244	**0.0385**
Sediment Organic Content	2010-2012	0.8467	0.4542	0.6109	0.9205	0.6935	0.2737	0.7354	0.4446	0.8830
	2011-2012	0.5938	0.4099				0.2763	0.6175	0.1108	0.7872
Aboveground Biomass	2011-2012	0.6601	**0.0079**						**0.0079**	0.9274
	Sep. 2012		0.1186				**0.0464**		0.1386	
Leaf Nitrogen	2011-2012	**0.0001**	**0.0004**						**0.0004**	0.5456
	Sep. 2012		**0.0408**				**0.0408**		**0.0651**	
Sediment Carbon	2010-2012	0.3356	0.1318				0.1096		**0.0609**	0.5124
Sediment Nitrogen	2010-2012	0.3997	**0.0237**				**0.0549**		**0.0077**	0.6416

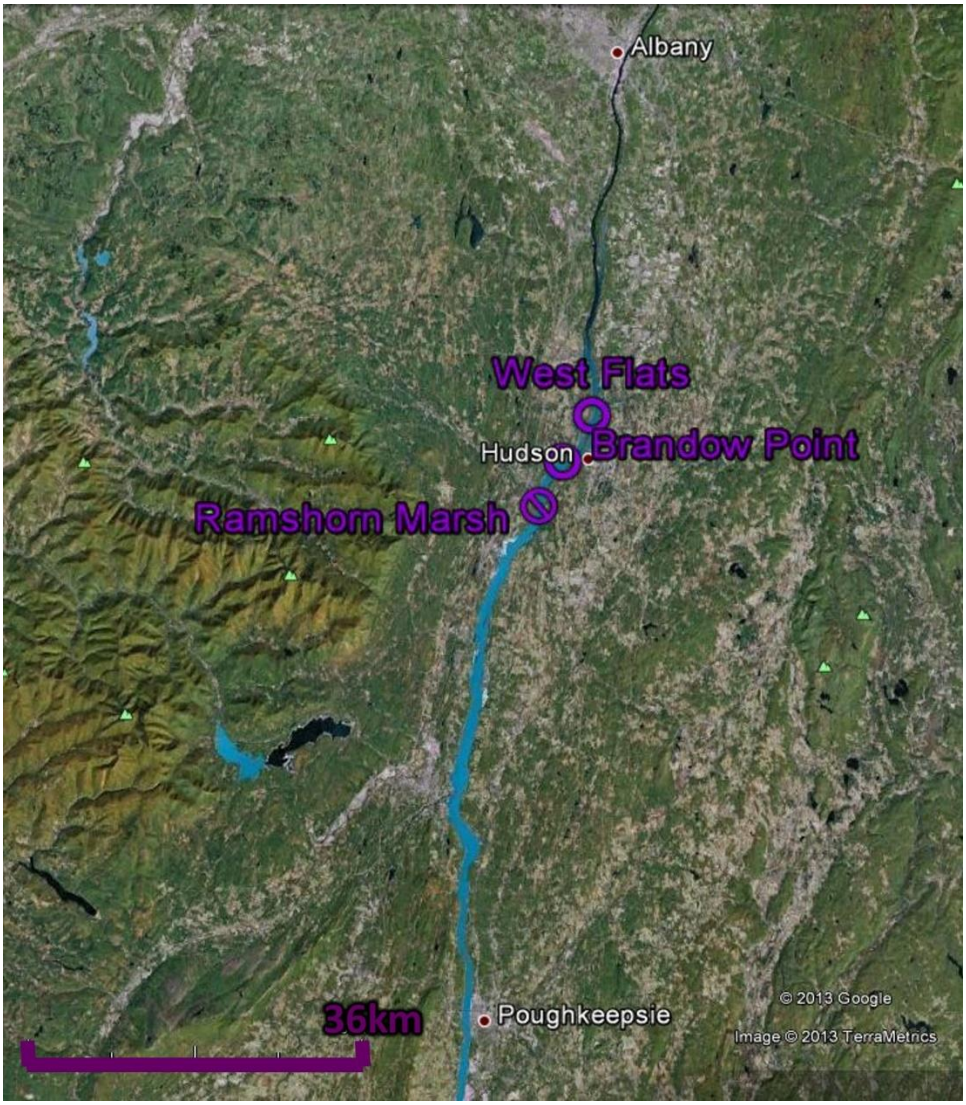

Figure 6.1: Map of sites included in field sampling. *Phragmites* removals ocurred at Ramshorn Marsh. Intact *Phragmites* stands were monitored at West Flats and Brandow Point (hereafter referred to as "Reference" sites). *Typha*-dominated communities were monitored at all sites.

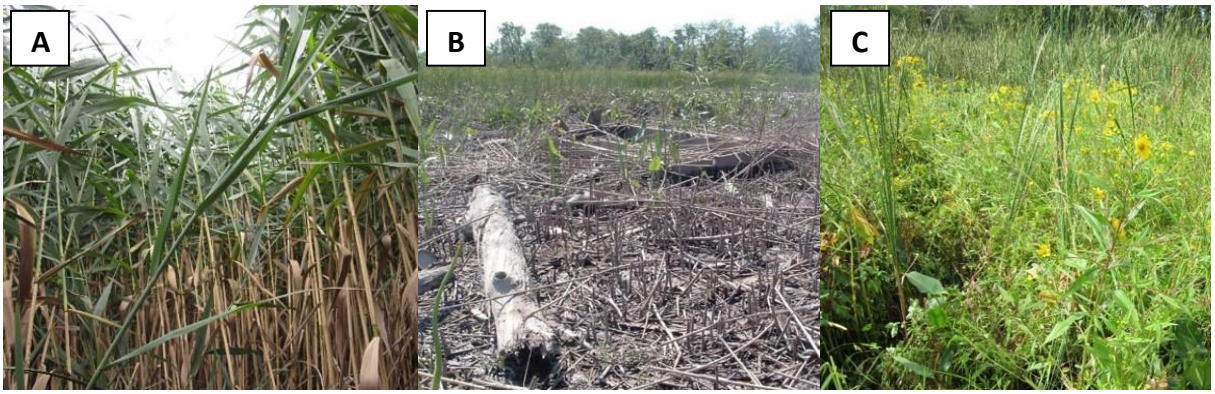

Figure 6.2: Photos from Ramshorn Marsh taken (A) prior to removal in August 2010, (B) one year following removal in September 2011, and (C) two years following removal in September 2012.

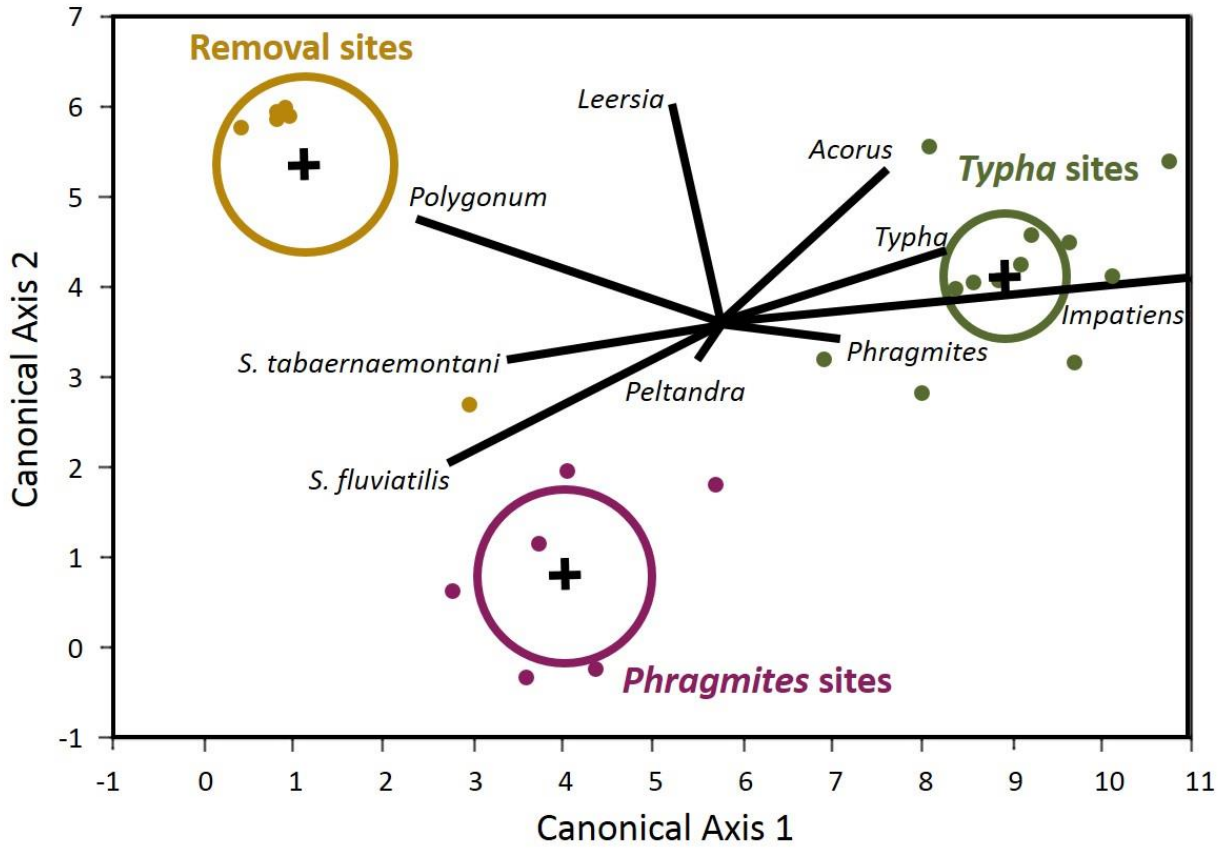

Figure 6.3: Biplot of dicriminant analysis for three dominant vegetation classifications [*Phragmites*, *Typha*, Removal] sampled in September 2012. Independent variables used to discriminate among the classifications were the biomasses of the component plant species at individual sampling plots. Rather than reverting from a *Phragmites*-dominated (purple) to a typical *Typha*-dominated community (green), communities shifted to a novel community characterized by *Leersia oryzoides* and *Polygonum arifolium* (brown) two years after initial herbicide treatment.

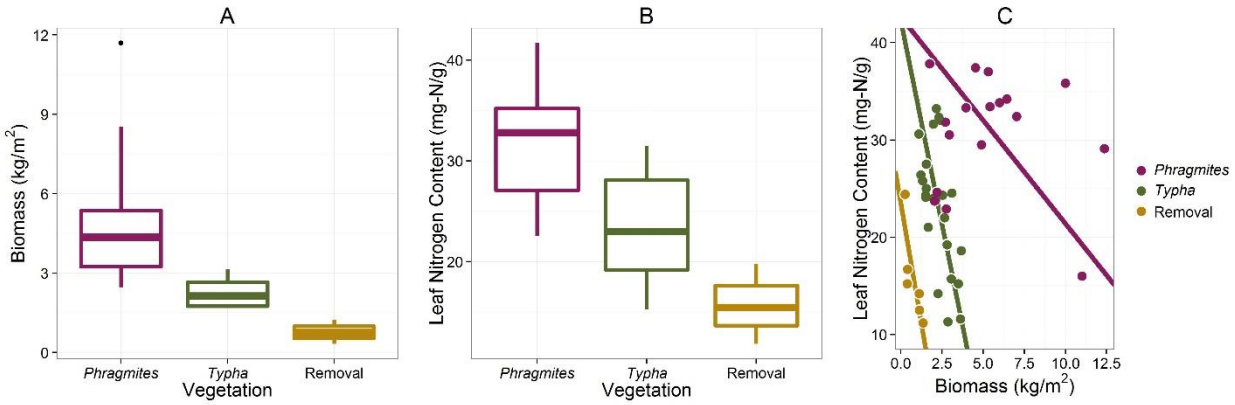

Figure 6.4: Differences in (A) aboveground biomass and (B) leaf nitrogen content among the three dominant vegetation classifications. *Phragmites*-dominated communities reach a higher peak biomass and assimilate more nitrogen per gram of leaf material than *Typha*-dominated and removal communities. Boxplots represent the median and interquartile range, and whiskers extend to the most extreme point within 1.5 times the interquartile range. (C) The nitrogen content of leaves decreases with increasing biomass in *Typha*-dominated (n = 24, $slope_{SMA}$ = -8.34, r = 0.59, p = 0.0023) and removal communties (n = 6, $slope_{SMA}$ = -9.92, r = 0.80, p = 0.0549), indicating nutrient limitation. Leaf nitrogen was not significantly correlated to aboveground biomass in *Phragmites*-dominated communities (n = 18, , $slope_{SMA}$ = -2.12, r = 0.23, p = 0.3584).

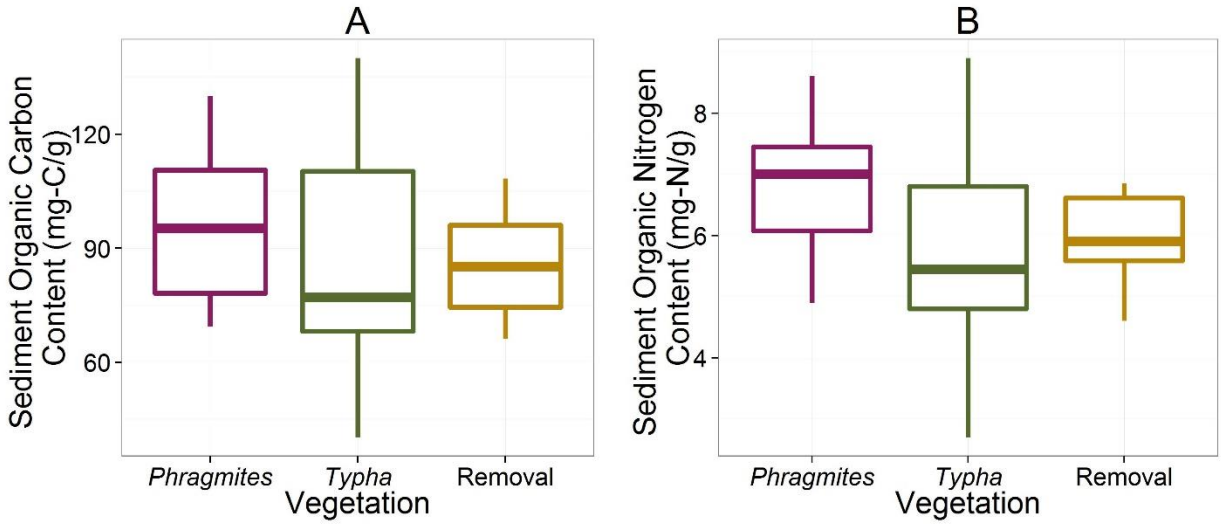

Figure 6.5: Sediments in *Phragmites*-dominated plant communities tend to contain (A) marginally higher organic-carbon content and (B) significantly higher organic nitrogen content than in *Typha*-dominated and removal communites. This results suggests the potential for higher organic-nitrogen storage in sediments in *Phragmites*-dominated sites. Boxplots represent the median and interquartile range, and whiskers extend to the most extreme point within 1.5 times the interquartile range.

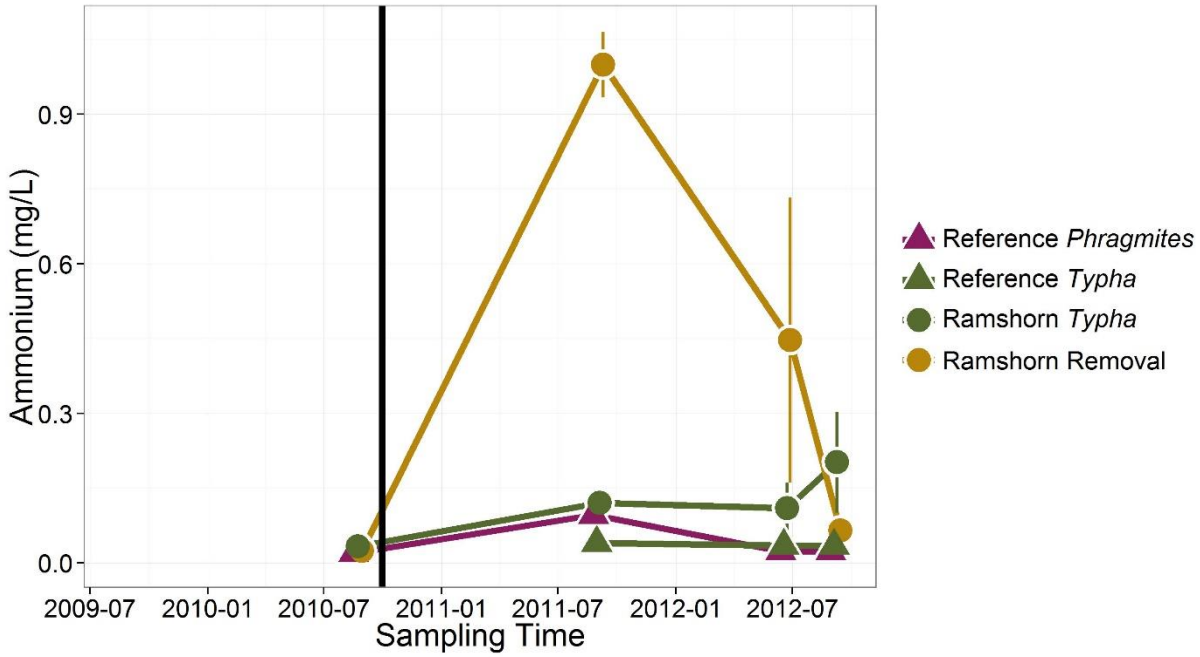

Figure 6.6: Following herbicide treatment in September 2010 (vertical black line), ammonium concentrations in sediments of treated sites increased by an order of magnitude relative to sites vegetated with *Phragmites* or *Typha*. Ammonium concentrations returned to pretreatment levels within two years of initial treatment. Error bars show standard errors.

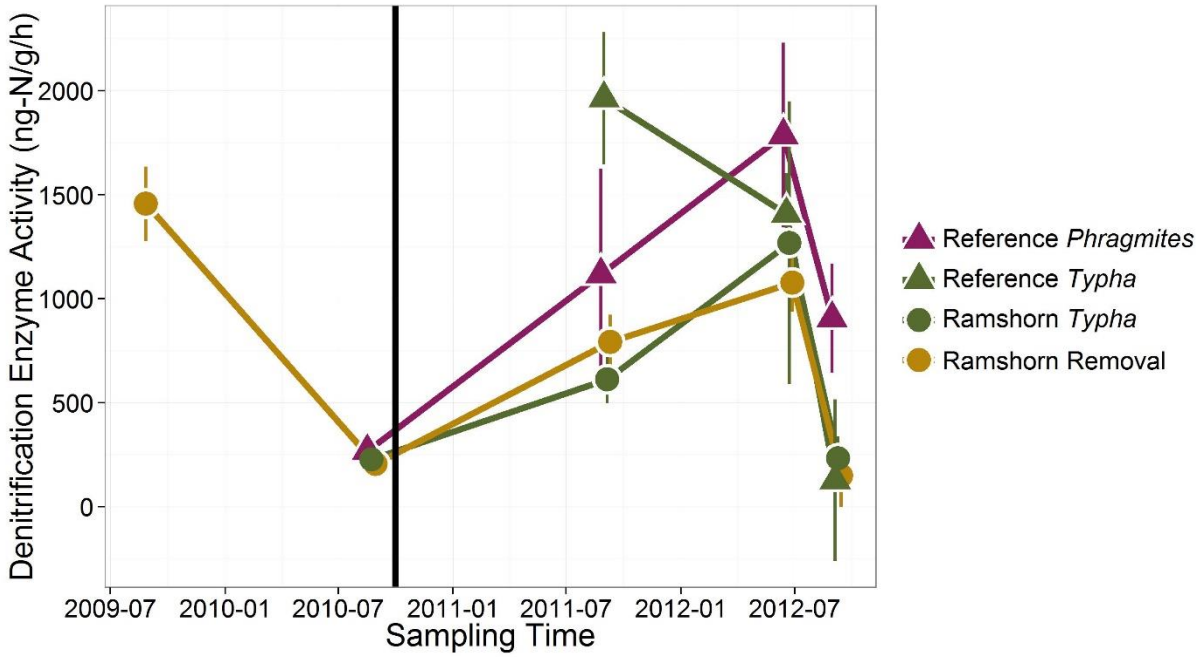

Figure 6.7: Denitrification potentials at all sites showed substantial interannual and interseasonal variability. Relative to *Phragmites*-dominated sites (purple), denitrification potentials in removal sites (brown) decreased by 50% following initial herbicide treatment (vertical black line). This effect persisted for two years following removal. Error bars show standard errors.

Chapter 7

Conclusions

Human activities have resulted in an unprecedented rate of global change in ecosystems worldwide (Millennium Ecosystem Assessment 2005). Ecological communities are changing rapidly due to global climate change, sea-level rise, species introductions, and land-use alterations (Chapin III et al. 2000). Because species composing ecological communities respond differently and at different rates to these various environmental pressures and have, in some cases, been artificially introduced to systems they would not inhabit naturally, humans have facilitated the emergence of novel, or "no analog," communities and ecosystems (Hobbs et al. 2006). To predict how these novel ecosystems will function and manage the services they may provide, we must extrapolate beyond observations in current and past ecosystems (Mitsch and Jørgensen 2003, Hooper et al. 2005). In this dissertation, I applied a trait-based theoretical framework to predict the effects that plant communities have on nitrogen cycling, based on hypothesized relationships between components of the nitrogen cycle and characteristics of wetland plants (Chapter 1). This approach has immediate practical applications for the difficult management challenge of predicting rates of microbial denitrification and associated nitrogen-removal ecosystem services, and provides a test of the utility of trait-based methods to describe and predict the influence of organisms on ecosystem functioning.

In Chapter 2, in a systematic review and meta-analysis of 419 published measurements of denitrification in plant communities dominated by different plant species I confirmed that wetland plants have a demonstrable effect on denitrification. The influence of vegetation on denitrification rates has been a missing component in understanding how to manage nitrogen removal in aquatic systems for some time (Boyer et al. 2006), and this study represented the first

generalizable estimate of this effect. Though isolated studies in the literature indicated that plants may exert control over microbial denitrification rates (Caffrey and Kemp 1990, Caffrey and Kemp 1992, Ehrenfeld and Scott 2001, Ehrenfeld 2003, Windham and Ehrenfeld 2003), the generality of plant-mediated effects and the variation in impact among species remained largely unresolved. I found that plants increased denitrification rates by 55% on average, and the impact was found to differ significantly among plant communities. My estimate was robust to the use of different experimental methods, which is a major concern in denitrification research (Groffman et al. 2006).

Having established that wetland plants differ in their impacts on sediment denitrification (Chapter 2), I investigated the mechanisms by which a dominant salt marsh grass, *Spartina alterniflora*, influences sediment oxygen and denitrification potential in greenhouse mesocosm experiments (Chapter 3). Using a novel combination of experimental methods, I determined that denitrification potentials correlated most strongly with plant traits that enhanced sediment aeration, most notably rhizome width. This finding supported the hypothesis that plant-mediated sediment aeration would indirectly enhance denitrification rates by promoting the production of nitrate via microbial nitrification. In Chapter 4, I addressed potential trait-process relationships by conducting field measurements in *Spartina alterniflora* salt marshes on Long Island, NY. Among eleven salt-marsh sites differing in nitrogen-loading intensity, I determined that simple linear models using plant-trait parameters provided comparable predictions of denitrification relative to those based on sediment chemistry. At the site level, root mass and leaf nitrogen content explained 52% of the total variation in denitrification rates. I further found that, among all sites, denitrification potentials in *Spartina*-dominated sediments were double those measured in adjacent non-vegetated control plots on average, with the influence of vegetation increasing

with total aboveground and belowground biomass of the plant community. Together with Chapter 3, these results support the utility of trait-based approaches in understanding the role of plant communities in promoting nitrogen-removal services in wetland ecosystems.

Belowground traits of *Spartina alterniflora*, which I found to be critical determinants of nitrogen-removal services and are also known to be critical determinants of salt-marsh stability, are expected to respond to both sea-level rise and increased nutrient loading. However, despite a long history of study (Valiela et al. 1976, Mendelssohn and Morris 2000), quantifying the multiple effects of nutrient loading on root biomass and marsh stability is an ongoing controversy in wetland research. In Chapter 5, I made use of two years of field-survey data from Long Island, NY to examine associations among root growth, nitrogen availability, and salinity. I found that total root mass correlated positively to salinity and negatively to extractable nitrogen content in sediments. These results indicate that further eutrophication may reduce marsh stability and that increasing salinity, perhaps as a result of future sea level rise (Craft et al. 2008), may increase marsh stability.

Removal of invasive plant species to conserve native plant diversity is a major management goal in many ecosystems, including wetlands (Tilman et al. 1997, Loreau et al. 2001, Zedler and Kercher 2005). However, substantial changes in the trait composition of plant communities, which are frequently observed following plant invasions, have the potential to alter sediment characteristics and processes of management interest, including denitrification (Ehrenfeld 2003, Ehrenfeld 2010). In Chapter 6, I monitored the impacts of removing *Phragmites australis*, an invasive marsh grass, from freshwater tidal wetlands of the Hudson River and compared treated sites to intact *Phragmites* communities and native *Typha angustifolia* communities. As I predicted, sediment ammonium increased following the removal

of vegetation, likely as a result of decreases in both plant uptake and nitrification. Concurrently, sediment denitrification rates decreased relative to untreated *Phragmites* sites. Plant communities that recolonized treated sites produced less aboveground biomass and removed less nitrogen than either *Phragmites*- or *Typha*-dominated communities. Taken together, these results suggest the potential for a trade-off between managing invasive plants to achieve conservation goals and maintaining nitrogen-removal services.

My dissertation demonstrates the utility of trait-based conceptual frameworks in understanding how the functional compositions of ecological communities are likely to change in the future and projecting how these changes may affect ecosystem processes. Though my research to date indicates great potential for plant traits to explain variation in denitrification rates, several questions remain that would benefit from data-synthesis, remote sensing, and/or survey approaches that examine traits among a greater variety of multi-species communities.

A considerable benefit of using physiological plant traits as variables in predictive modelling is the potential to measure them at the landscape scale using remote-sensing technology (Serbin et al. 2014, Asner et al. 2015). Leaf traits such as nitrogen content, which I found to be an important predictor of denitrification potential in Chapter 4, can now be measured and mapped for whole ecosystems using data from hyperspectral imaging (Serbin et al. 2014). In addition to incorporating the influence of plants on process rates, responses in plant traits at the community level may provide biologically relevant proxies of sediment variables such as moisture and nitrogen availability (Kulkarni et al. 2008). These new remote-sensing methods provide a potentially powerful solution to the difficult challenge of describing and predicting patterns in ecosystem processes such as denitrification that cannot be measured at the canopy level.

Ecosystem-level trait variables, whether they are assessed using remote-sensing or traditional ground-assessment methods, could enhance predictions of ecosystem processes and services within a variety of modeling frameworks (Boyer et al. 2006). For example, the structure of my trait-based conceptual framework linking nitrogen cycling processes to plant traits (Figure 1.1) naturally lends itself to structural equation modelling (SEM) or Bayesian hierarchical approaches. SEM could provide a method for evaluating the importance of specific pathways in my conceptual framework using existing data from plant-trait and ecological monitoring databases (Kattge et al. 2011) or newly collected data from a greater variety of multispecies communities. Bayesian approaches benefit from the ability to integrate prior knowledge from multiple data sources and provide more precise predictions. For example, Bayesian approaches have been successfully used to integrate plant-trait and ecosystem-flux data to explain dynamics of carbon uptake and allocation in terrestrial ecosystems (LeBauer et al. 2013). Trait-based models, once established, may greatly assist efforts to extrapolate beyond the current range of ecological observations to predict processes and potential services of no-analog ecosystems (Keddy 1992, Lavorel and Garnier 2002, McGill et al. 2006).

References

Alldred, M., and S. B. Baines. 2011. Invasive-species removals and nitrogen-removal ecosystem services in freshwater tidal marshes. Hudson River Foundation, New York, NY.

Anisfeld, S. C., and T. D. Hill. 2012. Fertilization effects on elevation change and belowground carbon balance in a Long Island Sound tidal marsh. Estuaries and Coasts **35**:201-211.

Armstrong, J., and W. Armstrong. 1990. Light-enhanced convective throughflow increases oxygenation in rhizomes and rhizosphere of *Phragmites australis* (Cav.) Trin. ex Steud. New Phytologist **114**:121-128.

Armstrong, J., W. Armstrong, P. M. Beckett, J. E. Halder, S. Lythe, R. Holt, and A. Sinclair. 1996. Pathways of aeration and the mechanisms and beneficial effects of humidity- and Venturi-induced convections in *Phragmites australis* (Cav.) Trin. ex Steud. Aquatic Botany **54**:177-197.

Armstrong, W., R. Brändle, and M. B. Jackson. 1994. Mechanisms of flood tolerance in plants. Acta Botanica Neerlandica **43**:307-358.

Asner, G. P., R. E. Martin, C. B. Anderson, and D. E. Knapp. 2015. Quantifying forest canopy traits: imaging spectroscopy versus field survey. Remote Sensing of Environment **158**:15-27.

Ayers, M. A., J. G. Kennen, and P. E. Stackelberg. 2000. Water quality in the Long Island–New Jersey coastal drainages, New York and New Jersey, 1996–98. U.S. Geological Survey Circular **1201**:1-40.

Bachand, P. A. M., and A. J. Horne. 2000. Denitrification in constructed free-water surface wetlands: II. Effects of vegetation and temperature. Ecological Engineering **14**:17-32.

Bédard, C., and R. Knowles. 1989. Physiology, biochemistry, and specific inhibitors of CH_4, NH_4^+, and CO oxidation by methanotrophs and nitrifiers. Microbiological Reviews **53**:68-84.

Benoit, L. K., and R. A. Askins. 1999. Impact of the spread of *Phragmites* on the distribution of birds in Connecticut tidal marshes. Wetlands **19**:194-208.

Benotti, M. J., M. Abbene, and S. A. Terracciano. 2007. Nitrogen loading in Jamaica Bay, Long Island, New York: predevelopment to 2005. U.S. Geological Survey Scientific Investigations Report 2007–5051:1-16.

Bertness, M. D., P. J. Ewanchuk, and B. R. Silliman. 2002. Anthropogenic modification of New England salt marsh landscapes. Proceedings of the National Academy of Sciences of the United States of America **99**:1395-1398.

Boutin, C., and P. A. Keddy. 1993. A functional classification of wetland plants. Journal of Vegetation Science **4**:591-600.

Bowden, W. B. 1986. Nitrification, nitrate reduction, and nitrogen immobilization in a tidal freshwater marsh sediment. Ecology **67**:88-99.

Boyer, E. W., R. B. Alexander, W. J. Parton, C. Li, K. Butterbach-Bahl, S. D. Donner, R. W. Skaggs, and S. J. D. Grosso. 2006. Modeling denitrification in terrestrial and aquatic ecosystems at regional scales. Ecological Applications **16**:2123-2142.

Bradley, P. M., and J. T. Morris. 1990. Influence of oxygen and sulfide concentration on nitrogen uptake kinetics in *Spartina alterniflora*. Ecology **71**:282-287.

Brix, H., B. K. Sorrel, and P. T. Orr. 1992. Internal pressurization and convective gas flow in some emergent freshwater macrophytes. Limnology and Oceanography **37**:1420-1433.

Caffrey, J., and W. Kemp. 1991. Seasonal and spatial patterns of oxygen production, respiration and root-rhizome release in *Potamogeton perfoliatus* L. and *Zostera marina* L. Aquatic Botany **40**:109-128.

Caffrey, J. M., and W. M. Kemp. 1990. Nitrogen cycling in sediments with estuarine populations of *Potamogeton perfoliatus* and *Zostera marina*. Marine Ecology Progress Series **66**:147-160.

Caffrey, J. M., and W. M. Kemp. 1992. Influence of the submersed plant, *Potamogeton perfoliatus*, on nitrogen cycling in estuarine sediments Limnology and Oceanography **37**:1483-1495.

Caffrey, J. M., M. C. Murrell, C. Wigand, and R. McKinney. 2007. Effect of nutrient loading on biogeochemical and microbial processes in a New England salt marsh. Biogeochemistry **82**:251–264.

Chambers, R. M., L. A. Meyerson, and K. Saltonstall. 1999. Expansion of *Phragmites australis* into tidal wetlands of North America. Aquatic Botany **64**:261-273.

Chapin III, F. S., E. S. Zavaleta, V. T. Eviner, R. L. Naylor, P. M. Vitousek, H. L. Reynolds, D. U. Hooper, S. Lavorel, O. E. Sala, and S. E. Hobbie. 2000. Consequences of changing biodiversity. Nature **405**:234-242.

Cornwell, J. C., W. M. Kemp, and T. M. Kana. 1999. Denitrification in coastal ecosystems: methods, environmental controls, and ecosystem level controls, a review. Aquatic Ecology **33**:41-54.

Costanza, R., O. Pérez-Maqueo, M. L. Martinez, P. Sutton, S. J. Anderson, and K. Mulder. 2008. The value of coastal wetlands for hurricane protection. Ambio **37**:241-248.

Craft, C., J. Clough, J. Ehman, S. Joye, R. Park, S. Pennings, H. Guo, and M. Machmuller. 2008. Forecasting the effects of accelerated sea-level rise on tidal marsh ecosystem services. Frontiers in Ecology and the Environment **7**:73-78.

Deegan, L. A., D. S. Johnson, R. S. Warren, B. J. Peterson, J. W. Fleeger, S. Fagherazzi, and W. M. Wollheim. 2012. Coastal eutrophication as a driver of salt marsh loss. Nature **490**:388-392.

Díaz, S., S. Lavorel, F. de Bello, F. Quétier, K. Grigulis, and T. M. Robson. 2007. Incorporating plant functional diversity effects in ecosystem service assessments. Proceedings of the National Academy of Sciences **104**:20684-20689.

Drake, B., and J. Gallagher. 1984. Osmotic potential and turgor maintenance in *Spartina alterniflora* Loisel. Oecologia **62**:368-375.

Ehrenfeld, J. 2003. Effects of exotic plant invasions on soil nutrient cycling processes. Ecosystems **6**:503-523.

Ehrenfeld, J. G. 2010. Ecosystem consequences of biological invasions. Annual Review of Ecology, Evolution, and Systematics **41**:59-80.

Ehrenfeld, J. G., and N. Scott. 2001. Invasive species and the soil: effects on organisms and ecosystem processes. Ecological Applications **11**:1259-1260.

Ericsson, T. 1995. Growth and shoot-root ratio of seedlings in relation to nutrient availability. Plant and Soil **168**:205-214.

Eviner, V. T., and F. S. Chapin III. 2003. Functional matrix: a conceptual framework for predicting multiple plant effects on ecosystem processes. Annual Review of Ecology Evolution and Systematics **34**:455-485.

Fell, P. E., R. S. Warren, J. K. Light, R. L. Rawson, Jr., and S. M. Fairley. 2003. Comparison of fish and macroinvertebrate use of *Typha angustifolia*, *Phragmites australis*, and treated *Phragmites* marshes along the lower Connecticut River. Estuaries **26**:534-551.

Findlay, S. E. G., P. M. Groffman, and S. Dye. 2003. Effects of *Phragmites australis* removal on marsh nutrient cycling. Wetlands Ecology and Management **11**:157-165.

Findlay, S. E. G., E. Kiviat, W. C. Nieder, and E. A. Blair. 2002. Functional assessment of a reference wetland set as a tool for science, management and restoration. Aquatic Sciences **64**:107-117.

Forbes, E. S., M. Larsen, F. Thomas, S. M. Thomas, and Z. G. Cardon. 2014. "Oxygen Probe": Using planar optodes to quantitatively measure oxygen concentrations and to describe oxygen dynamics in salt marsh sediments over time. 99th ESA Annual Convention. Ecological Society of America, Sacramento, CA.

Fox, L., I. Valiela, and E. L. Kinney. 2012. Vegetation cover and elevation in long-term experimental nutrient-enrichment plots in Great Sippewissett Salt Marsh, Cape Cod, Massachusetts: implications for eutrophication and sea level rise. Estuaries and Coasts **35**:445-458.

Freschet, G. T., J. H. C. Cornelissen, R. S. P. Van Logtestijn, and R. Aerts. 2010. Evidence of the 'plant economics spectrum' in a subarctic flora. Journal of Ecology **98**:362-373.

Galloway, J. N., F. J. Dentener, D. G. Capone, E. W. Boyer, R. W. Howarth, S. P. Seitzinger, G. P. Asner, C. C. Cleveland, P. A. Green, E. A. Holland, D. M. Karl, A. F. Michaels, J. H. Porter, A. R. Townsend, and C. J. Vöosmarty. 2004. Nitrogen Cycles: Past, Present, and Future. Biogeochemistry **70**:153-226.

Gedan, K. B., M. L. Kirwan, E. Wolanski, E. B. Barbier, and B. R. Silliman. 2011. The present and future role of coastal wetland vegetation in protecting shorelines: answering recent challenges to the paradigm. Climatic Change **106**:7-29.

Giblin, A. E., N. B. Weston, G. T. Banta, J. Tucker, and C. S. Hopkinson. 2010. The effects of salinity on nitrogen losses from an oligohaline estuarine sediment. Estuaries and Coasts **33**:1054-1068.

Goldman, J. C., D. A. Caron, and M. R. Dennett. 1987. Regulation of gross growth efficiency and ammonium regeneration in bacteria by substrate C: N ratio. Limnology and Oceanography **32**:1239-1252.

Graham, S. A., and I. A. Mendelssohn. 2014. Coastal wetland stability maintained through counterbalancing accretionary responses to chronic nutrient enrichment. Ecology **95**:3271-3283.

Grime, J. P. 1998. Benefits of plant diversity to ecosystems: immediate, filter and founder effects. Journal of Ecology **86**:902-910.

Groffman, P. M., M. A. Altabet, J. K. Bohlke, K. Butterbach-Bahl, M. B. David, M. K. Firestone, A. E. Giblin, T. M. Kana, L. P. Nielsen, and M. A. Voytek. 2006. Methods for measuring denitrification: diverse approaches to a difficult problem. Ecological Applications **16**:2091-2122.

Groffman, P. M., E. A. Davidson, and S. Seitzinger. 2009. New approaches to modeling denitrification. Biogeochemistry **93**:1-5.

Groffman, P. M., A. J. Gold, and R. C. Simmons. 1992. Nitrate dynamics in riparian forests - microbial studies. Journal of Environmental Quality **21**:666-671.

Gurevitch, J., and L. V. Hedges. 2001. Meta-analysis: combining the results of independent experiments. Pages 378–398 *in* S. M. Scheiner and J. Gurevitch, editors. Design and analysis of ecological experiments. Oxford University Press, New York, NY.

Hall, G. H. 1984. Measurement of nitrification rates in lake sediments - comparison of the nitrification inhibitors nitrapyrin and allylthiourea. Microbial Ecology **10**:25-36.

Hansson, L. A., C. Brönmark, P. Anders Nilsson, and K. Åbjörnsson. 2005. Conflicting demands on wetland ecosystem services: nutrient retention, biodiversity or both? Freshwater Biology **50**:705-714.

Harrell, F. E. 2014. Hmisc: Harrell miscellaneous. http://biostat.mc.vanderbilt.edu/Hmisc, https://github.com/harrelfe/Hmisc.

Hazelton, E. L. G., T. J. Mozdzer, D. Burdick, K. M. Kettenring, and D. Whigham. 2014. *Phragmites australis* management in the United States: 40 years of methods and outcomes. AoB Plants.

Hedges, L. V., J. Gurevitch, and P. S. Curtis. 1999. The meta-analysis of response ratios in experimental ecology. Ecology **80**:1150-1156.

Hesslein, R. H. 1976. An in situ sampler for close interval pore water studies. Limnology and Oceanography **21**:912-914.

Hinga, K. R., A. Batchelor, M. T. Ahmed, O. Osibanjo, N. Lewis, and M. Pilson. 2005. Chapter 15: Waste processing and detoxification. Pages 417-439 *in* N. Faruqui and A. Wagener, editors. Millennium Ecosystem Assessment. World Resources Institute, Washington, DC.

Hobbs, R. J., S. Arico, J. Aronson, J. S. Baron, P. Bridgewater, V. A. Cramer, P. R. Epstein, J. J. Ewel, C. A. Klink, and A. E. Lugo. 2006. Novel ecosystems: theoretical and management aspects of the new ecological world order. Global Ecology and Biogeography **15**:1-7.

Hooper, D. U., F. S. Chapin, J. J. Ewel, A. Hector, P. Inchausti, S. Lavorel, J. H. Lawton, D. M. Lodge, M. Loreau, and S. Naeem. 2005. Effects of biodiversity on ecosystem functioning: a consensus of current knowledge. Ecological Monographs **75**:3-35.

Hooper, D. U., and P. M. Vitousek. 1997. The effects of plant composition and diversity on ecosystem processes. Science **277**:1302-1305.

Hopfensperger, K. N., S. S. Kaushal, S. E. G. Findlay, and J. C. Cornwell. 2009. Influence of plant communities on denitrification in a tidal freshwater marsh of the Potomac River, United States. Journal of Environmental Quality **38**:618-626.

Howarth, R., F. Chan, D. J. Conley, J. Garnier, S. C. Doney, R. Marino, and G. Billen. 2011. Coupled biogeochemical cycles: eutrophication and hypoxia in temperate estuaries and coastal marine ecosystems. Frontiers in Ecology and the Environment **9**:18-26.

Howarth, R. W. 1988. Nutrient limitation of net primary production in marine ecosystems. Annual Review of Ecology and Systematics **19**:89-110.

Howes, N. C., D. M. Fitzgerald, Z. J. Hughes, I. Y. Georgiou, M. A. Kulp, M. D. Miner, J. M. Smith, and J. A. Barras. 2010. Hurricane-induced failure of low salinity wetlands. Proceedings of the National Academy of Sciences **107**:14014-14019.

Hume, N. P., M. S. Fleming, and A. J. Horne. 2002a. Denitrification potential and carbon quality of four aquatic plants in wetland microcosms. Soil Science Society of America Journal **66**:1706-1712.

Hume, N. P., M. S. Fleming, and A. J. Horne. 2002b. Plant carbohydrate limitation on nitrate reduction in wetland microcosms. Water Research **36**:577-584.

JMP(R). 1989-2007. JMP (R). SAS Institute Inc., Cary, NC.

Jones, M. N. 1984. Nitrate reduction by shaking with cadmium: alternative to cadmium columns. Water Research **18**:643-646.

Jordan, S., J. Stoffer, and J. Nestlerode. 2011. Wetlands as sinks for reactive nitrogen at continental and global scales: a meta-analysis. Ecosystems **14**:144-155.

Kana, T., C. Darkangelo, M. Hunt, J. Oldham, G. Bennett, and J. Cornwell. 1994. Membrane inlet mass spectrometer for rapid high-precision determination of N_2, O_2, and Ar in environmental water samples. Analytical Chemistry **66**:4166-4170.

Kattge, J., S. Díaz, S. Lavorel, I. C. Prentice, P. Leadley, G. Bönisch, E. Garnier, M. Westoby, P. B. Reich, I. J. Wright, J. H. C. Cornelissen, C. Violle, S. P. Harrison, P. M. Van Bodegom, M. Reichstein, B. J. Enquist, N. A. Soudzilovskaia, D. D. Ackerly, M. Anand, O. Atkin, M. Bahn, T. R. Baker, D. Baldocchi, R. Bekker, C. C. Blanco, B. Blonder, W. J. Bond, R. Bradstock, D. E. Bunker, F. Casanoves, J. Cavender-Bares, J. Q. Chambers, F. S. Chapin III, J. Chave, D. Coomes, W. K. Cornwell, J. M. Craine, B. H. Dobrin, L. Duarte, W. Durka, J. Elser, G. Esser, M. Estiarte, W. F. Fagan, J. Fang, F. Fernández-Méndez, A. Fidelis, B. Finegan, O. Flores, H. Ford, D. Frank, G. T. Freschet, N. M. Fyllas, R. V. Gallagher, W. A. Green, A. G. Gutierrez, T. Hickler, S. I. Higgins, J. G. Hodgson, A. Jalili, S. Jansen, C. A. Joly, A. J. Kerkhoff, D. Kirkup, K. Kitajima, M. Kleyer, S. Klotz, J. M. H. Knops, K. Kramer, I. Kühn, H. Kurokawa, D. Laughlin, T. D. Lee, M. Leishman, F. Lens, T. Lenz, S. L. Lewis, J. Lloyd, J. Llusiá, F. Louault, S. Ma, M. D. Mahecha, P. Manning, T. Massad, B. E. Medlyn, J. Messier, A. T. Moles, S. C. Müller, K. Nadrowski, S. Naeem, Ü. Niinemets, S. NöLlert, A. Nüske, R. Ogaya, J. Oleksyn, V. G. Onipchenko, Y. Onoda, J. Ordoñez, G. Overbeck, W. A. Ozinga, S. Patiño, S. Paula, J. G. Pausas, J. Peñuelas, O. L. Phillips, V. Pillar, H. Poorter, L. Poorter, P. Poschlod, A. Prinzing, R. Proulx, A. Rammig, S. Reinsch, B. Reu, L. Sack, B. Salgado-Negret, J. Sardans, S. Shiodera, B. Shipley, A. Siefert, E. Sosinski, J. F. Soussana, E. Swaine, N. Swenson, K. Thompson, P. Thornton, M. Waldram, E. Weiher, M. White, S. White, S. J. Wright, B. Yguel, S. Zaehle, A. E. Zanne, and C. Wirth. 2011. TRY – a global database of plant traits. Global Change Biology **17**:2905-2935.

Kattge, J., C. Wirth, W. Knorr, and T. Raddatz. 2009. Quantifying photosynthetic capacity and its relationship to leaf nitrogen content for global-scale terrestrial biosphere models. Global Change Biology **15**:976-991.

Kearney, M. S., J. Riter, and R. E. Turner. 2011. Freshwater river diversions for marsh restoration in Louisiana: Twenty-six years of changing vegetative cover and marsh area. Geophysical Research Letters **38**:1-6.

Keddy, P. A. 1992. A pragmatic approach to functional ecology. Functional Ecology **6**:621-626.

Keller, B. E. M. 2000. Plant diversity in *Lythrum*, *Phragmites*, and *Typha* marshes, Massachusetts, USA. Wetlands Ecology and Management **8**:391-401.

Kettenring, K. M., and C. R. Adams. 2011. Lessons learned from invasive plant control experiments: a systematic review and meta-analysis. Journal of Applied Ecology **48**:970-979.

Kettenring, K. M., S. de Blois, and D. P. Hauber. 2012. Moving from a regional to a continental perspective of *Phragmites australis* invasion in North America. AoB Plants **2012**:1-18.

Kim, B.-H., and H. J. Bokuniewicz. 1991. Estimates of sediment fluxes in Long Island Sound. Estuaries **14**:237-247.

Kirk, G. J. D., and H. J. Kronzucker. 2005. The Potential for nitrification and nitrate uptake in the rhizosphere of wetland plants: a modelling study. Annals of Botany **96**:639-646.

Kiviat, E. 2006. *Phragmites* management sourcebook for the tidal Hudson River. Hudson River Foundation, New York, New York, USA.

Kiviat, E. 2013. Ecosystem services of *Phragmites* in North America with emphasis on habitat functions. AoB Plants **5**:plt008.

Kleyer, M., R. M. Bekker, I. C. Knevel, J. P. Bakker, K. Thompson, M. Sonnenschein, P. Poschlod, J. M. V. Groenendael, L. Klimeš, J. Klimešová, S. Klotz, G. M. Rusch, M. Hermy, D. Adriaens, G. Boedeltje, B. Bossuyt, A. Dannemann, P. Endels, L. Götzenberger, J. G. Hodgson, A.-K. Jackel, I. Kühn, D. Kunzmann, W. A. Ozinga, C. Römermann, M. Stadler, J. Schlegelmilch, H. J. Steendam, O. Tackenberg, B. Wilmann, J. H. C. Cornelissen, O. Eriksson, E. Garnier, and B. Peco. 2008. The LEDA Traitbase: A database of life-history traits of Northwest European flora. Journal of Ecology **96**:1266-1274.

Kolker, A. S. 2005. The impacts of climate variability and anthropogenic activities on salt marsh accretion and loss on Long Island. Ph.D. State University of New York at Stony Brook, Ann Arbor.

Kralova, M., P. H. Masscheleyn, C. W. Lindau, and W. H. Patrick. 1992. Production of dinitrogen and nitrous oxide in soil suspensions as affected by redox potential. Water, Air, & Soil Pollution **61**:37-45.

Kremen, C. 2005. Managing ecosystem services: what do we need to know about their ecology? Ecology Letters **8**:468-479.

Kremen, C., and R. S. Ostfeld. 2005. A call to ecologists: measuring, analyzing, and managing ecosystem services. Frontiers in Ecology and the Environment **3**:540-548.

Kulkarni, M. V., P. M. Groffman, and J. B. Yavitt. 2008. Solving the global nitrogen problem: it's a gas! Frontiers in Ecology and the Environment **6**:199-206.

Larsen, M., S. M. Borisov, B. Grunwald, I. Klimant, and R. N. Glud. 2011. A simple and inexpensive high resolution color ratiometric planar optode imaging approach: application to oxygen and pH sensing. Limnology and Oceanography: Methods **9**:348-360.

Laughlin, D. C. 2011. Nitrification is linked to dominant leaf traits rather than functional diversity. Journal of Ecology **99**:1091-1099.

Lavorel, S., and E. Garnier. 2002. Predicting changes in community composition and ecosystem functioning from plant traits: revisiting the Holy Grail. Functional Ecology **16**:545-556.

Lavorel, S., and K. Grigulis. 2012. How fundamental plant functional trait relationships scale-up to trade-offs and synergies in ecosystem services. Journal of Ecology **100**:128-140.

Lavorel, S., K. Grigulis, P. Lamarque, M.-P. Colace, D. Garden, J. Girel, G. Pellet, and R. Douzet. 2011. Using plant functional traits to understand the landscape distribution of multiple ecosystem services. Journal of Ecology **99**:135-147.

Lawton, J. H. 1999. Are there general laws in ecology? Oikos **84**:177-192.

LeBauer, D. S., and K. K. Treseder. 2008. Nitrogen limitation of net primary productivity in terrestrial ecosystems is globally distributed. Ecology **89**:371-379.

LeBauer, D. S., D. Wang, K. T. Richter, C. C. Davidson, and M. C. Dietze. 2013. Facilitating feedbacks between field measurements and ecosystem models. Ecological Monographs **83**:133-154.

Legendre, P. 2013. lmodel2: Model II regression.*in* J. Oksanen, editor., http://cran.r-project.org/web/packages/lmodel2/index.html.

Lilliefors, H. W. 1967. On the Kolmogorov-Smirnov test for normality with mean and variance unknown. Journal of the American Statistical Association **62**:399-402.

Linthurst, R. A., and E. D. Seneca. 1981. Aeration, nitrogen and salinity as determinants of *Spartina alterniflora* Loisel. growth response. Estuaries **4**:53-63.

Lombard, K. B., D. Tomassi, and J. Ebersole. 2012. Long-term management of an invasive plant: lessons from seven years of *Phragmites australis* control. Northeastern Naturalist **19**:181-193.

Loreau, M., S. Naeem, P. Inchausti, J. Bengtsson, J. P. Grime, A. Hector, D. U. Hooper, M. A. Huston, D. Raffaelli, B. Schmid, D. Tilman, and D. A. Wardle. 2001. Biodiversity and ecosystem functioning: current knowledge and future challenges. Science **294**:804-808.

Martin, L. J., and B. Blossey. 2013. The runaway weed: costs and failures of *Phragmites australis* management in the USA. Estuaries and Coasts **36**:626-632.

McGill, B. J., B. J. Enquist, E. Weiher, and M. Westoby. 2006. Rebuilding community ecology from functional traits. Trends in Ecology & Evolution **21**:178-185.

McKee, K. L., I. A. Mendelssohn, and M. W. Hester. 1988. Reexamination of pore water sulfide concentrations and redox potentials near the aerial roots of *Rhizophora mangle* and *Avicennia germinans*. American Journal of Botany **75**:1352-1359.

Mendelssohn, I. A., and J. T. Morris. 2000. Eco-physiological controls on the productivity of *Spartina alterniflor*a Loisel. Pages 59-80 *in* M. P. Weinstein and D. A. Kreeger, editors. Concepts and Controversies in Tidal Marsh Ecology. Springer Netherlands.

Meyerson, L. A., R. M. Chambers, and K. A. Vogt. 1999. The effects of *Phragmites* removal on nutrient pools in a freshwater tidal marsh ecosystem. Biological Invasions **1**:129-136.

Meyerson, L. A., K. Saltonstall, L. Windham, E. Kiviat, and S. E. G. Findlay. 2000a. A comparison of *Phragmites australis* in freshwater and brackish marsh environments in North America. Wetlands Ecology and Management **8**:89-103.

Meyerson, L. A., K. A. Vogt, and R. M. Chambers. 2000b. Linking the success of *Phragmites* to the alteration of ecosystem nutrient cycles. Pages 827-844 *in* M. P. Weinstein and D. A. Kreeger, editors. Concepts and Controversies in Tidal Marsh Ecology. Kluwer Academic, Norwell, MA.

Millennium Ecosystem Assessment. 2005. Ecosystems and human well-being: Synthesis report. Island Press Washington, DC.

Mitsch, W. J., and S. E. Jørgensen. 2003. Ecological engineering: a field whose time has come. Ecological Engineering **20**:363-377.

Monti, J. J., and M. P. Scorca. 2003. Trends in nitrogen concentration and nitrogen loads entering the South Shore Estuary Reserve from streams and ground-water discharge in Nassau and Suffolk Counties, Long Island, New York, 1952-97. U.S. Geological Survey Water-Resources Investigations Report 02-4255:1-36.

Morris, J. T., and P. M. Bradley. 1999. Effects of nutrient loading on the carbon balance of coastal wetland sediments. Limnology and Oceanography **44**:699-702.

Morris, J. T., G. P. Shaffer, and J. A. Nyman. 2013. Brinson Review: Perspectives on the Influence of Nutrients on the Sustainability of Coastal Wetlands. Wetlands **33**:975-988.

Morris, J. T., P. V. Sundareshwar, C. T. Nietch, B. Kjerfve, and D. R. Cahoon. 2002. Responses of coastal wetlands to rising sea level. Ecology **83**:2869-2877.

Mozdzer, T. J., J. C. Zieman, and K. J. McGlathery. 2010. Nitrogen uptake by native and invasive temperate coastal macrophytes: importance of dissolved organic nitrogen. Estuaries and Coasts **33**:784-797.

Naeem, S. 2002. Ecosystem consequences of biodiversity loss: the evolution of a paradigm. Ecology **83**:1537-1552.

Nyman, J. A., R. J. Walters, R. D. Delaune, and W. H. Patrick Jr. 2006. Marsh vertical accretion via vegetative growth. Estuarine, Coastal and Shelf Science **69**:370-380.

O'Shea, M. L., and T. M. Brosnan. 2000. Trends in indicators of eutrophication in Western Long Island Sound and the Hudson-Raritan Estuary. Estuaries and Coasts **23**:877-901.

Orson, R. A. 1999. A paleoecological assessment of *Phragmites australis* in New England tidal marshes: Changes in plant community structure during the last few millennia. Biological Invasions **1**:149-158.

Osenberg, C. W., O. Sarnelle, S. D. Cooper, and R. D. Holt. 1999. Resolving ecological questions through meta-analysis: goals, metrics, and models. Ecology **80**:1105-1117.

Otto, S., P. M. Groffman, S. E. G. Findlay, and A. E. Arrcola. 1999. Invasive plant species and microbial processes in a tidal freshwater marsh. Journal of Environmental Quality **28**:1252-1257.

Parsons, T. R., Y. Maita, and C. M. Lalli. 1984a. 1.3 Determination of Ammonia (Oxidation Method). Pages 7-14 A Manual of Chemical and Biological Methods for Seawater Analysis. Pergamon Press, Elmsford, New York.

Parsons, T. R., Y. Maita, and C. M. Lalli. 1984b. 1.4 Determination of ammonia (alternative method). Pages 14-17 A Manual of Chemical and Biological Methods for Seawater Analysis. Pergamon Press, Elmsford, New York.

Perillo, G. M. E., E. Wolanski, D. R. Cahoon, and M. M. Brinson. 2009. Coastal wetlands: an integrated ecosystem approach. Elsevier, Amsterdam, the Netherlands.

R Core Team. 2012. R: A language and environment for statistical computing.*in* R Foundation for Statistical Computing, editor., Vienna, Austria.

Reich, P. B., I. J. Wright, and C. H. Lusk. 2007. Predicting leaf physiology from simple plant and climate attributes: a global Glopnet analysis. Ecological Applications **17**:1982-1988.

Rooth, J. E., and J. C. Stevenson. 2000. Sediment deposition patterns in *Phragmites australis* communities: Implications for coastal areas threatened by rising sea-level. Wetlands Ecology and Management **8**:173-183.

Rosenberg, M. S., D. C. Adams, and J. Gurevitch. 2000. MetaWin 2.0. Sinauer Associates, Inc., Sunderland, MA.

Saltonstall, K. 2002. Cryptic invasion by a non-native genotype of the common reed, *Phragmites australis*, into North America. Proceedings of the National Academy of Sciences **99**:2445-2449.

Sand-Jensen, K., C. Prahl, and H. Stokholm. 1982. Oxygen release from roots of submerged aquatic macrophytes. Oikos **38**:349-354.

Schimel, J. P., L. E. Jackson, and M. K. Firestone. 1989. Spatial and temporal effects on plant-microbial competition for inorganic nitrogen in a california annual grassland. Soil Biology and Biochemistry **21**:1059-1066.

Schlesinger, W. H. 2009. On the fate of anthropogenic nitrogen. Proceedings of the National Academy of Sciences **106**:203-208.

Schloerke, B., J. Crowley, D. Cook, H. Hofmann, H. Wickham, F. Briatte, M. Marbach, and E. Thoen. 2014. GGally: extension to ggplot2. http://cran.r-project.org/web/packages/GGally/index.html.

Schneider, C. A., W. S. Rasband, and K. W. Eliceiri. 2012. NIH Image to ImageJ: 25 years of image analysis. Nature Methods **9**:671-675.

Scorca, M. P., and J. J. Monti. 2001. Estimates of nitrogen loads entering Long Island Sound from ground water and streams on Long Island, New York, 1985-96. U.S. Geological Survey Water-Resources Investigations Report 00-4196:1-29.

Seitzinger, S. 2008. Nitrogen cycle: out of reach. Nature **452**:162-163.

Seitzinger, S., J. A. Harrison, J. K. Bohlke, A. F. Bouwman, R. Lowrance, B. Peterson, C. Tobias, and G. Van Drecht. 2006. Denitrification across landscapes and waterscapes: a synthesis. Ecological Applications **16**:2064-2090.

Serbin, S. P., A. Singh, B. E. McNeil, C. C. Kingdon, and P. A. Townsend. 2014. Spectroscopic determination of leaf morphological and biochemical traits for northern temperate and boreal tree species. Ecological Applications **24**:1651-1669.

Sherr, B. F., and W. J. Payne. 1978. Effect of the *Spartina alterniflora* root-rhizome system on salt marsh soil denitrifying bacteria. Applied and Environmental Microbiology **35**:724-729.

Silliman, B. R., and M. D. Bertness. 2004. Shoreline development drives invasion of *Phragmites australis* and the loss of plant diversity on New England salt marshes. Conservation Biology **18**:1424-1434.

Simberloff, D. 2004. Community ecology: is it time to move on? (An American Society of Naturalists presidential address). The American Naturalist **163**:787-799.

Simberloff, D. 2015. Non-native invasive species and novel ecosystems. F1000Prime Reports **7**.

Smith, M. D., and A. K. Knapp. 2003. Dominant species maintain ecosystem function with non-random species loss. Ecology Letters **6**:509-517.

Smith, M. S., and J. M. Tiedje. 1979a. Phases of denitrification following oxygen depletion in soil. Soil Biology & Biochemistry **11**:261-267.

Smith, M. S., and J. M. Tiedje. 1979b. Phases of denitrification following oxygen depletion in soil. Soil Biology and Biochemistry **11**:261-267.

Starry, O. S., H. M. Valett, and M. E. Schreiber. 2005. Nitrification rates in a headwater stream: influences of seasonal variation in C and N supply. Journal of the North American Benthological Society **24**:753-768.

Steever, E. Z., R. S. Warren, and W. A. Niering. 1976. Tidal energy subsidy and standing crop production of *Spartina alterniflora*. Estuarine and Coastal Marine Science **4**:473-478.

Stein, C., L. M. Hallett, W. S. Harpole, and K. N. Suding. 2014. Evaluating ecosystem services provided by non-native species: an experimental test in California grasslands. PLoS ONE **9**:7.

Strauss, E. A., and G. A. Lamberti. 2000. Regulation of nitrification in aquatic sediments by organic carbon. Limnology and Oceanography **45**:1854-1859.

Suding, K. N., S. Lavorel, F. S. Chapin III, J. H. C. Cornelissen, S. Diaz, E. Garnier, D. Goldberg, D. U. Hooper, S. T. Jackson, and M. L. Navas. 2008. Scaling environmental change through the community-level: a trait-based response-and-effect framework for plants. Global Change Biology **14**:1125-1140.

Tilman, D. 1999. The ecological consequences of changes in biodiversity: a search for general principles. Ecology **80**:1455-1474.

Tilman, D., J. Knops, D. Wedin, P. Reich, M. Ritchie, and E. Siemann. 1997. The influence of functional diversity and composition on ecosystem processes. Science **277**:1300-1302.

Truitt, A. M., E. F. Granek, M. J. Duveneck, K. A. Goldsmith, M. P. Jordan, and K. C. Yazzie. 2015. What is novel about novel ecosystems: managing change in an ever-changing world. Environmental Management **55**:1217-1226.

Turner, R. E. 2011. Beneath the salt marsh canopy: loss of soil strength with increasing nutrient loads. Estuaries and Coasts **34**:1084-1093.

Turner, R. E., B. L. Howes, J. M. Teal, C. S. Milan, E. M. Swenson, and D. D. Goehringer-Toner. 2009. Salt marshes and eutrophication: An unsustainable outcome. Limnology and Oceanography **54**:1634-1642.

United States Geological Survey (USGS). 2010. Long Island: State of the Aquifer System.

USDA, N. 2014. The PLANTS Database. National Resources Conservation Service. National Plant Data Team, Greensboro, NC 27401-4901 USA.

Valiela, I., J. M. Teal, and N. Y. Persson. 1976. Production and dynamics of experimentally enriched salt marsh vegetation: belowground biomass. Limnology and Oceanography **21**:245-252.

Verhagen, F. J. M., P. E. J. Hageman, J. W. Woldendorp, and H. J. Laanbroek. 1994. Competition for ammonium between nitrifying bacteria and plant-roots in soil in pots - effects of grazing by flagellates and fertilization. Soil Biology & Biochemistry **26**:89-96.

Verhagen, F. J. M., H. J. Laanbroek, and J. W. Woldendorp. 1995. Competition for ammonium between plant-roots and nitrifying and heterotrophic bacteria and the effects of protozoan grazing. Plant and Soil **170**:241-250.

Verhoeven, J. T. A., W. Koerselman, and A. F. M. Meuleman. 1996. Nitrogen- or phosphorus-limited growth in herbaceous, wet vegetation: relations with atmospheric inputs and management regimes. Trends in Ecology & Evolution **11**:494-497.

Vitousek, P. M., J. D. Aber, R. W. Howarth, G. E. Likens, P. A. Matson, D. W. Schindler, W. H. Schlesinger, and D. G. Tilman. 1997. Human alteration of the global nitrogen cycle: sources and consequences Ecological Applications **7**:737-750.

Vitousek, P. M., and L. R. Walker. 1989. Biological invasion by *Myrica faya* in Hawai'i: plant demography, nitrogen fixation, ecosystem effects. Ecological Monographs **59**:247-265.

Wainger, L. A., D. M. King, R. N. Mack, E. W. Price, and T. Maslin. 2010. Can the concept of ecosystem services be practically applied to improve natural resource management decisions? Ecological Economics **69**:978-987.

Watson, E. B., A. J. Oczkowski, C. Wigand, A. R. Hanson, E. W. Davey, S. C. Crosby, R. L. Johnson, and H. M. Andrews. 2014. Nutrient enrichment and precipitation changes do not enhance resiliency of salt marshes to sea level rise in the Northeastern U.S. Climatic Change **125**:501-509.

Watts, S. H., and S. P. Seitzinger. 2000. Denitrification rates in organic and mineral soils from riparian sites: a comparison of N_2 flux and acetylene inhibition methods. Soil Biology & Biochemistry **32**:1383-1392.

Weisner, S. E. B., P. G. Eriksson, W. Graneli, and L. Leonardson. 1994. Influence of macrophytes on nitrate removal in wetlands. Ambio **23**:363-366.

Wetzel, R. G., and G. E. Likens. 2000. Inorganic nutrients: nitrogen, phosphorus, and other nutrients. Pages 85-112 Limnological Analyses. Springer, New York, NY [u.a.].

Wickham, H., and W. Chang. 2015. ggplot2: elegant graphics for data analysis, http://cran.r-project.org/web/packages/ggplot2/index.html.

Windham, L., and J. G. Ehrenfeld. 2003. Net impact of a plant invasion on nitrogen-cycling processes within a brackish tidal marsh Ecological Applications **13**:883-896.

Windham, L., and L. A. Meyerson. 2003. Effects of common reed (*Phragmites australis*) expansions on nitrogen dynamics of tidal marshes of the Northeastern U.S. Estuaries **26**:452-464.

Windham, L., J. S. Weis, and P. Weis. 2001. Lead uptake, distribution, and effects in two dominant salt marsh macrophytes, *Spartina alterniflora* (cordgrass) and *Phragmites australis* (common reed). Marine Pollution Bulletin **42**:811-816.

Wright, I. J., P. B. Reich, M. Westoby, D. D. Ackerly, Z. Baruch, F. Bongers, J. Cavender-Bares, T. Chapin, J. H. C. Cornelissen, M. Diemer, J. Flexas, E. Garnier, P. K. Groom, J. Gulias, K. Hikosaka, B. B. Lamont, T. Lee, W. Lee, C. Lusk, J. J. Midgley, M. L. Navas, U. Niinemets, J. Oleksyn, N. Osada, H. Poorter, P. Poot, L. Prior, V. I. Pyankov, C. Roumet, S. C. Thomas, M. G. Tjoelker, E. J. Veneklaas, and R. Villar. 2004. The worldwide leaf economics spectrum. Nature **428**:821-827.

Wright, J. P., S. Naeem, A. Hector, C. Lehman, P. B. Reich, B. Schmid, and D. Tilman. 2006. Conventional functional classification schemes underestimate the relationship with ecosystem functioning. Pages 111-120. Blackwell Science Ltd.

Zedler, J. B. 2003. Wetlands at your service: reducing impacts of agriculture at the watershed scale. Frontiers in Ecology and the Environment **1**:65-72.

Zedler, J. B., and S. Kercher. 2004. Causes and consequences of invasive plants in wetlands: opportunities, opportunists, and outcomes. Critical Reviews in Plant Sciences **23**:431-452.

Zedler, J. B., and S. Kercher. 2005. Wetland resources: status, trends, ecosystem services, and restorability. Annual Review of Environment and Resources **30**:39-74.

Zimmerman, C., and R. Shirer. 2009. Hudson River invasive plant pre-treatment monitoring report. The Nature Conservancy, Albany, New York, USA.

Zimmerman, C., and R. Shirer. 2013. Trajectory of vegetation recovery in five *Phragmites australis* stands in response to management in a Hudson River freshwater tidal wetland. The Nature Conservancy in eastern New York, Albany, NY.

Appendix A: Supplement to Chapter 2

Table A1: Summary list of measurements included in this analysis, organized by the dominant plant species examined in each measurement.

Plant Species	N		Denitrification Measurement Method												Wetland System								Study Location	Reference
		Bare-sediment measurement	$^{15}NH_4$ addition	$^{15}NO_3$ addition	$^{15}N_2O$ addition	Acetylene inhibition	DEA	Mass balance	MIMS	N_2 flux	N_2:Ar	NH_4 removal	NO_3 removal	Constructed wetland	Depressional Wetland	Experimental estuarine pools	Mesocosm experiments	Microcosm experiments	Riparian wetland	Salt marsh	Tidal freshwater marsh		
Acer rubrum	2					X													X			Patuxent River, MD, USA	Verhoeven et al.. 2001
Acer rubrum	18						X												X			Kingson, RI, USA	Groffman et al. 1992
Acer rubrum	4						X												X			Kingson, RI, USA	Hanson et al. 1994
Acer rubrum	2	X					X												X			MD, USA	McCarty et al. 2007
Alnus glutinosa	1					X															X	Oude Maas, the Netherlands	Verhoeven et al. 2001
Alnus rugosa	1					X															X	Jug Bay, MD, USA	Verhoeven et al. 2001
Annual	3						X														X	Potomac River, VA, USA	Hopfensperger et al. 2009
Bulboschoenus medianus	1		X											X								New South Wales, Australia	Erler et al. 2010
Calamagrostis angustifolia	22					X									X							Sanjiang Plain, China	Sun & Liu 2007
Colocasia esculentus	1					X												X					Morgan et al. 2008
Cyperus papyrus	1					X												X					Morgan et al. 2008
Eichhornia crassipes	2							X									X					Marion, MA, USA	Hamersley et al. 2003
Eichhornia crassipes	1												X	X								Santo Tomé, Santa Fe, Argentina	Maine et al. 2007
Elodea canadensis	2						X							X								Linköping, Sweden	Bastviken et al. 2005
Elodea canadensis	26												X	X								Plönninge, Sweden	Bastviken et al. 2009
Elodea nuttallii	4					X								X								Everstekoog, the Netherlands	Toet et al. 2003
Glyceria maxima	4					X													X			Waal & IJssel Rivers, The Netherlands	Olde Venterink et al. 2006
Glyceria maxima	16						X							X								Kallby, Lund, Sweden	Bastviken et al. 2007
Glyceria maxima	2	X					X											X					Bodelier et al. 1998
Glyceria maxima	8	X					X												X			Elberg, The Netherlands	Bodelier et al. 1996
Halimione portulacoides	1	X		X																X		Lagoon of Venice, Italy	Eriksson et al. 2003
Hibiscus moscheutus	1					X												X					Morgan et al. 2008
Hydrocotyle umbellata	2												X					X					Hume et al. 2002b
Hydrocotyle umbellata	1												X					X					Hume et al. 2002a
Impatiens pallida	2	X					X												X			MD, USA	McCarty et al. 2007
Juncus effusus	1	X	X															X				Lake Okeechobee, FL, USA	Reddy et al. 1989
Juncus effusus	1					X													X			Patuxent River, MD, USA	Verhoeven et al. 2001
Juncus maritimus	1	X		X																X		Lagoon of Venice, Italy	Eriksson et al. 2003
Juncus roemerianus	3								X					X								Open Grounds Farm, NC, USA	Poe et al. 2003
Lemna minor	2												X						X				Hume et al. 2002b
Lemna minor	1												X						X				Hume et al. 2002a
Limonium serotinum	1	X		X																X		Lagoon of Venice, Italy	Eriksson et al. 2003
Littorella uniflora	1	X	X																X			Lake Hampen, Denmark	Ottosen et al. 1999

Lythrum salicaria	1						X													X	Tivoli Bay, NY, USA	Otto et al. 1999
Nuphar advena	1					X														X	Jug Bay, MD, USA	Verhoeven et al. 2001
Oryza sativa	1	X	X														X				Lake Okeechobee, FL, USA	Reddy et al. 1989
Oryza sativa	1					X							X								Sannogawa River, Japan	Zhou & Hosomi 2008
Perennial	3						X													X	Potomac River, VA, USA	Hopfensperger et al. 2009
Phalaris arundinacea	1	X		X													X				Rhin-Haveluch fen, Germany	Ruckauf et al. 2004
Phalaris arundinacea	7						X						X								Champaign County, IL, USA	Xue et al. 1999
Phragmites australis	1	X		X													X				Semitz-Welse lowland, Germany	Ruckauf et al. 2004
Phragmites australis	5					X							X								Everstekoog, the Netherlands	Toet et al. 2003
Phragmites australis	1	X				X											X					Munch 2005
Phragmites australis	4					X												X			Waal & IJssel Rivers, The Netherlands	Olde Venterink et al. 2006
Phragmites australis	2					X														X	Belgium & the Netherlands	Verhoeven et al. 2001
Phragmites australis	2						X						X								Linköping, Sweden	Bastviken et al. 2005
Phragmites australis	2	X					X						X								Costa Brava, Spain	Ruiz-Rueda et al. 2009
Phragmites australis	1						X												X		Tivoli Bay, NY, USA	Windham & Meyerson 2003
Phragmites australis	6						X													X	Connecticut River, CT, USA	Findlay et al. 2003
Phragmites australis	1						X													X	Tivoli Bay, NY, USA	Otto et al. 1999
Phragmites australis	1									X			X								Kodijärve, Estonia	Mander et al. 2008
Phragmites australis	4										X		X								Saxonia-Anhalt, Germany	Kuschk et al. 2003
Phragmites australis	26											X	X								Plönninge, Sweden	Bastviken et al. 2009
Phragmites australis	1											X							X		Mullica River Great Bay, NJ, USA	Windham & Ehrenfeld 2003
Pontederia cordata	1	X	X														X				Lake Okeechobee, FL, USA	Reddy et al. 1989
Potamogeton pectinatus	1	X	X															X			Lake Hampen, Denmark	Ottosen et al. 1999
Potamogeton pectinatus	16						X						X								Kallby, Lund, Sweden	Bastviken et al. 2007
Potamogeton perfoliatus	2	X	X												X						Chesapeake Bay, MD, USA	Caffrey & Kemp 1992
Potamogeton perfoliatus	3	X					X												X		Chesapeake Bay, MD, USA	Caffrey & Kemp 1990
Quercus spp.	18						X											X			Kingson, RI, USA	Groffman et al. 1992
Quercus spp.	4						X											X			Kingson, RI, USA	Hanson et al. 1994
Salix cineria	1	X	X														X				Lake Okareka, New Zealand	Lusby et al. 1998
Salix cineria	1	X					X											X			Lake Okareka, New Zealand	Lusby et al. 1998
Salix nigra	1					X											X					Morgan et al. 2008
Salix spp.	4					X												X			Waal & IJssel Rivers, The Netherlands	Olde Venterink et al. 2006
Salix spp.	1					X														X	Waal River, the Netherlands	Verhoeven et al. 2001
Schoenoplectus acutus	3	X						X					X								Hemet, CA, USA	Smith et al. 2000
Schoenoplectus californicus	4	X						X					X								Hemet, CA, USA	Smith et al. 2000
Schoenoplectus pungens	1	X							X										X		Narragansett Bay, RI, USA	Davis et al. 2004
Schoenoplectus spp.	1					X							X								Duplin County, NC, USA	Hunt et al. 2003
Schoenoplectus spp.	3					X							X								Duplin County, NC, USA	Hunt et al. 2009
Schoenoplectus spp.	1						X						X								Duplin County, NC, USA	Hunt et al. 2003
Schoenoplectus spp.	1						X						X								Duplin County, NC, USA	Hunt et al. 2009
Schoenoplectus tabernaemontani	1						X						X								Olentangy River, Columbus, OH, USA	Hernandez & Mitsch 2007
Schoenoplectus tabernaemontani	1							X								X						Tanner & Kadlec 2003
Schoenoplectus tabernaemontani	4							X								X						Tanner et al. 2002
Scirpus acutus	2											X					X					Hume et al. 2002b
Scirpus acutus	1											X					X					Hume et al. 2002a
Scirpus mariqueter	3	X				X													X		Yangtze River, China	Wang et al. 2007
Scirpus olneyi	6						X												X		Chesapeake Bay, USA	Matamala & Drake 1999
Scirpus spp.	1					X														X	Oude Maas, the Netherlands	Verhoeven et al. 2001

Scirpus spp.	2											X	X							Prado Basin, CA, USA	Bachand & Horne 2000
Scirpus spp.	6											X			X						Gebremariam 2008
Spartina alterniflora	4						X											X		Narragansett Bay, RI, USA	Wigand et al. 2004
Spartina alterniflora (short)	6	X			X													X		Virginia Coast Reserve, USA	Anderson et al. 1997
Spartina alterniflora (short)	2	X					X											X		SERF, Savannah, GA, USA	Dollhopf et al. 2004
Spartina alterniflora (short)	9	X								X								X		Great Sippewissett Marsh, USA	Kaplan et al. 1979
Spartina alterniflora (tall)	2	X					X											X		SERF, Savannah, GA, USA	Dollhopf et al. 2004
Spartina alterniflora (tall)	8	X								X								X		Great Sippewissett Marsh, USA	Kaplan et al. 1979
Spartina patens	4						X											X		Narragansett Bay, RI, USA	Wigand et al. 2004
Spartina patens	1						X											X		Tivoli Bay, NY, USA	Windham & Meyerson 2003
Spartina patens	4	X							X									X		Narragansett Bay, RI, USA	Davis et al. 2004
Spartina patens	8	X								X								X		Great Sippewissett Marsh, USA	Kaplan et al. 1979
Spartina patens	1											X						X		Mullica River Great Bay, NJ, USA	Windham & Ehrenfeld 2003
Symplocarpus foetidus	2	X					X										X			MD, USA	McCarty et al. 2007
Typha angustifolia	3						X												X	Connecticut River, USA	Findlay et al. 2003
Typha angustifolia	1						X												X	Tivoli Bay, NY, USA	Otto et al. 1999
Typha domingensis	1											X	X							Santo Tomé, Santa Fe, Argentina	Maine et al. 2007
Typha latifolia	2					X													X	Anacostia River, MD, USA	Verhoeven et al. 2001
Typha latifolia	2						X						X							Kallby, Lund, Sweden	Bastviken et al. 2005
Typha latifolia	16						X						X							Linköping, Sweden	Bastviken et al. 2007
Typha latifolia	2									X			X							Kõo, Estonia	Mander et al. 2008
Typha latifolia	2											X				X					Hume et al. 2002b
Typha latifolia	1											X				X					Hume et al. 2002a
Typha latifolia	3	X										X				X					Martin et al. 2003
Typha orientalis	3		X										X							New South Wales, Australia	Erler et al. 2010
Typha orientalis	1	X	X													X				Lake Okareka, New Zealand	Lusby et al. 1998
Typha orientalis	1	X					X										X			Lake Okareka, New Zealand	Lusby et al. 1998
Typha orientalis	2	X										X			X					Minumatanbo wetland, Japan	Sasikala et al. 2009
Typha spp.	1					X							X							Duplin County, NC, USA	Hunt et al. 2003
Typha spp.	3					X							X							Duplin County, NC, USA	Hunt et al. 2009
Typha spp.	1						X						X							Olentangy River, Colombus, OH, USA	Hernandez & Mitsch 2007
Typha spp.	1						X						X							Duplin County, NC, USA	Hunt et al. 2003
Typha spp.	1						X						X							Duplin County, NC, USA	Hunt et al. 2009
Typha spp.	2	X					X						X							Costa Brava, Spain	Ruiz-Rueda et al. 2009
Typha spp.	2											X	X							Prado Basin, CA, USA	Bachand & Horne 2000
Typha spp.	6											X			X						Gebremariam 2008
Typha spp.	1											X			X						Ingersoll & Baker 1998
Zostera marina	1	X	X															X		Limfjorden & Aarhus, Denmark	Ottosen et al. 1999
Zostera marina	4	X					X											X		Chesapeake Bay, MD, USA	Caffrey & Kemp 1990

Literature Cited

Anderson, I. C., C. R. Tobias, B. B. Neikirk, and R. L. Wetzel. 1997. Development of a process-based nitrogen mass balance model for a Virginia (USA) *Spartina alterniflora* salt marsh: implications for net DIN flux. Marine Ecology Progress Series **159**:13-27.

Bachand, P. A. M. and A. J. Horne. 2000. Denitrification in constructed free-water surface wetlands: II. Effects of vegetation and temperature. Ecological Engineering **14**:17-32.

Bastviken, S. K., P. G. Eriksson, A. Ekstrom, and K. Tonderski. 2007. Seasonal denitrification potential in wetland sediments with organic matter from different plant species. Water Air and Soil Pollution **183**:25-35.

Bastviken, S. K., P. G. Eriksson, A. Premrov, and K. Tonderski. 2005. Potential denitrification in wetland sediments with different plant species detritus. Ecological Engineering **25**:183-190.

Bastviken, S. K., S. E. B. Weisner, G. Thiere, J. M. Svensson, P. M. Ehde, and K. S. Tonderski. 2009. Effects of vegetation and hydraulic load on seasonal nitrate removal in treatment wetlands. Ecological Engineering **35**:946-952.

Bodelier, P. L. E., H. Duyts, C. W. P. M. Blom, and H. J. Laanbroek. 1998. Interactions between nitrifying and denitrifying bacteria in gnotobiotic microcosms planted with the emergent macrophyte *Glyceria maxima*. Fems Microbiology Ecology **25**:63-78.

Bodelier, P. L. E., J. A. Libochant, C. Blom, and H. J. Laanbroek. 1996. Dynamics of nitrification and denitrification in root-oxygenated sediments and adaptation of ammonia-oxidizing bacteria to low-oxygen or anoxic habitats. Applied and Environmental Microbiology **62**:4100-4107.

Caffrey, J. M. and W. M. Kemp. 1990. Nitrogen cycling in sediments with estuarine populations of *Potamogeton perfoliatus* and *Zostera marina*. Marine Ecology Progress Series **66**:147-160.

Caffrey, J. M. and W. M. Kemp. 1992. Influence of the submersed plant, *Potamogeton perfoliatus*, on nitrogen cycling in estuarine sediments. Limnology and Oceanography **37**:1483-1495.

Davis, J. L., B. Nowicki, and C. Wigand. 2004. Denitrification in fringing salt marshes of Narragansett Bay, Rhode Island, USA. Wetlands **24**:870-878.

Dollhopf, S. L., J.-H. Hyun, A. C. Smith, H. J. Adams, S. O'Brien, and J. E. Kostka. 2005. Quantification of ammonia-oxidizing bacteria and factors controlling nitrification in salt marsh sediments. Environmental Microbiology **71**:240-246.

Eriksson, P. G., J. M. Svensson, and G. M. Carrer. 2003. Temporal changes and spatial variation of soil oxygen consumption, nitrification and denitrification rates in a tidal salt marsh of the Lagoon of Venice, Italy. Estuarine, Coastal and Shelf Science **58**:861-871.

Findlay, S. E. G., P. M. Groffman, and S. Dye. 2003. Effects of *Phragmites australis* removal on marsh nutrient cycling. Wetlands Ecology and Management **11**:157-165.

Gebremariam, S. Y. and M. W. Beutel. 2008. Nitrate removal and DO levels in batch wetland mesocosms: Cattail (*Typha* spp.) versus bulrush (*Scirpus* spp.). Ecological Engineering **34**:1-6.

Groffman, P. M., A. J. Gold, and R. C. Simmons. 1992. Nitrate dynamics in riparian forests - microbial studies. Journal of Environmental Quality **21**:666-671.

Hamersley, M. R., B. L. Howes, and D. S. White. 2003. Particulates, not plants, dominate nitrogen processing in a septage-treating aerated pond system. Journal of Environtal Quality **32**:1895-1904.

Hanson, G. C., P. M. Groffman, and A. J. Gold. 1994. Denitrification in riparian wetlands receiving high and low groundwater nitrate inputs. Journal of Environmental Quality **23**:917-922.

Hernandez, M. E. and W. J. Mitsch. 2007. Denitrification potential and organic matter as affected by vegetation community, wetland age, and plant introduction in created wetlands. Journal of Environmental Quality **36**:333-342.

Hopfensperger, K. N., S. S. Kaushal, S. E. G. Findlay, and J. C. Cornwell. 2009. Influence of plant communities on denitrification in a tidal freshwater marsh of the Potomac River, United States. Journal of Environmental Quality **38**:618-626.

Hume, N. P., M. S. Fleming, and A. J. Horne. 2002a. Denitrification potential and carbon quality of four aquatic plants in wetland microcosms. Soil Science Society of America Journal **66**:1706-1712.

Hume, N. P., M. S. Fleming, and A. J. Horne. 2002b. Plant carbohydrate limitation on nitrate reduction in wetland microcosms. Water Research **36**:577-584.

Hunt, P. G., T. A. Matheny, and A. A. Szogi. 2003. Denitrification in constructed wetlands used for treatment of swine wastewater. Journal of Environmental Quality **32**:727-735.

Hunt, P. G., K. C. Stone, T. A. Matheny, M. E. Poach, M. B. Vanotti, and T. F. Ducey. 2009. Denitrification of nitrified and non-nitrified swine lagoon wastewater in the suspended sludge layer of treatment wetlands. Ecological Engineering **35**:1514-1522.

Ingersoll, T. L. and L. A. Baker. 1998. Nitrate removal in wetland microcosms. Water Research **32**:677-684.

Kaplan, W., I. Valiela, and J. M. Teal. 1979. Denitrification in a salt marsh ecosystem. Limnology and Oceanography **24**:726-734.

Kuschk, P., A. Wießner, U. Kappelmeyer, E. Weißbrodt, M. Kästner, and U. Stottmeister. 2003. Annual cycle of nitrogen removal by a pilot-scale subsurface horizontal flow in a constructed wetland under moderate climate. Water Research **37**:4236-4242.

Lusby, F. E., M. M. Gibbs, A. B. Cooper, and K. Thompson. 1998. The fate of groundwater ammonium in a lake edge wetland. Journal of Environmental Quality **27**:459-466.

Maine, M. A., N. Suñe, H. Hadad, G. Sánchez, and C. Bonetto. 2007. Removal efficiency of a constructed wetland for wastewater treatment according to vegetation dominance. Chemosphere **68**:1105-1113.

Mander, Ü., K. Lõhmus, S. Teiter, T. Mauring, K. Nurk, and J. Augustin. 2008. Gaseous fluxes in the nitrogen and carbon budgets of subsurface flow constructed wetlands. Science of The Total Environment **404**:343-353.

Martin, J., E. Hofherr, and M. F. Quigley. 2003. Effects of *Typha latifolia* transpiration and harvesting on nitrate concentrations in surface water of wetland microcosms. Wetlands **23**:835-844.

Matamala, R. and B. G. Drake. 1999. The influence of atmospheric CO_2 enrichment on plant-soil nitrogen interactions in a wetland plant community on the Chesapeake Bay. Plant and Soil **210**:93-101.

McCarty, G. W., S. Mookherji, and J. T. Angier. 2007. Characterization of denitrification activity in zones of groundwater exfiltration within a riparian wetland ecosystem. Biology and Fertility of Soils **43**:691-698.

Morgan, J. A., J. F. Martin, and V. Bouchard. 2008. Identifying plant species with root associated bacteria that promote nitrification and denitrification in ecological treatment systems. Wetlands **28**:220-231.

Munch, C., P. Kuschk, and I. Roske. 2005. Root stimulated nitrogen removal: only a local effect or important for water treatment? Water Science and Technology **51**:185-192.

Olde Venterink, H., J. E. Vermaat, M. Pronk, F. Wiegman, G. E. M. van der Lee, M. W. van den Hoorn, L. W. G. Higler, and J. T. A. Verhoeven. 2006. Importance of sediment deposition and denitrification for nutrient retention in floodplain wetlands. Applied Vegetation Science **9**:163-174.

Otto, S., P. M. Groffman, S. E. G. Findlay, and A. E. Arrcola. 1999. Invasive plant species and microbial processes in a tidal freshwater marsh. Journal of Environmental Quality **28**:1252-1257.

Poe, A. C., M. F. Piehler, S. P. Thompson, and H. W. Paerl. 2009. Denitrification in a constructed wetland receiving agricultural runoff. Wetlands **23**:817-826.

Reddy, K. R., W. H. Patrick, and C. W. Lindau. 1989. Nitrification-denitrification at the plant root-sediment interface in wetlands. Limnology and Oceanography **34**:1004-1013.

Rückauf, U., J. Augustin, R. Russow, and W. Merbach. 2004. Nitrate removal from drained and reflooded fen soils affected by soil N transformation processes and plant uptake. Soil Biology and Biochemistry **36**:77-90.

Ruiz-Rueda, O., S. Hallin, and L. Baneras. 2009. Structure and function of denitrifying and nitrifying bacterial communities in relation to the plant species in a constructed wetland. Fems Microbiology Ecology **67**:308-319.

Sasikala, S., N. Tanaka, H. S. Y. Wah Wah, and K. B. S. N. Jinadasa. 2009. Effects of water level fluctuation on radial oxygen loss, root porosity, and nitrogen removal in subsurface vertical flow wetland mesocosms. Ecological Engineering **35**:410-417.

Smith, L. K., J. J. Sartoris, J. S. Thullen, and D. C. Andersen. 2000. Investigation of denitrification rates in an ammonia-dominated constructed wastewater-treatment wetland. Wetlands **20**:684-696.

Sun, Z.-g. and J.-s. Liu. 2007. Nitrogen cycling of atmosphere-plant-soil system in the typical *Calamagrostis angustifolia* wetland in the Sanjiang Plain, Northeast China. Journal of Environmental Sciences **19**:986-995.

Tanner, C. C. and R. H. Kadlec. 2003. Oxygen flux implications of observed nitrogen removal rates in subsurface-flow treatment wetlands. Water Science and Technology **48**:191-198.

Tanner, C. C., R. H. Kadlec, M. M. Gibbs, J. P. S. Sukias, and M. L. Nguyen. 2002. Nitrogen processing gradients in subsurface-flow treatment wetlands--influence of wastewater characteristics. Ecological Engineering **18**:499-520.

Toet, S., L. Huibers, R. S. P. Van Logtestijn, and J. T. A. Verhoeven. 2003. Denitrification in the periphyton associated with plant shoots and in the sediment of a wetland system supplied with sewage treatment plant effluent. Hydrobiologia **501**:29-44.

Verhoeven, J. T. A., D. F. Whigham, R. van Logtestijn, and J. O'Neill. 2001. A comparative study of nitrogen and phosphorus cycling in tidal and non-tidal riverine wetlands. Wetlands **21**:210-222.

Wang, D., Z. Chen, J. Wang, S. Xu, H. Yang, H. Chen, L. Yang, and L. Hu. 2007. Summer-time denitrification and nitrous oxide exchange in the intertidal zone of the Yangtze Estuary. Estuarine, Coastal and Shelf Science **73**:43-53.

Wigand, C., R. A. McKinney, M. M. Chintala, M. A. Charpentier, and P. M. Groffman. 2004. Denitrification enzyme activity of fringe salt marshes in New England (USA). Journal of Environmental Quality **33**:1144-1151.

Windham, L. and J. G. Ehrenfeld. 2003. Net impact of a plant invasion on nitrogen-cycling processes within a brackish tidal marsh Ecological Applications **13**:883-896.

Windham, L. and L. A. Meyerson. 2003. Effects of common reed (*Phragmites australis*) expansions on nitrogen dynamics of tidal marshes of the Northeastern U.S. Estuaries **26**:452-464.

Xue, Y., M. B. David, L. E. Gentry, R. L. Mulvaney, D. A. Kovacic, and C. W. Lindau. 1999. In situ measurements of denitrification in constructed wetlands. Journal of Environmental Quality **28**:263-269.

Zhou, S. and M. Hosomi. 2008. Nitrogen transformations and balance in a constructed wetland for nutrient-polluted river water treatment using forage rice in Japan. Ecological Engineering **32**:147-155.

Appendix B: Supplement to Chapter 3

Packages

```
library(ggplot2)
library(bear)
library(Hmisc)
```

Data and formatting

```
setwd(filepath2)
# Import profile data
ExProfiles <- read.csv("20150204_WMExFPEx_ProfileData.csv")
# Import mesocosm-scale data
MesoScaleData <- read.csv("MesoScaleData_All.csv")
# Convert Microsite to an ordered variable
ExProfiles$Microsite <- ordered(ExProfiles$Microsite, levels = c("Edge", "Platform", "Mudflat"))
MesoScaleData$Microsite <- ordered(MesoScaleData$Microsite, levels = c("Edge", "Platform",
"Mudflat"))
# Create a dataframe that contains only rows with process measurements
ProcessProfiles <- ExProfiles[which(ExProfiles$Mineralization != "NA"), ]
```

Correlations among plant traits

```
# Compute Pearson correlations for plant-trait data
rcorr(as.matrix((MesoScaleData[, c("AGBiomass_g.m2", "Stem_density_m2", "RootMass_g.m..2",
   "Root_width_mm", "Max_Stem_height_cm", "SLA_cm2.g", "Veg_CN")])))
```

	AGBiomass_g.m2	Stem_density_m2	RootMass_g.m..2	Root_width_mm	Max_Stem_height_cm	SLA_cm2.g	Veg_CN
AGBiomass_g.m2	1	0.75	0.12	0.77	0.61	-0.5	-0.44
Stem_density_m2	0.75	1	0.19	-0.42	0.11	0.58	-0.17
RootMass_g.m..2	0.12	0.19	1	-0.05	0.36	0.45	-0.02
Root_width_mm	0.77	-0.42	-0.05	1	0.56	-0.63	-0.27
Max_Stem_height_cm	0.61	0.11	0.36	0.56	1	0.04	-0.73
SLA_cm2.g	-0.5	0.58	0.45	-0.63	0.04	1	-0.08
Veg_CN	-0.44	-0.17	-0.02	-0.27	-0.73	-0.08	1

n

	AGBiomass_g.m2	Stem_density_m2	RootMass_g.m..2	Root_width_mm	Max_Stem_height_cm	SLA_cm2.g	Veg_CN
AGBiomass_g.m2	12	12	12	8	8	8	8
Stem_density_m2	12	12	12	8	8	8	8
RootMass_g.m..2	12	12	12	8	8	8	8
Root_width_mm	8	8	8	12	8	8	8
Max_Stem_height_cm	8	8	8	8	12	8	8
SLA_cm2.g	8	8	8	8	8	12	8
Veg_CN	8	8	8	8	8	8	12

p

	AGBiomass_g.m2	Stem_density_m2	RootMass_g.m..2	Root_width_mm	Max_Stem_height_cm	SLA_cm2.g	Veg_CN
AGBiomass_g.m2		0.0054	0.7095	0.0253	0.1059	0.2076	0.2746
Stem_density_m2	0.0054		0.5448	0.3013	0.8029	0.1297	0.681
RootMass_g.m..2	0.7095	0.5448		0.9006	0.3803	0.26	0.9648
Root_width_mm	0.0253	0.3013	0.9006		0.1466	0.0919	0.5191
Max_Stem_height_cm	0.1059	0.8029	0.3803	0.1466		0.93	0.0389
SLA_cm2.g	0.2076	0.1297	0.26	0.0919	0.93		0.8432
Veg_CN	0.2746	0.681	0.9648	0.5191	0.0389	0.8432	

General linear models (GLMs) to predict sediment oxygen from plant traits

```
# Examine correlations of plant traits with O2 enrichment and extractable ammonium
rcorr(as.matrix(MesoScaleData[, c("O2Enrichment_ppt", "ExtNH4_uM", "AGBiomass_g.m2",
"Stem_density_m2", "RootMass_g.m..2", "Root_width_mm", "Max_Stem_height_cm", "SLA_cm2.g",
"Veg_CN")]))
```

	O2Enrichment_ppt	ExtNH4_uM	AGBiomass_g.m2	Stem_density_m2	RootMass_g.m..2	Root_width_mm	Max_Stem_height_cm	SLA_cm2.g	Veg_CN
O2Enrichment_ppt	1	0.53	0.55	0.11	-0.26	0.86	0.68	-0.53	-0.39
ExtNH4_uM	0.53	1	0.16	-0.27	-0.47	0.33	-0.13	-0.72	-0.16
AGBiomass_g.m2	0.55	0.16	1	0.75	0.12	0.77	0.61	-0.5	-0.44
Stem_density_m2	0.11	-0.27	0.75	1	0.19	-0.42	0.11	0.58	-0.17
RootMass_g.m..2	-0.26	-0.47	0.12	0.19	1	-0.05	0.36	0.45	-0.02
Root_width_mm	0.86	0.33	0.77	-0.42	-0.05	1	0.56	-0.63	-0.27
Max_Stem_height_cm	0.68	-0.13	0.61	0.11	0.36	0.56	1	0.04	-0.73
SLA_cm2.g	-0.53	-0.72	-0.5	0.58	0.45	-0.63	0.04	1	-0.08
Veg_CN	-0.39	-0.16	-0.44	-0.17	-0.02	-0.27	-0.73	-0.08	1

n

	O2Enrichment_ppt	ExtNH4_uM	AGBiomass_g.m2	Stem_density_m2	RootMass_g.m..2	Root_width_mm	Max_Stem_height_cm	SLA_cm2.g	Veg_CN
O2Enrichment_ppt	12	12	12	12	12	8	8	8	8
ExtNH4_uM	12	12	12	12	12	8	8	8	8
AGBiomass_g.m2	12	12	12	12	12	8	8	8	8
Stem_density_m2	12	12	12	12	12	8	8	8	8
RootMass_g.m..2	12	12	12	12	12	8	8	8	8
Root_width_mm	8	8	8	8	8	12	8	8	8
Max_Stem_height_cm	8	8	8	8	8	8	12	8	8
SLA_cm2.g	8	8	8	8	8	8	8	12	8
Veg_CN	8	8	8	8	8	8	8	8	12

p

	O2Enrichment_ppt	ExtNH4_uM	AGBiomass_g.m2	Stem_density_m2	RootMass_g.m..2	Root_width_mm	Max_Stem_height_cm	SLA_cm2.g	Veg_CN
O2Enrichment_ppt		0.0755	0.0631	0.7297	0.41	0.006	0.063	0.1737	0.3367
ExtNH4_uM	0.0755		0.6225	0.4019	0.1224	0.4184	0.7548	0.0437	0.7082
AGBiomass_g.m2	0.0631	0.6225		0.0054	0.7095	0.0253	0.1059	0.2076	0.2746
Stem_density_m2	0.7297	0.4019	0.0054		0.5448	0.3013	0.8029	0.1297	0.681
RootMass_g.m..2	0.41	0.1224	0.7095	0.5448		0.9006	0.3803	0.26	0.9648
Root_width_mm	0.006	0.4184	0.0253	0.3013	0.9006		0.1466	0.0919	0.5191
Max_Stem_height_cm	0.063	0.7548	0.1059	0.8029	0.3803	0.1466		0.93	0.0389
SLA_cm2.g	0.1737	0.0437	0.2076	0.1297	0.26	0.0919	0.93		0.8432
Veg_CN	0.3367	0.7082	0.2746	0.681	0.9648	0.5191	0.0389	0.8432	

```
# Predict O2 enrichment with root width, include microsite treatment as a categorical variable
mod1v <- lm(O2Enrichment_ppt ~ Microsite * Root_width_mm, data = MesoScaleData)
summary(mod1v)
```

```
Call:
lm(formula = O2Enrichment_ppt ~ Microsite * Root_width_mm, data = MesoScaleData)

Residuals:
    1     4     5     6     7     9    11    12
44.294  9.325 -37.298 -34.989  6.252 -15.557  43.083 -15.110

Coefficients:
                          Estimate Std.Error t       Pr(>|t|)
(Intercept)               -392.05    98.42  -3.983    0.016  *
Microsite.L                -56.94   139.19  -0.409    0.7035
Root_width_mm               47.04    15.81   2.975    0.0409 *
Microsite.L:Root_width_mm   11.06    22.36   0.495    0.6466
---
Signif. codes:  0 '***' 0.001 '**' 0.01 '*' 0.05 '.' 0.1 ' ' 1

Residual standard error: 41.92 on 4 degrees of freedom
  (4 observations deleted due to missingness)
Multiple R-squared:  0.766, Adjusted R-squared:  0.5906
F-statistic: 4.366 on 3 and 4 DF,  p-value: 0.09424
```

```
# Effect did not differ between treatments; remove 'Microsite' as a factor
mod2v <- lm(O2Enrichment_ppt ~ Root_width_mm, data = MesoScaleData)
summary(mod2v)
Call:
lm(formula = O2Enrichment_ppt ~ Root_width_mm, data = MesoScaleData)

Residuals:
    Min      1Q  Median      3Q     Max
-39.194 -21.232  -8.707  10.101  59.103

Coefficients:
                Estimate   Std.Error  t          Pr(>|t|)
 (Intercept)    -350.983     63.686   -5.511       0.002   **
 Root_width_mm    39.801      9.596    4.148     0.00603   **
---
Signif. codes:  0 '***' 0.001 '**' 0.01 '*' 0.05 '.' 0.1 ' ' 1

Residual standard error: 35.99 on 6 degrees of freedom
  (4 observations deleted due to missingness)
Multiple R-squared:  0.7414,    Adjusted R-squared:  0.6983
F-statistic:  17.2 on 1 and 6 DF,  p-value: 0.006027

# Test residuals for normality using Kolmogorov-Smirnov test
ks.test(x = mod2v$residuals, y = "pnorm", mean(mod2v$residuals), sd(mod2v$residuals))
One-sample Kolmogorov-Smirnov test
data:  mod2v$residuals
D = 0.2478, p-value = 0.624
alternative hypothesis: two-sided

# Compare fits of models with and without microsite treatment as a factor
anova(mod1v, mod2v)
Analysis of Variance Table
Model 1: O2Enrichment_ppt ~ Microsite * Root_width_mm
Model 2: O2Enrichment_ppt ~ Root_width_mm
  Res.Df    RSS Df Sum of Sq      F Pr(>F)
1      4 7029.8
2      6 7770.2 -2   -740.43 0.2107 0.8185

# Predict O2 enrichment with maximum stem height, include microsite
mod3v <- lm(O2Enrichment_ppt ~ Microsite * Max_Stem_height_cm, data = MesoScaleData)
summary(mod3v)
Call:
lm(formula = O2Enrichment_ppt ~ Microsite * Max_Stem_height_cm, data = MesoScaleData)

Residuals:
    1     4     5     6     7     9    11    12
-47.72 -58.43  28.82 -43.87  48.48  43.11  25.30   4.31

Coefficients:
```

```
                                Estimate  Std.Error     t      Pr(>|t|)
(Intercept)                     -576.553    275.089  -2.096    0.104
Microsite.L                      214.028    389.035   0.55     0.611
Max_Stem_height_cm                 4.193      2.302   1.822    0.143
Microsite.L:Max_Stem_height_cm    -1.461      3.255  -0.449    0.677

Residual standard error: 57.69 on 4 degrees of freedom
  (4 observations deleted due to missingness)
Multiple R-squared:  0.5569,    Adjusted R-squared:  0.2246
F-statistic: 1.676 on 3 and 4 DF,  p-value: 0.3082
```

```
# Effect did not differ between treatments; remove 'Microsite' as a factor
mod4v <- lm(O2Enrichment_ppt ~ Max_Stem_height_cm, data = MesoScaleData)
summary(mod4v)
Call:
lm(formula = O2Enrichment_ppt ~ Max_Stem_height_cm, data = MesoScaleData)

Residuals:
   Min     1Q Median     3Q    Max
-80.42 -34.24  12.73  35.77  51.64

Coefficients:
                    Estimate  Std.Error  t      Pr(>|t|)
(Intercept)         -357.39     117.89  -3.032  0.023    *
Max_Stem_height_cm     2.37       1.04   2.278  0.063    .
---
Signif. codes:  0 '***' 0.001 '**' 0.01 '*' 0.05 '.' 0.1 ' ' 1

Residual standard error: 51.83 on 6 degrees of freedom
  (4 observations deleted due to missingness)
Multiple R-squared:  0.4637,    Adjusted R-squared:  0.3743
F-statistic: 5.187 on 1 and 6 DF,  p-value: 0.06302
```

```
# Test residuals for normality using Kolmogorov-Smirnov test
ks.test(x = mod4v$residuals, y = "pnorm", mean(mod4v$residuals), sd(mod4v$residuals))
One-sample Kolmogorov-Smirnov test
data:  mod4v$residuals
D = 0.1766, p-value = 0.9293
alternative hypothesis: two-sided
```

```
# Compare fits of models with and without microsite treatment as a factor
anova(mod3v, mod4v)
Analysis of Variance Table
Model 1: O2Enrichment_ppt ~ Microsite * Max_Stem_height_cm
Model 2: O2Enrichment_ppt ~ Max_Stem_height_cm
  Res.Df   RSS Df Sum of Sq      F Pr(>F)
1      4 13314
2      6 16116 -2   -2801.9 0.4209 0.6825
```

```
# Compare fits of models including root width or max. stem height
anova(mod2v, mod4v)
Analysis of Variance Table
Model 1: O2Enrichment_ppt ~ Root_width_mm
Model 2: O2Enrichment_ppt ~ Max_Stem_height_cm
  Res.Df     RSS Df Sum of Sq F Pr(>F)
1      6  7770.2
2      6 16115.8  0   -8345.5
```

GLMs to predict sediment extractable ammonium from plant traits

```
# Predict NH4 with specific leaf area
mod5v <- lm(ExtNH4_uM ~ Microsite * SLA_cm2.g, data = MesoScaleData)
summary(mod5v)
Call:
lm(formula = ExtNH4_uM ~ Microsite * SLA_cm2.g, data = MesoScaleData)

Residuals:
     1      4      5      6      7      9     11     12
-20.96  35.27 -277.22 -50.11 -66.09 137.16  98.73 143.22

Coefficients:
                        Estimate  Std.Error  t        Pr(>|t|)
 (Intercept)             1138.37    419.887   2.711    0.054   .
 Microsite.L             -152.182    593.81  -0.256   0.8104
 SLA_cm2.g                 -8.409     3.793  -2.217   0.0909   .
 Microsite.L:SLA_cm2.g      1.94      5.365   0.362   0.7359
---
Signif. codes:  0 '***' 0.001 '**' 0.01 '*' 0.05 '.' 0.1 ' ' 1

Residual standard error: 183.4 on 4 degrees of freedom
  (4 observations deleted due to missingness)
Multiple R-squared:  0.5782,    Adjusted R-squared:  0.2619
F-statistic: 1.828 on 3 and 4 DF,  p-value: 0.2821

# Effect did not differ between treatments; remove 'Microsite' as a factor
mod6v <- lm(ExtNH4_uM ~ SLA_cm2.g, data = MesoScaleData)
summary(mod6v)
Call:
lm(formula = ExtNH4_uM ~ SLA_cm2.g, data = MesoScaleData)

Residuals:
   Min     1Q  Median     3Q    Max
-241.34  -99.84   18.57  113.05  172.28

Coefficients:
             Estimate  Std.Error  t        Pr(>|t|)
 (Intercept)  1075.741    341.706   3.148    0.020   *
 SLA_cm2.g      -7.829      3.075  -2.546   0.0437   *
```

Signif. codes: 0 '***' 0.001 '**' 0.01 '*' 0.05 '.' 0.1 ' ' 1

Residual standard error: 159.8 on 6 degrees of freedom
  (4 observations deleted due to missingness)
Multiple R-squared: 0.5193,   Adjusted R-squared: 0.4392
F-statistic: 6.482 on 1 and 6 DF, p-value: 0.04372

 # Test residuals for normality using Kolmogorov-Smirnov test
ks.test(x = mod6v$residuals, y = "pnorm", **mean**(mod6v$residuals), **sd**(mod6v$residuals))
One-sample Kolmogorov-Smirnov test
data: mod6v$residuals
D = 0.2579, p-value = 0.5762
alternative hypothesis: two-sided

 # Compare fits of models with and without microsite treatment as a factor
anova(mod5v, mod6v)
Analysis of Variance Table
Model 1: ExtNH4_uM ~ Microsite * SLA_cm2.g
Model 2: ExtNH4_uM ~ SLA_cm2.g
  Res.Df   RSS Df Sum of Sq   F Pr(>F)
1   4 134486
2   6 153267 -2   -18781 0.2793 0.7699

GLMs to predict net microbial mineralization rates from sediment ammonium and oxygen

 # Predict mineralization/immobilization using extractable ammonium and O2 enrichment
mod1m <- **lm**(Mineralization ~ ExtNH4_uM * O2Enrichment_ppt, data = MesoScaleData)
summary(mod1m)
Call:
lm(formula = Mineralization ~ ExtNH4_uM * O2Enrichment_ppt, data = MesoScaleData)

Residuals:
    Min   1Q Median   3Q   Max
-192.86 -91.16   21.61   93.82 165.87

Coefficients:

	Estimate	Std.Error	t	Pr(>|t|)	
(Intercept)	-2.65E+02	2.09E+02	-1.266	0.241	
ExtNH4_uM	-5.16E+00	6.17E-01	-8.362	3.17E-05	***
O2Enrichment_ppt	-1.58E+00	1.42E+00	-1.11	0.299	
ExtNH4_uM:O2Enrichment_ppt	1.26E-03	4.71E-03	0.268	0.796	

Signif. codes: 0 '***' 0.001 '**' 0.01 '*' 0.05 '.' 0.1 ' ' 1

Residual standard error: 145.8 on 8 degrees of freedom
Multiple R-squared: 0.9874,   Adjusted R-squared: 0.9827
F-statistic: 208.9 on 3 and 8 DF, p-value: 6.181e-08

```
# Remove insignificant interaction term
mod2m <- lm(Mineralization ~ ExtNH4_uM + O2Enrichment_ppt, data = MesoScaleData)
summary(mod2m)
Call:
lm(formula = Mineralization ~ ExtNH4_uM + O2Enrichment_ppt, data = MesoScaleData)

Residuals:
    Min      1Q  Median      3Q     Max
-189.693  -83.882    9.777   90.942  170.531

Coefficients:
                   Estimate     Std.Error    t           Pr(>|t|)
 (Intercept)       -2.21E+02    1.21E+02     -1.824        0.102
 ExtNH4_uM         -5.31E+00    2.47E-01    -21.463    4.87E-09    ***
 O2Enrichment_ppt  -1.26E+00    7.57E-01     -1.667         0.13
---
Signif. codes:  0 '***' 0.001 '**' 0.01 '*' 0.05 '.' 0.1 ' ' 1

Residual standard error: 138.1 on 9 degrees of freedom
Multiple R-squared:  0.9873,    Adjusted R-squared:  0.9845
F-statistic: 349.3 on 2 and 9 DF,  p-value: 2.95e-09

# Compare fits of models with and without interaction term
anova(mod1m, mod2m)
Analysis of Variance Table
Model 1: Mineralization ~ ExtNH4_uM * O2Enrichment_ppt
Model 2: Mineralization ~ ExtNH4_uM + O2Enrichment_ppt
  Res.Df    RSS Df Sum of Sq      F Pr(>F)
1      8 170073
2      9 171596 -1   -1522.7 0.0716 0.7958

# Remove insignificant effect of oxygen
mod3m <- lm(Mineralization ~ ExtNH4_uM, data = MesoScaleData)
summary(mod3m)
Call:
lm(formula = Mineralization ~ ExtNH4_uM, data = MesoScaleData)

Residuals:
    Min      1Q  Median      3Q     Max
-226.750  -93.348    2.842   84.724  217.712

Coefficients:
                Estimate     Std.Error    t           Pr(>|t|)
 (Intercept)    -4.48E+01    6.43E+01     -0.697        0.502
 ExtNH4_uM      -5.53E+00     2.28E-01    -24.306    3.17E-10    ***
---
Signif. codes:  0 '***' 0.001 '**' 0.01 '*' 0.05 '.' 0.1 ' ' 1

Residual standard error: 149.9 on 10 degrees of freedom
```

Multiple R-squared: 0.9834,   Adjusted R-squared: 0.9817
F-statistic: 590.8 on 1 and 10 DF, p-value: 3.166e-10

 # Test residuals for normality using Kolmogorov-Smirnov test
ks.test(x = mod3m$residuals, y = "pnorm", **mean**(mod3m$residuals), **sd**(mod3m$residuals))
One-sample Kolmogorov-Smirnov test
data: mod3m$residuals
D = 0.1157, p-value = 0.9911
alternative hypothesis: two-sided

 # Compare fits of models with and without oxygen
anova(mod2m, mod3m)
Analysis of Variance Table
Model 1: Mineralization ~ ExtNH4_uM + O2Enrichment_ppt
Model 2: Mineralization ~ ExtNH4_uM
  Res.Df   RSS Df Sum of Sq   F Pr(>F)
1   9 171596
2   10 224578 -1   -52982 2.7789 0.1299

GLMs to predict gross nitrification rates from sediment ammonium and oxygen

 # Predict nitrification using extractable ammonium and O2 enrichment
mod1n <- **lm**(Nitrification ~ ExtNH4_uM * O2Enrichment_ppt, data = MesoScaleData)
summary(mod1n)
Call:
lm(formula = Nitrification ~ ExtNH4_uM * O2Enrichment_ppt, data = MesoScaleData)

Residuals:
    Min   1Q Median   3Q   Max
-154.508 -29.911   -8.049   43.004 142.626

Coefficients:

	Estimate	Std.Error	t	Pr(>|t|)
(Intercept)	2.32E+02	1.27E+02	1.823	0.106
ExtNH4_uM	3.20E-01	3.75E-01	0.852	4.19E-01
O2Enrichment_ppt	1.06E+00	8.62E-01	1.235	0.252
ExtNH4_uM:O2Enrichment_ppt	-3.93E-03	2.86E-03	-1.372	0.207

Residual standard error: 88.56 on 8 degrees of freedom
Multiple R-squared: 0.8238,   Adjusted R-squared: 0.7577
F-statistic: 12.46 on 3 and 8 DF, p-value: 0.0022

 # Test residuals for normality using Kolmogorov-Smirnov test
ks.test(x = mod1n$residuals, y = "pnorm", **mean**(mod1n$residuals), **sd**(mod1n$residuals))
One-sample Kolmogorov-Smirnov test
data: mod1n$residuals
D = 0.1242, p-value = 0.9814
alternative hypothesis: two-sided
 # Interaction between ammonium and oxygen appears to be most important term

GLMs to predict denitrification rates from sediment ammonium and oxygen

```
# Predict denitrification using O2 and NH4
mod1d <- lm(log10(DEA_ngN.gC.h_Full) ~ ExtNH4_uM * O2Enrichment_ppt, data = MesoScaleData)
summary(mod1d)
```

```
Call:
lm(formula = log10(DEA_ngN.gC.h_Full) ~ ExtNH4_uM * O2Enrichment_ppt,
    data = MesoScaleData)

Residuals:
     Min       1Q   Median       3Q      Max
-0.48607 -0.26082 -0.07431  0.21285  0.87838

Coefficients:
                               Estimate   Std.Error  t        Pr(>|t|)
 (Intercept)                   5.80E+00   6.60E-01    8.784   2.21E-05   ***
 ExtNH4_uM                    -4.40E-03   1.95E-03   -2.261   5.37E-02   .
 O2Enrichment_ppt              1.88E-02   4.48E-03    4.208    0.00296   **
 ExtNH4_uM:O2Enrichment_ppt   -3.39E-05   1.49E-05   -2.277    0.05233   .
---
Signif. codes:  0 '***' 0.001 '**' 0.01 '*' 0.05 '.' 0.1 ' ' 1

Residual standard error: 0.4599 on 8 degrees of freedom
Multiple R-squared:  0.7676,    Adjusted R-squared:  0.6804
F-statistic: 8.806 on 3 and 8 DF,  p-value: 0.006479
```

```
# Test residuals for normality using Kolmogorov-Smirnov test
ks.test(x = mod1d$residuals, y = "pnorm", mean(mod1d$residuals), sd(mod1d$residuals))
```

```
One-sample Kolmogorov-Smirnov test
data:  mod1d$residuals
D = 0.1723, p-value = 0.811
alternative hypothesis: two-sided
```

```
# Interaction between ammonium and oxygen appears to be important
```

GLMs to predict N2 enrichment from sediment ammonium and oxygen

```
# Test for a potential correlation between DEA measurements and N2 measurements from MIMS
MesoScaleData$log10DEAC <- log10(MesoScaleData$DEA_ngN.gC.h_Full)
N2DEA <- MesoScaleData[, c("log10DEAC", "N2Enrichment_ppt")]
rcorr(as.matrix(N2DEA))
```

```
                log10DEAC N2Enrichment_ppt
log10DEAC            1.00            0.02
N2Enrichment_ppt     0.02            1.00

n= 12

p
                log10DEAC N2Enrichment_ppt
log10DEAC                0.9443
N2Enrichment_ppt 0.9443
```

```
# Predict N2 enrichment in sediment porewater using sediment O2 and NH4
mod1N <- lm(N2Enrichment_ppt ~ O2Enrichment_ppt * ExtNH4_uM, data = MesoScaleData)
summary(mod1N)
```

```
Call:
lm(formula = N2Enrichment_ppt ~ O2Enrichment_ppt * ExtNH4_uM,
    data = MesoScaleData)

Residuals:
    Min      1Q  Median      3Q     Max
-4.9199 -0.7264  0.3173  1.4275  2.5056

Coefficients:
                            Estimate   Std.Error  t        Pr(>|t|)
 (Intercept)                -1.83E+00  3.48E+00   -0.526    0.613
 O2Enrichment_ppt           -3.59E-02  2.36E-02   -1.522    0.167
 ExtNH4_uM                   1.56E-02  1.03E-02    1.521    0.167
 O2Enrichment_ppt:ExtNH4_uM  9.07E-05  7.84E-05    1.156    0.281

Residual standard error: 2.426 on 8 degrees of freedom
Multiple R-squared:  0.2609,    Adjusted R-squared:  -0.01633
F-statistic: 0.9411 on 3 and 8 DF,  p-value: 0.4649
```

```
# Remove interaction and rerun
mod2N <- lm(N2Enrichment_ppt ~ O2Enrichment_ppt + ExtNH4_uM, data = MesoScaleData)
summary(mod2N)
```

```
Call:
lm(formula = N2Enrichment_ppt ~ O2Enrichment_ppt + ExtNH4_uM,
    data = MesoScaleData)

Residuals:
    Min      1Q  Median      3Q     Max
-5.5018 -1.0109  0.1218  1.5306  2.5321

Coefficients
                   Estimate   Std.Error  t        Pr(>|t|)
 (Intercept)       1.36E+00   2.16E+00    0.628    0.546
 O2Enrichment_ppt  -1.34E-02  1.35E-02   -0.987    0.349
 ExtNH4_uM          4.86E-03  4.43E-03    1.098    0.301

Residual standard error: 2.471 on 9 degrees of freedom
Multiple R-squared:  0.1373,    Adjusted R-squared:  -0.05438
F-statistic: 0.7164 on 2 and 9 DF,  p-value: 0.5144
```

```
# No significant relationship detected
```

GLMs to predict denitrification potential from plant traits

```
# Predict effect of plants on denitrification rates using root width, include Microsite as a factor
mod2d <- lm(log10(DEA_ngN.gC.h_Full) ~ Microsite * Root_width_mm, data = MesoScaleData)
summary(mod2d)
```

```
Call:
lm(formula = log10(DEA_ngN.gC.h_Full) ~ Microsite * Root_width_mm,
    data = MesoScaleData)

Residuals:
      1       4       5       6       7       9      11      12
 1.04965 -0.11493 -0.06593 -0.86205  0.03557 -0.22317 -0.00684  0.18770

Coefficients:
                             Estimate   Std.Error  t        Pr(>|t|)
 (Intercept)                 1.11E+00   1.64E+00    0.676    0.536
 Microsite.L                -1.28E-01   2.32E+00   -0.055    0.959
 Root_width_mm               3.64E-01   2.63E-01    1.384    0.238
 Microsite.L:Root_width_mm  -2.53E-02   3.72E-01   -0.068    0.949

Residual standard error: 0.698 on 4 degrees of freedom
  (4 observations deleted due to missingness)
Multiple R-squared:  0.6212,    Adjusted R-squared:  0.3372
F-statistic: 2.187 on 3 and 4 DF,  p-value: 0.2322
```

```
# No significant differences in effect among Microsite treatments; remove Microsite factor and rerun
mod3d <- lm(log10(DEA_ngN.gC.h_Full) ~ Root_width_mm, data = MesoScaleData)
summary(mod3d)
Call:
lm(formula = log10(DEA_ngN.gC.h_Full) ~ Root_width_mm, data = MesoScaleData)

Residuals:
     Min       1Q   Median       3Q      Max
-0.61100 -0.23801 -0.14466  0.05454  1.26855

Coefficients:
              Estimate   Std.Error  t        Pr(>|t|)
 (Intercept)  4.98E-01   1.06E+00   0.469    0.656
 Root_width_mm  4.60E-01    1.60E-01   2.873    0.028    *
---
Signif. codes:  0 '***' 0.001 '**' 0.01 '*' 0.05 '.' 0.1 ' ' 1

Residual standard error: 0.6008 on 6 degrees of freedom
  (4 observations deleted due to missingness)
Multiple R-squared:  0.5791,    Adjusted R-squared:  0.509
F-statistic: 8.256 on 1 and 6 DF,  p-value: 0.0283
```

```
# Test residuals for normality using Kolmogorov-Smirnov test
ks.test(x = mod3d$residuals, y = "pnorm", mean(mod3d$residuals), sd(mod3d$residuals))
One-sample Kolmogorov-Smirnov test
data:  mod3d$residuals
D = 0.306, p-value = 0.3664
alternative hypothesis: two-sided
```

```
# Compare fits of models with and without Microsite factor
anova(mod2d, mod3d)
Analysis of Variance Table
Model 1: log10(DEA_ngN.gC.h_Full) ~ Microsite * Root_width_mm
Model 2: log10(DEA_ngN.gC.h_Full) ~ Root_width_mm
  Res.Df    RSS Df Sum of Sq      F Pr(>F)
1      4 1.9488
2      6 2.1655 -2  -0.21665 0.2223 0.8099

# Compare fit of model using root width to fit of model using ammonium and oxygen as predictors
mod1d <- lm(log10(DEA_ngN.gC.h_Full) ~ ExtNH4_uM * O2Enrichment_ppt, data =
MesoScaleData[which(MesoScaleData$Microsite != "Mudflat"), ])
anova(mod1d, mod3d)
Analysis of Variance Table
Model 1: log10(DEA_ngN.gC.h_Full) ~ ExtNH4_uM * O2Enrichment_ppt
Model 2: log10(DEA_ngN.gC.h_Full) ~ Root_width_mm
  Res.Df     RSS Df Sum of Sq      F Pr(>F)
1      4 0.36748
2      6 2.16546 -2    -1.798 9.7855 0.0288 *
---
Signif. codes:  0 '***' 0.001 '**' 0.01 '*' 0.05 '.' 0.1 ' ' 1

# Predict effect of plants on denitrification using maximum stem height, include Microsite as a factor
mod4d <- lm(log10(DEA_ngN.gC.h_Full) ~ Microsite * Max_Stem_height_cm, data = MesoScaleData)
summary(mod4d)
Call:
lm(formula = log10(DEA_ngN.gC.h_Full) ~ Microsite * Max_Stem_height_cm,
    data = MesoScaleData)

Residuals:
      1       4       5       6       7       9      11      12
-0.32601 -0.49048  0.19640 -0.46254  0.22777  0.56078  0.21870  0.07538

Coefficients:
                                Estimate     Std.Error    t          Pr(>|t|)
 (Intercept)                    -3.01E+00    2.41E+00    -1.251      0.279
 Microsite.L                     8.31E+00    3.40E+00     2.442      0.071   .
 Max_Stem_height_cm              5.16E-02     2.01E-02     2.561      0.0626  .
 Microsite.L:Max_Stem_height_cm -7.09E-02     2.85E-02    -2.49       0.0675  .
---
Signif. codes:  0 '***' 0.001 '**' 0.01 '*' 0.05 '.' 0.1 ' ' 1

Residual standard error: 0.5048 on 4 degrees of freedom
  (4 observations deleted due to missingness)
Multiple R-squared:  0.8019,    Adjusted R-squared:  0.6533
F-statistic: 5.397 on 3 and 4 DF,  p-value: 0.06852
```

```
# Remove microsite factor and rerun
mod5d <- lm(log10(DEA_ngN.gC.h_Full) ~ Max_Stem_height_cm, data = MesoScaleData)
summary(mod5d)
Call:
lm(formula = log10(DEA_ngN.gC.h_Full) ~ Max_Stem_height_cm, data = MesoScaleData)

Residuals:
    Min      1Q  Median      3Q     Max
-1.1105 -0.4177  0.3205  0.4348  0.5495

Coefficients:
                      Estimate     Std.Error    t          Pr(>|t|)
 (Intercept)          -8.65E-02    1.50E+00    -0.058     0.956
 Max_Stem_height_cm    3.20E-02     1.32E-02     2.415     0.052    .
---
Signif. codes:  0 '***' 0.001 '**' 0.01 '*' 0.05 '.' 0.1 ' ' 1

Residual standard error: 0.6595 on 6 degrees of freedom
  (4 observations deleted due to missingness)
Multiple R-squared:  0.4928,    Adjusted R-squared:  0.4083
F-statistic: 5.831 on 1 and 6 DF,  p-value: 0.05224

# Test residuals for normality using Kolmogorov-Smirnov test
ks.test(x = mod5d$residuals, y = "pnorm", mean(mod5d$residuals), sd(mod5d$residuals))
One-sample Kolmogorov-Smirnov test
data:  mod5d$residuals
D = 0.3073, p-value = 0.3613
alternative hypothesis: two-sided

# Compare fits of models with and without microsite factor
anova(mod4d, mod5d)
Analysis of Variance Table
Model 1: log10(DEA_ngN.gC.h_Full) ~ Microsite * Max_Stem_height_cm
Model 2: log10(DEA_ngN.gC.h_Full) ~ Max_Stem_height_cm
  Res.Df    RSS Df Sum of Sq      F Pr(>F)
1      4 1.0192
2      6 2.6094 -2   -1.5901 3.1203 0.1526

# Compare fit of model using max. stem height to model using ammonium and oxygen
anova(mod1d, mod5d)
Analysis of Variance Table
Model 1: log10(DEA_ngN.gC.h_Full) ~ ExtNH4_uM * O2Enrichment_ppt
Model 2: log10(DEA_ngN.gC.h_Full) ~ Max_Stem_height_cm
  Res.Df     RSS Df Sum of Sq      F  Pr(>F)
1      4 0.36748
2      6 2.60937 -2   -2.2419 12.202 0.01983 *
---
Signif. codes:  0 '***' 0.001 '**' 0.01 '*' 0.05 '.' 0.1 ' ' 1
```

GLMs to predict N_2 enrichment from plant traits

```
# Because O2 and NH4 were poor predictors, examine correlations among other
# traits that could influence ventilation and N2
rcorr(as.matrix(MesoScaleData[, c("N2Enrichment_ppt", "AGBiomass_g.m2",
   "Stem_density_m2", "RootMass_g.m..2", "Root_width_mm", "Max_Stem_height_cm",
   "SLA_cm2.g", "Veg_CN")]))
```

	N2Enrichment_ppt	AGBiomass_g.m2	Stem_density_m2	RootMass_g.m..2	Root_width_mm	Max_Stem_height_cm	SLA_cm2.g	Veg_CN
N2Enrichment_ppt	1	-0.65	-0.76	-0.1	0.08	0.33	0.06	-0.61
AGBiomass_g.m2	-0.65	1	0.75	0.12	0.77	0.61	-0.5	-0.44
Stem_density_m2	-0.76	0.75	1	0.19	-0.42	0.11	0.58	-0.17
RootMass_g.m..2	-0.1	0.12	0.19	1	-0.05	0.36	0.45	-0.02
Root_width_mm	0.08	0.77	-0.42	-0.05	1	0.56	-0.63	-0.27
Max_Stem_height_cm	0.33	0.61	0.11	0.36	0.56	1	0.04	-0.73
SLA_cm2.g	0.06	-0.5	0.58	0.45	-0.63	0.04	1	-0.08
Veg_CN	-0.61	-0.44	-0.17	-0.02	-0.27	-0.73	-0.08	1

n

	N2Enrichment_ppt	AGBiomass_g.m2	Stem_density_m2	RootMass_g.m..2	Root_width_mm	Max_Stem_height_cm	SLA_cm2.g	Veg_CN
N2Enrichment_ppt	12	12	12	12	8	8	8	8
AGBiomass_g.m2	12	12	12	12	8	8	8	8
Stem_density_m2	12	12	12	12	8	8	8	8
RootMass_g.m..2	12	12	12	12	8	8	8	8
Root_width_mm	8	8	8	8	12	8	8	8
Max_Stem_height_cm	8	8	8	8	8	12	8	8
SLA_cm2.g	8	8	8	8	8	8	12	8
Veg_CN	8	8	8	8	8	8	8	12

p

	N2Enrichment_ppt	ExtNH4_uM	AGBiomass_g.m2	Stem_density_m2	RootMass_g.m..2	Root_width_mm	Max_Stem_height_cm	SLA_cm2.g	Veg_CN
N2Enrichment_ppt		0.5131	0.0227	0.0044	0.7653	0.8539	0.424	0.8813	0.1061
ExtNH4_uM	0.5131		0.6225	0.4019	0.1224	0.4184	0.7548	0.0437	0.7082
AGBiomass_g.m2	0.0227	0.6225		0.0054	0.7095	0.0253	0.1059	0.2076	0.2746
Stem_density_m2	0.0044	0.4019	0.0054		0.5448	0.3013	0.8029	0.1297	0.681
RootMass_g.m..2	0.7653	0.1224	0.7095	0.5448		0.9006	0.3803	0.26	0.9648
Root_width_mm	0.8539	0.4184	0.0253	0.3013	0.9006		0.1466	0.0919	0.5191
Max_Stem_height_cm	0.424	0.7548	0.1059	0.8029	0.3803	0.1466		0.93	0.0389
SLA_cm2.g	0.8813	0.0437	0.2076	0.1297	0.26	0.0919	0.93		0.8432
Veg_CN	0.1061	0.7082	0.2746	0.681	0.9648	0.5191	0.0389	0.8432	

```
# Stem density appears to be the best candidate

mod3N <- lm(N2Enrichment_ppt ~ Microsite * Stem_density_m2, data = MesoScaleData)
summary(mod3N)
```

```
Call:
lm(formula = N2Enrichment_ppt ~ Microsite * Stem_density_m2,
    data = MesoScaleData)

Residuals:
     Min       1Q   Median       3Q      Max
-1.78440 -0.62496  0.09186  0.30902  2.77570

Coefficients: (1 not defined because of singularities)
                              Estimate   Std.Error  t        Pr(>|t|)
 (Intercept)                   7.52E+00   1.27E+00   5.926       0.001  ***
 Microsite.L                   1.06E+00   1.15E+00   0.923       0.387
 Microsite.Q                  -5.61E+00   2.89E+00  -1.943    0.093142  .
 Stem_density_m2              -3.19E-02   1.07E-02  -2.971    0.020768  *
 Microsite.L:Stem_density_m2   -0.03931    0.01628  -2.415    0.046429  *
 Microsite.Q:Stem_density_m2   NA          NA        NA        NA
---
Signif. codes:  0 '***' 0.001 '**' 0.01 '*' 0.05 '.' 0.1 ' ' 1

Residual standard error: 1.367 on 7 degrees of freedom
Multiple R-squared:  0.7946,    Adjusted R-squared:  0.6772
F-statistic:  6.77 on 4 and 7 DF,  p-value: 0.01485
```

```
# Remove microsite as a factor
mod4N <- lm(N2Enrichment_ppt ~ Stem_density_m2, data = MesoScaleData)
summary(mod4N)
```

```
Call:
lm(formula = N2Enrichment_ppt ~ Stem_density_m2, data = MesoScaleData)

Residuals:
    Min      1Q  Median      3Q     Max
-4.3350 -0.3287  0.3663  0.6342  1.9982

Coefficients:
                  Estimate    Std.Error   t        Pr(>|t|)
 (Intercept)      5.79E+00    7.31E-01     7.914   1.29E-05   ***
 Stem_density_m2  -9.71E-03   2.65E-03    -3.665   4.36E-03   **
---
Signif. codes:  0 '***' 0.001 '**' 0.01 '*' 0.05 '.' 0.1 ' ' 1

Residual standard error: 1.649 on 10 degrees of freedom
Multiple R-squared:  0.5732,    Adjusted R-squared:  0.5305
F-statistic: 13.43 on 1 and 10 DF,  p-value: 0.004356
```

```
# Test residuals for normality using Kolmogorov-Smirnov test
ks.test(x = mod4N$residuals, y = "pnorm", mean(mod4N$residuals), sd(mod4N$residuals))
One-sample Kolmogorov-Smirnov test
data:  mod4N$residuals
D = 0.2516, p-value = 0.3702
alternative hypothesis: two-sided
```

```
# Compare fits of models with and without Microsite factor
anova(mod3N, mod4N)
Analysis of Variance Table
Model 1: N2Enrichment_ppt ~ Microsite * Stem_density_m2
Model 2: N2Enrichment_ppt ~ Stem_density_m2
  Res.Df    RSS Df Sum of Sq      F Pr(>F)
1      7 13.086
2     10 27.195 -3   -14.109 2.5157  0.142
```

Figures

```
# Change base text size for figures
theme_set(theme_bw(base_size = 16))
```

```
# O2 enrichment versus rhizome width
Rootwidth_O2 <- ggplot(MesoScaleData, aes(x = Root_width_mm, y = O2Enrichment_ppt))
Rootwidth_O2 + geom_point(size = 4) + stat_smooth(method = lm, size = 2, color = "black") +
xlab("Rhizome width (mm)") + ylab(expression(paste(O[2], " Enrichment (ppt)"))) + ggtitle("(A)")
```

```
# O2 enrichment versus maximum stem height
MaxStemHeight_O2 <- ggplot(MesoScaleData, aes(x = Max_Stem_height_cm, y = O2Enrichment_ppt))
MaxStemHeight_O2 + geom_point(size = 4) + stat_smooth(method = lm, size = 2, color = "black") +
xlab("Maximum stem height (mm)") + ylab(expression(paste(O[2], " Enrichment (ppt)"))) +
ggtitle("(B)")
```

```
# Extractable ammonium versus specific leaf area
SLA_ammonium <- ggplot(MesoScaleData, aes(x = SLA_cm2.g, y = ExtNH4_uM))
SLA_ammonium + geom_point(size = 4) + stat_smooth(method = lm, size = 2, color = "black") +
xlab(expression(paste("Specific leaf area (", cm^2, g^-1, ")"))) + ylab(expression(paste("Extractable
N", H[4], " (", mu, "M"))) + ggtitle("(C)")

# Extractable ammonium verus immobilization
AmmoniumMin <- ggplot(ExProfiles, aes(x = ExtNH4_uM, y = -1 * Mineralization))
AmmoniumMin + geom_point(size = 4, color = "black") + stat_smooth(method = lm, size = 2, color =
"black") + xlab(expression(paste("Extractable N", H[4], "(", mu, "M"))) +
lab(expression(paste("Immobilization Rate (", mu, "gN ", cm^-3, h^-1, ")"))) + ggtitle("(A)")

# Interaction plot: Nitrification Predictors = Ammonium (NH4) and O2 Enrichment
AmmoniumNit <- ggplot(MesoScaleData, aes(x = O2Enrichment_ppt, y = Nitrification,
   color = NH4LowHigh))
AmmoniumNit + geom_point(size = 4) + stat_smooth(method = lm, size = 2) +
xlab(expression(paste(O[2], "Enrichment"))) + ylab(expression(paste("Nitrification Rate (", mu, "gN ",
cm^-3, h^-1, ")"))) + scale_color_manual(values = c("black", "grey50"), labels =
c(expression(paste("High ", NH[4])), expression(paste("Low ", NH[4])))) + theme(legend.title =
element_blank()) + theme(legend.text.align = 0) + theme(legend.position = c(0.8, 0.85)) + ggtitle("(B)")

# Interaction plot: log10(Denitrification/C) Predictors = Ammonium (NH4) and O2 Enrichment
MesoScaleData$log10DEAC_meso <- log10(MesoScaleData$DEA_ngN.gC.h_Full)
AmmoniumDEAC <- ggplot(MesoScaleData, aes(x = O2Enrichment_ppt, y =
DEA_ngN.gC.h_Full/1000, color = NH4LowHigh))
AmmoniumDEAC + geom_point(size = 4) + stat_smooth(method = lm, size = 2) +
xlab(expression(paste(O[2], "Enrichment"))) + ylab(expression(paste("Denitrification Rate (", mu, "gN
", gC^-1, h^-1, ")"))) + scale_color_manual(values = c("black", "grey50"), labels =
c(expression(paste("High ", NH[4])), expression(paste("Low ", NH[4])))) + scale_y_log10() +
theme(legend.title = element_blank()) + theme(legend.text.align = 0) + theme(legend.position = c(0.8,
0.2)) + ggtitle("(C)")

# Root width versus denitrification
RootWidth_Denit <- ggplot(MesoScaleData[which(MesoScaleData$Microsite != "Mudflat"),
   ], aes(x = Root_width_mm, y = DEA_ngN.gC.h_Full/1000))
RootWidth_Denit + geom_point(size = 4, aes(color = Microsite)) + stat_smooth(method = lm, size = 2,
color = "black") + xlab("Rhizome width (mm)") + ylab(expression(paste("Denitrification Rate (", mu,
"gN ", gC^-1, h^-1, ")"))) + scale_color_manual(values = c("springgreen4", "springgreen",
"darkgoldenrod"), labels = c("Marsh Edge", "Marsh Platform")) + scale_y_log10() + ggtitle("(A)")

# Maximum stem height versus denitrification
Maxstemheight_Denit <- ggplot(MesoScaleData[which(MesoScaleData$Microsite != "Mudflat"), ],
aes(x = Max_Stem_height_cm, y = DEA_ngN.gC.h_Full/1000))
Maxstemheight_Denit + geom_point(size = 4, aes(color = Microsite)) + stat_smooth(method = lm, size
= 2, color = "black") + xlab("Maximum stem height (cm)") + ylab(expression(paste("Denitrification
Rate (", mu, "gN ", gC^-1, h^-1, ")"))) + scale_color_manual(values = c("springgreen4", "springgreen",
"darkgoldenrod"), labels = c("Marsh Edge", "Marsh Platform")) + scale_y_log10() + ggtitle("(B)")

# Stem density versus N2 enrichment
Stemdens_N2 <- ggplot(MesoScaleData, aes(x = Stem_density_m2, y = N2Enrichment_ppt))
Stemdens_N2 + geom_point(size = 4, aes(color = Microsite)) + stat_smooth(method = lm, size = 2,
```

```
color = "black") + xlab(expression(paste("Stem density (", m^-2, ")"))) + ylab(expression(paste(N[2], " Enrichment (ppt)"))) + scale_color_manual(values = c("springgreen4", "springgreen", "darkgoldenrod"), labels = c("Marsh Edge", "Marsh Platform", "Mudflat")) + ggtitle("(C)") + theme(legend.position = c(0.3, 0.2), legend.text = element_text(size = 11))
```

Appendix C: Supplement to Chapter 4

Packages

```
library(ggplot2)
library(bear)
library(Hmisc)
library(scatterplot3d)
```

Data and Formatting

```
setwd(filepath3)
LIall <- read.csv("20141107_LI_AllData_2012-2013.csv")
# Convert 'Month_Year' from factor to ordered factor
LIall$Month_Year <- ordered(LIall$Month_Year, levels = c("April2012", "June2012",
   "August2012", "April2013", "June2013", "August2013"))
# Convert Site from a Factor to an Ordered Factor
LIall$Site <- ordered(LIall$Site, levels = c("East Creek", "Frost Creek", "Oceanside",
   "Lido", "Gardiners", "West Meadow", "Smith Point", "Indian Island", "Hubbard",
   "Mashomack", "Accabonac"))
# Create dataframe for measurements collected in vegetated plots only
LIallVEG <- droplevels(LIall[LIall$Tall_short != "sediment", ])
# Create dataframe for measurements collected in non-vegetated, or 'sediment,' plots
LIallSED <- droplevels(LIall[LIall$Tall_short == "sediment", ])
# Create dataframe for all plots measured in 2013
LIall2013 <- LIall[which(LIall$Sample_Year == "2013"), ]
# Create dataframe for all vegetated plots measured in 2013
LIallVEG2013 <- LIallVEG[which(LIallVEG$Month_Year == "June2013" | LIallVEG$Month_Year ==
   "August2013"), ]
LIallSED2013 <- LIallSED[which(LIallSED$Month_Year == "June2013" | LIallSED$Month_Year ==
   "August2013"), ]
#Change base text size for figures
theme_set(theme_bw(base_size = 16))
```

Examine pairwise correlations among plant traits

I used rcorr{Hmisc} to compute Pearson correlations for a matrix of plant traits.

```
# Create a matrix of plant traits for all vegetated plots measured in 2013
cordata_veg <- LIallVEG2013[, c("DryWeight_g.m2", "RootMass_g.m2", "RhizomeWidth_mm",
   "Photosyn_uMCO2.m2.s1", "Conduct_molH2O.m2.s1", "VegN_mg.gDW", "SLA_cm2g.1")]
# Compute pairwise Pearson correlations for trait variables
rcorr(as.matrix(cordata_veg))
```

	DryWeight_g.m2	RootMass_g.m2	RhizomeWidth_mm	Photosyn_uMCO2.m2.s1	Conduct_molH2O.m2.s1	VegN_mg.gDW	SLA_cm2g.1
DryWeight_g.m2	1	-0.34	-0.07	-0.07	-0.08	-0.09	-0.2
RootMass_g.m2	-0.34	1	0.05	0.17	0.05	-0.05	0.13
RhizomeWidth_mm	-0.07	0.05	1	0.06	-0.12	0.16	0.15
Photosyn_uMCO2.m2.s1	-0.07	0.17	0.06	1	0.35	0.24	0.15
Conduct_molH2O.m2.s1	-0.08	0.05	-0.12	0.35	1	0.06	-0.09
VegN_mg.gDW	-0.09	-0.05	0.16	0.24	0.06	1	0.41
SLA_cm2g.1	-0.2	0.13	0.15	0.15	-0.09	0.41	1

n= 220

p

	DryWeight_g.m2	RootMass_g.m2	RhizomeWidth_mm	Photosyn_uMCO2.m2.s1	Conduct_molH2O.m2.s1	VegN_mg.gDW	SLA_cm2g.1
DryWeight_g.m2		0.0000	0.3308	0.2926	0.2680	0.2011	0.0032
RootMass_g.m2	0.0000		0.4945	0.0113	0.4675	0.4669	0.0620
RhizomeWidth_mm	0.3308	0.4945		0.4129	0.0667	0.0189	0.0254
Photosyn_uMCO2.m2.s1	0.2926	0.0113	0.4129		0.0000	0.0004	0.0315
Conduct_molH2O.m2.s1	0.2680	0.4675	0.0667	0.0000		0.3523	0.1843
VegN_mg.gDW	0.2011	0.4669	0.0189	0.0004	0.3523		0.0000
SLA_cm2g.1	0.0032	0.0620	0.0254	0.0315	0.1843	0.0000	

Determine which traits are most correlated with denitrification

```
# Transform denitrification rates to meet assumptions of normality for all data sets
LIallVEG2013$log10DEAC <- log10(LIallVEG2013$Denitrification_ng.N.g.C.hr)
LIallVEG2013$log10DEA <- log10(LIallVEG2013$Denitrification_ng.N.g.hr)
# Examine correlations between log10-transformed denitrification rates and plant traits
cordata_logdenit_traits <- LIallVEG2013[, c("log10DEA", "log10DEAC", "DryWeight_g.m2",
  "RootMass_g.m2", "RhizomeWidth_mm", "Photosyn_uMCO2.m2.s1", "Conduct_molH2O.m2.s1",
  "VegN_mg.gDW", "SLA_cm2g.1")]
rcorr(as.matrix(cordata_logdenit_traits))
```

	log10DEA	log10DEAC	DryWeight_g.m2	RootMass_g.m2	RhizomeWidth_mm	Photosyn_uMCO2.m2.s1	Conduct_molH2O.m2.s1	VegN_mg.gDW	SLA_cm2g.1
log10DEA	1.00	0.93	0.28	-0.42	0.08	-0.02	-0.03	0.32	0.16
log10DEAC	0.93	1.00	0.34	-0.33	0.02	0.06	0.02	0.35	0.21
DryWeight_g.m2	0.28	0.34	1.00	-0.34	-0.07	-0.07	-0.08	-0.09	-0.20
RootMass_g.m2	-0.42	-0.33	-0.34	1.00	0.05	0.17	0.05	-0.05	0.13
RhizomeWidth_mm	0.08	0.02	-0.07	0.05	1.00	0.06	-0.12	0.16	0.15
Photosyn_uMCO2.m2.s1	-0.02	0.06	-0.07	0.17	0.06	1.00	0.35	0.24	0.15
Conduct_molH2O.m2.s1	-0.03	0.02	-0.08	0.05	-0.12	0.35	1.00	0.06	-0.09
VegN_mg.gDW	0.32	0.35	-0.09	-0.05	0.16	0.24	0.06	1.00	0.41
SLA_cm2g.1	0.16	0.21	-0.20	0.13	0.15	0.15	-0.09	0.41	1.00

n

	log10DEA	log10DEAC	DryWeight_g.m2	RootMass_g.m2	RhizomeWidth_mm	Photosyn_uMCO2.m2.s1	Conduct_molH2O.m2.s1	VegN_mg.gDW	SLA_cm2g.1
log10DEA	220	218	218	218	218	218	218	218	218
log10DEAC	218	220	218	218	218	218	218	218	218
DryWeight_g.m2	218	218	220	220	220	220	220	220	220
RootMass_g.m2	218	218	220	220	220	220	220	220	220
RhizomeWidth_mm	218	218	220	220	220	220	220	220	220
Photosyn_uMCO2.m2.s1	218	218	220	220	220	220	220	220	220
Conduct_molH2O.m2.s1	218	218	220	220	220	220	220	220	220
VegN_mg.gDW	218	218	220	220	220	220	220	220	220
SLA_cm2g.1	218	218	220	220	220	220	220	220	220

p

	log10DEA	log10DEAC	DryWeight_g.m2	RootMass_g.m2	RhizomeWidth_mm	Photosyn_uMCO2.m2.s1	Conduct_molH2O.m2.s1	VegN_mg.gDW	SLA_cm2g.1
log10DEA		0.000	0.000	0.000	0.235	0.821	0.701	0.000	0.016
log10DEAC	0.000		0.000	0.000	0.755	0.354	0.751	0.000	0.002
DryWeight_g.m2	0.000	0.000		0.000	0.331	0.293	0.268	0.201	0.003
RootMass_g.m2	0.000	0.000	0.000		0.495	0.011	0.468	0.467	0.062
RhizomeWidth_mm	0.235	0.755	0.331	0.495		0.413	0.067	0.019	0.025
Photosyn_uMCO2.m2.s1	0.821	0.354	0.293	0.011	0.413		0.000	0.000	0.032
Conduct_molH2O.m2.s1	0.701	0.751	0.268	0.468	0.067	0.000		0.352	0.184
VegN_mg.gDW	0.000	0.000	0.201	0.467	0.019	0.000	0.352		0.000
SLA_cm2g.1	0.016	0.002	0.003	0.062	0.025	0.032	0.184	0.000	

Create summary dataframes of site means and errors for Denitrification, log10-transformed Denitrification rates, BGBiomass, and Leaf N

I used the summarySE{bear} function to create summary data frames for each variable of interest at the site level. I used the rename function to rename the error variables with unique column headings. Finally, I used cbind to merge all of the summary tables into a single data frame (order is important for this function).

```
# For each summary dataframe, rename error variables with unique column headings
Denit <- summarySE(measurevar = "Denitrification_ng.N.g.hr", groupvars = c("Month_Year",
   "Site"), data = LIallVEG2013)
Denit <- rename(Denit, c(se = "Denit_se", sd = "Denit_sd", ci = "Denit_ci"))
log10DEA <- summarySE(measurevar = "log10DEA", groupvars = c("Month_Year", "Site"),
   data = LIallVEG2013, na.rm = T)
log10DEA <- rename(log10DEA, c(se = "log10DEA_se", sd = "log10DEA_sd", ci = "log10DEA_ci"))
RootMass <- summarySE(measurevar = "RootMass_g.m2", groupvars = c("Month_Year",
   "Site"), data = LIallVEG2013)
RootMass <- rename(RootMass, c(se = "RootMass_se", sd = "RootMass_sd", ci = "RootMass_ci"))
LeafN <- summarySE(measurevar = "VegN_mg.gDW", groupvars = c("Month_Year", "Site"),
   data = LIallVEG2013)
LeafN <- rename(LeafN, c(se = "LeafN_se", sd = "LeafN_sd", ci = "LeafN_ci"))
denit_trait_site <- cbind(Denit, log10DEA, RootMass, LeafN)
```

Construct GLMs to predict denitrification rates with plant traits for site-level data

Initial models contain Month_Year as a categorical predictor and the two plant traits most correlated with denitrification rates that are not intercorrelated (redundant). In this case, the two most correlated plant traits were total Root mass and leaf nitrogen content.

```
# Run denitrification model at site level
mod1dt <- lm(log10DEA ~ Month_Year * RootMass_g.m2 * VegN_mg.gDW, data = denit_trait_site)
summary(mod1dt)
Call:
lm(formula = log10DEA ~ Month_Year * RootMass_g.m2 * VegN_mg.gDW,
    data = denit_trait_site)

Residuals:
     Min       1Q   Median       3Q      Max
-0.66804 -0.04400  0.03585  0.14754  0.27036

Coefficients:
                                  Estimate   Std.Error  t value  Pr(>|t|)
   (Intercept)                    3.16E-01   2.22E+00     0.143     0.889
   Month_Year.L                  -1.11E+00   3.14E+00    -0.355     0.728
   RootMass_g.m2                 -3.70E-04   1.06E-03    -0.349     0.732
   VegN_mg.gDW                    1.88E-01   1.58E-01      1.19     0.254
   Month_Year.L:RootMass_g.m2    -8.92E-04   1.50E-03    -0.597      0.56
   Month_Year.L:VegN_mg.gDW       6.73E-02   2.23E-01     0.302     0.767
   RootMass_g.m2:VegN_mg.gDW      1.03E-05   7.72E-05     0.134     0.895
   Month_Year.L:RootMass_g.m2:    6.63E-05   1.09E-04     0.607     0.553
   VegN_mg.gDW

Residual standard error: 0.2717 on 14 degrees of freedom
Multiple R-squared:  0.7814,    Adjusted R-squared:  0.672
F-statistic: 7.148 on 7 and 14 DF,  p-value: 0.0009519
# Seasonality is not an important component; remove and rerun
mod2dt <- lm(log10DEA ~ RootMass_g.m2 * VegN_mg.gDW, data = denit_trait_site)
summary(mod2dt)
Call:
lm(formula = log10DEA ~ RootMass_g.m2 * VegN_mg.gDW, data = denit_trait_site)

Residuals:
     Min       1Q   Median       3Q      Max
-0.70748 -0.11176  0.01732  0.17788  0.67539

Coefficients:
                           Estimate  Std.Error  t         Pr(>|t|)
  (Intercept)                 0.261      1.189    0.220    0.829
  RootMass_g.m2               0.000      0.000    0.813    0.427
  VegN_mg.gDW                 0.194      0.074    2.608    0.018   *
  RootMass_g.m2:VegN_mg.gDW   0.000      0.000   -1.577    0.132
---
Signif. codes:  0 '***' 0.001 '**' 0.01 '*' 0.05 '.' 0.1 ' ' 1

Residual standard error: 0.3335 on 18 degrees of freedom
Multiple R-squared:  0.5764,    Adjusted R-squared:  0.5058
F-statistic: 8.165 on 3 and 18 DF,  p-value: 0.001216
```

```
# No significant interaction between BGBiomass and Leaf N; remove
# interaction and rerun model
mod3dt <- lm(log10DEA ~ RootMass_g.m2 + VegN_mg.gDW, data = denit_trait_site)
summary(mod3dt)
Call:
lm(formula = log10DEA ~ RootMass_g.m2 + VegN_mg.gDW, data = denit_trait_site)

Residuals:
    Min      1Q  Median      3Q     Max
-0.64008 -0.15953  0.03293  0.25169  0.70461

Coefficients:
                Estimate  Std.Error  t        Pr(>|t|)
 (Intercept)       1.994      0.472   4.225    4.59E-04   ***
 RootMass_g.m2     0.000      0.000  -3.465    2.60E-03    **
 VegN_mg.gDW       0.084      0.027   3.103    5.86E-03    **
---
Signif. codes:  0 '***' 0.001 '**' 0.01 '*' 0.05 '.' 0.1 ' ' 1

Residual standard error: 0.3464 on 19 degrees of freedom
Multiple R-squared:  0.5179,    Adjusted R-squared:  0.4671
F-statistic: 10.21 on 2 and 19 DF,  p-value: 0.0009769
# Test normality of residuals with KS Lilliefors test
ks.test(x = mod3dt$residuals, y = "pnorm", mean(mod3dt$residuals), sd(mod3dt$residuals))
One-sample Kolmogorov-Smirnov test
data:  mod3dt$residuals
D = 0.0949, p-value = 0.9779
alternative hypothesis: two-sided

# Visualize relationship between log10DEA BGBiomass and Leaf N in 3
# dimensions
s1d <- scatterplot3d(x = denit_trait_site$RootMass_g.m2, y = denit_trait_site$VegN_mg.gDW, z =
denit_trait_site$log10DEA, xlab = expression(paste("Root mass (g ",  m^-2, ")")), ylab =
expression(paste("Leaf nitrogen content (mgN ", g^-1, ")")), zlab = expression(paste(log[10],
"[Denitrification rate (ngN ", g^-1, h^-1, ")]")), color = "black", pch = 19)
s1d$plane3d(mod3dt)

# Plot Denitrification versus Root Mass at the site level
Denit_RootMass2 <- ggplot(denit_trait_site, aes(x = RootMass_g.m2, y =
Denitrification_ng.N.g.hr/1000))
Denit_RootMass2 + geom_point(size = 6, color = "gray24") + stat_smooth(method = lm, size = 2, color
= "black") + ylab(expression(paste("Denitrification Rate (", mu, "gN ", g^-1, h^-1, ")"))) +
xlab(expression(paste("Root mass (g ", m^-2, ")"))) + theme(legend.title = element_blank()) +
scale_y_log10()

# Plot Denitrification versus Leaf N at the site level
Denit_LeafN2 <- ggplot(denit_trait_site, aes(x = VegN_mg.gDW, y = Denitrification_ng.N.g.hr/1000))
Denit_LeafN2 + geom_point(size = 6, color = "gray24") + stat_smooth(method = lm, size = 2, color =
"black") + ylab(expression(paste("Denitrification Rate (", mu, "gN ", g^-1, h^-1, ")"))) +
```

```
xlab(expression(paste("Leaf nitrogen content (mgN ", g^-1, ")"))) + theme(legend.title =
element_blank()) + scale_y_log10()
```

Determine which sediment variables are most correlated with denitrification rates

```
cordata_denit_sed <- LIallVEG2013[, c("log10DEA", "log10DEAC", "SedC_mg.gDW",
  "SedN_mg.gDW", "NH4_Extractable_uM", "NO3_Extractable_uM", "Salinity_ppt",
  "Sed_temp")]
rcorr(as.matrix(cordata_denit_sed))
```

	log10DEA	log10DEAC	SedC_mg.gDW	SedN_mg.gDW	NH4_Extractable_uM	NO3_Extractable_uM	Salinity_ppt	Sed_temp
log10DEA	1.00	0.93	0.28	0.32	0.39	0.52	-0.21	-0.10
log10DEAC	0.93	1.00	-0.05	0.05	0.35	0.48	-0.18	-0.11
SedC_mg.gDW	0.28	-0.05	1.00	0.79	0.10	0.30	-0.33	-0.12
SedN_mg.gDW	0.32	0.05	0.79	1.00	0.04	0.33	-0.27	-0.14
NH4_Extractable_uM	0.39	0.35	0.10	0.04	1.00	0.30	-0.07	0.03
NO3_Extractable_uM	0.52	0.48	0.30	0.33	0.30	1.00	-0.34	-0.24
Salinity_ppt	-0.21	-0.18	-0.33	-0.27	-0.07	-0.34	1.00	0.48
Sed_temp	-0.10	-0.11	-0.12	-0.14	0.03	-0.24	0.48	1.00

n

	log10DEA	log10DEAC	SedC_mg.gDW	SedN_mg.gDW	NH4_Extractable_uM	NO3_Extractable_uM	Salinity_ppt	Sed_temp
log10DEA	220	218	218	218	217	216	216	218
log10DEAC	218	220	218	218	217	216	216	218
SedC_mg.gDW	218	218	220	220	219	218	218	220
SedN_mg.gDW	218	218	220	220	219	218	218	220
NH4_Extractable_uM	217	217	219	219	220	218	217	219
NO3_Extractable_uM	216	216	218	218	218	220	216	218
Salinity_ppt	216	216	218	218	217	216	220	218
Sed_temp	218	218	220	220	219	218	218	220

p

	log10DEA	log10DEAC	SedC_mg.gDW	SedN_mg.gDW	NH4_Extractable_uM	NO3_Extractable_uM	Salinity_ppt	Sed_temp
log10DEA		0.0000	0.0000	0.0000	0.0000	0.0000	0.0016	0.1529
log10DEAC	0.0000		0.4861	0.4457	0.0000	0.0000	0.0085	0.1074
SedC_mg.gDW	0.0000	0.4861		0.0000	0.1439	0.0000	0.0000	0.0853
SedN_mg.gDW	0.0000	0.4457	0.0000		0.5402	0.0000	0.0000	0.0323
NH4_Extractable_uM	0.0000	0.0000	0.1439	0.5402		0.0000	0.2752	0.6697
NO3_Extractable_uM	0.0000	0.0000	0.0000	0.0000	0.0000		0.0000	0.0003
Salinity_ppt	0.0016	0.0085	0.0000	0.0000	0.2752	0.0000		0.0000
Sed_temp	0.1529	0.1074	0.0853	0.0323	0.6697	0.0003	0.0000	

 # DEAs appear to be correlated with sediment organic matter and nitrate; will build models with these variables

Create summary dataframes of site means and errors for Denitrification, log10-transformed Denitrificaiton rates, BGBiomass, and Leaf N

```
# Create dataframe of site means for denitrification, sediment carbon, and nitrate
SedC <- summarySE(measurevar = "SedC_mg.gDW", groupvars = c("Month_Year", "Site"),
   data = LIallVEG2013)
SedC <- rename(SedC, c(se = "SedC_se", sd = "SedC_sd", ci = "SedC_ci"))
ExtNO3 <- summarySE(measurevar = "NO3_Extractable_uM", groupvars = c("Month_Year",
   "Site"), data = LIallVEG2013, na.rm = T)
ExtNO3 <- rename(ExtNO3, c(se = "ExtNO3_se", sd = "ExtNO3_sd", ci = "ExtNO3_ci"))
Denit_sed_site <- cbind(Denit, log10DEA, SedC, ExtNO3)
```

Construct GLMs to predict denitrification rates using sediment data at the site level

```
# Run denitrification/sediment model at site level
mod1ds <- lm(log10DEA ~ Month_Year * SedC_mg.gDW * NO3_Extractable_uM, data =
Denit_sed_site)
summary(mod1ds)
Call:
lm(formula = log10DEA ~ Month_Year * SedC_mg.gDW * NO3_Extractable_uM,
   data = Denit_sed_site)

Residuals:
    Min      1Q  Median      3Q     Max
-0.70788 -0.14646 -0.05757  0.11143  0.56904

Coefficients:
                                    Estimate     Std.Error   t value   Pr(>|t|)
   (Intercept)                      1.50E+00   4.92E-01      3.055    **0.00857
```

Month_Year.L	5.83E-01	6.95E-01	0.838	0.41615
SedC_mg.gDW	3.25E-03	2.69E-03	1.206	0.24785
NO3_Extractable_uM	1.26E-02	9.05E-03	1.397	0.18421
Month_Year.L:SedC_mg.gDW	-8.07E-04	3.81E-03	-0.212	0.83528
Month_Year.L:NO3_Extractable_uM	-1.41E-02	1.28E-02	-1.101	0.28961
SedC_mg.gDW:NO3_Extractable_uM	-1.76E-05	3.87E-05	-0.456	0.65533
Month_Year.L:SedC_mg.gDW: NO3_Extractable_uM	3.71E-05	5.47E-05	0.678	0.50855

Signif. codes: 0 '***' 0.001 '**' 0.01 '*' 0.05 '.' 0.1 ' ' 1

Residual standard error: 0.3388 on 14 degrees of freedom
Multiple R-squared: 0.6602, Adjusted R-squared: 0.4902
F-statistic: 3.885 on 7 and 14 DF, p-value: 0.01474

```
# Remove season variable and rerun
mod2ds <- lm(log10DEA ~ SedC_mg.gDW * NO3_Extractable_uM, data = Denit_sed_site)
summary(mod2ds)
```

Call:
lm(formula = log10DEA ~ SedC_mg.gDW * NO3_Extractable_uM, data = Denit_sed_site)

Residuals:
Min	1Q	Median	3Q	Max
-0.55816	-0.15092	-0.07691	0.12355	0.68625

Coefficients:

	Estimate	Std.Error	t	Pr(>|t|)	
(Intercept)	1.641	0.445	3.684	1.70E-03	**
SedC_mg.gDW	0.003	0.002	1.347	0.195	
NO3_Extractable_uM	0.012	0.007	1.703	0.106	
SedC_mg.gDW:NO3_Extractable_uM	0.000	0.000	-0.728	0.476	

Signif. codes: 0 '***' 0.001 '**' 0.01 '*' 0.05 '.' 0.1 ' ' 1

Residual standard error: 0.3354 on 18 degrees of freedom
Multiple R-squared: 0.5716, Adjusted R-squared: 0.5002
F-statistic: 8.006 on 3 and 18 DF, p-value: 0.001341

```
# Remove non-significant interaction and rerun
mod3ds <- lm(log10DEA ~ SedC_mg.gDW + NO3_Extractable_uM, data = Denit_sed_site)
summary(mod3ds)
```

Call:
lm(formula = log10DEA ~ SedC_mg.gDW + NO3_Extractable_uM, data = Denit_sed_site)

Residuals:
Min	1Q	Median	3Q	Max
-0.65828	-0.19823	-0.04106	0.18050	0.64631

Coefficients:

	Estimate	Std.Error	t	Pr(>|t|)	
(Intercept)	1.924	0.214	8.971	2.93E-08	***
SedC_mg.gDW	0.002	0.001	1.353	0.192	
NO3_Extractable_uM	0.007	0.002	3.600	0.002	**

Signif. codes: 0 '***' 0.001 '**' 0.01 '*' 0.05 '.' 0.1 ' ' 1

Residual standard error: 0.3312 on 19 degrees of freedom
Multiple R-squared: 0.559, Adjusted R-squared: 0.5126
F-statistic: 12.04 on 2 and 19 DF, p-value: 0.0004187

```
# Test model residuals for normality using KS Lilliefors test
ks.test(x = mod3ds$residuals, y = "pnorm", mean(mod3ds$residuals), sd(mod3ds$residuals))
```

One-sample Kolmogorov-Smirnov test
data: mod3ds$residuals
D = 0.1339, p-value = 0.7771
alternative hypothesis: two-sided

```
# Visualize relationship in 3 dimensions
s2d <- scatterplot3d(x = Denit_sed_site$SedC_mg.gDW, y = Denit_sed_site$NO3_Extractable_uM, z =
Denit_sed_site$log10DEA, xlab = expression(paste("Sediment carbon content (mgC ", g^-1, ")")), ylab
= expression(paste("Extractable nitrate (", mu, "M")), zlab = expression(paste(log[10],
"[Denitrification rate (ngN ", g^-1, h^-1, ")]")), color = "black", pch = 19)
s2d$plane3d(mod3ds)
```

```
# Plot Denitrification versus Sediment carbon at the site level
Denit_SedC <- ggplot(Denit_sed_site, aes(x = SedC_mg.gDW, y = Denitrification_ng.N.g.hr/1000))
Denit_SedC + geom_point(size = 6, color = "gray24") + stat_smooth(method = lm, size = 2, color =
"black") + ylab(expression(paste("Denitrification Rate (", mu, "gN ", g^-1, h^-1, ")"))) +
xlab(expression(paste("Sediment carbon (mgC ", gDW^-1, ")"))) + theme(legend.title =
element_blank()) + scale_y_log10() + ggtitle("(E)")
```

```
# Plot Denitrification versus Sediment extractable nitrate content at the site level
Denit_NO3 <- ggplot(Denit_sed_site, aes(x = NO3_Extractable_uM, y =
Denitrification_ng.N.g.hr/1000))
Denit_NO3 + geom_point(size = 6, color = "gray24") + stat_smooth(method = lm, size = 2, color =
"black") + ylab(expression(paste("Denitrification Rate (", mu, "gN ", g^-1, h^-1, ")"))) +
xlab(expression(paste("Extractable nitrate (", mu, "M")))) + theme(legend.title = element_blank()) +
scale_y_log10() + ggtitle("(F)")
```

Determine which traits are most correlated with nitrification

```
# Create a matrix of nitrification rates and plant traits
cordata_nit_traits <- LIallVEG2013[, c("Nitrification_ug.N.cm3.hr", "DryWeight_g.m2",
   "RootMass_g.m2", "RhizomeWidth_mm", "Photosyn_uMCO2.m2.s1", "Conduct_molH2O.m2.s1",
   "VegN_mg.gDW", "SLA_cm2g.1")]
rcorr(as.matrix(cordata_nit_traits))
```

	Nitrification_ug.N.cm3.hr	DryWeight_g.m2	RootMass_g.m2	RhizomeWidth_mm	Photosyn_uMCO2.m2.s1	Conduct_molH2O.m2.s1	VegN_mg.gDW	SLA_cm2g.1
Nitrification_ug.N.cm3.hr	1.00	0.18	-0.24	-0.12	0.03	0.1	-0.05	-0.03
DryWeight_g.m2	0.18	1.00	-0.34	-0.07	-0.07	-0.08	-0.09	-0.2
RootMass_g.m2	-0.24	-0.34	1	0.05	0.17	0.05	-0.05	0.13
RhizomeWidth_mm	-0.12	-0.07	0.05	1	0.06	-0.12	0.16	0.15
Photosyn_uMCO2.m2.s1	0.03	-0.07	0.17	0.06	1	0.35	0.24	0.15
Conduct_molH2O.m2.s1	0.10	-0.08	0.05	-0.12	0.35	1	0.06	-0.09
VegN_mg.gDW	-0.05	-0.09	-0.05	0.16	0.24	0.06	1	0.41
SLA_cm2g.1	-0.03	-0.20	0.13	0.15	0.15	-0.09	0.41	1

n

	Nitrification_ug.N.cm3.hr	DryWeight_g.m2	RootMass_g.m2	RhizomeWidth_mm	Photosyn_uMCO2.m2.s1	Conduct_molH2O.m2.s1	VegN_mg.gDW	SLA_cm2g.1
Nitrification_ug.N.cm3.hr	220	219	219	219	219	219	219	219
DryWeight_g.m2	219	220	220	220	220	220	220	220
RootMass_g.m2	219	220	220	220	220	220	220	220
RhizomeWidth_mm	219	220	220	220	220	220	220	220
Photosyn_uMCO2.m2.s1	219	220	220	220	220	220	220	220
Conduct_molH2O.m2.s1	219	220	220	220	220	220	220	220
VegN_mg.gDW	219	220	220	220	220	220	220	220
SLA_cm2g.1	219	220	220	220	220	220	220	220

p

	Nitrification_ug.N.cm3.hr	DryWeight_g.m2	RootMass_g.m2	RhizomeWidth_mm	Photosyn_uMCO2.m2.s1	Conduct_molH2O.m2.s1	VegN_mg.gDW	SLA_cm2g.1
Nitrification_ug.N.cm3.hr		0.0072	0.0004	0.0739	0.6382	0.1254	0.4985	0.7010
DryWeight_g.m2	0.0072		0.0000	0.3308	0.2926	0.2680	0.2011	0.0032
RootMass_g.m2	0.0004	0.0000		0.4945	0.0113	0.4675	0.4669	0.0620
RhizomeWidth_mm	0.0739	0.3308	0.4945		0.4129	0.0667	0.0189	0.0254
Photosyn_uMCO2.m2.s1	0.6382	0.2926	0.0113	0.4129		0.0000	0.0004	0.0315
Conduct_molH2O.m2.s1	0.1254	0.2680	0.4675	0.0667	0.0000		0.3523	0.1843
VegN_mg.gDW	0.4985	0.2011	0.4669	0.0189	0.0004	0.3523		0.0000
SLA_cm2g.1	0.7010	0.0032	0.0620	0.0254	0.0315	0.1843	0.0000	

```
# log10 transform nitrification rates to meet assumptions of normality
LIall2013$log10Nitrification <- log10(LIall2013$Nitrification_ug.N.cm3.hr)
LIallVEG2013$log10Nitrification <- log10(LIallVEG2013$Nitrification_ug.N.cm3.hr)
LIallSED2013$log10Nitrification <- log10(LIallSED2013$Nitrification_ug.N.cm3.hr)
# Rerun correlation analysis with log10 transformed nitrification rates
cordata_nit_traits <- LIallVEG2013[, c("log10Nitrification", "DryWeight_g.m2",
  "RootMass_g.m2", "RhizomeWidth_mm", "Photosyn_uMCO2.m2.s1", "Conduct_molH2O.m2.s1",
  "VegN_mg.gDW", "SLA_cm2g.1")]
rcorr(as.matrix(cordata_nit_traits))
```

	log10Nitrification	DryWeight_g.m2	RootMass_g.m2	RhizomeWidth_mm	Photosyn_uMCO2.m2.s1	Conduct_molH2O.m2.s1	VegN_mg.gDW	SLA_cm2g.1
log10Nitrification	1.00	0.15	-0.28	-0.20	0.09	0.12	0.07	0.14
DryWeight_g.m2	0.15	1.00	-0.34	-0.07	-0.07	-0.08	-0.09	-0.20
RootMass_g.m2	-0.28	-0.34	1.00	0.05	0.17	0.05	-0.05	0.13
RhizomeWidth_mm	-0.20	-0.07	0.05	1.00	0.06	-0.12	0.16	0.15
Photosyn_uMCO2.m2.s1	0.09	-0.07	0.17	0.06	1.00	0.35	0.24	0.15
Conduct_molH2O.m2.s1	0.12	-0.08	0.05	-0.12	0.35	1.00	0.06	-0.09
VegN_mg.gDW	0.07	-0.09	-0.05	0.16	0.24	0.06	1.00	0.41
SLA_cm2g.1	0.14	-0.20	0.13	0.15	0.15	-0.09	0.41	1.00

n

	log10Nitrification	DryWeight_g.m2	RootMass_g.m2	RhizomeWidth_mm	Photosyn_uMCO2.m2.s1	Conduct_molH2O.m2.s1	VegN_mg.gDW	SLA_cm2g.1
log10Nitrification	220	155	155	155	155	155	155	155
DryWeight_g.m2	155	220	220	220	220	220	220	220
RootMass_g.m2	155	220	220	220	220	220	220	220
RhizomeWidth_mm	155	220	220	220	220	220	220	220
Photosyn_uMCO2.m2.s1	155	220	220	220	220	220	220	220
Conduct_molH2O.m2.s1	155	220	220	220	220	220	220	220
VegN_mg.gDW	155	220	220	220	220	220	220	220
SLA_cm2g.1	155	220	220	220	220	220	220	220

p

	log10Nitrification	DryWeight_g.m2	RootMass_g.m2	RhizomeWidth_mm	Photosyn_uMCO2.m2.s1	Conduct_molH2O.m2.s1	VegN_mg.gDW	SLA_cm2g.1
log10Nitrification		0.0628	0.0004	0.0127	0.2822	0.1417	0.3789	0.0908
DryWeight_g.m2	0.0628		0.0000	0.3308	0.2926	0.2680	0.2011	0.0032
RootMass_g.m2	0.0004	0.0000		0.4945	0.0113	0.4675	0.4669	0.0620
RhizomeWidth_mm	0.0127	0.3308	0.4945		0.4129	0.0667	0.0189	0.0254
Photosyn_uMCO2.m2.s1	0.2822	0.2926	0.0113	0.4129		0.0000	0.0004	0.0315
Conduct_molH2O.m2.s1	0.1417	0.2680	0.4675	0.0667	0.0000		0.3523	0.1843
VegN_mg.gDW	0.3789	0.2011	0.4669	0.0189	0.0004	0.3523		0.0000
SLA_cm2g.1	0.0908	0.0032	0.0620	0.0254	0.0315	0.1843	0.0000	

```
# Potential correlations with BGBiomass and Rhizome Width
```

Create data frame of site-level means and errors for Nitrification, BGBiomass, and Rhizome width

```
Nitrification <- summarySE(measurevar = "Nitrification_ug.N.cm3.hr", groupvars = c("Month_Year",
   "Site"), data = LIallVEG2013, na.rm = T)
Nitrification <- rename(Nitrification, c(se = "Nit_se", sd = "Nit_sd", ci = "Nit_ci"))
log10Nit <- summarySE(measurevar = "log10Nitrification", groupvars = c("Month_Year",
   "Site"), data = LIallVEG2013, na.rm = T)
```

```
log10Nit <- rename(log10Nit, c(se = "log10Nit_se", sd = "log10Nit_sd", ci = "log10Nit_ci"))
RhizomeWidth <- summarySE(measurevar = "RhizomeWidth_mm", groupvars = c("Month_Year",
   "Site"), data = LIallVEG2013, na.rm = T)
RhizomeWidth <- rename(RhizomeWidth, c(se = "RW_se", sd = "RW_sd", ci = "RW_ci"))
Nit_trait_site <- cbind(Nitrification, log10Nit, RootMass, RhizomeWidth)
```

Construct GLMs to predict nitrification rates using plant traits at the site level

Both weighted and unweighted models were attempted. Weighted models weighted observations of nitrification by the inverse of the sampling mean.

```
mod1n <- lm(log10Nitrification ~ Month_Year * RootMass_g.m2 * RhizomeWidth_mm,
   weights = 1/(log10Nit_sd)^2, data = Nit_trait_site)
summary(mod1n)
Call:
lm(formula = log10Nitrification ~ Month_Year * RootMass_g.m2 *
   RhizomeWidth_mm, data = Nit_trait_site, weights = 1/(log10Nit_sd)^2)

Weighted Residuals:
   Min     1Q  Median     3Q    Max
-1.7298 -0.7333 -0.1001  0.2923  1.4508

Coefficients:
                                          Estimate    Std.Error   t value  Pr(>|t|)
   (Intercept)                            5.22E+00    1.96E+00     2.659   *0.0197
   Month_Year.L                           1.67E+00    2.78E+00     0.603    0.5568
   RootMass_g.m2                         -1.59E-03    9.12E-04    -1.74     0.1055
   RhizomeWidth_mm                       -6.29E-01    4.73E-01    -1.331    0.2062
   Month_Year.L:RootMass_g.m2            -1.36E-03    1.29E-03    -1.056    0.3104
   Month_Year.L:RhizomeWidth_mm          -3.55E-01    6.68E-01    -0.531    0.6044
   RootMass_g.m2:RhizomeWidth_mm          3.62E-04    2.27E-04     1.592    0.1353
   Month_Year.L:RootMass_g.m2:RhizomeWidth_mm  3.19E-04  3.21E-04  0.992    0.3395
---
Signif. codes:  0 '***' 0.001 '**' 0.01 '*' 0.05 '.' 0.1 ' ' 1

Residual standard error: 1.112 on 13 degrees of freedom
  (1 observation deleted due to missingness)
Multiple R-squared:  0.3748,    Adjusted R-squared:  0.03818
F-statistic: 1.113 on 7 and 13 DF,  p-value: 0.4106
# Remove seasonality variable and rerun
mod2n <- lm(log10Nitrification ~ RootMass_g.m2 * RhizomeWidth_mm, data = Nit_trait_site)
summary(mod2n)
Call:
lm(formula = log10Nitrification ~ RootMass_g.m2 * RhizomeWidth_mm,
   data = Nit_trait_site)

Residuals:
     Min       1Q   Median       3Q      Max
-0.70804 -0.30917  0.04335  0.28035  0.72747
```

Coefficients:

	Estimate	Std.Error	t	Pr(>|t|)
(Intercept)	2.137	1.682	1.270	0.220
RootMass_g.m2	0.000	0.001	0.021	0.983
RhizomeWidth_mm	0.135	0.403	0.336	0.741
RootMass_g.m2:RhizomeWidth_mm	0.000	0.000	-0.285	0.779

Residual standard error: 0.4454 on 18 degrees of freedom
Multiple R-squared: 0.1518, Adjusted R-squared: 0.01048
F-statistic: 1.074 on 3 and 18 DF, p-value: 0.3849

```
# Remove non-significant interaction and rerun
mod3n <- lm(log10Nitrification ~ RootMass_g.m2 + RhizomeWidth_mm, data = Nit_trait_site)
summary(mod3n)
```

Call:
lm(formula = log10Nitrification ~ RootMass_g.m2 + RhizomeWidth_mm, data = Nit_trait_site)

Residuals:

Min	1Q	Median	3Q	Max
-0.70635	-0.31428	0.03237	0.28641	0.71265

Coefficients:

	Estimate	Std.Error	t	Pr(>|t|)	
(Intercept)	2.587	0.569	4.545	0.000	***
RootMass_g.m2	0.000	0.000	-1.751	0.096	.
RhizomeWidth_mm	0.026	0.117	0.221	0.828	

Signif. codes: 0 '***' 0.001 '**' 0.01 '*' 0.05 '.' 0.1 ' ' 1

Residual standard error: 0.4345 on 19 degrees of freedom
Multiple R-squared: 0.148, Adjusted R-squared: 0.05834
F-statistic: 1.65 on 2 and 19 DF, p-value: 0.2183

```
ks.test(mod3n$residuals, "pnorm", mean(mod3n$residuals), sd(mod3n$residuals))
```

One-sample Kolmogorov-Smirnov test
data: mod3n$residuals
D = 0.091, p-value = 0.9853
alternative hypothesis: two-sided

```
# Trait models not successful in predicting variation in nitrification rates at the site level Note: Weighted GLM (see GLM performed for sediment variables below) also not successful in explaining significant variation in Nitrification rates with plant traits.
```

Determine which sediment variables are most correlated with nitrification rates

```
# Examine correlations between nitrification rates and sediment data
cordata_lognit_sed <- LIallVEG2013[, c("Nitrification_ug.N.cm3.hr", "log10Nitrification",
  "SedC_mg.gDW", "SedN_mg.gDW", "NH4_Extractable_uM", "NO3_Extractable_uM",
  "Salinity_ppt", "Sed_temp")]
rcorr(as.matrix(cordata_lognit_sed))
```

	Nitrification_ug.N.cm3.hr	log10Nitrification	SedC_mg.gDW	SedN_mg.gDW	NH4_Extractable_uM	NO3_Extractable_uM	Salinity_ppt	Sed_temp
Nitrification_ug.N.cm3.hr	1.00	0.73	0.19	0.18	0.34	0.21	-0.19	-0.22
log10Nitrification	0.73	1.00	0.04	0.03	0.39	0.23	-0.17	-0.20
SedC_mg.gDW	0.19	0.04	1.00	0.79	0.10	0.30	-0.33	-0.12
SedN_mg.gDW	0.18	0.03	0.79	1.00	0.04	0.33	-0.27	-0.14
NH4_Extractable_uM	0.34	0.39	0.10	0.04	1.00	0.30	-0.07	0.03
NO3_Extractable_uM	0.21	0.23	0.30	0.33	0.30	1.00	-0.34	-0.24
Salinity_ppt	-0.19	-0.17	-0.33	-0.27	-0.07	-0.34	1.00	0.48
Sed_temp	-0.22	-0.20	-0.12	-0.14	0.03	-0.24	0.48	1.00

n

	Nitrification_ug.N.cm3.hr	log10Nitrification	SedC_mg.gDW	SedN_mg.gDW	NH4_Extractable_uM	NO3_Extractable_uM	Salinity_ppt	Sed_temp
Nitrification_ug.N.cm3.hr	220	155	219	219	218	217	217	219
log10Nitrification	155	220	155	155	154	154	153	155
SedC_mg.gDW	219	155	220	220	219	218	218	220
SedN_mg.gDW	219	155	220	220	219	218	218	220
NH4_Extractable_uM	218	154	219	219	220	218	217	219
NO3_Extractable_uM	217	154	218	218	218	220	216	218
Salinity_ppt	217	153	218	218	217	216	220	218
Sed_temp	219	155	220	220	219	218	218	220

p

	Nitrification_ug.N.cm3.hr	log10Nitrification	SedC_mg.gDW	SedN_mg.gDW	NH4_Extractable_uM	NO3_Extractable_uM	Salinity_ppt	Sed_temp
Nitrification_ug.N.cm3.hr		0.0000	0.0042	0.0093	0.0000	0.0020	0.0044	0.0012
log10Nitrification	0.0000		0.6592	0.6971	0.0000	0.0049	0.0393	0.0123
SedC_mg.gDW	0.0042	0.6592		0.0000	0.1439	0.0000	0.0000	0.0853
SedN_mg.gDW	0.0093	0.6971	0.0000		0.5402	0.0000	0.0000	0.0323
NH4_Extractable_uM	0.0000	0.0000	0.1439	0.5402		0.0000	0.2752	0.6697
NO3_Extractable_uM	0.0020	0.0049	0.0000	0.0000	0.0000		0.0000	0.0003
Salinity_ppt	0.0044	0.0393	0.0000	0.0000	0.2752	0.0000		0.0000
Sed_temp	0.0012	0.0123	0.0853	0.0323	0.6697	0.0003	0.0000	

Create data frame of site-level means and errors for Nitrification, log10Nitrification, Salinity and total extractable ammonium in sediment porewater

```
Salinity <- summarySE(measurevar = "Salinity_ppt", groupvars = c("Month_Year",
   "Site"), data = LIallVEG2013, na.rm = T)
Salinity <- rename(Salinity, c(se = "Sal_se", sd = "Sal_sd", ci = "Sal_ci"))
Ammonium <- summarySE(measurevar = "NH4_Extractable_uM", groupvars = c("Month_Year",
   "Site"), data = LIallVEG2013, na.rm = T)
Ammonium <- rename(Ammonium, c(se = "NH4_se", sd = "NH4_sd", ci = "NH4_ci"))
Nit_sed_site <- cbind(Nitrification, log10Nit, Salinity, Ammonium)
```

Run weighted linear regression using sediment variables to predict nitrification rates

Weights were calculated as the inverse of the variance in microbial rates at the site level.

```
# Create initial model with seasonality, salinity, and ammonium
mod1ns <- lm(Nitrification_ug.N.cm3.hr ~ Month_Year * Salinity_ppt * NH4_Extractable_uM,
   weights = 1/(Nit_sd)^2, data = Nit_sed_site)
summary(mod1ns)
```

```
Call:
lm(formula = Nitrification_ug.N.cm3.hr ~ Month_Year * Salinity_ppt *
   NH4_Extractable_uM, data = Nit_sed_site, weights = 1/(Nit_sd)^2)

Weighted Residuals:
    Min      1Q  Median      3Q     Max
-1.11874 -0.07423  0.14862  0.34496  1.26988

Coefficients:
                                    Estimate   Std.Error  t value  Pr(>|t|)
   (Intercept)                      5.22E+00   1.96E+00    2.659   *0.0197
   Month_Year.L                     1.67E+00   2.78E+00    0.603    0.5568
```

```
   RootMass_g.m2                              -1.59E-03  9.12E-04   -1.74  0.1055
   RhizomeWidth_mm                            -6.29E-01  4.73E-01   -1.331 0.2062
   Month_Year.L:RootMass_g.m2                 -1.36E-03  1.29E-03   -1.056 0.3104
   Month_Year.L:RhizomeWidth_mm               -3.55E-01  6.68E-01   -0.531 0.6044
   RootMass_g.m2:RhizomeWidth_mm               3.62E-04  2.27E-04    1.592 0.1353
   Month_Year.L:RootMass_g.m2:RhizomeWidth_mm  3.19E-04  3.21E-04    0.992 0.3395
---
Signif. codes:  0 '***' 0.001 '**' 0.01 '*' 0.05 '.' 0.1 ' ' 1

Residual standard error: 0.7283 on 14 degrees of freedom
Multiple R-squared:  0.6411,    Adjusted R-squared:  0.4616
F-statistic: 3.572 on 7 and 14 DF,  p-value: 0.02036
```

```
# Remove seasonality and rerun model
mod2ns <- lm(Nitrification_ug.N.cm3.hr ~ Salinity_ppt * NH4_Extractable_uM,
   weights = 1/(Nit_sd)^2, data = Nit_sed_site)
summary(mod2ns)
```

```
Call:
lm(formula = Nitrification_ug.N.cm3.hr ~ Salinity_ppt * NH4_Extractable_uM,
   data = Nit_sed_site, weights = 1/(Nit_sd)^2)

Weighted Residuals:
   Min     1Q  Median     3Q    Max
-1.1204 -0.1234  0.3189  0.5584  1.8888

Coefficients:
                               Estimate  Std.Error  t        Pr(>|t|)
 (Intercept)                   -163.400    340.600  -0.480    0.637
 Salinity_ppt                    -0.211     11.640  -0.018    0.986
 NH4_Extractable_uM               3.335      4.869   0.685    0.502
 Salinity_ppt:NH4_Extractable_uM -0.006      0.168  -0.034    0.973

Residual standard error: 0.7876 on 18 degrees of freedom
Multiple R-squared:  0.4604,    Adjusted R-squared:  0.3704
F-statistic: 5.119 on 3 and 18 DF,  p-value: 0.009795
```

```
# Remove non-significant interaction term and rerun model
mod3ns <- lm(Nitrification_ug.N.cm3.hr ~ Salinity_ppt + NH4_Extractable_uM,
   weights = 1/(Nit_sd)^2, data = Nit_sed_site)
summary(mod3ns)
```

```
Call:
lm(formula = Nitrification_ug.N.cm3.hr ~ Salinity_ppt + NH4_Extractable_uM,
   data = Nit_sed_site, weights = 1/(Nit_sd)^2)

Weighted Residuals:
   Min     1Q  Median     3Q    Max
-1.1175 -0.1237  0.3234  0.5665  1.8799

Coefficients:
```

```
                     Estimate   Std.Error  t        Pr(>|t|)
 (Intercept)         -152.780     133.227  -1.147      0.266
 Salinity_ppt          -0.584       3.977  -0.147      0.885
 NH4_Extractable_uM     3.171       0.790   4.015  7.41E-04  ***
---
Signif. codes:  0 '***' 0.001 '**' 0.01 '*' 0.05 '.' 0.1 ' ' 1

Residual standard error: 0.7666 on 19 degrees of freedom
Multiple R-squared:  0.4603,    Adjusted R-squared:  0.4035
F-statistic: 8.104 on 2 and 19 DF,  p-value: 0.002852
```

```
# Remove non-significant Salinity term and rerun model
mod4ns <- lm(Nitrification_ug.N.cm3.hr ~ NH4_Extractable_uM, weights = 1/(Nit_sd)^2,
   data = Nit_sed_site)
summary(mod4ns)
Call:
lm(formula = Nitrification_ug.N.cm3.hr ~ NH4_Extractable_uM,
   data = Nit_sed_site, weights = 1/(Nit_sd)^2)

Weighted Residuals:
   Min     1Q  Median     3Q    Max
-1.1080 -0.1278  0.3181  0.5873  1.8667

Coefficients:
                     Estimate   Std.Error  t        Pr(>|t|)
 (Intercept)         -169.967      61.934  -2.744  1.25E-02    *
 NH4_Extractable_uM     3.175       0.770   4.125  5.25E-04  ***
---
Signif. codes:  0 '***' 0.001 '**' 0.01 '*' 0.05 '.' 0.1 ' ' 1

Residual standard error: 0.7476 on 20 degrees of freedom
Multiple R-squared:  0.4597,    Adjusted R-squared:  0.4327
F-statistic: 17.02 on 1 and 20 DF,  p-value: 0.0005248
```

```
ks.test(mod4ns$residuals, "pnorm", mean(mod4ns$residuals), sd(mod4ns$residuals))
One-sample Kolmogorov-Smirnov test
data:  mod4ns$residuals
D = 0.1853, p-value = 0.3891
alternative hypothesis: two-sided
```

```
# Plot relationship between ammonium and nitrification
Nit_NH4 <- ggplot(Nit_sed_site, aes(x = NH4_Extractable_uM, y = Nitrification_ug.N.cm3.hr))
Nit_NH4 + geom_errorbar(aes(ymin = Nitrification_ug.N.cm3.hr - Nit_se, ymax =
Nitrification_ug.N.cm3.hr + Nit_se), width = 0) + geom_errorbarh(aes(xmin = NH4_Extractable_uM -
NH4_se, xmax = NH4_Extractable_uM + NH4_se), width = 0) + geom_point(size = 6, color = "gray24")
+ geom_abline(intercept = -169.9668, slope = 3.1753, color = "black", size = 2) +
xlab(expression(paste("Extractable ammonium (", mu, "M")))) + ylab(expression(paste("Nitrification
rate (", mu, "gN ", cm^-3, h^-1, ")"))) + ggtitle("(A)")
```

Examine potential relationship between nitrification and denitrification at the site level

```
# Create data frame of site-level means for denitrification and nitrification rates
Nit_DEA_site <- cbind(Denit, Nitrification, log10DEA, log10Nit)
# Use nitrification rates as predictor of denitrification rates
mod1dn <- lm(log10DEA ~ log10Nitrification, data = Nit_DEA_site)
summary(mod1dn)
```

```
Call:
lm(formula = log10DEA ~ log10Nitrification, data = Nit_DEA_site)

Residuals:
     Min       1Q   Median       3Q      Max
-0.81810 -0.21134 -0.02627  0.24174  0.99431

Coefficients:
                   Estimate Std.Error t       Pr(>|t|)
 (Intercept)          1.594     0.485 3.284   3.71E-03  **
 log10Nitrification   0.450     0.215 2.097   4.89E-02   *
---
Signif. codes:  0 '***' 0.001 '**' 0.01 '*' 0.05 '.' 0.1 ' ' 1

Residual standard error: 0.4402 on 20 degrees of freedom
Multiple R-squared:  0.1802,    Adjusted R-squared:  0.1392
F-statistic: 4.397 on 1 and 20 DF,  p-value: 0.04892
```

```
# Test residuals of model for normality using KS Lilliefors test
ks.test(mod1dn$residuals, "pnorm", mean(mod1dn$residuals), sd(mod1dn$residuals))
```

```
One-sample Kolmogorov-Smirnov test
data:  mod1dn$residuals
D = 0.0778, p-value = 0.9978
alternative hypothesis: two-sided
```

```
# Plot denitrification versus nitrification rates at the site level
Nit_Denit_site <- ggplot(Nit_DEA_site, aes(x = Nitrification_ug.N.cm3.hr, y =
Denitrification_ng.N.g.hr/1000))
Nit_Denit_site + geom_point(size = 6, color = "gray24") + stat_smooth(method = "lm", color = "black",
size = 2) + ylab(expression(paste("Denitrification rate (", mu, "gN ", g^-1, h^-1, ")"))) +
xlab(expression(paste("Nitrification rate (", mu, "gN ", cm^-3, h^-1, ")"))) + scale_y_log10() +
scale_x_log10()
```

Determine which traits are most correlated with net (mineralization-immobilization)

```
# Examine correlations among immobilization, min, and plant traits
cordata_min_traits <- LIallVEG2013[, c("Mineralization_ug.N.cm3.hr", "DryWeight_g.m2",
   "RootMass_g.m2", "RhizomeWidth_mm", "Photosyn_uMCO2.m2.s1", "Conduct_molH2O.m2.s1",
   "VegN_mg.gDW", "SLA_cm2g.1")]
rcorr(as.matrix(cordata_min_traits))
```

	Mineralization_ug.N.cm3.hr	DryWeight_g.m2	RootMass_g.m2	RhizomeWidth_mm	Photosyn_uMCO2.m2.s1	Conduct_molH2O.m2.s1	VegN_mg.gDW	SLA_cm2g.1
Mineralization_ug.N.cm3.hr	1.00	-0.01	0.04	-0.09	0.01	0.23	-0.11	-0.04
DryWeight_g.m2	-0.01	1.00	-0.34	-0.07	-0.07	-0.08	-0.09	-0.20
RootMass_g.m2	0.04	-0.34	1.00	0.05	0.17	0.05	-0.05	0.13
RhizomeWidth_mm	-0.09	-0.07	0.05	1.00	0.06	-0.12	0.16	0.15
Photosyn_uMCO2.m2.s1	0.01	-0.07	0.17	0.06	1.00	0.35	0.24	0.15
Conduct_molH2O.m2.s1	0.23	-0.08	0.05	-0.12	0.35	1.00	0.06	-0.09
VegN_mg.gDW	-0.11	-0.09	-0.05	0.16	0.24	0.06	1.00	0.41
SLA_cm2g.1	-0.04	-0.20	0.13	0.15	0.15	-0.09	0.41	1.00

n= 220

p

	Mineralization_ug.N.cm3.hr	DryWeight_g.m2	RootMass_g.m2	RhizomeWidth_mm	Photosyn_uMCO2.m2.s1	Conduct_molH2O.m2.s1	VegN_mg.gDW	SLA_cm2g.1
Mineralization_ug.N.cm3.hr		0.8875	0.5523	0.2045	0.9274	0.0005	0.1065	0.5759
DryWeight_g.m2	0.8875		0.0000	0.3308	0.2926	0.2680	0.2011	0.0032
RootMass_g.m2	0.5523	0.0000		0.4945	0.0113	0.4675	0.4669	0.0620
RhizomeWidth_mm	0.2045	0.3308	0.4945		0.4129	0.0667	0.0189	0.0254
Photosyn_uMCO2.m2.s1	0.9274	0.2926	0.0113	0.4129		0.0000	0.0004	0.0315
Conduct_molH2O.m2.s1	0.0005	0.2680	0.4675	0.0667	0.0000		0.3523	0.1843
VegN_mg.gDW	0.1065	0.2011	0.4669	0.0189	0.0004	0.3523		0.0000
SLA_cm2g.1	0.5759	0.0032	0.0620	0.0254	0.0315	0.1843	0.0000	

Create data frame of site-level means and errors for Mineralization, root mass, leaf nitrogen, rhizome width, and stomatal conductance

```
Mineralization <- summarySE(measurevar = "Mineralization_ug.N.cm3.hr", groupvars =
c("Month_Year", "Site"), data = LIallVEG2013, na.rm = T)
```

```
Mineralization <- rename(Mineralization, c(se = "Min_se", sd = "Min_sd", ci = "Min_ci"))
Conductance <- summarySE(measurevar = "Conduct_molH2O.m2.s1", groupvars = c("Month_Year",
   "Site"), data = LIallVEG2013, na.rm = T)
Conductance <- rename(Conductance, c(se = "Conduct_se", sd = "Conduct_sd", ci = "Conduct_ci"))
Min_trait_site <- cbind(Mineralization, RootMass, LeafN, RhizomeWidth, Conductance)
```

Construct weighted GLMs to predict net mineralization rates using plant traits at the site level

Because net mineralization rates range from negative (net immobilization) to positive (net mineralization) values, log10 transformations could not be performed for the whole dataset. Therfore, weighted regressions are used to construct initial GLMs, where weights are equal to the inverse of the sampling variance.

```
mod1m <- lm(Mineralization_ug.N.cm3.hr ~ Month_Year * RootMass_g.m2 * Conduct_molH2O.m2.s1,
   weights = 1/(Min_sd)^2, data = Min_trait_site)
summary(mod1m)
Call:
lm(formula = Mineralization_ug.N.cm3.hr ~ Month_Year * RootMass_g.m2 *
   Conduct_molH2O.m2.s1, data = Min_trait_site, weights = 1/(Min_sd)^2)

Weighted Residuals:
    Min      1Q  Median      3Q     Max
-1.69367 -0.26253  0.08222  0.33115  1.74122

Coefficients:
                                          Estimate  Std.Error       t  Pr(>|t|)
 (Intercept)                           -1784.988    475.428  -3.754  0.00213  **
 Month_Year.L                            945.565    672.357   1.406  0.18143
 RootMass_g.m2                             0.484      0.180   2.681  0.01792  *
 Conduct_molH2O.m2.s1                   9345.307   4605.710   2.029  0.06191  .
 Month_Year.L:RootMass_g.m2               -0.282      0.255  -1.106  0.28756
 Month_Year.L:Conduct_molH2O.m2.s1     -4648.054   6513.457  -0.714  0.4872
 RootMass_g.m2:Conduct_molH2O.m2.s1        -3.124      2.126  -1.47  0.16374
 Month_Year.L:RootMass_g.m2:               1.252      3.006   0.416  0.68343
   Conduct_molH2O.m2.s1
---
Signif. codes:  0 '***' 0.001 '**' 0.01 '*' 0.05 '.' 0.1 ' ' 1

Residual standard error: 0.8867 on 14 degrees of freedom
Multiple R-squared:  0.493, Adjusted R-squared:  0.2395
F-statistic: 1.945 on 7 and 14 DF,  p-value: 0.1371

# Remove seasonality and rerun
mod2m <- lm(Mineralization_ug.N.cm3.hr ~ RootMass_g.m2 * Conduct_molH2O.m2.s1,
   weights = 1/(Min_sd)^2, data = Min_trait_site)
summary(mod2m)
Call:
lm(formula = Mineralization_ug.N.cm3.hr ~ RootMass_g.m2 * Conduct_molH2O.m2.s1,
   data = Min_trait_site, weights = 1/(Min_sd)^2)
```

```
Weighted Residuals:
    Min      1Q  Median      3Q     Max
-2.18609 -0.27330 -0.02539  0.38994  1.96689

Coefficients:
                                    Estimate  Std.Error       t  Pr(>|t|)
 (Intercept)                      -1147.359    290.995  -3.943  9.54E-04 ***
 RootMass_g.m2                        0.285      0.126   2.257  0.036658 *
 Conduct_molH2O.m2.s1              4659.377   2880.973   1.617  0.123205
 RootMass_g.m2:Conduct_molH2O.m2.s1   -1.454      1.252  -1.161  0.260612
---
Signif. codes:  0 '***' 0.001 '**' 0.01 '*' 0.05 '.' 0.1 ' ' 1

Residual standard error: 0.8631 on 18 degrees of freedom
Multiple R-squared:  0.3823,    Adjusted R-squared:  0.2793
F-statistic: 3.713 on 3 and 18 DF,  p-value: 0.0307
```

```
# Remove non-significant interaction term and rerun
mod3m <- lm(Mineralization_ug.N.cm3.hr ~ RootMass_g.m2 + Conduct_molH2O.m2.s1,
   weights = 1/(Min_sd)^2, data = Min_trait_site)
summary(mod3m)
Call:
lm(formula = Mineralization_ug.N.cm3.hr ~ RootMass_g.m2 + Conduct_molH2O.m2.s1,
   data = Min_trait_site, weights = 1/(Min_sd)^2)

Weighted Residuals:
   Min     1Q  Median     3Q    Max
-2.1861 -0.3718  0.1973  0.4215  1.6296

Coefficients:
                    Estimate  Std.Error  t       Pr(>|t|)
 (Intercept)        -864.405    160.614  -5.382  3.41E-05 ***
 RootMass_g.m2         0.156      0.061   2.561    0.0191 *
 Conduct_molH2O.m2.s1 1457.518  844.782   1.725    0.1007
---
Signif. codes:  0 '***' 0.001 '**' 0.01 '*' 0.05 '.' 0.1 ' ' 1

Residual standard error: 0.871 on 19 degrees of freedom
Multiple R-squared:  0.336, Adjusted R-squared:  0.2661
F-statistic: 4.807 on 2 and 19 DF,  p-value: 0.02045
```

```
# Test residuals of model for normality using KS Lilliefors test
ks.test(mod3m$residuals, "pnorm", mean(mod3m$residuals), sd(mod3m$residuals))
One-sample Kolmogorov-Smirnov test
data:  mod3m$residuals
D = 0.1305, p-value = 0.8021
alternative hypothesis: two-sided
```

```
# Visualize final model in 3d
s1m <- scatterplot3d(x = Min_trait_site$RootMass_g.m2, y = Min_trait_site$Conduct_molH2O.m2.s1,
z = Min_trait_site$Mineralization_ug.N.cm3.hr, xlab = expression(paste("Root mass (g ", m^-2, ")")),
ylab = expression(paste("Stomatal conductance (mol ", H[2], O, m^-2, s^-1, ")")), zlab =
expression(paste("Mineralization rate (", mu, "gN ", cm^-3, h^-1, ")")), color = "black", pch = 19)
s1m$plane3d(mod3m)
```

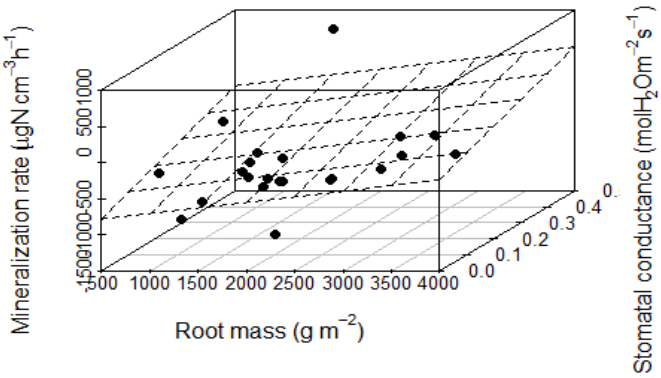


```
# Plot relationship between BGBiomass and Mineralization
Min_RootMass_site <- ggplot(Min_trait_site, aes(x = RootMass_g.m2, y =
Mineralization_ug.N.cm3.hr))
Min_RootMass_site + geom_errorbar(aes(ymin = Mineralization_ug.N.cm3.hr - Min_se, ymax =
Mineralization_ug.N.cm3.hr + Min_se), width = 0) + geom_errorbarh(aes(xmin = RootMass_g.m2 -
RootMass_se, xmax = RootMass_g.m2 + RootMass_se), width = 0) + geom_point(size = 6, color =
"gray24") + geom_abline(intercept = -864.40514, slope = 0.15618, color = "black", size = 2) +
ylab(expression(paste("Mineralization rate (", mu, "gN ", cm^-3, h^-1, ")"))) +
xlab(expression(paste("Root mass (g ", m^-2, ")")))
```

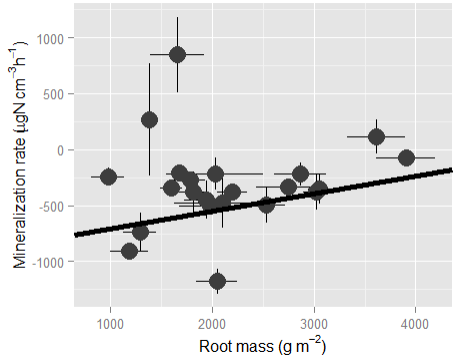


```
# Plot relationship between stomatal conductance and Immobilization
Min_conduct_site <- ggplot(Min_trait_site, aes(x = Conduct_molH2O.m2.s1, y =
Mineralization_ug.N.cm3.hr))
Min_conduct_site + geom_errorbar(aes(ymin = Mineralization_ug.N.cm3.hr - Min_se, ymax =
Mineralization_ug.N.cm3.hr + Min_se), width = 0) + geom_errorbarh(aes(xmin =
Conduct_molH2O.m2.s1 - Conduct_se, xmax = Conduct_molH2O.m2.s1 + Conduct_se), width = 0) +
geom_point(size = 6, color = "gray24") + geom_abline(intercept = -864.40514, slope = 1457.51833) +
ylab(expression(paste("Mineralization rate (", mu, "gN ", cm^-3, h^-1, ")"))) +
xlab(expression(paste("Stomatal conductance (mol ", H[2], O, m^-2, s^-1, ")")))
```

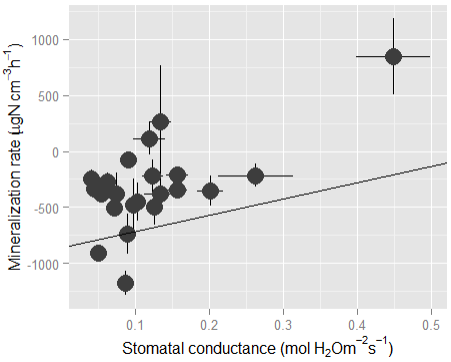

Determine which sediment variables are most correlated with net (mineralization-immobilization)

```
# Examine correlations between sediment variables and mineralization and immobilization rates
cordata_min_sed <- LIallVEG2013[, c("Mineralization_ug.N.cm3.hr", "SedC_mg.gDW",
   "SedN_mg.gDW", "NH4_Extractable_uM", "NO3_Extractable_uM", "Salinity_ppt", "Sed_temp")]
rcorr(as.matrix(cordata_min_sed))
```

	Mineralization_ug.N.cm3.hr	SedC_mg.gDW	SedN_mg.gDW	NH4_Extractable_uM	NO3_Extractable_uM	Salinity_ppt	Sed_temp
Mineralization_ug.N.cm3.hr	1.00	0.20	0.19	-0.44	0.06	-0.23	-0.24
SedC_mg.gDW	0.20	1.00	0.79	0.10	0.30	-0.33	-0.12
SedN_mg.gDW	0.19	0.79	1.00	0.04	0.33	-0.27	-0.14
NH4_Extractable_uM	-0.44	0.10	0.04	1.00	0.30	-0.07	0.03
NO3_Extractable_uM	0.06	0.30	0.33	0.30	1.00	-0.34	-0.24
Salinity_ppt	-0.23	-0.33	-0.27	-0.07	-0.34	1.00	0.48
Sed_temp	-0.24	-0.12	-0.14	0.03	-0.24	0.48	1.00

n

	Mineralization_ug.N.cm3.hr	SedC_mg.gDW	SedN_mg.gDW	NH4_Extractable_uM	NO3_Extractable_uM	Salinity_ppt	Sed_temp
Mineralization_ug.N.cm3.hr	220	220	220	219	218	218	220
SedC_mg.gDW	220	220	220	219	218	218	220
SedN_mg.gDW	220	220	220	219	218	218	220
NH4_Extractable_uM	219	219	219	220	218	217	219
NO3_Extractable_uM	218	218	218	218	220	216	218
Salinity_ppt	218	218	218	217	216	220	218
Sed_temp	220	220	220	219	218	218	220

p

	Mineralization_ug.N.cm3.hr	SedC_mg.gDW	SedN_mg.gDW	NH4_Extractable_uM	NO3_Extractable_uM	Salinity_ppt	Sed_temp
Mineralization_ug.N.cm3.hr		0.0023	0.0043	0.0000	0.3478	0.0005	0.0004
SedC_mg.gDW	0.0023		0.0000	0.1439	0.0000	0.0000	0.0853
SedN_mg.gDW	0.0043	0.0000		0.5402	0.0000	0.0000	0.0323
NH4_Extractable_uM	0.0000	0.1439	0.5402		0.0000	0.2752	0.6697
NO3_Extractable_uM	0.3478	0.0000	0.0000	0.0000		0.0000	0.0003
Salinity_ppt	0.0005	0.0000	0.0000	0.2752	0.0000		0.0000
Sed_temp	0.0004	0.0853	0.0323	0.6697	0.0003	0.0000	

Create data frame of site-level means and errors for Mineralization, salinity, and extractable ammonium content

```
Min_sed_site <- cbind(Mineralization, Salinity, Ammonium)
```

Construct weighted GLMs to predict net mineralization rates using sediment variables at the site level

```
# Build model to predict immobilization, initialize with seasonality, salinity, and ammonium
mod1ms <- lm(Mineralization_ug.N.cm3.hr ~ Month_Year * Salinity_ppt * NH4_Extractable_uM,
   weights = 1/(Min_sd)^2, data = Min_sed_site)
summary(mod1ms)
```

```
Call:
lm(formula = Mineralization_ug.N.cm3.hr ~ Month_Year * Salinity_ppt *
   NH4_Extractable_uM, data = Min_sed_site, weights = 1/(Min_sd)^2)

Weighted Residuals:
    Min      1Q  Median      3Q     Max
-1.07175 -0.29176  0.09653  0.50605  1.06406

Coefficients:
                                          Estimate   Std.Error  t value  Pr(>|t|)
   (Intercept)                            3.15E+02   5.35E+02    0.589    0.5652   .
   Month_Year.L                           1.59E+03   7.56E+02    2.107    0.0536
   Salinity_ppt                          -8.14E+00   1.82E+01   -0.447     0.662
   NH4_Extractable_uM                    -7.42E+00   6.75E+00   -1.099    0.2903   .
   Month_Year.L:Salinity_ppt             -5.29E+01   2.58E+01   -2.052    0.0593   *
   Month_Year.L:NH4_Extractable_uM       -2.37E+01   9.55E+00   -2.478    0.0266
   Salinity_ppt:NH4_Extractable_uM        4.31E-02   2.31E-01    0.187    0.8546   *
   Month_Year.L:Salinity_ppt:NH4_Extractable_uM  8.38E-01   3.27E-01    2.565    0.0224
---
Signif. codes:  0 '***' 0.001 '**' 0.01 '*' 0.05 '.' 0.1 ' ' 1

Residual standard error: 0.6598 on 14 degrees of freedom
Multiple R-squared:  0.7192,    Adjusted R-squared:  0.5788
F-statistic: 5.123 on 7 and 14 DF,  p-value: 0.004616
```

```
# Remove salinity and rerun model
mod2ms <- lm(Mineralization_ug.N.cm3.hr ~ Month_Year * NH4_Extractable_uM, weights =
1/(Min_sd)^2, data = Min_sed_site)
summary(mod2ms)
```

```
Call:
lm(formula = Mineralization_ug.N.cm3.hr ~ Month_Year * NH4_Extractable_uM,
   data = Min_sed_site, weights = 1/(Min_sd)^2)

Weighted Residuals:
   Min     1Q  Median     3Q    Max
-1.7233 -0.1809  0.1979  0.5728  1.2374

Coefficients:
                      Estimate  Std.Error      t  Pr(>|t|)
 (Intercept)            -17.470     92.399 -0.189  0.852154
 Month_Year.L            12.899    130.672  0.099  0.922458
 NH4_Extractable_uM      -4.799      1.068 -4.491  0.000282  ***
```

```
  Month_Year.L:NH4_Extractable_uM        0.229        1.511    0.152    0.881061
---
Signif. codes:  0 '***' 0.001 '**' 0.01 '*' 0.05 '.' 0.1 ' ' 1

Residual standard error: 0.7305 on 18 degrees of freedom
Multiple R-squared:  0.5576,    Adjusted R-squared:  0.4838
F-statistic: 7.562 on 3 and 18 DF,  p-value: 0.001774
```

```
# Remove non-significant interaction and rerun model
mod3ms <- lm(Mineralization_ug.N.cm3.hr ~ Month_Year + NH4_Extractable_uM, weights =
1/(Min_sd)^2, data = Min_sed_site)
summary(mod3ms)
```

```
Call:
lm(formula = Mineralization_ug.N.cm3.hr ~ Month_Year + NH4_Extractable_uM,
    data = Min_sed_site, weights = 1/(Min_sd)^2)

Weighted Residuals:
    Min      1Q  Median      3Q     Max
-1.6886 -0.1836  0.1916  0.5844  1.2323

Coefficients:
                      Estimate   Std.Error  t          Pr(>|t|)
  (Intercept)          -13.886      87.004   -0.16    0.874875
  Month_Year.L          30.007      64.362    0.466   0.646355
  NH4_Extractable_uM    -4.808       1.039   -4.627   0.000184   ***
---
Signif. codes:  0 '***' 0.001 '**' 0.01 '*' 0.05 '.' 0.1 ' ' 1

Residual standard error: 0.7114 on 19 degrees of freedom
Multiple R-squared:  0.557, Adjusted R-squared:  0.5104
F-statistic: 11.95 on 2 and 19 DF,  p-value: 0.0004372
```

```
# Remove non-significant effect of seasonality and rerun model
mod4ms <- lm(Mineralization_ug.N.cm3.hr ~ NH4_Extractable_uM, weights = 1/(Min_sd)^2,
    data = Min_sed_site)
summary(mod4ms)
```

```
Call:
lm(formula = Mineralization_ug.N.cm3.hr ~ NH4_Extractable_uM,
    data = Min_sed_site, weights = 1/(Min_sd)^2)

Weighted Residuals:
    Min      1Q  Median      3Q     Max
-1.6637 -0.2570  0.1898  0.5817  1.2036

Coefficients:
                      Estimate   Std.Error  t          Pr(>|t|)
  (Intercept)          -22.535      83.324   -0.270       0.790
  NH4_Extractable_uM    -4.608       0.928   -4.964    7.47E-05   ***
```

```
---
Signif. codes:  0 '***' 0.001 '**' 0.01 '*' 0.05 '.' 0.1 ' ' 1

Residual standard error: 0.6974 on 20 degrees of freedom
Multiple R-squared:  0.5519,    Adjusted R-squared:  0.5295
F-statistic: 24.64 on 1 and 20 DF,  p-value: 7.473e-05
```

```
# Test residuals of model for normality using KS Lilliefors test
ks.test(mod4ms$residuals, "pnorm", mean(mod4ms$residuals), sd(mod4ms$residuals))
One-sample Kolmogorov-Smirnov test
data:  mod4ms$residuals
D = 0.2285, p-value = 0.1718
alternative hypothesis: two-sided
```

```
# Plot univariate relationship between ammonium and immobilization rates
Min_Ammonium_site <- ggplot(Min_sed_site, aes(x = NH4_Extractable_uM, y =
Mineralization_ug.N.cm3.hr))
Min_Ammonium_site + geom_errorbar(aes(ymin = Mineralization_ug.N.cm3.hr - Min_se, ymax =
Mineralization_ug.N.cm3.hr + Min_se), width = 0) + geom_errorbarh(aes(xmin =
NH4_Extractable_uM - NH4_se, xmax = NH4_Extractable_uM + NH4_se), width = 0) +
geom_point(size = 6, color = "gray24") + geom_abline(intercept = -22.5353, slope = -4.6084, size = 2) +
xlab(expression(paste("Extractable ammonium (", mu, "M")))) + ylab(expression(paste("Mineralization
rate (", mu, "gN ", cm^-3, h^-1, ")"))) + ggtitle("(B)")
```

Calculate an "effect of vegetation" log-response ratio for denitrification rates

To estimate the effect that vegetation exerts on denitrification rates, I calculated a log response ratio of denitrification rates in vegetated sediments to denitrification rates in non-vegetated sediments for site-level means.

```
# Create a table of site means for denitrification rates in non-vegetated sediments
Denit_sed <- summarySE(data = LIallSED2013, measurevar = "Denitrification_ng.N.g.hr",
   groupvars = c("Month_Year", "Site"))
Denit_sed <- rename(Denit_sed, c(se = "Denit_sed_se", sd = "Denit_sed_sd", ci = "Denit_sed_ci"))
# Rename column names in Denit and Denit_sed to reflect treatment
Denit$Denit_VEG <- Denit$Denitrification_ng.N.g.hr
Denit_sed$Denit_SED <- Denit_sed$Denitrification_ng.N.g.hr
# Create table of site means for AGBiomass
AGBiomass <- summarySE(LIallVEG2013, measurevar = "DryWeight_g.m2", groupvars =
c("Month_Year", "Site"))
AGBiomass <- rename(AGBiomass, c(se = "AGBiomass_se", sd = "AGBiomass_sd", ci =
"AGBiomass_ci"))
# Merge tables of means for Denit, Denit_sed, and plant traits
Denit_Plant_traits <- cbind(Denit, Denit_sed, AGBiomass, RootMass, LeafN)
```

```
# Calculate log response ratio as log10(Denit_VEG/Denit_SED)
Denit_Plant_traits$logR <- log10(Denit_Plant_traits$Denit_VEG/Denit_Plant_traits$Denit_SED)

# Calculate standard deviation of log response ratios as mean of independent standard deviations of each
treatment group
Denit_Plant_traits$logR_sd <- log10((Denit_Plant_traits$Denit_sd^2 +
Denit_Plant_traits$Denit_sed_sd^2)^0.5)
```

```
# Examine distribution of plant effects on denitrification, where 0 = no effect
hist(Denit_Plant_traits$logR)
```

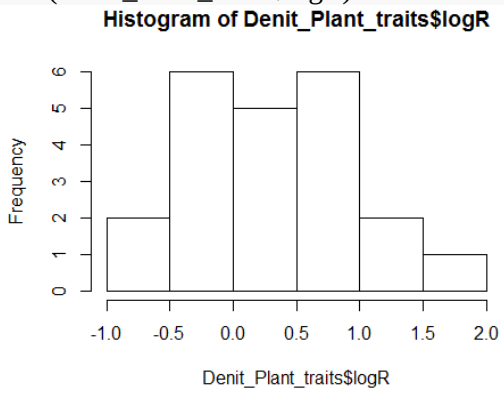


```
# Calculate mean effect of plants on denit at site level
mean(Denit_Plant_traits$logR)
[1] 0.3203291
# Back transform mean effect
10^0.3203291
[1] 2.09088
# Mean effect of vegetation is an approximate doubling of denitrification rates
```

Use plant traits to predict the effect of vegetation on denitrification rates

Initial model was a GLM, weighted by the inverse of the propagated sampling error in logR. Initial continuous predictors were total root mass, total aboveground biomass, and leaf nitrogen content.

```
# Create model, initialize with AGBiomass, BGBiomass, and Leaf N
mod1logR <- lm(logR ~ DryWeight_g.m2 * RootMass_g.m2 * VegN_mg.gDW, weights = 1/logR_sd^2,
   data = Denit_Plant_traits)
summary(mod1logR)
Call:
lm(formula = logR ~ DryWeight_g.m2 * RootMass_g.m2 * VegN_mg.gDW,
   data = Denit_Plant_traits, weights = 1/logR_sd^2)

Weighted Residuals:
    Min      1Q  Median      3Q     Max
-0.47090 -0.12953  0.00197  0.08182  0.47043

Coefficients:
```

	Estimate	Std.Error	t value	Pr(>|t|)
(Intercept)	2.49E+00	1.48E+01	0.168	0.869
DryWeight_g.m2	-6.20E-03	3.09E-02	-0.201	0.844
RootMass_g.m2	-8.98E-04	5.24E-03	-0.172	0.866
VegN_mg.gDW	-1.73E-01	9.21E-01	-0.187	0.854
DryWeight_g.m2:RootMass_g.m2	2.67E-06	1.22E-05	0.219	0.83
DryWeight_g.m2:VegN_mg.gDW	3.77E-04	2.06E-03	0.183	0.857
RootMass_g.m2:VegN_mg.gDW	4.88E-05	3.31E-04	0.147	0.885

```
   DryWeight_g.m2:RootMass_g.m2:VegN_mg.gDW    -1.13E-07     8.37E-07    -0.136      0.894

Residual standard error: 0.2776 on 14 degrees of freedom
Multiple R-squared:  0.2806,    Adjusted R-squared:  -0.07906
F-statistic: 0.7802 on 7 and 14 DF,  p-value: 0.6144
```

```
# Remove Leaf N and rerun model
mod2logR <- lm(logR ~ DryWeight_g.m2 * RootMass_g.m2, weights = 1/logR_sd^2,
   data = Denit_Plant_traits)
summary(mod2logR)
Call:
lm(formula = logR ~ DryWeight_g.m2 * RootMass_g.m2, data = Denit_Plant_traits,
   weights = 1/logR_sd^2)

Weighted Residuals:
    Min      1Q  Median      3Q     Max
-0.47905 -0.13575 -0.00166  0.11270  0.46915

Coefficients:
                                Estimate  Std.Error  t        Pr(>|t|)
 (Intercept)                      -0.197      1.260  -0.156     0.878
 DryWeight_g.m2                    0.000      0.002  -0.245     0.809
 RootMass_g.m2                     0.000      0.000  -0.268     0.792
 DryWeight_g.m2:RootMass_g.m2      0.000      0.000   1.084     0.293

Residual standard error: 0.2455 on 18 degrees of freedom
Multiple R-squared:  0.2763,    Adjusted R-squared:  0.1557
F-statistic: 2.291 on 3 and 18 DF,  p-value: 0.1128
```

```
# Remove non-significant interaction and rerun model
mod3logR <- lm(logR ~ DryWeight_g.m2 + RootMass_g.m2, weights = 1/logR_sd^2,
   data = Denit_Plant_traits)
summary(mod3logR)
Call:
lm(formula = logR ~ DryWeight_g.m2 + RootMass_g.m2, data = Denit_Plant_traits,
   weights = 1/logR_sd^2)

Weighted Residuals:
    Min      1Q  Median      3Q     Max
-0.49353 -0.17863  0.00935  0.11240  0.51154

Coefficients:
                 Estimate  Std.Error  t        Pr(>|t|)
 (Intercept)       -1.295      0.752  -1.723    0.1011
 DryWeight_g.m2     0.002      0.001   2.133    0.0462  *
 RootMass_g.m2      0.000      0.000   1.808    0.0865  .
---
Signif. codes:  0 '***' 0.001 '**' 0.01 '*' 0.05 '.' 0.1 ' ' 1
```

```
Residual standard error: 0.2466 on 19 degrees of freedom
Multiple R-squared:  0.2291,    Adjusted R-squared:  0.1479
F-statistic: 2.823 on 2 and 19 DF,  p-value: 0.08443
```

```
# Test residuals of model for normality using KS Lilliefors test
ks.test(mod3logR$residuals, "pnorm", mean(mod3logR$residuals), sd(mod3logR$residuals))
One-sample Kolmogorov-Smirnov test
data:  mod3logR$residuals
D = 0.1124, p-value = 0.915
alternative hypothesis: two-sided
```

```
# Visualize final model in 3 dimensions
logR_AGBGBiomass <- scatterplot3d(x = Denit_Plant_traits$DryWeight_g.m2, y =
Denit_Plant_traits$RootMass_g.m2, z = Denit_Plant_traits$logR, xlab = expression(paste("AG Biomass
(g ", m^-2, ")")), ylab = expression(paste("BG Biomass (g ", m^-2, ")")), zlab =
expression(paste(log[10], "(", DEA[VEG], "/", DEA[SED], ")")), color = "black", pch = 19)
logR_AGBGBiomass$plane3d(mod3logR)
```

```
# Plot relationship between AGBiomass and Effect of Plant
logR_AGBiomass <- ggplot(Denit_Plant_traits, aes(y = logR, x = DryWeight_g.m2))
logR_AGBiomass + geom_point(aes(size = logR_sd * 2), color = "gray24") + geom_hline(yintercept =
0, size = 1, color = "gray24") + geom_abline(intercept = -1.2954225, slope = 0.0015582, size = 2) +
ylab(expression(paste(log[10], "(", DEA[VEG], "/", DEA[SED], ")"))) + xlab(expression(paste("AG
Biomass (g ", m^-2, ")"))) + theme(legend.position = "none") + ggtitle("(B)")
```

```
# Plot relationship between BGBiomass and Effect of Plant
logR_BGBiomass <- ggplot(Denit_Plant_traits, aes(y = logR, x = RootMass_g.m2))
logR_BGBiomass + geom_point(aes(size = logR_sd * 2), color = "gray24") + geom_hline(yintercept =
0, size = 1, color = "gray24") + geom_abline(intercept = -1.2954225, slope = 0.0003559, size = 2) +
ylab(expression(paste(log[10], "(", DEA[VEG], "/", DEA[SED], ")"))) + xlab(expression(paste("Root
mass (g ", m^-2, ")"))) + theme(legend.position = "none") + ggtitle("(C)")
```

Appendix D: Supplement to Chapter 5

Packages

```
library(ggplot2)
library(bear)
library(car)
library(lmodel2)
library(Hmisc)
library(GGally)
library(smatr)
```

Data and Formatting

```
# Set working directory and import data
setwd(filepath1)
LIall <- read.csv("20141107_LI_AllData_2012-2013.csv")
# Convert 'Month_Year' from factor to ordered factor
LIall$Month_Year <- ordered(LIall$Month_Year, levels = c("April2012", "June2012",
   "August2012", "April2013", "June2013", "August2013"))
# Convert Site from a Factor to an Ordered Factor, West to East
LIall$Site <- ordered(LIall$Site, levels = c("East Creek", "Frost Creek", "Oceanside",
   "Lido", "Gardiners", "West Meadow", "Smith Point", "Indian Island", "Hubbard",
   "Mashomack", "Accabonac"))
# Drop levels to show only vegetated plots
LIallVEG <- droplevels(LIall[LIall$Tall_short != "sediment", ])
# Create dataframe for all vegetated plots measured in 2013
LIallVEG2013 <- LIallVEG[which(LIallVEG$Month_Year =="June2013" | LIallVEG$Month_Year ==
    "August2013"),]
```

Dependent variables

I created tables of means, standard deviations, standard errors, and confidence intervals for each dependent variable, grouped by Sampling Time (Month_Year) and Site. Initial groupings also included whether measurements were conducted in tall- or short-form vegetation (Tall_short), but these groupings were not useful in partitioning variation.

```
BGBiomassMeans <- summarySE(LIallVEG, measurevar = "RootMass_g.m2", groupvars =
c("Month_Year", "Site", na.rm = T))
AGBiomassMeans <- summarySE(LIallVEG, measurevar = "DryWeight_g.m2", groupvars =
c("Month_Year", "Site", na.rm = T))
RhizomeMeans <- summarySE(LIallVEG, measurevar = "RhizomeWidth_mm", groupvars =
c("Month_Year", "Site", na.rm = T))
```

Independent Variables

```
PW_DINMeans <- summarySE(LIallVEG, measurevar = "DIN_uM", groupvars = c("Month_Year",
   "Site", na.rm = T))
PW_PhosphateMeans <- summarySE(LIallVEG, measurevar = "PO4_uM", groupvars =
c("Month_Year", "Site", na.rm = T))
PW_SalinityMeans <- summarySE(LIallVEG, measurevar = "Salinity_ppt", groupvars =
c("Month_Year", "Site", na.rm = T))
Ext_DINMeans <- summarySE(LIallVEG, measurevar = "DIN_Extractable", groupvars =
c("Month_Year", "Site", na.rm = T))
Ext_PhosphateMeans <- summarySE(LIallVEG, measurevar = "PO4_Extractable_um",
   groupvars = c("Month_Year", "Site", na.rm = T))
```

```
SedCMeans <- summarySE(LIallVEG, measurevar = "SedC_mg.gDW", groupvars = c("Month_Year",
   "Site", na.rm = T))
SedNMeans <- summarySE(LIallVEG, measurevar = "SedN_mg.gDW", groupvars = c("Month_Year",
   "Site", na.rm = T))
FracSandMeans <- summarySE(LIallVEG, measurevar = "Frac_Sand", groupvars = c("Month_Year",
   "Site", na.rm = T))
```

Variable Correlations and Distributions

I created a data frame of site means for all variables included in initial models. I examined variables for distribution and correlation, then transformed as needed to meet assumptions of normality.

```
# Create data frame of site means for variables of interest
ancova1data <- cbind(PW_DINMeans, Ext_DINMeans, PW_PhosphateMeans, Ext_PhosphateMeans,
   PW_SalinityMeans, BGBiomassMeans, AGBiomassMeans, RhizomeMeans, SedCMeans,
   FracSandMeans)
# Examine correlations and distributions of independent variables in 2013 model
pcdata_ind <- ancova1data[, c("Salinity_ppt", "DIN_uM", "DIN_Extractable", "PO4_uM",
   "PO4_Extractable_um")]
ggpairs(pcdata_ind)
```

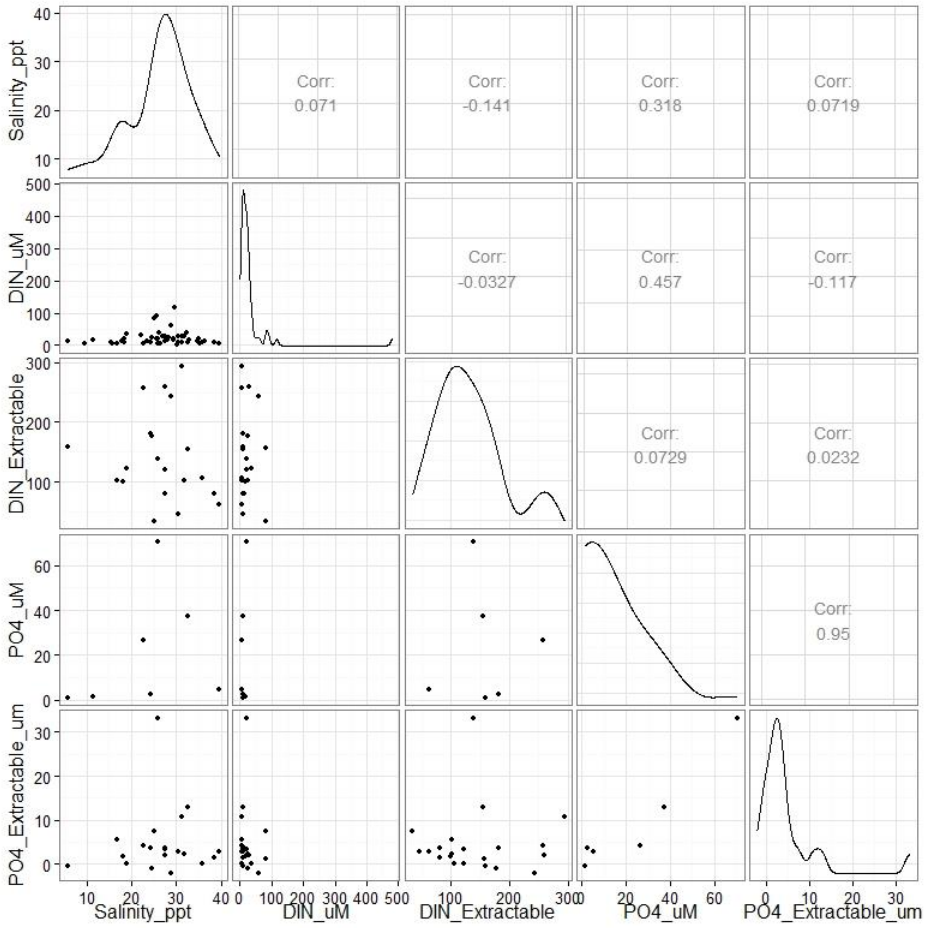


```
# Log10 transform PWPO4, PWDIN, ExtPO4
ancova1data$log10_PWPO4 <- log10(ancova1data$PO4_uM)
ancova1data$log10_ExtPO4 <- log10(ancova1data$PO4_Extractable_um)
```

```
ancova1data$log10_PWDIN <- log10(ancova1data$DIN_uM)
# Re-examine distributions for independent variables after transformations
pcdata_ind2 <- ancova1data[, c("Salinity_ppt", "log10_PWDIN", "DIN_Extractable",
   "log10_PWPO4", "log10_ExtPO4")]
ggpairs(pcdata_ind2)
```

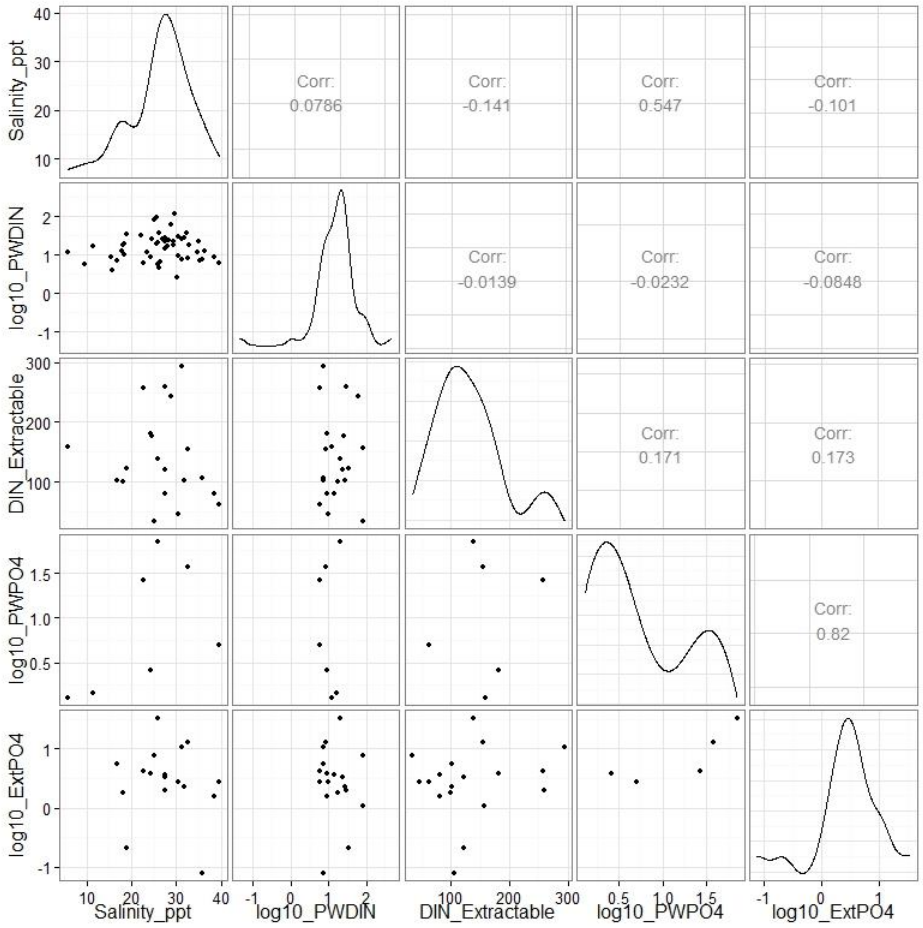


```
# Test correlations among independent varaibles for significance
rcorr(as.matrix(pcdata_ind2))
```

	Salinity_ppt	log10_PWDIN	DIN_Extractable	log10_PWPO4	log10_ExtPO4
Salinity_ppt	1.00	0.08	-0.14	0.55	-0.10
log10_PWDIN	0.08	1.00	-0.01	-0.02	-0.08
DIN_Extractable	-0.14	-0.01	1.00	0.17	0.17
log10_PWPO4	0.55	-0.02	0.17	1.00	0.82
log10_ExtPO4	-0.10	-0.08	0.17	0.82	1.00

n

	Salinity_ppt	log10_PWDIN	DIN_Extractable	log10_PWPO4	log10_ExtPO4
Salinity_ppt	64.00	52.00	20.00	7.00	17
log10_PWDIN	52.00	64.00	21.00	7.00	18
DIN_Extractable	20.00	21.00	64.00	6.00	18
log10_PWPO4	7.00	7.00	6.00	64.00	5
log10_ExtPO4	17.00	18.00	18.00	5.00	64

p

	Salinity_ppt	log10_PWDIN	DIN_Extractable	log10_PWPO4	log10_ExtPO4
Salinity_ppt		0.5796	0.5536	0.2041	0.7010
log10_PWDIN	0.5796		0.9522	0.9606	0.7381
DIN_Extractable	0.5536	0.9522		0.7455	0.4933
log10_PWPO4	0.2041	0.9606	0.7455		0.0893
log10_ExtPO4	0.7010	0.7381	0.4933	0.0893	

```
# Examine correlations and distributions of dependent variables
pcdata_dep <- ancova1data[, c("DryWeight_g.m2", "RootMass_g.m2", "RhizomeWidth_mm")]
ggpairs(pcdata_dep)
```

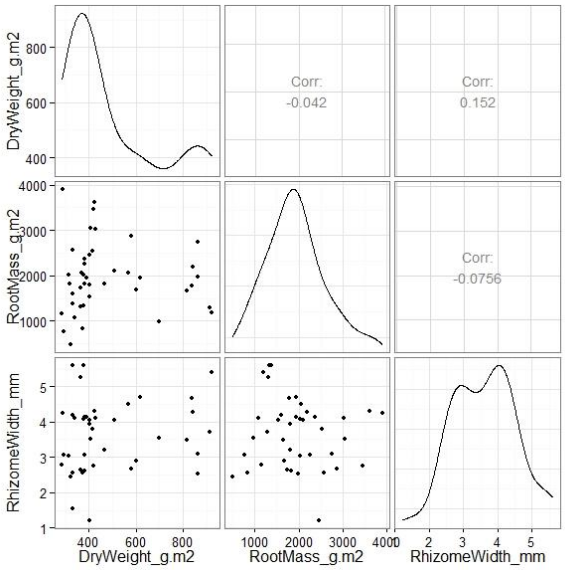


```
# Transform Aboveground Biomass (DryWeight_g.m2) to meet assumptions of normality
ancova1data$log10_DryWeight <- log10(ancova1data$DryWeight)
pcdata_dep2 <- ancova1data[, c("log10_DryWeight", "RootMass_g.m2", "RhizomeWidth_mm")]
ggpairs(pcdata_dep2)
```

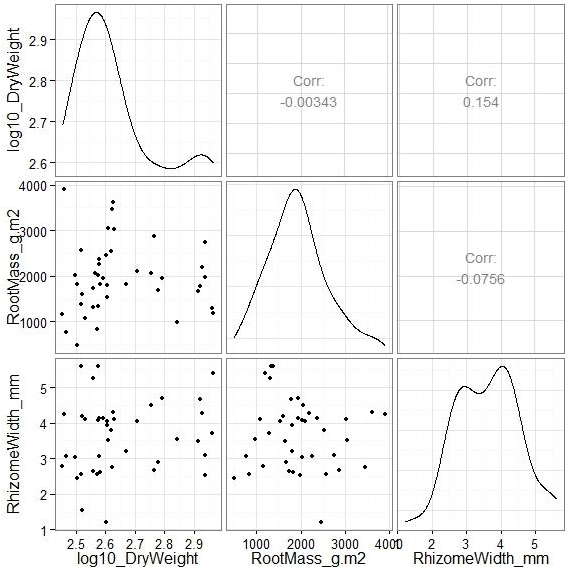

```
# Test correlations among dependent variables for significance
rcorr(as.matrix(pcdata_dep2))
```

	log10_DryWeight	RootMass_g.m2	RhizomeWidth_mm
log10_DryWeight	1.00	0.00	0.15
RootMass_g.m2	0.00	1.00	-0.08
RhizomeWidth_mm	0.15	-0.08	1.00

n

	log10_DryWeight	RootMass_g.m2	RhizomeWidth_mm
log10_DryWeight	64	42	41
RootMass_g.m2	42	64	40
RhizomeWidth_mm	41	40	64

p

	log10_DryWeight	RootMass_g.m2	RhizomeWidth_mm
log10_DryWeight		0.9828	0.3351
RootMass_g.m2	0.9828		0.6430
RhizomeWidth_mm	0.3351	0.6430	

Longitudinal Patterns in Independent Variables

I plotted site means of DIN (Dissolved inorganic nitrogen) and Salinity by longitude (west to east) to examine patterns and potential gradients in these variables among sites. I found variation in both of these variables among sites but no linear gradients.

```
# Create summaries of site means for Salinity and DIN by Longitude
DIN <- summarySE(data = LIallVEG2013, measurevar = "DIN_Extractable", groupvar = "Site",
   na.rm = T)
DIN <- rename(DIN, c(se = "DINse", sd = "DINsd", ci = "DINci"))
Sal <- summarySE(data = LIallVEG2013, measurevar = "Salinity_ppt", groupvar = "Site", na.rm = T)
Sal <- rename(Sal, c(se = "Salse", sd = "Salsd", ci = "Salci"))
UTM <- summarySE(data = LIallVEG2013, measurevar = "UTM_W", groupvar = "Site", na.rm = T)
UTM <- rename(UTM, c(se = "UTMse", sd = "UTMsd", ci = "UTMci"))
DIN_Sal_UTM <- cbind(DIN, Sal, UTM)
# Change base text size and background for figures
theme_set(theme_bw(base_size = 16))
# DIN by Longitude
DIN_UTMmeans <- ggplot(DIN_Sal_UTM, aes(x = UTM_W, y = DIN_Extractable))
DIN_UTMmeans + stat_smooth(size = 2, color = "grey40") + geom_errorbar(aes(ymin =
DIN_Extractable - DINse, ymax = DIN_Extractable + DINse, width = 0), size = 1.5, color = "gray34") +
   geom_point(size = 7, color = "white") + geom_point(size = 5, color = "grey40") +
   xlab("Longitude (UTM west)") + ylab(expression(paste("Extractable inorganic nitrogen ( ",
   mu, "M)")))
```

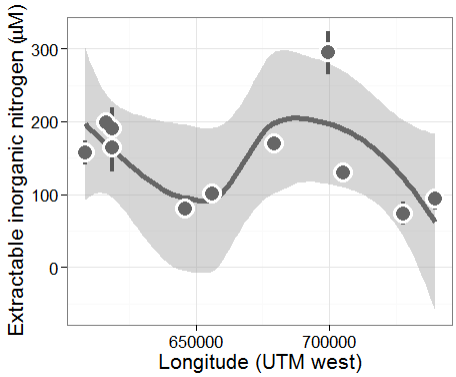


```
# Salinity by Longitude
Sal_UTMmeans <- ggplot(DIN_Sal_UTM, aes(x = UTM_W, y = Salinity_ppt))
Sal_UTMmeans + stat_smooth(size = 2, color = "grey40") + geom_errorbar(aes(ymin = Salinity_ppt -
Salse, ymax = Salinity_ppt + Salse, width = 0), size = 1.5, color = "gray34") + geom_point(size = 7,
color = "white") + geom_point(size = 5, color = "grey40") + xlab("Longitude (UTM west)") +
ylab("Salinity (ppt)")
```

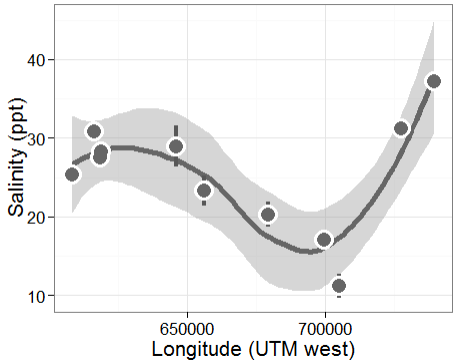

Ancova 1

Independent Variables measured in 2013

Dependent variable = RootMass_g.m2

Categorical variable = Month_Year[June2013, August2013]

Initial Continuous variables = Salinity_ppt, DIN_Extractable, log10_PO4

This model was initiated first with porewater nutrient values; due to insufficient sample volume to perform phosphate analyses for some sites, the model was run without interactions. Models including porewater nutrient values had no predictive power, and were discarded in favor of full-factorial models initiated with extractable nutrient values.

```
# Create data frame of site means for variables of interest
ancova1data <- cbind(PW_DINMeans, Ext_DINMeans, PW_PhosphateMeans, Ext_PhosphateMeans,
   PW_SalinityMeans, BGBiomassMeans, AGBiomassMeans, RhizomeMeans, SedCMeans,
   FracSandMeans)
# Log10 transform variables to meet assumptions of normality
ancova1data$log10_PWPO4 <- log10(ancova1data$PO4_uM)
ancova1data$log10_ExtPO4 <- log10(ancova1data$PO4_Extractable_um)
ancova1data$log10_PWDIN <- log10(ancova1data$DIN_uM)
# Subset data frame to include only measurements collected in 2013
ancova1data2013 <- ancova1data[which(ancova1data == "June2013" | ancova1data == "August2013"), ]
```

```
# Initial model, all independent variables and interactions
mod1.1 <- aov(RootMass_g.m2 ~ Month_Year * Salinity_ppt * DIN_Extractable * log10_ExtPO4, data = ancova1data2013)
summary(mod1.1)
```

	Df	SumSq	MeanSq	F	Pr(>F)	
Month_Year	1	3.33E+06	3334812	16.9	0.0261	*
Salinity_ppt	1	1.45E+06	1453740	7.367	0.0729	.
DIN_Extractable	1	1.36E+06	1355247	6.868	0.079	.
log10_ExtPO4	1	1.16E+05	116283	0.589	0.4986	
Month_Year:Salinity_ppt	1	6.02E+04	60194	0.305	0.6192	
Month_Year:DIN_Extractable	1	4.95E+05	495153	2.509	0.2113	
Salinity_ppt:DIN_Extractable	1	2.64E+04	26406	0.134	0.7388	
Month_Year:log10_ExtPO4	1	1.53E+05	152504	0.773	0.4441	
Salinity_ppt:log10_ExtPO4	1	1615573	1615573	8.188	0.0645	.
DIN_Extractable:log10_ExtPO4	1	1170398	1170398	5.931	0.0929	.
Month_Year:Salinity_ppt:DIN_Extractable	1	220521	220521	1.118	0.368	
Month_Year:Salinity_ppt:log10_ExtPO4	1	119784	119784	0.607	0.4927	
Salinity_ppt:DIN_Extractable:log10_ExtPO4	1	753322	753322	3.818	0.1457	
Residuals	3	591963	197321			

```
---
Signif. codes:  0 '***' 0.001 '**' 0.01 '*' 0.05 '.' 0.1 ' ' 1
203 observations deleted due to missingness
```

```
# Model with phosphate eliminated
mod1.2 <- aov(RootMass_g.m2 ~ Month_Year * Salinity_ppt * DIN_Extractable, data = ancova1data2013)
summary(mod1.2)
```

	Df	SumSq	MeanSq	F	Pr(>F)	
Month_Year	1	2.05E+06	2050883	4.773	0.0495	*
Salinity_ppt	1	1.69E+06	1694707	3.944	0.0704	.
DIN_Extractable	1	2.22E+06	2224973	5.178	0.042	*
Month_Year:Salinity_ppt	1	4.90E+01	49	0	0.9917	
Month_Year:DIN_Extractable	1	4.95E+05	495071	1.152	0.3042	
Salinity_ppt:DIN_Extractable	1	8.87E+03	8874	0.021	0.8881	
Month_Year:Salinity_ppt:DIN_Extractable	1	6.56E+02	656	0.002	0.9695	
Residuals	12	5.16E+06	429704			

```
---
Signif. codes:  0 '***' 0.001 '**' 0.01 '*' 0.05 '.' 0.1 ' ' 1
200 observations deleted due to missingness
```

```
# Model with interactions eliminated
mod1.3 <- aov(RootMass_g.m2 ~ Month_Year + Salinity_ppt + DIN_Extractable, data = ancova1data2013)
summary(mod1.3)
```

	Df	SumSq	MeanSq	F	Pr(>F)	
Month_Year	1	2.05E+06	2050883	5.796	0.0285	*

```
   Salinity_ppt          1   1.69E+06   1694707    4.79   0.0438   *
   DIN_Extractable       1   2.22E+06   2224973   6.288   0.0233   *
   Residuals            16   5.66E+06    353818
---
Signif. codes:  0 '***' 0.001 '**' 0.01 '*' 0.05 '.' 0.1 ' ' 1
200 observations deleted due to missingness
```

```
# Evaluate difference between models
anova(mod1.2, mod1.3)
```

```
Analysis of Variance Table
Model 1: RootMass_g.m2 ~ Month_Year * Salinity_ppt * DIN_Extractable
Model 2: RootMass_g.m2 ~ Month_Year + Salinity_ppt + DIN_Extractable
  Res.Df     RSS Df Sum of Sq      F Pr(>F)
1     12 5156443
2     16 5661093 -4   -504650 0.2936 0.8765
```

```
# Run mod1.3 as linear model to evaluate fit
mod1.3lm <- lm(RootMass_g.m2 ~ Month_Year + Salinity_ppt + DIN_Extractable,
   data = ancova1data2013)
summary(mod1.3lm)
```

```
Call:
lm(formula = RootMass_g.m2 ~ Month_Year + Salinity_ppt + DIN_Extractable,
   data = ancova1data2013)

Residuals:
   Min     1Q  Median     3Q    Max
-986.12 -287.48   78.36  404.48  825.76

Coefficients:
                     Estimate   Std. Error   t          Pr(>|t|)
   (Intercept)           2067   6.00E+02     3.443      0.00334   **
   Month_Year.L          -524   1.99E+02    -2.636      0.01799   *
   Salinity_ppt            32   1.82E+01     1.738      0.10148
   DIN_Extractable         -5   1.86E+00    -2.508      0.02331   *
---
Signif. codes:  0 '***' 0.001 '**' 0.01 '*' 0.05 '.' 0.1 ' ' 1

Residual standard error: 594.8 on 16 degrees of freedom
  (200 observations deleted due to missingness)
Multiple R-squared:  0.5133,    Adjusted R-squared:  0.422
F-statistic: 5.625 on 3 and 16 DF,  p-value: 0.00791
```

```
# Inspect residuals of final model
hist(mod1.3lm$residuals)
```

Ancova 1

Independent Variables measured in 2013

Dependent variable = DryWeight_g.m2

Categorical variable = Month_Year[June2013, August2013]

Initial Continuous variables = Salinity_ppt, DIN_Extractable, log10_PO4

This model was initiated first with porewater nutrient values; due to insufficient sample volume to perform phosphate analyses for some sites, the model was run without interactions. Models including porewater nutrient values had no predictive power, and were discarded in favor of full-factorial models initiated with extractable nutrient values.

```
# Create data frame of site means for variables of interest
ancova1data <- cbind(PW_DINMeans, Ext_DINMeans, PW_PhosphateMeans, Ext_PhosphateMeans,
   PW_SalinityMeans, BGBiomassMeans, AGBiomassMeans, RhizomeMeans, SedCMeans,
   FracSandMeans)
# Log10 transform variables to meet assumptions of normality
ancova1data$log10_PWPO4 <- log10(ancova1data$PO4_uM)
ancova1data$log10_ExtPO4 <- log10(ancova1data$PO4_Extractable_um)
ancova1data$log10_PWDIN <- log10(ancova1data$DIN_uM)
ancova1data$log10_DryWeight <- log10(ancova1data$DryWeight_g.m2)
# Subset data frame to include only measurements collected in 2013
ancova1data2013 <- ancova1data[which(ancova1data == "June2013" | ancova1data == "August2013"), ]

# Initial model, all independent variables and interactions
mod1.1a <- aov(DryWeight_g.m2 ~ Month_Year * Salinity_ppt * DIN_Extractable *
   log10_ExtPO4, data = ancova1data2013)
summary(mod1.1a)
```

	Df	SumSq	MeanSq	F	Pr(>F)	
Month_Year	1	3.28E+05	327527	5.575	0.0993	.
Salinity_ppt	1	2.26E+04	22585	0.384	0.5791	
DIN_Extractable	1	6.41E+04	64088	1.091	0.373	
log10_ExtPO4	1	6.40E+04	63988	1.089	0.3733	
Month_Year:Salinity_ppt	1	8.00E+00	8	0	0.9913	
Month_Year:DIN_Extractable	1	1.95E+03	1948	0.033	0.8671	
Salinity_ppt:DIN_Extractable	1	5.71E+02	571	0.01	0.9277	
Month_Year:log10_ExtPO4	1	1.11E+05	111423	1.897	0.2622	
Salinity_ppt:log10_ExtPO4	1	222	222	0.004	0.9549	

DIN_Extractable:log10_ExtPO4	1	186	186	0.003	0.9587
Month_Year:Salinity_ppt:DIN_Extractable	1	315	315	0.005	0.9463
Month_Year:Salinity_ppt:log10_ExtPO4	1	15321	15321	0.261	0.6448
Salinity_ppt:DIN_Extractable:log10_ExtPO4	1	6927	6927	0.118	0.754
Residuals	3	176248	58749		

Signif. codes: 0 '***' 0.001 '**' 0.01 '*' 0.05 '.' 0.1 ' ' 1
203 observations deleted due to missingness

```
# Model with salinity eliminated
mod1.2a <- aov(DryWeight_g.m2 ~ Month_Year * DIN_Extractable * log10_ExtPO4,
   data = ancova1data2013)
summary(mod1.2a)
```

	Df	SumSq	MeanSq	F	Pr(>F)	
Month_Year	1	2.34E+05	234486	8.259	0.0166	*
DIN_Extractable	1	1.10E+05	109598	3.86	0.0778	.
log10_ExtPO4	1	5.44E+04	54406	1.916	0.1964	
Month_Year:DIN_Extractable	1	1.04E+04	10383	0.366	0.5588	
Month_Year:log10_ExtPO4	1	1.25E+05	124577	4.388	0.0626	.
DIN_Extractable:log10_ExtPO4	1	5.93E+02	593	0.021	0.888	
Month_Year:DIN_Extractable:log10_ExtPO4	1	1.36E+04	13626	0.48	0.5042	
Residuals	10	2.84E+05	28391			

Signif. codes: 0 '***' 0.001 '**' 0.01 '*' 0.05 '.' 0.1 ' ' 1
202 observations deleted due to missingness

```
# Model with phosphate eliminated
mod1.3a <- aov(DryWeight_g.m2 ~ Month_Year * DIN_Extractable, data = ancova1data2013)
summary(mod1.3a)
```

	Df	SumSq	MeanSq	F	Pr(>F)	
Month_Year	1	272259	272259	8.628	0.0092	**
DIN_Extractable	1	113797	113797	3.606	0.0747	.
Month_Year:DIN_Extractable	1	0	0	0	0.9975	
Residuals	17	536420	31554			

Signif. codes: 0 '***' 0.001 '**' 0.01 '*' 0.05 '.' 0.1 ' ' 1
199 observations deleted due to missingness

```
# Model with interactions eliminated
mod1.4a <- aov(DryWeight_g.m2 ~ Month_Year + DIN_Extractable, data = ancova1data2013)
summary(mod1.4a)
```

	Df	SumSq	MeanSq	F	Pr(>F)	
Month_Year	1	272259	272259	9.136	0.00732	**
DIN_Extractable	1	113797	113797	3.819	0.06641	.
Residuals	18	536420	29801			

Signif. codes: 0 '***' 0.001 '**' 0.01 '*' 0.05 '.' 0.1 ' ' 1
199 observations deleted due to missingness

```
# Evaluate difference between models
anova(mod1.3a, mod1.4a)
```
Analysis of Variance Table
Model 1: DryWeight_g.m2 ~ Month_Year * DIN_Extractable
Model 2: DryWeight_g.m2 ~ Month_Year + DIN_Extractable

Res.Df	RSS	Df	Sum of Sq	F	Pr(>F)
1	17	536420			
2	18	536420	-1	-0.31054	0 0.9975

```
# Run mod1.3 as linear model to evaluate fit
mod1.4alm <- lm(DryWeight_g.m2 ~ Month_Year + DIN_Extractable, data = ancova1data2013)
summary(mod1.4alm)
```
Call:
lm(formula = DryWeight_g.m2 ~ Month_Year + DIN_Extractable, data = ancova1data2013)

Residuals:

Min	1Q	Median	3Q	Max
-283.05	-104.22	4.56	112.30	311.69

Coefficients:

	Estimate	Std.Error	t	Pr(>|t|)	
(Intercept)	453.305	83.978	5.398	3.96E-05	***
Month_Year.L	155.69	53.41	2.915	0.00924	**
DIN_Extractable	1.036	0.53	1.954	0.06641	.

Signif. codes: 0 '***' 0.001 '**' 0.01 '*' 0.05 '.' 0.1 ' ' 1

Residual standard error: 172.6 on 18 degrees of freedom
  (199 observations deleted due to missingness)
Multiple R-squared: 0.4185,   Adjusted R-squared: 0.3539
F-statistic: 6.477 on 2 and 18 DF, p-value: 0.007602

```
# Inspect residuals of final model, Residuals were more normally distributed for non-transformed
variable; fit simple linear model instead
hist(mod1.4alm$residuals)
```

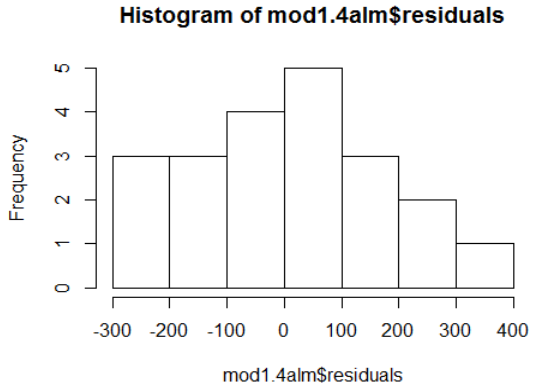

Ancova 2

Independent Variables measured in 2012-2013

Dependent variable = RootMass_g.m2

Categorical variable = Month_Year[June2012, August2012, June2013, August2013]

Initial Continuous variables = Salinity_ppt, log10_DIN

```
# Create data frame of site means for variables of interest
ancova2data <- cbind(PW_DINMeans, PW_SalinityMeans, BGBiomassMeans, AGBiomassMeans,
   RhizomeMeans)
# Log transform DIN to meet assumptions of normality
ancova2data$log10_DIN <- log10(ancova2data$DIN_uM)
# Subset data to include only sampling times of interest
ancova2data20122013 <- ancova2data[which(ancova2data == "June2012" | ancova2data ==
   "August2012" | ancova2data == "June2013" | ancova2data == "August2013"), ]

# Initial model, all independent variables and interactions
mod2.1 <- aov(RootMass_g.m2 ~ Month_Year * Salinity_ppt * log10_DIN, data =
ancova2data20122013)
summary(mod2.1)
```

	Df	SumSq	MeanSq	F	Pr(>F)	
Month_Year	3	3904434	1301478	2.623	0.07277	.
Salinity_ppt	1	4251230	4251230	8.568	0.00719	**
log10_DIN	1	260238	260238	0.524	0.47566	
Month_Year:Salinity_ppt	3	157055	52352	0.106	0.95609	
Month_Year:log10_DIN	3	747186	249062	0.502	0.68437	
Salinity_ppt:log10_DIN	1	109109	109109	0.22	0.64318	
Month_Year:Salinity_ppt:log10_DIN	3	1974228	658076	1.326	0.2881	
Residuals	25	12404507	496180			

Signif. codes: 0 '***' 0.001 '**' 0.01 '*' 0.05 '.' 0.1 ' ' 1

174 observations deleted due to missingness

```
# Model with DIN eliminated
mod2.2 <- aov(RootMass_g.m2 ~ Month_Year * Salinity_ppt, data = ancova2data20122013)
summary(mod2.2)
```

	Df	SumSq	MeanSq	F	Pr(>F)	
Month_Year	3	3904434	1301478	2.790	0.05579	.
Salinity_ppt	1	4251230	4251230	9.115	0.00486	**
Month_Year:Salinity_ppt	3	260632	86877	0.186	0.90498	
Residuals	33	15391690	466415			

Signif. codes: 0 '***' 0.001 '**' 0.01 '*' 0.05 '.' 0.1 ' ' 1

174 observations deleted due to missingness

```
# Model with interaction term eliminated
mod2.3 <- aov(RootMass_g.m2 ~ Month_Year + Salinity_ppt, data = ancova2data20122013)
summary(mod2.3)
```

	Df	SumSq	MeanSq	F	Pr(>F)

```
   Month_Year     3    3904434  1301478   2.993  0.04349   *
   Salinity_ppt   1    4251230  4251230   9.778  0.00349   **
   Residuals     36   15652322   434787
---
Signif. codes:  0 '***' 0.001 '**' 0.01 '*' 0.05 '.' 0.1 ' ' 1
174 observations deleted due to missingness
```

```
# Evaluate difference between models
anova(mod2.2, mod2.3)
```

```
Analysis of Variance Table
Model 1: RootMass_g.m2 ~ Month_Year * Salinity_ppt
Model 2: RootMass_g.m2 ~ Month_Year + Salinity_ppt
  Res.Df      RSS Df Sum of Sq      F Pr(>F)
1     33 15391690
2     36 15652322 -3   -260632 0.1863  0.905
```

```
# Run mod2.3 as linear model to evaluate fit
mod2.3lm <- lm(RootMass_g.m2 ~ Month_Year + Salinity_ppt, data = ancova2data20122013)
summary(mod2.3lm)
```

```
Call:
lm(formula = RootMass_g.m2 ~ Month_Year + Salinity_ppt, data = ancova2data20122013)

Residuals:
   Min     1Q  Median     3Q    Max
-1144.6  -471.7  -127.3   264.8  1398.2

Coefficients:
                Estimate  Std.Error  t        Pr(>|t|)
   (Intercept)    675.48     425.71   1.587      0.121
   Month_Year.L   371.6      204.27   1.819    0.07721   .
   Month_Year.Q  -509.44     207.99  -2.449    0.01931   *
   Month_Year.C  -510.77     219.54  -2.327    0.02573   *
   Salinity_ppt    47.81      15.29   3.127    0.00349   **
---
Signif. codes:  0 '***' 0.001 '**' 0.01 '*' 0.05 '.' 0.1 ' ' 1

Residual standard error: 659.4 on 36 degrees of freedom
  (174 observations deleted due to missingness)
Multiple R-squared:  0.3426,    Adjusted R-squared:  0.2695
F-statistic: 4.689 on 4 and 36 DF,  p-value: 0.003773
```

```
# Inspect residuals of final model
hist(mod2.3lm$residuals)
```

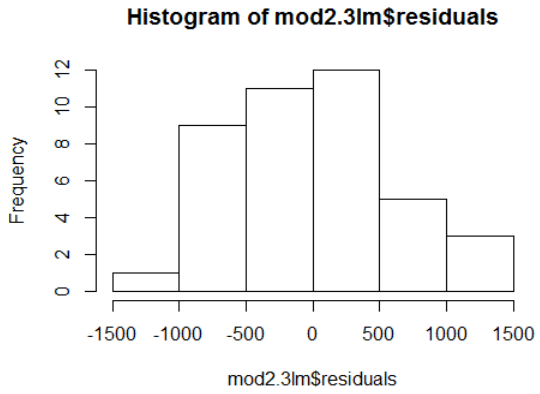

Ancova 2

Independent Variables measured in 2012-2013

Dependent variable = DryWeight_g.m2

Categorical variable = Month_Year[June2012, August2012, June2013, August2013]

Initial Continuous variables = Salinity_ppt, log10_DIN

```
# Create data frame of site means for variables of interest
ancova2data <- cbind(PW_DINMeans, PW_SalinityMeans, BGBiomassMeans, AGBiomassMeans,
   RhizomeMeans)
# Log transform DIN to meet assumptions of normality
ancova2data$log10_DIN <- log10(ancova2data$DIN_uM)
# Subset data to include only sampling times of interest
ancova2data20122013 <- ancova2data[which(ancova2data == "June2012" | ancova2data ==
   "August2012" | ancova2data == "June2013" | ancova2data == "August2013"), ]

# Initial model, all independent variables and interactions
mod2.1a <- aov(DryWeight_g.m2 ~ Month_Year * Salinity_ppt * log10_DIN, data =
ancova2data20122013)
summary(mod2.1a)
```

	Df	SumSq	MeanSq	F	Pr(>F)	
Month_Year	3	914710	304903	18.306	1.36E-06	***
Salinity_ppt	1	839	839	0.05	0.824	
log10_DIN	1	5195	5195	0.312	0.581	
Month_Year:Salinity_ppt	3	47915	15972	0.959	0.427	
Month_Year:log10_DIN	3	6875	2292	0.138	0.937	
Salinity_ppt:log10_DIN	1	7287	7287	0.438	0.514	
Month_Year:Salinity_ppt:log10_DIN	3	61673	20558	1.234	0.317	
Residuals	26	433043	16655			

Signif. codes: 0 '***' 0.001 '**' 0.01 '*' 0.05 '.' 0.1 ' ' 1

173 observations deleted due to missingness

```
# Model with Salinity eliminated
mod2.2a <- aov(DryWeight_g.m2 ~ Month_Year * log10_DIN, data = ancova2data20122013)
summary(mod2.2a)
```

	Df	SumSq	MeanSq	F	Pr(>F)	
Month_Year	3	899779	299926	16.829	6.16E-07	***

```
   log10_DIN                 1     29470     29470   1.654      0.207
   Month_Year:log10_DIN      3     41216     13739   0.771      0.518
   Residuals                35    623766     17822
---
Signif. codes:  0 '***' 0.001 '**' 0.01 '*' 0.05 '.' 0.1 ' ' 1
172 observations deleted due to missingness
```

```
# Model with interaction term eliminated
mod2.3a <- aov(DryWeight_g.m2 ~ Month_Year + log10_DIN, data = ancova2data20122013)
summary(mod2.3a)
```

```
                Df   SumSq   MeanSq   F        Pr(>F)
   Month_Year    3  899779   299926  17.139  3.36E-07  ***
   log10_DIN     1   29470    29470   1.684      0.202
   Residuals    38  664982    17500
---
Signif. codes:  0 '***' 0.001 '**' 0.01 '*' 0.05 '.' 0.1 ' ' 1
172 observations deleted due to missingness
```

Fit RMA regressions for Extractable Inorganic Nitrogen and Salinity versus Root Mass

Because both my independent and dependent variables include measurement error, it is appropriate to visualize relationships using reduced-major-axis (RMA) regression, as opposed to ordinary-least-squares (OLS) regression. The lmodel2 package refers to RMA regressions as SMA (or standardized-major-axis) regressions. I also created tables of coefficients for easy insertion of RMA lines into plots.

```
# DIN v BG Biomass June 2013
data_June2013 <- ancova1data[which(ancova1data == "June2013"), ]
DIN_fit_June2013 <- lmodel2(RootMass_g.m2 ~ DIN_Extractable, data = data_June2013)
DIN_coef_June2013 <- with(data_June2013, line.cis(RootMass_g.m2, DIN_Extractable))
DIN_fit_June2013
```

```
Model II regression

Call: lmodel2(formula = RootMass_g.m2 ~ DIN_Extractable, data =
data_June2013)

n = 10   r = -0.6986631   r-square = 0.4881302
Parametric P-values:   2-tailed = 0.02459641    1-tailed = 0.0122982
Angle between the two OLS regression lines = 3.874798 degrees

Regression results
  Method Intercept      Slope Angle (degrees) P-perm (1-tailed)
1    OLS  3513.804  -7.492212       -82.39755              NA
2     MA  4587.043 -15.280769       -86.25580              NA
3    SMA  3959.085 -10.723640       -84.67247              NA

Confidence intervals
  Method 2.5%-Intercept 97.5%-Intercept 2.5%-Slope 97.5%-Slope
1    OLS       2539.463       4488.145  -13.74735   -1.237071
2     MA       3626.321      15101.628  -91.58570   -8.308758
```

```
3    SMA      3330.160       5054.038  -18.66978   -6.159498

Eigenvalues: 676904.3 2987.493
H statistic used for computing C.I. of MA: 0.002959727

# DIN v BG Biomass August 2013
data_August2013 <- ancova1data[which(ancova1data == "August2013"), ]
DIN_fit_August2013 <- lmodel2(RootMass_g.m2 ~ DIN_Extractable, data = data_August2013)
DIN_coef_August2013 <- with(data_August2013, line.cis(RootMass_g.m2, DIN_Extractable))
DIN_fit_August2013
Model II regression

Call: lmodel2(formula = RootMass_g.m2 ~ DIN_Extractable, data =
data_August2013)

n = 11   r = -0.3593934   r-square = 0.1291636
Parametric P-values:   2-tailed = 0.2776882    1-tailed = 0.1388441
Angle between the two OLS regression lines = 14.97878 degrees

Regression results
  Method Intercept      Slope Angle (degrees) P-perm (1-tailed)
1    OLS  2396.341  -3.214648       -72.72034              NA
2     MA  5506.925 -24.617738       -87.67386              NA
3    SMA  3229.102  -8.944652       -83.62090              NA

Confidence intervals
  Method 2.5%-Intercept 97.5%-Intercept 2.5%-Slope 97.5%-Slope
1    OLS       1382.036       3410.646  -9.508743    3.079446
2     MA       3133.574      -1806.235  25.702152   -8.287352
3    SMA       2603.944       4433.428 -17.231297   -4.643109

Eigenvalues: 427368.5 4636.558
H statistic used for computing C.I. of MA: 0.006304798

# Salinity v BG Biomass June 2012
data_June2012 <- ancova1data[which(ancova1data == "June2012"), ]
Sal_fit_June2012 <- lmodel2(RootMass_g.m2 ~ Salinity_ppt, data = data_June2012)
Sal_coef_June2012 <- with(data_June2012, line.cis(RootMass_g.m2, Salinity_ppt))
Sal_fit_June2012
Model II regression

Call: lmodel2(formula = RootMass_g.m2 ~ Salinity_ppt, data =
data_June2012)

n = 10   r = 0.2317316   r-square = 0.05369952
Parametric P-values:   2-tailed = 0.5194423    1-tailed = 0.2597212
Angle between the two OLS regression lines = 1.753331 degrees

Regression results
  Method  Intercept     Slope Angle (degrees) P-perm (1-tailed)
```

```
1    OLS    743.845  30.91206        88.14714              NA
2     MA -14028.580 575.61800        89.90046              NA
3    SMA  -2035.518 133.39596        89.57049              NA

Confidence intervals
  Method 2.5%-Intercept 97.5%-Intercept 2.5%-Slope 97.5%-Slope
1    OLS      -2180.768       3668.4582  -74.88469    136.7088
2     MA       8026.164      -1947.5872  130.15366   -237.6100
3    SMA      -5904.396       -165.9811   64.46022    276.0537

Eigenvalues: 567044.6 30.15493
H statistic used for computing C.I. of MA: 3.535228e-05
```

```
# Salinity v BG Biomass August 2012
data_August2012 <- ancova1data[which(ancova1data == "August2012"), ]
Sal_fit_August2012 <- lmodel2(RootMass_g.m2 ~ Salinity_ppt, data = data_August2012)
Sal_coef_August2012 <- with(data_August2012, line.cis(RootMass_g.m2, Salinity_ppt))
Sal_fit_August2012
Model II regression

Call: lmodel2(formula = RootMass_g.m2 ~ Salinity_ppt, data =
data_August2012)

n = 10   r = 0.645659   r-square = 0.4168755
Parametric P-values:   2-tailed = 0.04375435    1-tailed = 0.02187717
Angle between the two OLS regression lines = 0.4730375 degrees

Regression results
  Method  Intercept     Slope Angle (degrees) P-perm (1-tailed)
1    OLS  -163.1501  70.62235        89.18876              NA
2     MA -3053.3977 169.40047        89.66178              NA
3    SMA -1297.2067 109.38027        89.47619              NA

Confidence intervals
  Method 2.5%-Intercept 97.5%-Intercept 2.5%-Slope 97.5%-Slope
1    OLS      -2193.649       1867.3484    2.52430    138.7204
2     MA    -136704.094       -620.1054   86.23942   4737.0934
3    SMA      -3859.334        125.7642   60.74832    196.9444

Eigenvalues: 437665.3 21.33021
H statistic used for computing C.I. of MA: 3.239855e-05
```

```
# Salinity v BG Biomass June 2013
data_June2013 <- ancova1data[which(ancova1data == "June2013"), ]
Sal_fit_June2013 <- lmodel2(RootMass_g.m2 ~ Salinity_ppt, data = data_June2013)
Sal_coef_June2013 <- with(data_June2013, line.cis(RootMass_g.m2, Salinity_ppt))
Sal_fit_June2013
Model II regression

Call: lmodel2(formula = RootMass_g.m2 ~ Salinity_ppt, data =
```

data_June2013)

n = 10 r = 0.5211492 r-square = 0.2715965
Parametric P-values: 2-tailed = 0.122417 1-tailed = 0.06120849
Angle between the two OLS regression lines = 0.8976689 degrees

Regression results
  Method Intercept   Slope Angle (degrees) P-perm (1-tailed)
1   OLS 1386.3047 46.48238   88.76756   NA
2   MA -1475.5884 171.12929   89.66519   NA
3   SMA   405.6902 89.19206   89.35764   NA

Confidence intervals
  Method 2.5%-Intercept 97.5%-Intercept 2.5%-Slope 97.5%-Slope
1   OLS   -146.592   2919.2013 -15.57984   108.5446
2   MA   14176.780   771.0308   73.28002   -510.5941
3   SMA   -1466.237   1383.6605   46.59754   170.7220

Eigenvalues: 732757.7 67.08885
H statistic used for computing C.I. of MA: 6.086949e-05

```
# Salinity v BG Biomass August 2013
data_August2013 <- ancova1data[which(ancova1data == "August2013"), ]
Sal_fit_August2013 <- lmodel2(RootMass_g.m2 ~ Salinity_ppt, data = data_August2013)
Sal_coef_August2013 <- with(data_August2013, line.cis(RootMass_g.m2, Salinity_ppt))
Sal_fit_August2013
```
Model II regression

Call: lmodel2(formula = RootMass_g.m2 ~ Salinity_ppt, data =
data_August2013)

n = 11 r = 0.4342889 r-square = 0.1886068
Parametric P-values: 2-tailed = 0.1819802 1-tailed = 0.0909901
Angle between the two OLS regression lines = 1.055763 degrees

Regression results
  Method Intercept   Slope Angle (degrees) P-perm (1-tailed)
1   OLS   664.4365 44.02468   88.69878   NA
2   MA -4775.8563 233.40196   89.75452   NA
3   SMA -982.9921 101.37188   89.43481   NA

Confidence intervals
  Method 2.5%-Intercept 97.5%-Intercept 2.5%-Slope 97.5%-Slope
1   OLS   -1358.306   2687.1788 -24.83020   112.8796
2   MA   13817.520   -685.8218   91.02734   -413.8358
3   SMA   -3569.248   386.7776   53.69002   191.3998

Eigenvalues: 426679.9 33.68857
H statistic used for computing C.I. of MA: 4.490059e-05

Fit RMA regressions for Extractable Inorganic Nitrogen versus Aboveground Biomass

```
# DIN v AG Biomass June 2013
data_June2013 <- ancova1data[which(ancova1data == "June2013"), ]
DIN_fit2_June2013 <- lmodel2(DryWeight_g.m2 ~ DIN_Extractable, data = data_June2013)
DIN_coef2_June2013 <- with(data_June2013, line.cis(DryWeight_g.m2, DIN_Extractable))
DIN_fit2_June2013
```

```
Model II regression

Call: lmodel2(formula = DryWeight_g.m2 ~ DIN_Extractable, data =
data_June2013)

n = 10   r = 0.4793113   r-square = 0.2297393
Parametric P-values:   2-tailed = 0.1609991    1-tailed = 0.08049957
Angle between the two OLS regression lines = 31.51547 degrees

Regression results
  Method Intercept    Slope Angle (degrees) P-perm (1-tailed)
1    OLS 343.45312 1.034006        45.95783              NA
2     MA -37.28324 3.797031        75.24541              NA
3    SMA 188.67017 2.157275        65.13002              NA

Confidence intervals
  Method 2.5%-Intercept 97.5%-Intercept 2.5%-Slope 97.5%-Slope
1    OLS      103.00952        583.8967 -0.5096103    2.577623
2     MA     1638.64861         298.5268  1.3600388   -8.365300
3    SMA      -92.29751        333.1137  1.1090400    4.196273

Eigenvalues: 28873.74 4265.164
H statistic used for computing C.I. of MA: 0.1351749
```

```
# DIN v AG Biomass August 2013
data_August2013 <- ancova1data[which(ancova1data == "August2013"), ]
DIN_fit2_August2013 <- lmodel2(DryWeight_g.m2 ~ DIN_Extractable, data = data_August2013)
DIN_coef2_August2013 <- with(data_August2013, line.cis(DryWeight_g.m2, DIN_Extractable))
DIN_fit2_August2013
```

```
Model II regression

Call: lmodel2(formula = DryWeight_g.m2 ~ DIN_Extractable, data =
data_August2013)

n = 11   r = 0.3765868   r-square = 0.1418176
Parametric P-values:   2-tailed = 0.2536335    1-tailed = 0.1268167
Angle between the two OLS regression lines = 36.16343 degrees

Regression results
  Method Intercept    Slope Angle (degrees) P-perm (1-tailed)
1    OLS  563.1471 1.037428        46.05242              NA
2     MA -231.4784 6.505033        81.26050              NA
3    SMA  313.5529 2.754818        70.04908              NA
```

Confidence intervals
  Method 2.5%-Intercept 97.5%-Intercept 2.5%-Slope 97.5%-Slope
1   OLS   253.03430   873.2598 -0.8869227   2.961779
2   MA   1827.54980   401.0308 2.1529064   -7.662588
3   SMA   -54.12773   505.2171 1.4360285   5.284730

Eigenvalues: 41322.37 4482.445
H statistic used for computing C.I. of MA: 0.07760072

Figure 2A: Extractable Inorganic Nitrogen versus Root Mass

```
# Change base text size and background for figures
theme_set(theme_bw(base_size = 16))
# Create data table for figure
ExtDIN_BGbiomass_means <- merge(Ext_DINMeans, BGBiomassMeans, by = c("Month_Year",
   "Site"))
ExtDIN_BGbiomass_means2 <- ExtDIN_BGbiomass_means[which(ExtDIN_BGbiomass_means ==
   "June2013" | ExtDIN_BGbiomass_means == "August2013"), ]
# Create plot
ExtDIN_BGbiomass <- ggplot(ExtDIN_BGbiomass_means2, aes(x = DIN_Extractable,
   y = RootMass_g.m2, color = Month_Year))
ExtDIN_BGbiomass + geom_errorbar(aes(ymin = RootMass_g.m2 - se.y, ymax = RootMass_g.m2 +
se.y, width = 0), size = 1) + geom_errorbarh(aes(xmin = DIN_Extractable - se.x, xmax =
DIN_Extractable + se.x, width = 0), size = 1) + geom_point(size = 6, color = "white") +
geom_point(size = 5) + geom_abline(aes(intercept = DIN_coef_June2013[1, 1], slope =
DIN_coef_June2013[2, 1]), size = 2, color = "Dark Blue") + geom_abline(aes(intercept =
DIN_coef_August2013[1, 1], slope = DIN_coef_August2013[2, 1]), size = 2, color = "Dark Red") +
xlab(expression(paste("Extractable Inorganic Nitrogen (", mu, "M")))) + ylab(expression(paste("Root
mass (g/", m^{2}, ")"))) + scale_color_manual(values = c("Dark Blue", "Dark Red"), labels = c("June
2013", "August 2013")) + theme(legend.title = element_blank()) + scale_y_continuous(limits = c(0,
5000)) + ggtitle("A")
```

Figure 2B: Salinity versus Root Mass

```
# Create data table for figure
Salinity_BGbiomass_means <- merge(PW_SalinityMeans, BGBiomassMeans, by = c("Month_Year",
   "Site"))
Salinity_BGbiomass_means2 <- Salinity_BGbiomass_means[which(Salinity_BGbiomass_means ==
   "June2012" | Salinity_BGbiomass_means == "August2012" | Salinity_BGbiomass_means ==
   "June2013" | Salinity_BGbiomass_means == "August2013"), ]
# Create plot
Salinity_BGbiomass <- ggplot(Salinity_BGbiomass_means2, aes(x = Salinity_ppt,
   y = RootMass_g.m2, color = Month_Year, shape = Month_Year))
Salinity_BGbiomass + geom_errorbar(aes(ymin = RootMass_g.m2 - se.y, ymax = RootMass_g.m2 +
se.y, width = 0), size = 1) + geom_errorbarh(aes(xmin = Salinity_ppt - se.x, xmax = Salinity_ppt + se.x,
width = 0), size = 1) + geom_point(size = 6, color = "white") + geom_point(size = 5) +
geom_abline(aes(intercept = Sal_coef_June2012[1, 1], slope = Sal_coef_June2012[2, 1]), size = 2, color
= "Dark Cyan") + geom_abline(aes(intercept = Sal_coef_August2012[1, 1], slope =
Sal_coef_August2012[2, 1]), size = 2, color = "Orange") + geom_abline(aes(intercept =
Sal_coef_June2013[1, 1], slope = Sal_coef_June2013[2, 1]), size = 2, color = "Dark Blue") +
geom_abline(aes(intercept = Sal_coef_August2013[1, 1], slope = Sal_coef_August2013[2, 1]), size = 2,
color = "Dark Red") + scale_color_manual(values = c("Dark Cyan", "Orange", "Dark Blue", "Dark
```

```
Red"), labels = c("June 2012", "August 2012", "June 2013", "August 2013")) +
scale_shape_manual(values = c(17, 17, 19, 19), labels = c("June 2012", "August 2012", "June 2013",
"August 2013")) + xlab("Salinity (ppt)") + ylab(expression(paste("Root mass (g/", m^{ 2}, ")"))) +
theme(legend.title = element_blank()) + scale_y_continuous(limits = c(0, 5000)) + ggtitle("B")
```

Figure 2C: Extractable Inorganic Nitrogen versus Aboveground Biomass

```
# Change base text size and background for figures
theme_set(theme_bw(base_size = 16))
# Create data table for figure
ExtDIN_AGbiomass_means <- merge(Ext_DINMeans, AGBiomassMeans, by = c("Month_Year",
   "Site"))
ExtDIN_AGbiomass_means2 <- ExtDIN_AGbiomass_means[which(ExtDIN_AGbiomass_means ==
   "June2013" | ExtDIN_AGbiomass_means == "August2013"), ]
# Create plot
ExtDIN_AGbiomass <- ggplot(ExtDIN_AGbiomass_means2, aes(x = DIN_Extractable,
   y = DryWeight_g.m2, color = Month_Year))
ExtDIN_AGbiomass + geom_errorbar(aes(ymin = DryWeight_g.m2 - se.y, ymax = DryWeight_g.m2 +
se.y, width = 0), size = 1) + geom_errorbarh(aes(xmin = DIN_Extractable - se.x, xmax =
DIN_Extractable + se.x, width = 0), size = 1) + geom_point(size = 6, color = "white") +
geom_point(size = 5) + geom_abline(aes(intercept = DIN_coef2_June2013[1, 1], slope =
DIN_coef2_June2013[2, 1]), size = 2, color = "Dark Blue") + geom_abline(aes(intercept =
DIN_coef2_August2013[1, 1], slope = DIN_coef2_August2013[2, 1]), size = 2, color = "Dark Red") +
xlab(expression(paste("Extractable Inorganic Nitrogen (", mu, "M"))) +
ylab(expression(paste("Aboveground Biomass (g/", m^{2}, ")"))) +  scale_color_manual(values =
c("Dark Blue", "Dark Red"), labels = c("June 2013", "August 2013")) + theme(legend.title =
element_blank()) + scale_y_continuous(limits = c(0, 1200)) + ggtitle("C")
```

Figure 2D: Salinity versus Aboveground Biomass

```
# Create data table for figure
Salinity_AGbiomass_means <- merge(PW_SalinityMeans, AGBiomassMeans, by = c("Month_Year",
   "Site"))
Salinity_AGbiomass_means2 <- Salinity_AGbiomass_means[which(Salinity_AGbiomass_means ==
   "June2012" | Salinity_AGbiomass_means == "August2012" | Salinity_AGbiomass_means ==
   "June2013" | Salinity_AGbiomass_means == "August2013"), ]
# Create plot
Salinity_AGbiomass <- ggplot(Salinity_AGbiomass_means2, aes(x = Salinity_ppt,
   y = DryWeight_g.m2, color = Month_Year, shape = Month_Year))
Salinity_AGbiomass + geom_errorbar(aes(ymin = DryWeight_g.m2 - se.y, ymax = DryWeight_g.m2 +
se.y, width = 0), size = 1) + geom_errorbarh(aes(xmin = Salinity_ppt - se.x, xmax = Salinity_ppt + se.x,
width = 0), size = 1) + geom_point(size = 6, color = "white") + geom_point(size = 5) +
scale_color_manual(values = c("Dark Cyan", "Orange", "Dark Blue", "Dark Red"), labels = c("June
2012", "August 2012", "June 2013", "August 2013")) + scale_shape_manual(values = c(17, 17, 19, 19),
labels = c("June 2012", "August 2012", "June 2013", "August 2013")) + xlab("Salinity (ppt)") +
ylab(expression(paste("Aboveground Biomass (g/", m^{2}, ")"))) + theme(legend.title =
element_blank()) + scale_y_continuous(limits = c(0, 1200)) + ggtitle("D")
```

Supplementary Figure: Aboveground Biomass versus Sediment C

```
SedC_AGbiomass_means <- merge(SedCMeans, AGBiomassMeans, by = c("Month_Year",
   "Site"))
SedC_AGbiomass_means2 <- SedC_AGbiomass_means[which(SedC_AGbiomass_means ==
```

```
    "June2012" | SedC_AGbiomass_means == "August2012" | SedC_AGbiomass_means ==
    "June2013" | SedC_AGbiomass_means == "August2013"), ]
# Create plot
SedC_AGbiomass <- ggplot(SedC_AGbiomass_means2, aes(x = SedC_mg.gDW, y = DryWeight_g.m2,
    color = Month_Year, shape = Month_Year))
SedC_AGbiomass + geom_errorbar(aes(ymin = DryWeight_g.m2 - se.y, ymax = DryWeight_g.m2 +
se.y, width = 0), size = 1) + geom_errorbarh(aes(xmin = SedC_mg.gDW - se.x, xmax = SedC_mg.gDW
+ se.x, width = 0), size = 1) + geom_point(size = 6, color = "white") + geom_point(size = 5) +
scale_color_manual(values = c("Dark Cyan", "Orange", "Dark Blue", "Dark Red"), labels = c("June
2012", "August 2012", "June 2013", "August 2013")) + scale_shape_manual(values = c(17, 17, 19, 19),
labels = c("June 2012", "August 2012", "June 2013", "August 2013")) + xlab("Sediment Carbon Content
(mg/g)") + ylab(expression(paste("Aboveground Biomass (g/", m^{2}, ")"))) + theme(legend.title =
element_blank()) + scale_y_continuous(limits = c(0, 1200))
```

Supplementary Figure: Aboveground Biomass versus Sand Content

```
Sand_AGbiomass_means <- merge(FracSandMeans, AGBiomassMeans, by = c("Month_Year",
    "Site"))
Sand_AGbiomass_means2 <- Sand_AGbiomass_means[which(Sand_AGbiomass_means ==
    "June2012" | Sand_AGbiomass_means == "August2012" | Sand_AGbiomass_means ==
    "June2013" | Sand_AGbiomass_means == "August2013"), ]
# Create plot
Sand_AGbiomass <- ggplot(Sand_AGbiomass_means2, aes(x = Frac_Sand, y = DryWeight_g.m2,
    color = Month_Year, shape = Month_Year))
Sand_AGbiomass + geom_errorbar(aes(ymin = DryWeight_g.m2 - se.y, ymax = DryWeight_g.m2 +
se.y, width = 0), size = 1) + geom_errorbarh(aes(xmin = Frac_Sand - se.x, xmax = Frac_Sand + se.x,
width = 0), size = 1) + geom_point(size = 6, color = "white") + geom_point(size = 5) +
stat_smooth(method = "lm", size = 2) + scale_color_manual(values = c("Dark Cyan", "Orange", "Dark
Blue", "Dark Red"), labels = c("June 2012", "August 2012", "June 2013", "August 2013")) +
scale_shape_manual(values = c(17, 17, 19, 19), labels = c("June 2012", "August 2012", "June 2013",
"August 2013")) + xlab("Fraction Sand Content") + ylab(expression(paste("Aboveground Biomass (g/",
    m^{2}, ")"))) + theme(legend.title = element_blank()) + scale_y_continuous(limits = c(0, 1200))
```

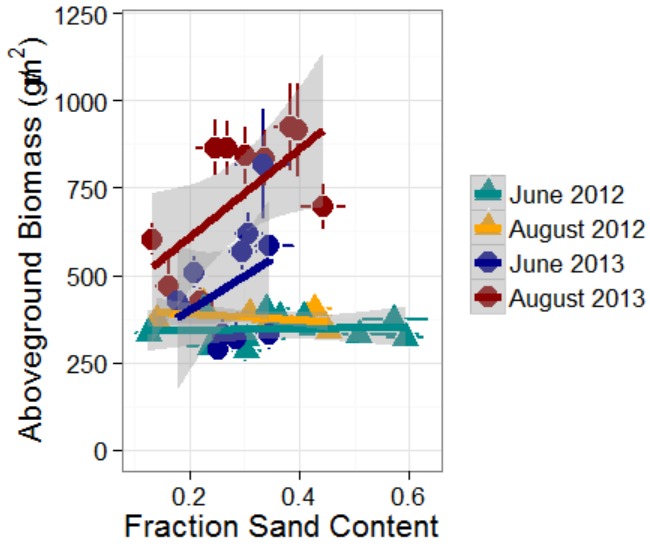

```
# Test association between fraction sand and aboveground biomass
SandAGBiomass <- Sand_AGbiomass_means2[, c("Frac_Sand", "DryWeight_g.m2")]
rcorr(as.matrix(SandAGBiomass))
              Frac_Sand DryWeight_g.m2
Frac_Sand          1.00         -0.01
DryWeight_g.m2     -0.01          1.00

n= 43

p
              Frac_Sand DryWeight_g.m2
Frac_Sand               0.9662
DryWeight_g.m2 0.9662

# Test association between fraction sand and aboveground biomass for 2013 data only
Sand_AGbiomass2013 <- Sand_AGbiomass_means[which(Sand_AGbiomass_means == "June2013" |
  Sand_AGbiomass_means == "August2013"), ]
SandAGBiomass2013 <- Sand_AGbiomass2013[, c("Frac_Sand", "DryWeight_g.m2")]
rcorr(as.matrix(SandAGBiomass2013))
              Frac_Sand DryWeight_g.m2
Frac_Sand          1.00          0.48
DryWeight_g.m2      0.48          1.00

n= 22

p
              Frac_Sand DryWeight_g.m2
Frac_Sand               0.0244
DryWeight_g.m2 0.0244
```

Appendix E: Supplement to Chapter 6

Output from JMP

Table E1: Summary of one-way ANOVAs of plant traits collected in September 2012 for three vegetation cover types [*Phragmites*, *Typha*, Removal], two-way ANOVAs of plant traits collected September 2011-September 2012 for *Phragmites* and *Typha* communities only, and two-way ANOVAs of sediment carbon and nitrogen content collected August 2010-September 2012. Leaf nitrogen content in September 2012 was calculated as an average of the component species of the community, weighted by their biomass. Effects significant at $\alpha = 0.05$ are shown in bold. Analyses performed in JMP.

Source	df	Sum of Squares	F Ratio	p
Aboveground Biomass, September 2012				
Vegetation	2	35.12	2.73	0.1186
Contrast: *Phragmites* v. Removal	1	34.30	5.33	**0.0464**
Contrast: *Phragmites* v. *Typha*	1	17.00	2.64	0.1386
Error	9	57.94		
Total	11	93.07		
Aboveground Biomass, 2011-2012, Reference *Phragmites* and *Typha* only				
Time	2	4.13	0.42	0.6601
Vegetation	1	45.49	9.39	**0.0079**
Time x Vegetation	2	0.73	0.07	0.9274
Error	15	72.64		
Total	20	121.56		
Leaf Nitrogen Content, September 2012				
Vegetation	2	117.67	4.66	**0.0408**
Contrast: *Phragmites* v. Removal	1	115.28	9.13	**0.0144**
Contrast: *Phragmites* v. *Typha*	1	55.65	4.41	0.0651
Error	9	113.58		
Total	11	231.25		
Leaf Nitrogen Content, 2011-2012, Reference *Phragmites* and *Typha* only				
Time	2	459.31	19.80	**<0.0001**
Vegetation	1	241.12	20.78	**0.0004**
Time x Vegetation	2	14.64	0.63	0.5456
Error	15	173.99		
Total	20	1001.32		
Sediment Carbon Content, August 2010-September 2012				
Time	3	1576.98	1.17	0.3356
Vegetation	2	1931.61	2.14	0.1318
Contrast: *Phragmites* v. Removal	1	1211.47	2.69	0.1096
Contrast: *Phragmites* v. *Typha*	1	1685.38	3.74	0.0609
Time x Vegetation	6	2404.57	0.89	0.5124
Error	36	16208.37		
Total	47	21914.03		
Sediment Nitrogen Content, August 2010-September 2012				

Time	3	4.4462	1.01	0.3997
Vegetation	2	12.2090	4.16	**0.0237**
Contrast: *Phragmites* v. Removal	1	5.7760	3.94	0.0549
Contrast: *Phragmites* v. *Typha*	1	11.6806	7.96	**0.0077**
Time x Vegetation	6	6.2764	0.71	0.6416
Error	36	52.8383		
Total	47	73.6617		

Table E2: Summary of two-way ANOVAs comparing denitrification potential and sediment properties of three vegetation treatments [Ramshorn-Removal, Ramshorn-*Typha*, Reference-*Phragmites*] before [August 2010] and after [September 2011, June 2012, September 2012] herbicide application. Effects significant at $\alpha = 0.05$ are shown in bold. Analyses performed in JMP.

Source	**df**	**Sum of Squares**	**F Ratio**	**P**
Denitrification Potential, 2010-2012				
Time	3	7.32×10^{6}	6.57	**0.0018**
Vegetation	2	1.76×10^{6}	2.37	0.1122
Time x Vegetation	6	7.68×10^{5}	0.34	0.9066
Contrast: *Phragmites* v Removal 2010	1	7.29×10^{3}	0.02	0.8896
Contrast: *Typha* v Removal 2010	1	6.38×10^{2}	0.00	0.9675
Contrast: *Phragmites* v *Typha* 2010	1	3.19×10^{3}	0.01	0.9269
Contrast: *Phragmites* v Removal 2011-2012	1	1.61×10^{6}	4.33	**0.0471**
Contrast: *Typha* v Removal 2011-2012	1	4.47×10^{3}	0.01	0.9134
Contrast: *Phragmites* v *Typha* 2011-2012	1	1.44 x 106	3.88	0.0591
Error	27	1.00×10^{7}		
Total	38	1.97×10^{7}		
Ammonium, 2010-2012				
Time	3	0.6398	3.42	**0.0335**
Vegetation	2	0.6145	4.92	**0.0162**
Time x Vegetation	6	1.0480	2.79	**0.0330**
Contrast: *Phragmites* v Removal 2010	1	0.0000	0.00	0.9858
Contrast: *Typha* v Removal 2010	1	0.0000	0.00	0.9772
Contrast: *Phragmites* v *Typha* 2010	1	0.0003	0.00	0.9472
Contrast: *Phragmites* v Removal 2011-2012	1	0.9370	15.00	**0.0007**
Contrast: *Typha* v Removal 2011-2012	1	0.5831	9.34	**0.0054**
Contrast: *Phragmites* v *Typha* 2011-2012	1	0.0418	0.67	0.4215
Error	24	1.4987		
Total	35	4.1843		
Organic Content, 2010-2012				
Time	3	1.44×10^{-3}	0.26	0.8467
Vegetation	2	2.89×10^{-3}	0.81	0.4542
Time x Vegetation	6	4.01×10^{-3}	0.38	0.8830
Contrast: *Phragmites* v Removal 2010	1	4.71×10^{-4}	0.26	0.6109
Contrast: *Typha* v Removal 2010	1	1.80×10^{-5}	0.01	0.9205
Contrast: *Phragmites* v *Typha* 2010	1	2.82×10^{-4}	0.16	0.6935

Contrast: *Phragmites* v Removal 2011-2012	1	2.22×10^{-3}	1.25	0.2737
Contrast: *Typha* v Removal 2011-2012	1	2.07×10^{-4}	0.12	0.7354
Contrast: *Phragmites* v *Typha* 2011-2012	1	1.07×10^{-3}	0.60	0.4446
Error	27	4.79×10^{-2}		
Total	38	5.67×10^{-2}		

Table E3: Summary of two-way ANOVAs comparing denitrification potential and sediment properties of four vegetation treatments [Ramshorn-Removal, Ramshorn-*Typha*, Reference-*Typha*, Reference-*Phragmites*] only after [September 2011, June 2012, September 2012] herbicide application. Effects significant at $\alpha = 0.05$ are shown in bold. Analyses performed in JMP.

Source	**df**	**Sum of Squares**	**F Ratio**	**p**
Denitrification Potential, 2011-2012				
Time	2	6.88×10^{6}	6.80	**0.0046**
Vegetation	3	2.58×10^{6}	1.70	0.1938
Contrast: Reference-*Phragmites* v Ramshorn-Removal	1	1.61×10^{6}	3.18	0.0874
Contrast: Ramshorn-*Typha* v Ramshorn-Removal	1	4.47×10^{3}	0.01	0.9259
Contrast: Reference-*Phragmites* v Reference-*Typha*	1	4.85×10^{4}	0.10	0.7594
Time x Vegetation	6	2.71×10^{6}	0.89	0.2590
Error	27	1.21×10^{7}		
Total	38	2.43×10^{7}		
Ammonium, 2011-2012				
Time	2	0.3402	2.72	0.0861
Vegetation	3	1.2993	6.93	**0.0016**
Contrast: Reference-*Phragmites* v Ramshorn-Removal	1	0.9370	14.99	**0.0007**
Contrast: Ramshorn-*Typha* v Ramshorn-Removal	1	0.5831	9.33	**0.0055**
Contrast: Reference-*Phragmites* v Reference-*Typha*	1	0.0092	0.01	0.9244
Time x Vegetation	6	1.0091	2.69	**0.0385**
Error	24	1.5005		
Total	35	4.1490		
Organic Content, 2010-2012				
Time	2	4.60×10^{-4}	0.53	0.5938
Vegetation	3	1.30×10^{-3}	1.00	0.4099
Contrast: Reference-*Phragmites* v Ramshorn-Removal	1	5.37×10^{-4}	1.24	0.2763
Contrast: Ramshorn-*Typha* v Ramshorn-Removal	1	1.11×10^{-4}	0.26	0.6175
Contrast: Reference-*Phragmites* v Reference-*Typha*	1	1.19×10^{-3}	2.74	0.1108
Time x Vegetation	6	1.35×10^{-3}	0.52	0.7872
Error	27	1.04×10^{-2}		
Total	38	1.35×10^{-2}		

Output from R

Packages

```
library(ggplot2)
library(bear)
```

Data and Formatting

```
setwd(filepath5)
hudson <- read.csv("20141022_Sediment_AllYears.csv")
treatmentmeans <- read.csv("20140428_Sediment_AllYears_Treatmentmeans.csv")
# Convert 'Time' from factor to date
hudson$Time <- as.Date(hudson$Time)
# Convert 'Vegetation' from factor to ordered factor
hudson$Vegetation <- ordered(hudson$Vegetation, levels = c("Phragmites", "Typha",
"Removal"))
# Convert 'Time' from factor to date
treatmentmeans$Time <- as.Date(treatmentmeans$Time)
# Convert 'Vegetation' from factor to ordered factor
treatmentmeans$Vegetation <- ordered(treatmentmeans$Vegetation, levels = c("Phragmites",
   "Typha", "Removal"))
# Convert 'Site_Treatment' from factor to ordered factor
treatmentmeans$Site_Treatment <- ordered(treatmentmeans$Site_Treatment, levels =
c("Reference Phragmites", "Reference Typha", "Ramshorn Typha", "Ramshorn Removal"))
# Change base text size for figures
theme_set(theme_bw(base_size = 20))
```

Plot Biomass by Vegetation Type

```
# Create a summary table for Biomass data at the plot level using summarySE{bear}
Biomass <- summarySE(hudson, measurevar = "AGBiomass_kg.m2", groupvar = c("Time",
   "ReplicateCode", "Vegetation"), na.rm = T)
# Create a boxpolot for biomass
biomass <- ggplot(Biomass, aes(x = Vegetation, y = AGBiomass_kg.m2, color = Vegetation))
biomass + geom_boxplot(size = 1.5) + scale_color_manual(values = c("maroon4",
"darkolivegreen", "darkgoldenrod")) + ylab(expression(paste("Biomass (kg/", m^{2}, ")"))) +
theme(legend.position = "none") + theme(axis.text.x = element_text(face = c("italic", "italic",
"plain"), color = "black")) + theme(axis.text.y = element_text(color = "black")) + ggtitle("A")
```

Plot Leaf N Content by Vegetation Type

```
LeafN <- summarySE(hudson, measurevar = "PlantN_mg.gDW", groupvar = c("Time",
   "ReplicateCode", "Vegetation"), na.rm = T)
LeafNcontent <- ggplot(LeafN, aes(x = Vegetation, y = PlantN_mg.gDW, color = Vegetation))
LeafNcontent + geom_boxplot(size = 1.5) + scale_color_manual(values = c("maroon4",
"darkolivegreen", "darkgoldenrod")) + ylab("Leaf Nitrogen Content (mg-N/g)") +
theme(legend.position = "none") + theme(axis.text.x = element_text(face = c("italic", "italic",
"plain"), color = "black")) + theme(axis.text.y = element_text(color = "black")) + ggtitle("B")
```

Graph aboveground biomass v Leaf nitrogen content

A negative slope would indicate nutrient competition

```
Biomass_LeafN_means <- cbind(Biomass, LeafN)
Biomass_LeafN <- ggplot(Biomass_LeafN_means, aes(x = AGBiomass_kg.m2, y =
PlantN_mg.gDW,
   color = Vegetation))
Biomass_LeafN + geom_abline(intercept = 42.61210463, slope = -2.120325886, color =
"maroon4",     size = 2) + geom_abline(intercept = 42.14073928, slope = -8.3415148, color =
"darkolivegreen", size = 2) + geom_abline(intercept = 23.3532942, slope = -9.917019514, color
= "darkgoldenrod", size = 2) + geom_point(size = 5, color = "white") + geom_point(size = 4) +
scale_color_manual(values = c("maroon4", "darkolivegreen", "darkgoldenrod"), labels =
expression(paste(italic("Phragmites")), paste(italic("Typha")), paste("Removal"))) +
xlab(expression(paste("Biomass (kg/", m^{2}, ")"))) + ylab("Leaf Nitrogen Content (mg-N/g)")
+ theme(legend.title = element_blank(), legend.key = element_blank(), legend.text.align = 0) +
ggtitle("C") + scale_y_continuous(limits = c(10, 40))
```

Create Plot for Sediment C content

```
SedC <- summarySE(hudson, measurevar = "SedCmg.gDW", groupvar = c("Time",
"ReplicateCode",
   "Vegetation"), na.rm = T)
SedCcontent <- ggplot(SedC, aes(x = Vegetation, y = SedCmg.gDW, color = Vegetation))
SedCcontent + geom_boxplot(size = 1.5) + scale_color_manual(values = c("maroon4",
"darkolivegreen", "darkgoldenrod")) + ylab("Sediment Organic Carbon \nContent (mg-N/g)") +
theme(legend.position = "none") + theme(axis.text.x = element_text(face = c("italic", "italic",
"plain"), color = "black")) + theme(axis.text.y = element_text(color = "black")) + ggtitle("A")
```

Create Plot for Sediment N content

```
SedN <- summarySE(hudson, measurevar = "SedNmg.gDW", groupvar = c("Time",
"ReplicateCode",
   "Vegetation"), na.rm = T)
SedNcontent <- ggplot(SedN, aes(x = Vegetation, y = SedNmg.gDW, color = Vegetation))
SedNcontent + geom_boxplot(size = 1.5) + scale_color_manual(values = c("maroon4",
"darkolivegreen", "darkgoldenrod")) + ylab("Sediment Organic Nitrogen \nContent (mg-N/g)")
+ theme(legend.position = "none") + theme(axis.text.x = element_text(face = c("italic", "italic",
"plain"), color = "black")) + theme(axis.text.y = element_text(color = "black")) + ggtitle("B")
```

Plot Sediment Ammonium over Time

```
# Create an object that refers to my ammonium variable
NH4 <- treatmentmeans$Mean.NH4_mgL.
# Create an object that refers to standard errors for y error bars
NH4se <- treatmentmeans$Std.Err.NH4_mgL.
# Create a position_dodge to keep treatment points and errorbars from overlapping
pd <- position_dodge(width = 20)
# Create an object indicating the date when herbicide application was performed (for v line)
herbicide <- as.Date("2010-09-15")
# Create an object that indicates whether sites were reference or treatment sites (for ease of
```

```
reading legend title)
Site_Treatment <- treatmentmeans$Site_Treatment

# Create plot
NH4Time <- ggplot(treatmentmeans, aes(x = Time, y = NH4, color = Site_Treatment,
   shape = Site_Treatment))
NH4Time + geom_line(size = 2, position = pd, aes(color = Site_Treatment)) +
geom_errorbar(aes(ymin = NH4 - NH4se, ymax = NH4 + NH4se, width = 0), position = pd,
size = 1) + geom_point(size = 9, position = pd, color = "white") + geom_point(size = 7, position
= pd) + geom_vline(xintercept = as.numeric(as.Date("2010-09-30", format = "%Y-%m-%d")),
size = 2) + scale_color_manual(name = "Site and Vegetation", values = c("maroon4",
"darkolivegreen", "darkolivegreen", "darkgoldenrod"),   labels = expression(paste("Reference ",
italic("Phragmites")), paste("Reference ", italic("Typha")), paste("Ramshorn ",
italic("Typha")), paste("Ramshorn Removal")), guide = guide_legend(title = NULL)) +
scale_shape_manual(values = c(17, 17, 19, 19), name = "Site and Vegetation", labels =
expression(paste("Reference ", italic("Phragmites")), paste("Reference ", italic("Typha")),
paste("Ramshorn ", italic("Typha")), paste("Ramshorn Removal")), guide = guide_legend(title
= NULL)) + theme(legend.key = element_blank(), legend.text.align = 0) + ylab("Ammonium
(mg/L)") + xlab("Sampling Time") + theme(axis.text.x = element_text(color = "black")) +
theme(axis.text.y = element_text(color = "black"))
```

Plot Denitrification Rates over Time

```
# Create an object that refers to my dentirification variable
DEA <- treatmentmeans$Mean.DEA..ng.N.g.hr..
# Create an object that refers to standard errors for y error bars
DEAse <- treatmentmeans$Std.Err.DEA..ng.N.g.hr..

# Create plot
DenitTime <- ggplot(treatmentmeans, aes(x = Time, y = DEA, color = Site_Treatment,
   shape = Site_Treatment))
DenitTime + geom_line(size = 2, position = pd, aes(color = Site_Treatment)) +
geom_errorbar(aes(ymin = DEA - DEAse, ymax = DEA + DEAse, width = 0), position = pd,
size = 1) + geom_point(size = 9, position = pd, color = "white") + geom_point(size = 7, position
= pd) + geom_vline(xintercept = as.numeric(as.Date("2010-09-30", format = "%Y-%m-%d")),
size = 2) + scale_color_manual(name = "Site and Vegetation", values = c("maroon4",
"darkolivegreen", "darkolivegreen", "darkgoldenrod"), labels = expression(paste("Reference ",
italic("Phragmites")), paste("Reference ", italic("Typha")), paste("Ramshorn ",
italic("Typha")), paste("Ramshorn Removal")), guide = guide_legend(title = NULL)) +
scale_shape_manual(values = c(17, 17, 19, 19), name = "Site and Vegetation", labels =
expression(paste("Reference ", italic("Phragmites")), paste("Reference ", italic("Typha")),
paste("Ramshorn ", italic("Typha")), paste("Ramshorn Removal")), guide = guide_legend(title
= NULL)) + theme(legend.key = element_blank(), legend.text.align = 0) +
ylab("Denitrification Enzyme Activity (ng-N/g/h)") + xlab("Sampling Time") +
theme(axis.text.x = element_text(color = "black")) + theme(axis.text.y = element_text(color =
"black"))
```